UNIVERSITÀ DI SIENA 1240

Department of Biotechnology, Chemistry and Pharmacy

PhD in Chemical and Pharmaceutical Sciences

Cycle XXXV

Coordinator: Prof. Maurizio Taddei

Micellar catalysis for eco-friendly hydroaminomethylation (HAM)

Tutor: Prof. Elena Petricci

CHIM/06- Organic Chemistry

PhD candidate: Elisabetta Monciatti

Academic year 2021/2022

Abstract

Hydroaminomethylation (HAM) is one of the most interesting atom economic metal catalysed process for the production of amines. Despite the large application of HAM in the synthesis of aliphatic amines, anilines, interesting intermediates in APIs synthesis, are still challenging substrates for this reaction. Herein it is reported the development of a protocol that combines micellar catalysis and microwave heating for the eco-friendly HAM of anilines by using water as the reaction medium. Secondary and tertiary anilines are obtained in good yields and regioselectivity with a full recovery of the catalyst in the water/micellar media that can be reused several times without drastic impacts on the reaction yields and regioselcetivity. The final amines are obtained as pure products by filtration on SCX columns. The characterization of the possible active catalytic species involved in the process is also reported. Mechanistic investigations suggest a different pathway compared to the commonly observed mechanism with homogeneous catalysts for the reported HAM reaction.

Finally, LCA analysis of the protocol was performed, that demontrates the greeness and low environmental impact of the process.

Beside this work, the synthesis of a small library of potential inhibitors of SIRT1, deacetylase involved in noumerous biological pathways and pathologies, included anxiety and depression, is reported.

Finally, a third section is dedicated to design and early stage synthesis of a photolabeling probe precursor, by functionalization of quinoline compounds endowed with a good antibacterial activity, for the future further investigation of the interactions between these compounds and bacteria.

INDEX

LIST OF ACRONYMS

5-HT 5-hydroxytriptamine

AcOH acetic acid

AE Atom Economy

ACN acetonitrile

ADP adenosindiphosphate

API Active Pharmacetical Ingredient

API-IL Active Pharmacetical Ingredient-Ionic Liquid

AQNO 2-alkyl-4(1H)-quinolone N-oxides

AQs alkyl quinolines

Biphephos 6′-[(3,3′-Di-tert-butyl-5,5′-dimethoxy-1,1′-biphenyl-2,2′-diyl)bis(oxy)]bis(dibenzo[d,f][1,3,2]dioxaphosphepin)

Bs broad singlet

CDCl₃ Deuterated chloroform

CE carbon economy

CED cumulative energy demand

cEF complete E-factor

CTAB cetyltrimethylammonium bromide

CMC critical micellar concentration

CPME cyclopentyl methyl ether

CXLs carbon dioxide expanded liquid

d doublet

dd double of doublets

ddd doublet of doublets of doublets

DFT density functional theory

dppf 1,1′-Ferrocenediyl-bis(diphenylphosphine)

DCM dichloromethane

DELs DNA Encoded Libraries

DES deep eutectic solvent

DMAC *N,N*-dimethylacetammide

DMF *N,N*-dimethylformamide

DMSO dimethylsulfoxide

DLS dynamic light scattering

EHS environment, health and safety

EMS Enhanced Microwaves Synthesis

EMY Effective Mass Yield

ETBE ethyl-butyl ether

EtOAC ethyl acetate

EtOH ethanol

Et₂O diethyl ether

FLASC™ Fast Cycle Assessment of Synthetic Chemistry

FOXO Forehead box protein O

GABA γ-aminobutirric acid

GC-MS gas chromatography-mass spectrometry

GVL γ-valerolactone

HBA hydrogen bond acceptor

HBD hydrogen bond donor

HLB hydrophilic lipophilic balance

HESI heated electrospray ionization

HHQ hydroxy-2-heptilquinoline

HOSA hydroxylamine-*O*-sulfonic

ILs ionic liquids

LA levulinic acid

LCA life cycle assessment

LC-MS liquid chromatography-mass spectrometry

LDA lithium diisopropylamine

LiHMDS lithium bis(trimethylsilyl)amide

LIFDI liquid injection field desorption ionization

m multiplet

MAO-A monoamine oxidase A

MAOS microwaved assisted organic synthesis

m-CPBA meta-chloroperbenzoic acid

Me-THF methyl tetrahydrofuran

MeOD deuterated methanol

MeOH methanol

MI Mass Intensity

MIC minimum inhibitory concentration

MH menaquinone

MKH$_2$ menaquinol

MP mass productivity

MPEG methyl polymethylene glycol

mPFC medial prefrontal cortex

MSNs medium spiny neurons

MWs microwaves

NAc Nucleus Accumbens

NAD⁺ adenine dinucleotide

NAM nicotinamide

NBS *N*-bromosuccinimide

NCW near critical water

NF-kB nuclear factor kappa-light-chain-enhancer of activated B cells

NHLH₂ nescient helix-loop-helix 2

NMP N-methylpirrolidone

PAG photoaffinity group

PAL photoaffinity labelling

PBD pyrrolo-benzodiazepines

PCG1a peroxisome proliferator-activated receptor gamma coactivator-1α

PEG polyethylene glycole

PMB para-methoxy benzyl

PMI Process Mass Intensity

PPARα proliferator-activated receptor α

PPARγ proliferator-activated receptor γ

PQS Pseudomonas Quinolone Signal

PTS polyhoxyehanyl-α-tocopherol sebacate

***p*TSA** para-toluensulfonic acid

q quartet

QS quorum sensing

Q-SAvESS Quick Sustainability Assessment via Experimental Solvent Selection

RME reaction mass efficiency

rt room temperature

s singlet

sCO₂ supercritical carbon dioxide

SCFs super critical fluids

SCX Strong Cationic EXchange

SDS sodium dodecylsulfate

SDBS sodium dodecylbenzenesufonate

sEF simple E-factor

SM starting material

SHSs switchable hydrophobicity solvents

SI Solvent Intensity

SIR2 Silent Information Regulator 2

SPSs switchable polar solvents

SPGS-550-M β-sitosterol methoxypolyethyleneglycol succinate

SW switchable water

t triplet

TAME tert-amyl-methyl ether

TBAC *tert*-butyl acetate

TEM transmission electron microscopy

TEMPO 2,2,6,6-tetramethyl-1-piperidinyloxy

Tetrabi 2, 2′, 6, 6′-tetrakis ((diphenylphosphino)methyl)-1, 1′-biphenyl

TBAI tetrabutylammonium iodide

TPPTS trisodium 3,3′,3″-phosphanetriyltri(benzene-1-sulfonate)

THF tetrahydrofuran

TLC thin layer chromatography

TMEDA *N,N,N,N*-tetramethylendiamine

TPGS-750-M DL-α-Tocopherol methoxypolyethylene glycol succinate

Xantphos 4,5-bis(diphenylphosphino)-9,9-dimethylxanthene

XRD X-ray diffraction analysis

WWI Waste Water Intensity

I - Micellar catalysis for eco-friendly hydroaminomethylation

1. INTRODUCTION

1.1 Green chemistry and circular chemistry

The term *Green Chemistry* was introduced in the early 1990s and used in the modern meaning for the first time by Anastas and Williamson in a publication in 1996.[1] In 1998, Anastas and Warner proposed for the first time the so called 12 Principles of *Green Chemistry* (Figure 1)[2].
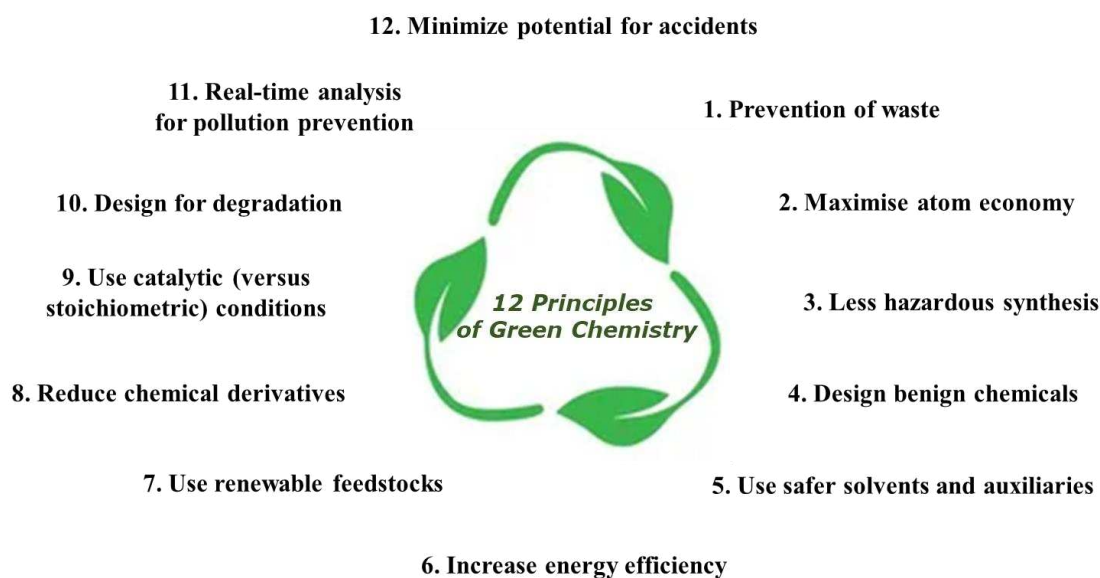
Figure 1. The twelve principles of green chemistry.

In 2005, the term *PRODUCTIVELY* was introduced by Poliarkoff and co-worker as a mnemonic to summarize all these principles:[3]

Prevent waste

Renewable materials

Omit derivatization steps

Degradable chemical products inputs

Use of safe synthetic methods

Catalytic reagents

Temperature, pressure ambient

In-process monitoring

Very few auxiliary substances

E-factor, maximize feed in product

Low toxicity of chemical products

Yes, it is safe!

Elimination of waste and of the use of toxic or hazardous reactants and solvents, the efficient use of preferably renewable raw materials and energy resources will be analysed more in detail.

Green Chemistry principally focuses on the design of chemicals and their production processes reducing or eliminating the use or generation of substances hazardous for humans, animals, plants and environment.[4]

Green Chemistry allowed the general optimization of several chemical processes, enhancing their sustainability and making them less environmentally demanding, in many important fields, included the pharmaceutical one.[5] However, since they are mostly focused on the assessment on chemical reactions, the 12 principles of Green chemistry result perfectly suitable for the optimization of linear processes.[6]

To have a fully sustainability, a transition to circular economy was necessary, with the development of novel chemical reactions and close-loop-waste-free chemical processes, through reuse or recycle of chemicals, especially at industrial level.[7] To facilitate this transition, 12 principles of circular chemistry were formulated along the line of the green chemistry principles (Figure 2).[6]

Figure 2. 12 Principles of Circular Chemistry.

Sustainability is strictly dependent on the rates of two factors: i) resource utilization and ii) waste production.[8] The rate of exploitation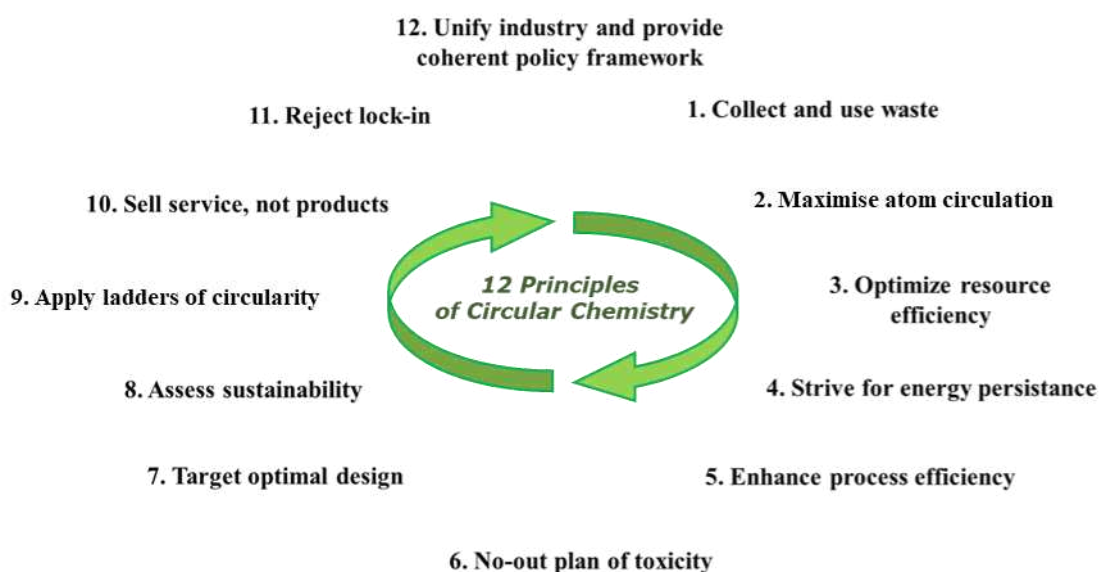 of natural resources should not deplete supplies over the long term and residues of waste products should not overcome the capability of the environment to assimilate them. According to the "new" principles,[6] reuse of waste materials as chemical feedstock making it marketable value-added product is the first prerequisite. To make it possible, process design should be optimized to guarantee an efficient separation and purification and a correct recycling of the waste, in respect of the environment.

Renewability and stability of materials for many cycles is valued over their degradability.[9] In fact, recirculation of material is indispensable to reduce the use of primary feedstocks and of harmful effects, avoiding release of waste in the environment. For this purpose, redistribution of material in the same place and its reuse in situ is preferable since transportation is not required.

Different ladders of circularity have been proposed as means to find the best life-end option for every material and the original "3 Rs" (**R**educe, **R**euse, **R**ecycle) approach has been gradually expanded to reach "11 Rs" (**R**eject, **R**educe, **R**euse, **R**edistribute, **R**epair, **R**efurbish, **R**epurpose, **R**emanufacture, **R**ecycle, **R**ecover, **R**eturn) as guide for resource hierarchy.[10]

The achievement of the maximum grade of sustainability needs an effort from the chemical industry world, that must focus its goal on the promotion of efficiency over the production rate, demonstrating to be flexible to implementation of innovation and united to policy to create the optimal environment to enable circularity in chemical processes.

1.2 Catalysis and atom economy

The production of waste represents not only an economic but even an environmental and a social problem, due to its impact on the ecosystem and workers and consumers' health.[5] Pharmaceutical industry represents a very good example for waste prevention strategies, due both to process intensification in terms of improvement of yields, product quality and efficiency, and to process simplification in terms of design of synthetic strategies with a minor number of steps for the manufacturing of Active Pharmaceutical Ingredients (APIs).

One pot synthesis is a perfect approach for waste production prevention, that avoids isolation and purification of intermediates, with reduction of solvents and separation aids necessity. In this context, in 2002 Pfizer won the U.S. Environmental Protection Agency (EPA)

Presidential Green Chemistry award, for designing an alternative process that reduced a multi-step synthesis of an intermediate of sertraline (Zoloft®) to only one step.[11]

1.2.1 Catalysis

One pot synthesis if often accomplished by catalysis as we can see in reactions as Grubbs olefin methatesis,[12] selective C-H activation,[13] aryl-aryl bond formation,[14] catalytic hydrogenation,[15] hydroformylation[16] and hydroaminomethylation,[17] very exploited in industrial processes, including the manufacturing of APIs.

The use of stoichiometric amounts of Cr or Mn salts in oxidation, metal hydrides (i.e $NaBH_4$, $LiAlH_4$) or metals (Na, Mg, Zn, Fe) necessary for reductions, as well as mineral (H_2SO_4, HF, H_3PO_4) and Lewis ($AlCl_3$, $ZnCl_2$, BF_3) acids and bases employed in classical stoichiometric reactions, leads to the production of a major amount of waste. On the other hand, catalysts are very important tools in Green Chemistry, since their use improves selectivity, included regio- and stereoselectivity, and atom economy and lower the energy demand by accelerating the rate of chemical reactions without being consumed and, consequently, without producing waste.[18,19]

Catalysis is defined homogeneous when the catalyst reacts in the same phase of reactants: it is more efficient, but the recovery of the catalyst, soluble in organic phase, can be very difficult. Some improvements have been achieved by catalyst immobilization using solid supports,[20] or by using biphasic systems,[21] where organic reactants stay in the organic phase, while the catalyst remains in the aqueous one: under high stirring, reaction occurs at the liquid-liquid interface,[22] without transfer of the species in the other phase.

Considerations about the toxicity of metal catalysts should always be done.[23] Leaching of metals can cause a spread of metal ions or nanoparticles (very difficult to separate from solvents, products or by-products) in the environment, some of them even in bioavailable forms. Moreover, relative abundance of the metals used must be evaluated. Many benefits can derive by the study and effective use of abundant "light" metals as iron, nickel, cobalt or copper, that are much less expensive (i. e. $Pd(OAc)_2$ $75/gram, while $Ni(OAc)_2$ $10/gram), more available and usually less impactive on health or environment than rare precious metals as palladium, platinum, rhodium and ruthenium. However, a very less toxicity of lighter metals should not always be taken for granted, since it depends on bioavailability of the species formed and released.

In 2021, David W.C. Mc Millan won a Nobel prize for Chemistry for the development of asymmetric organo-catalysis. Natural and non-hazardous no-metal organocatalysts[20,24] can bring advantages from both a toxicological and economic point of view. Among them, biological organocatalysts have been developed, widely more accessible than enzymes, that can operate in aqueous media and enable the access to new transformations.[25] Efforts have been done to enhance activity and efficiency of non-metal catalysts, but challenges like the necessity of high loading and the difficulty to recycle the catalyst remain.[24,26]

Heterogeneous catalysis happens at the surface of the solid catalyst that promotes the reaction in gaseous or liquid environments:[27] heterogeneous catalysts are usually more stable and easier to purify. If mineral and Lewis acids are among the biggest causes of waste production, solid acids or bases can be exploited as good heterogeneous catalysts, as porous silica-supported Bronsted acids efficiently used for different transformations by modification with different metal catalysts.[28]

Biocatalysis affords a lot of benefits at environmental and economic level,[29] and now finds a very large application in the production of APIs.[30,31] Catalyst is usually an unmodified or recombinant enzyme, generally non-toxic, biodegradable and biocompatible.[29] Enzymatic reactions can be carried on in very mild conditions, at physiological pH in water at ambient temperature and pressure, avoiding the use of metallic catalysts. Their selectivity also allows to perform reactions on complex molecules with different functional groups avoiding protection/deprotection steps. Thanks to the improvement in DNA technology and protein engineering, enzymes can be designed for specific chemical processes,[32] isolated or even in cellular environment.

1.2.2 Atom economy and mass green metrics

Ideally, a synthetic process should be designed to maximise the incorporation of all materials used in the process in the products, namely economic in atoms. Atom economy is the ratio between the molecular weight of the products and the molecular weight of the starting materials:[33] the highest degree is obviously obtained when all the atoms in the reactants are finally included in the products, possible by combining a maximum of two or three building blocks, while the other reactants are catalytic.

$$\text{Atom Economy (AE) (\%)} = \frac{\text{mol wt. of product}}{\text{mol wt of reactants}} \text{ X } 100$$

Certain chemical bond-forming and breaking are intrinsically atom economic: olefin methatesis,[12] which is the carbon-carbon atom economic reaction for excellence, rearrangement reactions (i. e. Claisen,[34] Cope,[35] Curtius[36] rearrangements), coupling reactions (i. e. Suzuki-Miyaura cross-coupling),[37] ring contraction/expansion reactions (i. e. Buchner reaction),[38] cycloadditions (i.e. Diels-Alder reaction),[39] or aromatization reactions (i. e. Biginelli's reaction).[40]

Atom economy can give a rapid prediction of the waste that will be generated in a single step, without experimentation, but it is just a theoretical value; even when an experimental atom economy value is calculated, it only considers reactants.

Instead, the E-factor can be applied to multi-step processes: it assures a holistic assessment of an entire process expressing the actual amount of waste produced,[41] with a value given by the ratio between the total amount of waste produced and the actual yield.

$$\text{E-factor (E) (kg)} = \frac{\text{total mass of waste}}{\text{mass of products}}$$

The ideal E-factor value is zero, while a high value indicates a high impact on the environment. Initially, water was not considered in the E-factor value calculation, with the risk of an underestimation of the real total amount of waste produced. The actual E-factor value falls between simple E-factor (sEF), that takes count of all the materials excluded solvents and water, and complete E-factor (cEF), that considers all process materials, water included, in case they are not recycled, more appropriate especially for that processes that suffer the most for solvent loss, as the manufacturing of APIs.

Other mass metrics can be considered (Table 1), as Reaction Mass Efficiency (RME),[42] Mass Productivity (MP), Effective Mass Yield (EMY), and Carbon Economy (CE),[42] related to Atom Economy (AE) and expressed in percentage, and the ones based ok kg/kg ratio, as well as the E-factor, as Mass Intensity (MI),[42] Process Mass Intensity (PMI),[43] Waste Water Intensity (WWI), and Solvent Intensity (SI).

Table 1. Mass green metrics.

Atom Economy (AE) (%)	
Reaction Mass Efficiency (RME)	$\dfrac{\text{mass of product}}{\text{total mass of reactants}} \times 100$
Mass Productivity (MP)	$\dfrac{\text{mass of product}}{\text{total mass (+ solvents)}} \times 100$
Effective Mass Yield (EMY)	$\dfrac{\text{mass of}}{\text{mass of hazardous reactants}} \times 100$
Carbon Economy (CE)	$\dfrac{\text{carbons in product}}{\text{carbons in reactants}} \times 100$
E-Factor (E) (kg/kg)	
Mass Intensity (MI)	$\dfrac{\text{total mass of waste}}{\text{mass of reactants}}$
Process Mass Intensity (PMI)	$\dfrac{\text{total mass in process (+ H}_2\text{O)}}{\text{mass of reactants}}$
Waste Water Intensity (WWI)	$\dfrac{\text{total mass of water}}{\text{mass of reactants}}$
Solvent Intensity (SI)	$\dfrac{\text{total mass of solvent}}{\text{mass of reactants}}$

1.3 Solvents

To improve the safety of the processes, synthetic routes that avoid or limit the use of toxic chemicals should be preferred and final chemicals must be designed to be less toxic as possible and to decompose in harmless products without persistence in the environment at the end of their life. The elimination or the substitution of toxic solvents with alternatives with lower or no toxicity is highly recommended.

Even the use of auxiliary solvents and reagents should be avoided, when it is possible, or they should be substituted with less toxic materials. Unnecessary derivatization processes should be minimized since they need the use of ulterior reagents and solvents and cause a bigger production of waste.

1.3.1 Solvent guides

Conventional toxic solvents, that have potential for greater exposure because of their volatility, often exceed the quantity of raw materials, reagents and products in many chemical reactions.[44] A large quantity of solvent is often necessary for a reaction to proceed, since solvation guarantees major advantages as selectivity, control, safety and better handling, and also to obtain clean products by extractions or purifications (auxiliary solvents).

In 2007 it was estimated that 80-90% of the non-aqueous materials to produce APIs was represented by organic solvents,[45] and in 2011 it was reported that organic solvents counted the 56% of all the materials used in APIs manufacture.[46] Only the 28% of solvents is recovered, measure that would reduce the necessity of use virgin solvent and the production of waste at the same time.

For many years costs and availability of "greener" solvents, consistency of purity, lack of guidance and environmental studies made industries reluctant to the adoption of new solvents; then it became clear that the replacement and/or minimization of use of toxic solvents was necessary:[47] this led many pharmaceutical industries to the development of solvent guides, based on scores and colour highlights. AstraZeneca categorized 46 solvents using environmental, health and safety (EHS) indicators.[48] From 1999 to 2016 GlaxoSmithKline (GSK) published and expanded the first solvent guide, assigning a score for every solvent in four main categories (divided in sub-categories):[49] waste disposal, environment, health and safety. Pfizer divided the solvents in "preferred", "usable" and "undesirable" highlighted in green, orange and red respectively,[50] while Sanofi classified 96 solvents in "recommended", "substitution advisable", "substitution request" and "banned" labelled with green, amber, red and brown.[51]

A survey of all the solvent guides, mostly in large agreement, that switched 51 solvents in four categories (Figure 3), "recommended", "problematic", "hazardous" and "highly hazardous" was published.[52] 17 solvents could not be ranked, but they remained borderline because of the disagreement about them between the different companies.

Recommended	Water, EtOH, *i*-PrOH,*n*-BuOH, AcOEt, *i*-PrOAc, *n*-BuOAc, anisole, sulfolane
Recommended or problematic?	MeOH, *t*-BuOH, Benzyl alcohol, ethylene glycol, acetone, MEK, MIBK, cyclohexanone, MeOAc, AcOH, Ac$_2$O
Problematic	Me-THF, heptane, Me-cyclohexane, toluene, xylenes, chlorobenzene, acetonitrile, DMPU, DMSO
Problematic or hazardous?	MTBE, THF, cyclohexane, DCM, formic acid, pyridine
Hazardous	Diisopropyl ether, 1,4-dioxane, DME, pentane, hexane, DMAc, NMP, methoxy-ethanol, TEA
Higly hazardous	Diethyl ether, benzene, chloroform, CCl$_4$ DCE, nitromethane

Figure 3. Survey of all industries' solvent guides.[52]

Starting from this, ACS Green Chemistry Institute's Pharmaceutical Round Table consortium and the European collaborative research project CHEM21 developed a solvent guide that is not limited to a ranking, but that also takes consideration of EHS criteria and that includes also the 17 borderline solvents with the addition of newer solvents, as bio-derived ones.[53]

Among the classic solvents, water, alcohols, ketones and esters resulted the best choices; hydrocarbons, chlorinated hydrocarbons, as dichloromethane (DCM), and ethers are classified as hazardous or highly hazardous because of their toxicity and/or flammability issues. Less hazardous ethers as ethyl-tert-butyl ether (ETBE), cyclopentyl methyl ether (CPME), tert-amyl-methyl ether (TAME), dimethyl isosorbide and 2-methyl tetrahydrofuran (Me-THF) are considered greener.

Polar aprotic solvents are usually considered fundamental for important reaction as nucleophilic substitutions. Acetonitrile is one of the less problematic, while dimethyl sulfoxide (DMSO) is considered problematic for his stability/safety issues at high temperatures and dimethylformamide (DMF), N-methyl pyrrolidone (NMP) and dimethylacetamide (DMAC) are classified as substances of very high concern. Minimizing or avoiding the use of these solvents, by choosing more sustainable and safer ones, has become a very important goal.

1.3.2 Alternative solvents

1.3.2.1 Ionic liquids (ILs) and deep eutectic solvents (DESs)

Ionic liquids (ILs) are organic salts differently designed by mixing and matching cations and anions to obtain specific characteristics as thermal stability, low volatility (that decreases their inhalation and toxicity), high polarity, strong solubility and relatively high conductibility.[54] They can be an interesting alternative to volatile organic solvents in chemical synthesis and catalysis, sometimes going beyond the role of solvents and acting as reagents or catalysts themselves.[55] ILs are not easily available and have to be synthesized, so they are not intrinsically green. Since all ionic liquids are different from the others depending on their composition, toxicity must be evaluated case by case.[44] Thanks to their tunable and physicochemical biological properties, ionic liquids now find many different applications as drug delivery systems,[56] enhancing bioavailability and pharmacokinetic and pharmacodynamic profile of drugs, and a series of novel-active pharmaceutical ingredient-ionic liquids (API-ILs) have been developed with antibiotic,[57,58] antifungal,[59] antitumoral[60] and other different activities.

Deep eutectic solvents (DESs) are prepared mixing two (or three) solid reagents (sometimes with a little amount of water), Bronsted or Lewis acid or bases to obtain a liquid product with a lower melting point compared to the individual components.[61] They contain at least one hydrogen-bond acceptor (HBAs, *e. g.* choline chloride) and one hydrogen-bond donor (HBDs, *e. g.* urea), that interact with hydrogens bonds decreasing the lattice energy of the system, and sometimes metal or hydrated metal salts. DESs mostly derive from renewable sources or can be prepared in a green way, by mechanochemistry technology, and present low or no-toxicity. Among all the chemical process, DESs are excellent solvents for organometallic synthesis, allowing to effectively exploit organolithium reagents under non-inert atmosphere,[62] and metal-catalysed reactions as Pd-catalysed couplings as Suzuki-Miyaura, effective even for synthesis of APIs as Felbinac and Diflunisal, Heck and Sonogashira,[63] or Ullman type reactions[64] and copper C-N bond formation reactions and click chemistry protocols. DESs also find a large application in enzymatic catalysis.

1.3.2.2 CO$_2$ tunable solvents, expanded liquids and switchable solvents

Subcritical and supercritical fluids, as gas expanded fluids, are very attractive in Green Chemistry field.

Supercritical CO_2 (sCO_2) is non-toxic, non-flammable, non-explosive, natural, abundantly available and cheap. With its low polarity, it can represent a promising alternative to organic solvents. It can be separated by the products without leaving traces only by pressure release, without necessity of any distillation. sCO_2 is largely used for extractions, mostly in the food, beverage, flavours and cosmetics production.[65] sCO_2 is very miscible with gases, as H_2, so it was successfully used in hydrogenation reactions. The use of sCO_2 can improve the reaction rate of olefin hydrogenation compared with usual organic solvents, and in some cases its use combined with different catalytic complexes resulted very effective and superior to organic solvents in the stereoselective hydrogenation of prochiral olefins for the obtainment of enantiomerically pure compounds,[66] and of chiral amines from imines[67] or chiral alcohols from ketones.[68]

CO_2 can also be dissolved in organic solvents to produce carbon dioxide expanded liquids (CXLs),[69] divided in three classes, I, II, III based on the volumetric amount of the expansion. Expanded liquids have intermediate properties between organic solvents and super critical fluids (SCFs) and are particularly useful for catalysed reactions in presence of gas reagents, as hydrogenations or hydroformylation[70] in mild conditions, mostly due to the high solubility of gases, with a less quantity of solvent needed. As SCFs, they are very interesting alternatives as solvents for biomass-based extractions.

Switchable solvents can exist in two states with distinct properties and the capability to switch from one to the other under specific conditions of heat, light or pH.[69] Switchable solvents are divided in three classes: switchable polar solvents (SPSs) and switchable hydrophobicity solvents (SHSs), which undergo under polarity switches upon CO_2 addition, and switchable water (SW)[71] that undergoes under ionic strength changes. One of the most representative switchable solvent is piperylene sulfone,[72] a DMSO mimic liquid synthesized from *trans*-piperylene and SO_2, useful for reactions carried out at temperatures between room temperature, in which it is liquid, and 100 °C, above which it collapses in the two gaseous starting materials. This is particularly interesting for solvent recycle, since after the reaction it can be recovered in two steps by firstly heating the mixture above 100 °C to decompose the solvent and then, after removing the products, by lowering the temperature to reconstitute the liquid solvent.

1.3.2.3 Solvents derived from cellulose and starch

Cellulose and starch are readily available from renewable sources since they are the major components of biomasses. Their chemical or enzymatical hydrolysis produce glucose, the starting material for the synthesis of products as solvents that can be used as alternatives to polar aprotic ones. With its low water miscibility, higher stability, lower volatility ad toxicity, 2-methyl THF (2-MeTHF) is considered a renewable substitute to THF, approved for use in pharmaceutical processes.[73] Despite it derives from renewable sources, its flammability led to label it as problematic in CHEM21 solvent guide.

γ-valerolactone (GVL) is a green, biodegradable alternative for dipolar aprotic solvent. GVL is easily prepared from highly abundant lignocellulosic biomass in a multi-step process that involves the hydrolysis of cellulose and levulinic acid (LA) hydrogenation-cyclization to GVL[74] following two different pathways, using both noble and not-noble metal catalysis, and exploiting H_2 or hydrogen donors, even in aqueous medium.[75] Furthermore, it can also be obtained by one pot dehydration of fructose to LA and formic acid and subsequent hydrogenation of LA to GVL.[76] GVL has a high boiling point (207°C) and dielectric constant of 36.5, similar to dipolar aprotic solvents, and is completely miscible in water, less toxic and biodegradable. GVL is a very good alternative for C-H activation reactions,[77,78] C-C bond [79] or C-N bond formation, exploited for the synthesis as APIs as fedratinib and abemaciclib, with better results compared with classical dipolar solvents.[80]

1.3.2.4 Water and biphasic aqueous systems

The problem of using organic solvents is not only related to their volatility or toxicity but some issues can also be found in their containment, recover and rapid removal from the product and reuse.

The best solvent is no-solvent, but in case it is necessary, water represents the best alternative, since it is non-toxic, non-flammable, abundantly available and cheap.[81] Water possesses a series of optimal characteristics as high electric constant and high heating capacity, that make it a very good medium for the activation of exothermic reactions. Water also owns the capability to form hydrogen bonds and shows an hydrophobic effect, modulable by salting in or salting-out effects: hydrophobic effects accelerate organic reactions between poorly water-soluble compounds, as well as for Diels-Alder transformation,[82] while they can promote even better chemo-and regioselectivity. Water can also provide the so called "on-water effect",[83]

accelerating the reaction of suspended organic reactants, sometimes with the auxilium of only a minimal amount of water non-soluble solvents.

Despite all its good qualities, the limited use of water is often determined by the scarce solubility of the organic reactants.[84] Nonetheless, reaction products are often scarcely soluble in water, so they can be recovered just by phase separation, avoiding the conventional extraction operations. Moreover, biologically active molecules as protein, carbohydrates and nucleic acids, drugs and alkaloids, as well as bio-mass based chemical feedstocks, are soluble in water, while they need to be modified to increase their solubility in organic solvents, ususally disproportionally used for their synthesis: exploration of novel chemical reactions to undercover new reactivities and biocatalysis, or a proper synthesis design, could solve the problem of protection/deprotection steps or allow the exploitation of more naturally abundant feedstocks.

As aforementioned, aqueous biphasic systems can be exploited both for solubilization of water-immiscible reactants and for the recycle of catalysts by phase separation.[21] Organic phase with reactants can be just separated, while the aqueous one can be left in the reactor for another cycle and be reused together with the catalyst, limiting the amount of water necessary. Horkheimer/Rhône Poulenc is one of the most famous processes that exploits a water-soluble Rhodium (I) in biphasic complex of trisulfonated triphenylphosphine (tppts) for the aqueous alkene hydroformylation in large scale at industrial level.[85]

Supercritical water can also be an excellent solvent for non-polar reactions:[86] in fact, it possesses interesting opposite properties to "regular" water at room temperature, as low dielectric constant or low polarity, that make it behave more like an organic solvent. Moreover, it has contemporary properties of strong acid or base, due to the increased dissociation in H^+ and OH^-, making it possible the conduction of reaction in neutral conditions, avoiding the use of strong acids and bases and preventing waste production.

1.3.2.5 Surfactants in water and micellar catalysis

The use of surfactants under micellar conditions is very effective to perform catalytic reactions in water.[87]

Surfactants are amphiphilic molecules composed by a hydrophilic group (head) and a hydrophobic portion (tail). Driven by hydrophobic forces, surfactants spontaneously aggregate in micelles in water, when they reach the typical critical micellar concentration (CMC) of 10^{-3}-10^{-4} M.[88] Assemblies are usually formed by 50-100 monomers in a

thermodynamic equilibrium where monomers rapidly exchange between aggregates. The hydrophilic heads exposed outside ensures the solubility in water, creating a polar external surface, around which water molecules have a different behaviour than in the rest of the bulk;[87] the hydrophobic tails orient themselves inside of the aggregate in a core, shielded from the aqueous environment, were the contact between water-insoluble reactants and catalyst occurs (Figure 4).
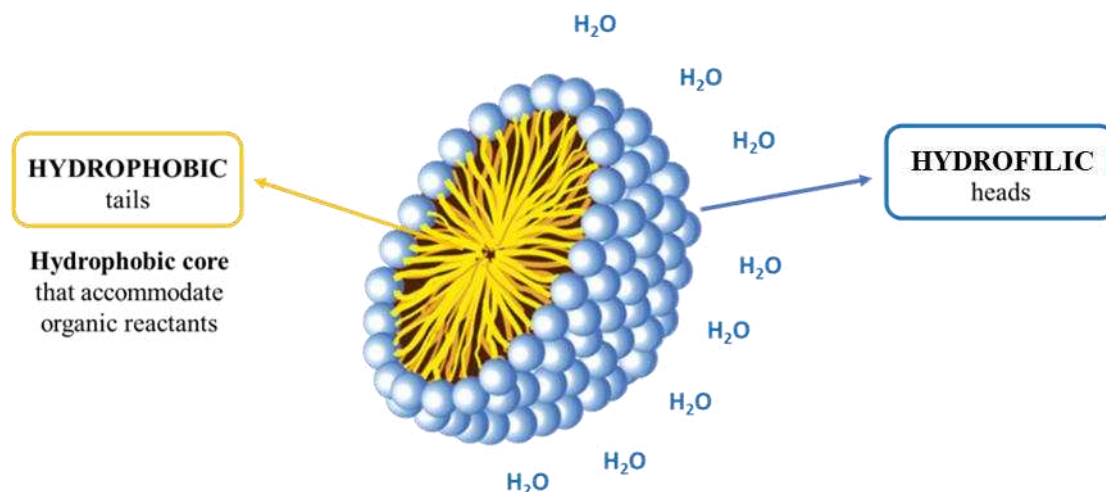

Figure 4. Micelle's structure.

Micelles play a doble role: they are fundamental for the solubilization of organic compounds in water, but they also act as small nanoreactors,[89,90] favouring the accommodation and compartmentalization of the hydrophobic reagents in their core. A limited amount of reactants can be loaded, but since solubilization occurs mostly inside micelles, the concentration of the organic substrates in contact with catalyst in the lipidic core is higher than in the rest of the solution and reactivity is enhanced.[87] High selectivity obtained working with micelles also compensates the disadvantage of working in diluted conditions.

Surfactant can be divided in cationic, anionic, non-ionic, zwitterionic and gemini.[91] The choice of the surfactant is crucial, as well as the choice of the solvent, for the success of a reaction, since it determines lipophilicity, size and shape of the aggregates. The molecular structure of micelles depends on several variables, as the molecular structure and the balance between hydrophilic and hydrophobic portions, the molecule geometry and the experimental conditions of pH, temperature and ionic strength.[92] Concentration plays a very important role: aggregates are initially spherical, but an increased concentration provides the formation of micelles of different shapes or can lead to a change of polarity.

Ionic surfactants

Charged surfactants, as the cationic hexadecyltrimethylammonium bromide (CTAB) and the anionic sodium dodecyl sulfate (SDS), can act like ligands or nucleophiles because of their charges, giving side-reactions problems.[93]

Cationic micelles are less attractive, since the anionic counter ion can coordinate metal catalysts, causing the loss of their activity. Nonetheless, the affinity toward negatively charged reagents and special space confinement confer unique properties, useful for some kind of reactions: Mn-catalyst functionalized with long aliphatic chains can be confined in CTAB micelles and shows a high catalytic activity for the enantioselective epoxidation of alkenes.[94] Cationic surfactants find more interest in non-catalysed reactions, i.e. *C*-arylarylations, for which CTAB can be optimal over non-ionic surfactants.[95]

On the other hand, in SDS environment, water non-soluble reagents are "trapped" in the core, while the polar heads efficiently interact with positive charged catalysts based, for example, charged species of copper[96] or iron.[97]

Anionic surfactants can play a role in the stabilization of silver nanoparticles.[98] They are also compatible with biocatalysts at low concentration, but the denaturation of enzymes probably occurs at higher concentrations; in fact, H_2O/surfactant ratio plays a fundamental role in the enzymatic activity.[99]

PEG-based non-ionic surfactants

Ionic micelles' limits can be overcome using more stable non-ionic surfactants, that are definitely more exploited for organic metal-catalysed transformations.

Lipshutz and co-workers developed efficient, "benign by design" green non-ionic amphiphiles (Figure 5), broadly employed by industry and academia for a large amount of transformations: polyhoxyehanyl-α-tocopherol succinate (TPGS-750-M),[100] derived from polyhoxyehanyl-α-tocopherol sebacate (PTS)[101] and based on racemic vitamin E, and the more recent β-sitosterol methoxypolyethyleneglycol succinate (SPGS-550-M).[102]
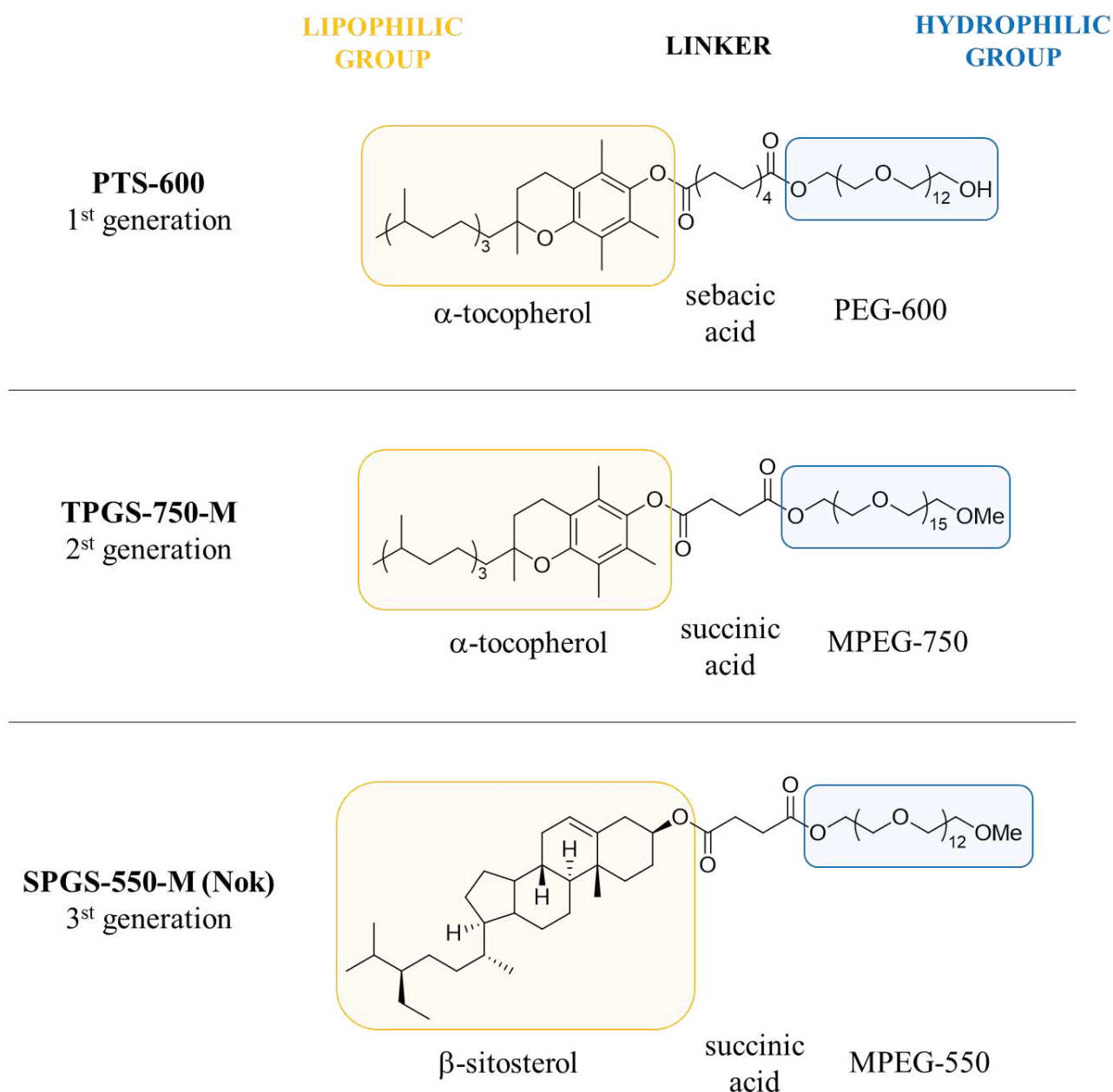
Figure 5. Structures of PTS (1st generation), TPGS-750-M (2nd generation), and SPGS-550-M (3rd generation).

Micelles have typically diameters between 15 and 100 nm: 50-60 nm is the optimal diameter to perform catalytic transformations, since it allows the accommodation of the reactants to effectively perform different kind of metal catalysed transformations, still leaving enough "grease" between different micelles. The formation of too big micelles determines the presence of heterogeneous mixtures.[93] Polyethylene glycol (PEG) and methyl polyethylene glycol (MPEG), that constitute the hydrophilic heads, influence the size of micelles, since longer chains determine the formation of micelles of smaller diameter. PEG also have a "nano-nano effect", absent in organic solvents, stabilizing heterogenous nanometal catalysts

acting as a ligand and allowing the leading of heterogenous catalysed reactions in water in mild conditions.[103]

PTS (Figure 5,) is composed by racemic vitamin E as lipophilic part, sebacic acid as linker and PEG600 or PEG1000 as hydrophilic portion. Different reactions involving Pd catalysts, as Buchwald-Hartwig amination,[104] Suzuki-Miyaura[105] or Heck coupling,[106] and Ru catalysed olefin cross-metathesis[107] can be successfully performed in micellar environment in presence of PTS.

Taking inspiration also from the commercially available and cheaper TPGS-1000, PTS was modified to obtain TPGS-750-M (Figure 5), by substitution of sebacic linker with cheaper succinic one and the use of a methylated PEG as hydrophilic portion:[100] the aim was the maintenance of the chemical versatility of PTS, tuning the hydrophilic-lipophilic balance (HLB) of TPGS-1000 by balancing the length of PEG chains. HLB is an important property that determines the affinity of the surfactant for water or hydrophobic phase, influencing the shape and size of micelles. HLB > 10 determines a major affinity to water, while HLB < 10 determines the opposite. Non-ionic solvents have an HLB value between 0 and 20: TPGS surfactants are more balanced in the hydrophilic portion and have a major affinity for aqueous environment, due to their higher HLB value of 13 compared with an HLB of 10 of PTS.

Longer PEG chains decrease the size of micelles. Dynamic light scattering (DLS) experiments confirmed that TPGS-750-M aggregates in bigger micelles of 53 nm compared both to PTS-PEG600 (24 nm)[101] and TPGS-1000 (13 nm) and provides mostly spherical particles, as it can be seen by Cryo-TEM analysis. Larger nanoparticles offer good or better-quality cross-coupling compared to PTS. TPGS-750-M micelles can accommodate different types of Ru and Pd-catalysed reaction; different couplings in water at room temperature were performed comparing the results obtained with these different surfactants: TPGS-750-M demonstrated to be a superior choice in terms of reaction yields, economics of preparation and purity.

Many kinds of metal catalysed reactions can be performed in water with the auxilium of TPGS-750-M, as olefin metathesis,[108,109] Suzuki-Miyaura couplings,[110–112] Buchwald-Hartwig aminations,[113,114] Ullman-type reaction,[115] Fe/Pd nanoparticles (NPs) nitro-reduction[116] and S_NAr,[117] as well as other important reactions as amidation[118] or click chemistry reactions.[109] The possibility to achieve excellent results in gram-scale[119] makes micellar catalysis with TPGS-750-M in water a valid alternative to organic solvents for an industrial use, as for APIs synthesis.[115] Lipshutz and co-workers proposed protocols for the complete synthesis of various APIs in micellar catalysis. Two different synthetic pathways were design, that almost exploit reactions in micellar media and that differ for the sequence Suzuki-Myiaura coupling-

amide bond formation, that lead to the obtainment of the antitumoral compound Sonidegib (Odomzo)[120] in more than 80% yield and with an E-factor six time lower compared with the original route. The antitumoral Lapatinib can be synthesised in five steps:[121] while the old synthesis was carried out only in organic solvents, in this case only the last two steps are not performed in micellar environment for matter of solubility, but in biomass derived ethanol. Two different pathways, a linear and a convergent one, were proposed for the synthesis of the antimalarial compound Pyronidarine starting with CuI catalysed Ullman-type reaction, both atomi economically attractive and with a low environmental impact.[122] Lipshutz and co-workers' synthetic route for the synthesis of Tezacaftor, used for the treatment of cystic fibrosis, is not only interesting for the reduction of steps number, from the original six ones performed in organic solvents to the four performed in micellar medium:[123] moreover, one step for the formation of an indole intermediate, performed in micellar catalysis in presence of ppm quantity of Au as catalyst, provides the desired compound in a 93% yield (compared to 30% of the original procedure). The total yield of the process was increased four times, with a reduction of the E-factor value. Finally, a one-pot three steps (Suzuki-Miyaura cross coupling, nitro reduction and Shotten Bauman reaction) procedure for the synthesis of intermediate Boscalid in TPGS-750-M, in presence of only little amount of organic co-solvent, was developed, with visible improvement compared to classic procedure.[124]

Moreover, TPGS-750-M can find application in biocatalysis[125] and, very interestingly, in the synthesis of DNA-encoded libraries (DELs).[126]

SPGS-550-M (Figure 5), or Nok, was designed as third generation surfactant to reduce the cost of the amphiphiles.[102] Racemic vitamin E is substituted with less expensive β-sitosterol, a phytosterol mimic of cholesterol, that is combined with succinate as spacer and MPEG-550. This surfactant was designed to form micelles with 45-60 nm of diameter, similar to TPGS-750-M: DLS studies showed a diameter of 46 nm at a concentration of 2% of Nok in water, overlapping with TPGS-750-M, while characterization via Cryo-TEM images showed an intricate array of worm-like micelles, instead of spherical ones. Once again, different reactions with Nok, in comparison with TPGS-750-M, were performed: in most cases Nok gave similar or better results, demonstrating to be a good alternative for effective micellar catalysis in water.

Both TPGS-750-M and Nok are synthesized in two steps, in >10g scale in almost quantitative yields. After the reaction (metathesis close ring was selected as example), products can be extracted with little amounts of organic solvents (i. e. ethyl acetate) and, after the addition of new reactants, surfactants can be reused respectively eight and six times.

The success of micellar catalysis and PEG non-ionic surfactant is depicted by the large synthesis of new surfactants inspired by TPGS-750-M and modified to perform a wide range of catalysed reactions[127] as TPG lite,[128] Coolade,[129] designed to avoid the tendence of foaming, rosin-based amphiphiles DAPGS-750-M[130] and APGS-550-M,[131] Fi-750-M[132] (or PS-750-M) and MC-1,[133] designed to form micelles with slightly "polar" core, BTB-750-M and PiNap-750-M.[134]

Biosurfactants

Most surfactants derive from petroleum stocks, while neutral bio-surfactants, based on neutral lipids, glycolipids, lipopeptides, phospholipids and fatty acids, are synthesized through yeast, bacteria, and plant transformation.[87] Bio-surfactants are intrinsically biodegradable and biocompatible, with self-assembling properties, and they could find different applications in the environment, food, cosmetics and medicines fields.[135] They still do not find these applications, but a future employment as eco-friendly reaction media is advisable.

1.4 Microwave-assisted reactions

One of the purposes of Green chemistry is the improvement of energy efficiency, possible by developing techniques that guarantee efficient reactions in milder condition and in shorter times, especially useful at industrial level, where the energy demand of large scale synthesis has an high cost.[5] Sonochemistry, electrochemistry, photochemistry and microwave irradiation are unconventional energy delivery systems very attractive to reach this goal.

Microwaves (MWs) are electromagnetic waves with a frequency between 0.3 and 300 GHz and a wavelength between 1 cm^{-1} and 1 m^{-1}. They are composed of two different fields that move perpendicularly to each other both at the speed of light: a magnetic field and an electric one that is the only one that transfers energy and heat substances (Figure 6).[136,137]
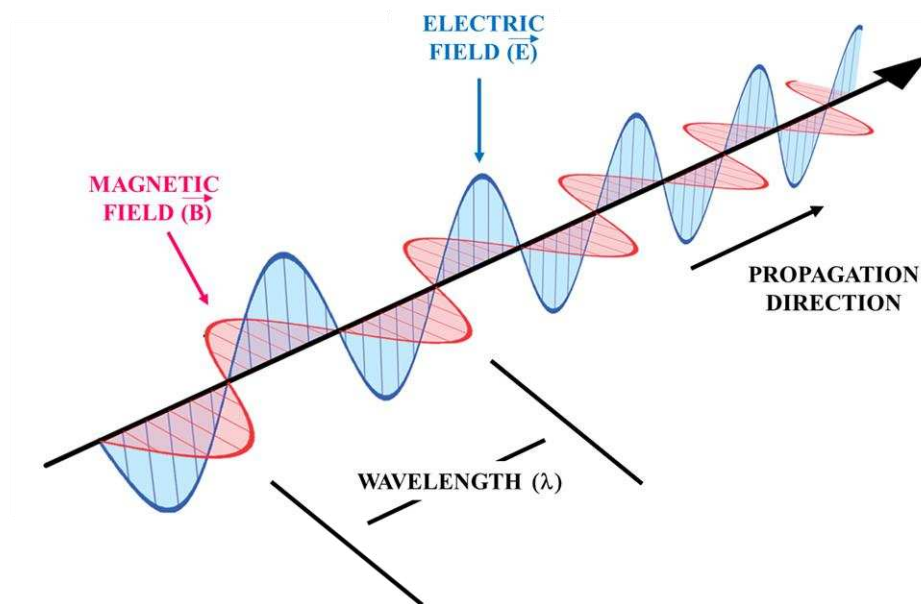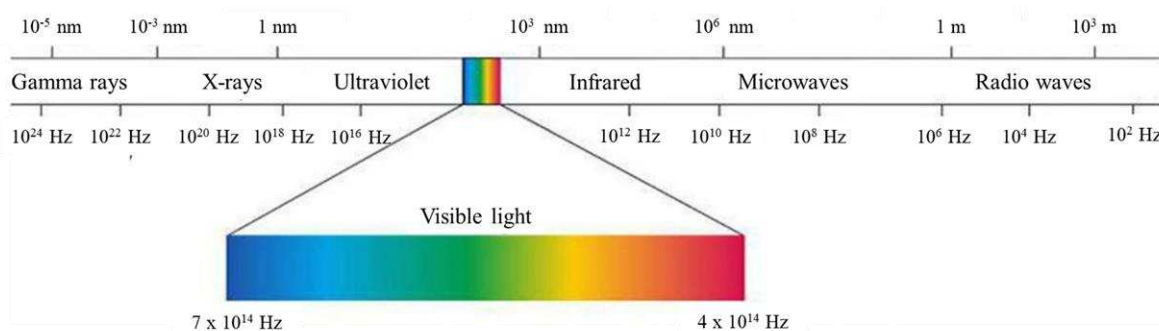
Figure 6. The electromagnetic spectrum and the schematic representation of an electromagnetic wave, where an electric field and a magnetic one spread perpendicularly to each other.[137]

Microwave (MW) technology finds its original great diffusion in '50s and '60s of the past century with the use of home MW oven, while Microwave-Assisted Organic Synthesis (MAOS) and the use of microwaves in laboratories started in the mid '80s.[137]

Initially, MAOS were performed in home MW ovens, with a series of significant limits. Pressure and temperature could not be regulated; heating was not homogenous and hot spots were often formed. Since the use of refrigerants was impossible, the use of organic solvents that could boil or evaporate, giving raise to flames or explosions, was forbidden. The impossibility to control the reaction parameters also determined a lack of reproducibility. Moreover, only open-vessel reactions could be performed. Finally, in the late '90s different companies started to develop MW oven that work in a single mode, specifically designed for small-scale MAOS.

Microwave reactions are performed in cavities operating at a fixed frequency of 2.45 GHz (wavelength of 12.245 cm) established by international agreements: in this condition, the

corresponding quantum of energy of a MW photon is 1 x 10^{-5},[138] many orders of magnitude lower than the energy necessary to induce electronic transition that determines the break of a chemical bond.[136] Only molecular rotation is affected by MWs.

Microwaves provide a dielectric heating effect, due to the contribution of dipole rotation and ionic conduction. The transfer of energy by dipole rotation depends on the fact that the rapid change of electric field determines the alignment of polar molecules (Figure 7). In ionic conduction, electromagnetic waves interact with ions or ionic species providing their oscillation back and forth that promotes a superheating effect and the increase of the temperature.[137] The electric field is responsible for heating: when a dipole tries to reorient itself with respect to an alternating electric field, it loses energy in the form of heating, by molecular friction.
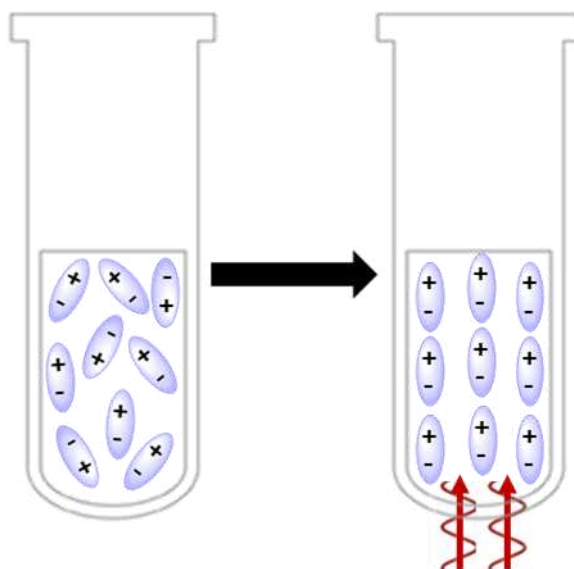

Figure 7. MW dielectring heating.

The dielectric heating is influenced by the solvent used for the reaction.[137,139,140] Solvents are more or less able to absorb microwave energy and transform it into heating fundamental to break bonds and provide products. This ability is determined by their loss tangent value (δ), given by the ratio between the dielectric loss (ε'), the efficiency in converting microwave irradiation into heating, and the dielectric constant of the medium (ε) measured as polarizability of a molecule when hit by an electric field:

$$\tan \delta = \varepsilon' / \varepsilon$$

Highest values of δ correspond to a better capability of the solvent to transform the MWs energy in heating at a certain temperature and frequency. Considering their δ value, solvents can be classified as high (δ > 0.5), medium (0.1 > δ > 0.5), and low (δ < 0.1) microwave absorbing.

Table 2. Tan δ of different solvents.

HIGH (> 0.5)		MEDIUM (0.1-0.5)		LOW (< 0.5)	
Solvent	**tan δ**	**Solvent**	**tan δ**	**Solvent**	**tan δ**
Ethylene glycol	1.350	2-Butanol	0.447	Chloroform	0.091
Ethanol	0.941	Dichlorobenzene	0.280	Acetonitrile	0.062
DMSO	0.825	NMP	0.275	Ethyl acetate	0.059
2-Propanol	0.799	Acetic acid	0.174	Acetone	0.054
Formic acid	0.722	DMF	0.161	THF	0.047
Methanol	0.659	Dichloroethane	0.127	Dichloromethane	0.042
Nitrobenzene	0.589	Water	0.123	Toluene	0.040
1-Butanol	0.571	Chlorobenzene	0.101	*n*-Hexane	0.020

According to the loss tangent δ values, polar organic solvents can absorb microwaves and transform the energy in heating in a very efficient and rapid way. On the other side, non-polar solvents such as toluene and *n*-Hexane are transparent to microwaves and cannot provide good results alone. In that case, it is still possible to have good performances by adding polar additives, as ionic liquids.

Loss tangent is strictly dependent by the temperature and can change during the reaction, so polarity is a more indicative parameter to consider the influence of microwaves on the solvent.

Dielectric heating confers some advantages over conventional conductive heating,[139,140] that exploits convectional thermal sources, basically reflux systems, as oil and sand baths, or heating blocks systems. In conventional mode, heating must firstly penetrate through the walls of reaction container, which temperature results higher than the temperature of the core, then it can reach the solvent and the reactants (Figure 8, left): in this way, the process is slow and scarcely efficient, and it depends on a vigorous stirring to guarantee a homogenous heating. Instead, glass, Teflon or quartz are transparent to MWs, so these are not absorbed but they directly reach the core (Figure 8, right). Dielectric heating selectivity is determined by

the fact that different materials respond differently to MWs and does not depend on the difference upon conductivity of solvents and reactants. These properties allow an instant rise of temperature and a homogenous internal heating, that results in more efficient and faster processes. Reaction can be performed both in open vessel and under pressure.
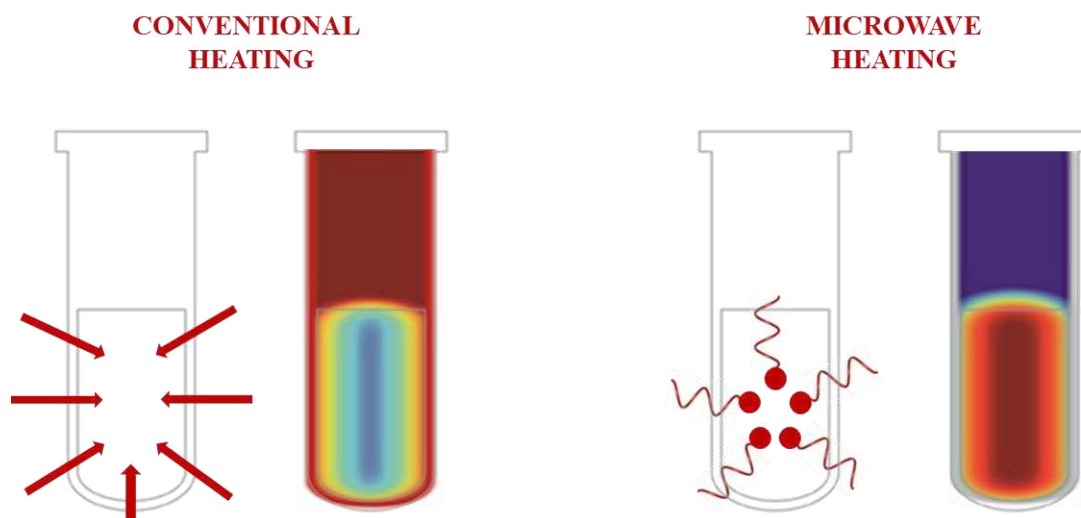

Figure 8. Comparison between conventional (left) and microwave heating (right).

The effect of dielectric heating alone is not sufficient to explain the great enhancement in the efficiency of some reactions. The term "microwave catalysis"[141] was used to underline the improvement of efficiency obtained in microwave assisted olefin-metathesis and a "non-thermal" (or "specific") effect of highly polarization mechanism of microwaves was hypothesized.[142] The debate is still open,[143] but microwave heating can have an influence on the A parameter of the Arrhenius equation or a greater impact due to the capability of reducing the value of the apparent activation energy. In any case, microwave heating incredibly enhances the rates of reactions, that are carried out faster, due to the fact that higher temperatures can be achieved, together with a reduced formation of by-products and easier purifications, translated in better yields. Moreover, MWs guarantee a high reproducibility, due to the uniform heating and a better control of the reaction parameters, as reaction temperature.[144]

An alternative efficient method to perform MAOS is the Enhanced Microwave Synthesis (EMS), that allows the introduction of greater amounts of MWs energy maintaining low temperatures:[144] in these experiments microwave irradiation is performed while the reaction

vessel is simultaneously externally cooled with compressed air. Microwave energy level is high and constant and leads to obtain great yields and cleaner products.

1.4.1 Hot spots

A large amount of homogenous and heterogeneous catalysed reactions,[145] especially Pd-catalysed processes,[146] can be performed with high success under microwaves irradiation. A homogeneous heat is fundamental to avoid the formation of so-called hot spots, zones where temperature is very higher than in the rest of the solution, due to arching phenomena that happen during the irradiation, especially because metal catalysts have a differential heating.[147] The generation of hot spots represents a safety and efficiency problem: in fact, hot spots can create explosive phenomena or cause a loss of materials, and consequently lower reaction yields, due to the less efficiency of catalyst or the degradation of the solvent.

Metals (and organometallic compounds) are very good conductors, so they are sensitive to electric fields and interact with MWs.[147,148] Usually, hot spot formation is higher when heterogenous catalysts are used in combination with low boiling point solvents at high electric fields. Discharge phenomena for both magnetic and diamagnetic metals strictly depend on their particles size: metals can be heated with MWs when present in small particle sizes, while hot spot formation is higher when heterogenous catalyst are in form of aggregates.

Hot-spots formation can have a detrimental impact on the reaction: for example, an excessive formation of hot spots on the surface of activated carbon catalysts has a negative impact on Pd catalysed reactions, as Suzuki-Miyaura couplings.[149,150] Avoiding the formation of hot spot in Pd catalysed reactions is challenging when non-absorbing solvents are used. Sometimes, the use of solvents with higher boiling points can be useful to avoid the formation of hot spots, if they are suitable for the specific reaction: Petricci and coworkers solved the problem of the formation of hot-spot in Pd catalysed formation of benzyl-imidazoles by substitution of toluene with the green GVL.[151]

On the other hand, some reactions, as formation of Grignard reagents, can take advantages from formation of hot spots: discharges generate highly active magnesium particles, but only at low fields.[152,153] Using high field density, discharges are high and produce the decomposition of solvent, resulting in the formation of a layer on the metal surface that deactivates magnesium towards the formation of Grignard reagent.

1.4.2 Microwave-assisted reactions with gas reagents

In 2006, the first example of use of gas reagents under MW dielectric heating was described by the research group in which I worked for my PhD.[154] For this purpose, a Discover CEM monomodal microwave was modified and adapted by modification of the external pressure control system (Figure 9).

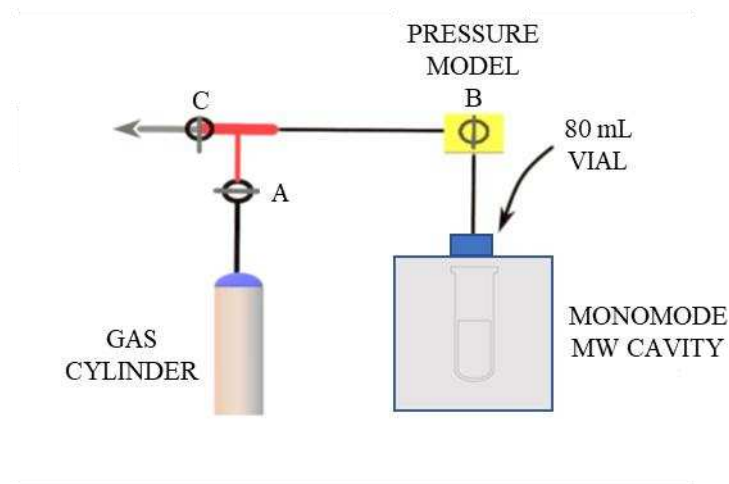**Figure 9.** Monomodal Discover CEM adapted with external pressure control system for MWs assisted reaction in presence of gas reagents.

This modified MW is equipped with an 80 mL vessel glass vial tested to resist up to a pressure of 17 bar (250 psi). The vessel is connected to an external pressure control system equipped with a valve and an exit tube for venting the vial, connected to a cylinder containing the gas necessary for the reaction through a three-way connector equipped with two taps. After the gas is introduced and the necessary pressure is reached, tap B is closed and pressure is maintained stable during all the reaction time; at the end of the reaction, tap C is opened and the gas is released. The regioselective hydroformylation of terminal alkenes was performed with this system using $Rh(CO)H(PPh_3)_3$ and Xantphos in toluene and a ionic liquid, necessary to reach the desired temperature.[154] MW assisted hydroformylation gave excellent results in both regioselectivity and yields in milder conditions of gas pressure (3 bar) and in extremely shorter reaction times (4 min), compared to the same reaction performed in a traditional autoclave. Nonanal was obtained in an 80% yield from 1-octene, and also various olefin substrates were hydroformylated with high regioselectivity. Many different transformations related to hydroformylation were performed with the same system, as hydroaminomethylation,[155] tandem hydroformylation-hydrocondensation[156] and solid

supported hydroformylation. MW irradiation is also an important tool for homogeneous and heterogeneous carbonylation reactions using gaseous CO,[157] starting point for the obtainment of amides, esters or heterocycle compounds.

Other systems have been developed for the microwave-assisted reactions with gaseous reagents, that gave the possibility to perform efficient hydrogenation reactions as Pd-catalysed olefins hydrogenation, triple bond reduction, nitroarene reduction and other processes carried out in few minutes:[158] in comparison with thermal heating, MWs not only accelerated the reaction rate, but also contributed to a better outcome of the reaction in terms of yields. Pd-catalysed hydrogenation of styrene was successfully performed under MW heating and 50 psi of H_2 in 20 minutes thank to a gas addition kit:[159] reaction was carried out in green EtOH/H_2O, using very little amount of Pd-NPs on polystyrene resin, that can also be recycled and used for several times. Cravotto and co-workers reported a very interesting procedure for the microwave-assisted hydrogenation of levulinic acid, precursor of GVL:[160] value added 1,4-pentanediol was selectively provided using two supported gold catalysts, in water or no-solvent conditions, under 50 bar of H_2.

1.4.3 Microwave-assisted reactions in green solvents and micellar catalysis

Microwave assisted reactions have the advantage that can be efficiently performed in absence of any solvent. Reactions between neat reactants can occur when one of them is a MWs absorbent liquid. Under neat condition, a series of reactions that provide biologically active compounds, such as coumarin derivatives[161] and quinolines,[162] in few minutes were developed.

Green solvents have been exploited for microwaves assisted reactions, starting from water,[163,164] exploited for procedure as Suzuki-Miyaura[165] or Sonogashira couplings.[166]

Under microwave assisted conditions, near to critical point, water "switches" to Near Critical Water (NCW) changing its properties and acting more like an organic solvent.[167] When water is heated at 250 °C the dielectric constant drops from 78.5 to 27.5, acting as a strong base or acid due to the increase of the ionic products, very useful condition to perform hydrolysis reactions.

Ionic liquids[168,169] and DESs[170] represent a very interesting alternative to organic solvents, because of their ionic character that confers them the capability to transform microwaves in heating. GVL shows a high stability under MWs irradiation: it was successfully exploited for

Pd catalysed reactions of C-H activation,[171] benzimidazole formation,[151] solid phase peptide synthesis as good substituent of DMF.[172]

Coupling between microwave and micellar catalysis produced interesting results in different kind of transformations and is very exploited in the laboratory where I worked for my PhD. 3% TPGS-750-M was crucial for MW-assisted alkylation of anilines with lipophilic alcohols in water through a Ru-catalysed hydrogen borrowing protocol:[173] microwaves have a crucial role since, in this conditions, Ru based Shvo catalyst turns into Ru NPs-nano micelles combination that acts as effective recyclable catalyst. The protocol can be performed in only water as solvent, or with addition of 2-Me-THF or GVL when necessary, it does not need purification steps and the catalyst can be recycled several times. Also, it is useful for the synthesis of pyrrolo-benzodiazepines (PBD) without use of protecting groups. The same system resulted efficient even for the microwave assisted hydroamination of terminal alkynes in water in presence of a little amount of TPGS-750-M:[174] in presence of Shvo catalyst, Ru nano micelles are formed and this system provides the hydration of terminal alkynes, giving only the Markovnikov product. Moreover, it is the first example of one pot- single step hydroamination of terminal alkynes in presence of equimolar amines and sodium formate. Once again, the catalyst can be recycled several times.

Recently, a fully sustainable process that exploits both micellar catalysis and MW heating for the regioselective hydroformylation of terminal alkenes in water was published.[175] This protocol provides linear aldehydes and hemiacetals in very mild conditions of syngas pressure (9 bar) and temperature (70 °C) in short reaction times (40-60 min) using water as unique solvent. The addition of $NaHCO_3$ and the formation of Bertagnini's salt of the aldehyde that precipitates in the reaction environment consents to recover the pure aldehyde by filtration and treatment with HCl 4N or NaOH 10 N without any further chromatographic purification. Micellar phase, catalyst and ligand can be recovered and reused at least 5 times without impact regioselectivity and yield.

1.4.4 Scale-up and industrial exploitation of MW-assisted reactions

Microwaves technology advantages, as high selectivity and reproducibility, shorter reaction times, easier discover of new chemical reactions and rapid reactions optimization, are exploited even in pharmaceutical industry, especially in medicinal chemistry departments, for small-scale production of small molecules.[176]

Small-scale reactions are not always suitable for an industrial application, so efforts were made to adapt microwave heating to a large-scale production, by using several parallel closed vessels with a total of 1L of capacity, designed Teflon vessels with 350 mL volume or 5L reactors used at temperatures below the solvent boiling point and limited to open vessel reactions. Larger volumes are prohibitive: at 2.45 GHz microwaves penetrates only few centimetres, so dielectric heating can reach only the surface, while in the core heating is conductive. Plus, an increased power output and extra sized cooling systems are required.

An interesting solution is represented by the combination of MWs heating and flow chemistry. Flow reactors represent a valid alternative to batch reactors because of their fast heating and their mass transfer properties.[177] Flow rectors can be applied to both single- and multi-modal microwave ovens and can also be tailor-made designed for specific processes.[137] They can work both in continuous mode, exploitable even to perform combinatorial synthesis, or in stop-flow mode, more efficient in heterogenous catalysis.

1.5 Life cycle assessment (LCA)

Life cycle assessment (LCA) is a broadly applicable "from cradle-to grave" process, that considers all the mass- and energy-flows of the entire "life" of a product, from the acquisition of raw materials, over distribution, to the production of waste, so specifically designed to determine the environmental impact of a whole process.[41]

LCA analysis usually foresees four different stages:[178] i) the definition of the goal and scope, including system boundaries ii) the inventory analysis (LCI), during which all the mass and energy flows are recorded, iii) the impact assessment (LCIA), and, finally, iv) the interpretation of the data.

LCI phase regards the documentation of data concerning energy and materials input (substrates, reagents and solvents-resources extracted from the environment) and output flows (products, waste and emission), within the boundaries outlined, and the data relating to different environmental impact categories for the chemicals exploiting, for example, the LCI database Ecoinvent.[179] These data are the starting point for LCIA: in this phase, determined impact categories, that represent potential environmental consequences, are assigned to mass and energy flows quantified using representative units, i.e. carbon dioxide equivalents, generally following common procedure reported in standard EN ISO 14040 and 14044.[180,181]

Different LCIA methods can be exploited or are in development.[182] A consistent and standardized LCIA method, based on international approvement or agreement, must be

chosen to have reliable results. CML 2002[178] and IMPACT 2002,[183] midpoint oriented, and Eco-indicator99,[184] endpoint oriented, are examples of well-established methods. ReCiPe[185] is one of the most up-date methods, combination of mid-point and end-point, based on 18 impact categories as climate change, human and eco-toxicity, acidification and eutrophication, water, fossil fuel and mineral depletion.

The energy demand of an industrial process naturally contributes to its final environmental impact. The Cumulative Energy Demand (CED),[186] or "primary energy consumption" is a well-established category of LCIA: CED value represents the energy demand of the entire process and is a screening indicator of related environmental impacts as global warming or acidification.

Data collected in the described phases are then processed, and results presented must be consistent and in accordance with initial goal and scope. Results can be reviewed both with a revision of the initial scope and the nature and quality of the data collected.
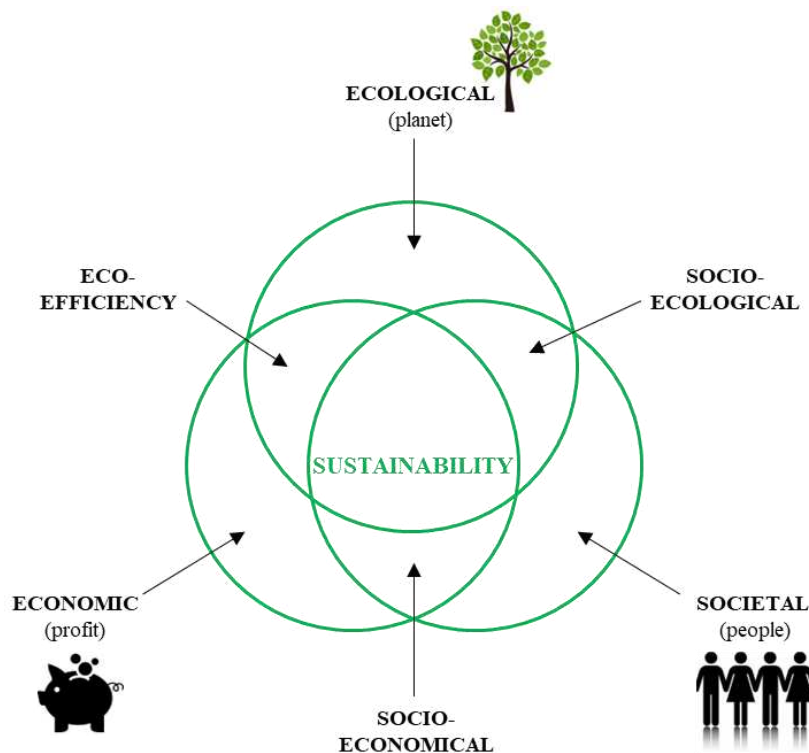
Figure 10. Venn diagram of sustainability.

Sustainability highly depends on the maintenance of the fundamental balance between environmental impact, economic development and social equity, by following three basic sustainability metrics (or indicators):[187] economic, ecological and societal, that can be

29

expressed with the so-called 3Ps, **P**rofit, **P**lanet and **P**eople (Figure 10). "Overlapping" these three parameters, three other hybrid metrics, socio-economic, socio-ecological and eco-efficiency are obtained, that describe the more important aspects of a sustainable process. For this reason, LCA is coupled with other assessing method. For example, Life Cycle Costing is an important tool exploited to measure the impact of a process in economic terms considering the economic dimension of sustainability.[188]

LCA is a fully comprehensive method, with many advantages but it is not specifically design for chemical synthesis. Despite this, a method can be selected, among the high number of different developed approaches, that fits in the best way possible. Especially in a chemical process, the evaluation of risk concerning environment, but also human health and safety, is strictly necessary. The Environmental Safety and Health (ESH) risk assessment method is useful to evaluate the risks of chemical handling and can be coupled with complete or simplified LCA.[178]

LCA is crucial especially in the early stages of the development of new compounds to identify and fix the weak points of the process and to guarantee that they can be avoided in further stages. However, the full analysis can be long and expensive, so sometimes a simplification of the method, without losing achieved standards, could be necessary. One simplification approach is to focus the analysis on the most relevant stages, performing a gate-to-gate analysis of the potential impact caused by particular steps.

1.5.1 LCA of APIs

During the last years, pharmaceutical industry made many efforts to develop "green-by-design" synthetic strategies.[189,190] Despite the long work needed, LCA analysis is determinant to improve the potential toward the development of greener processes in this field. A good improvement can derive by the coupling of LCA with the Process Mass Intensity (PMI), a mass metric (very close to the E-factor and atomic economy) that defines the total mass of input resources per unit mass of step product of API.[43]

In a pharmaceutical production, LCA must consider not only the analysis of the APIs, with attention to the use of solvents, but also an analysis regarding excipients and formulation must be evaluated, also considering the impact of their production process.

GSK developed a software tool for fast LCA of synthetic chemistry processes to be applied especially for APIs, that is now considered a tool for determination, comparison and benchmark assignment for the "greenness" of APIs' production process.[191] This software,

called Fast Cycle Assessment of Synthetic Chemistry (FLASC™), exploits chosen material classes to generate an average LCI profile that can be applied with materials for which LCI does not exist. Using a combination of average and actual data of this LCI and the mass of the material, a cradle-to-gate life cycle impact of a batch chemical process for APIs' synthesis can be predicted. This is particularly useful to select and highly optimise the process from the earlier steps of research and development (R&D) when environmental impact data are still not available. FLASC™ is based on eight sustainability metrics: score between 1 and 5 is assigned to each one. To flag the scores a colour labelling method is exploited, that assigns i) green for a score > 4 (LCA mass and energy impact < 25% of the benchmark), ii) yellow for a score between 4 and 2 and iii) red when the score is < 2 (LCA mass and energy impact > 120% of the benchmark).

Solvents represent the 80-90% of the materials needed to produce APIs. A particular concern is also given by the fact that these solvents can be released in the environment during their life cycle. The Quick Sustainability Assessment via Experimental Solvent Selection (Q-SAvESS) is a methodology that can be exploited for the selection of solvents in the early stages of an API production process.[192] It is a three stages full cradle-to-grave life cycle of ten solvents that i) exploits metrics that reflect the environmental and economic impact of solvents, with a comparison between fossil and renewable biomass feedstocks, ii) collects energy and mass data pertaining the process in which every solvent is used, also considering type and quantity of solvent used to clean machines and finally iii) evaluates the end of use treatment that can consist in its reuse/recycle, distillation (most common) or disposal by incineration.

1.6 Hydroaminomethylation (HAM)

According to the studies of Roughley and co-workers,[193] a quarter of C-N bond-forming reactions in the pharmaceutical industry for the synthesis of commercially successful drugs are performed via reductive amination.[194] However, hydroaminomethylation (HAM) is a one pot-three steps elegant and more environmental benign approach to obtain amines directly from an olefin (Figure 11) in respect of the principles of atom economy and catalysis, superior to reductive amination and other traditional procedures, mostly multi-step and less atom-economic and that provide different by-products.
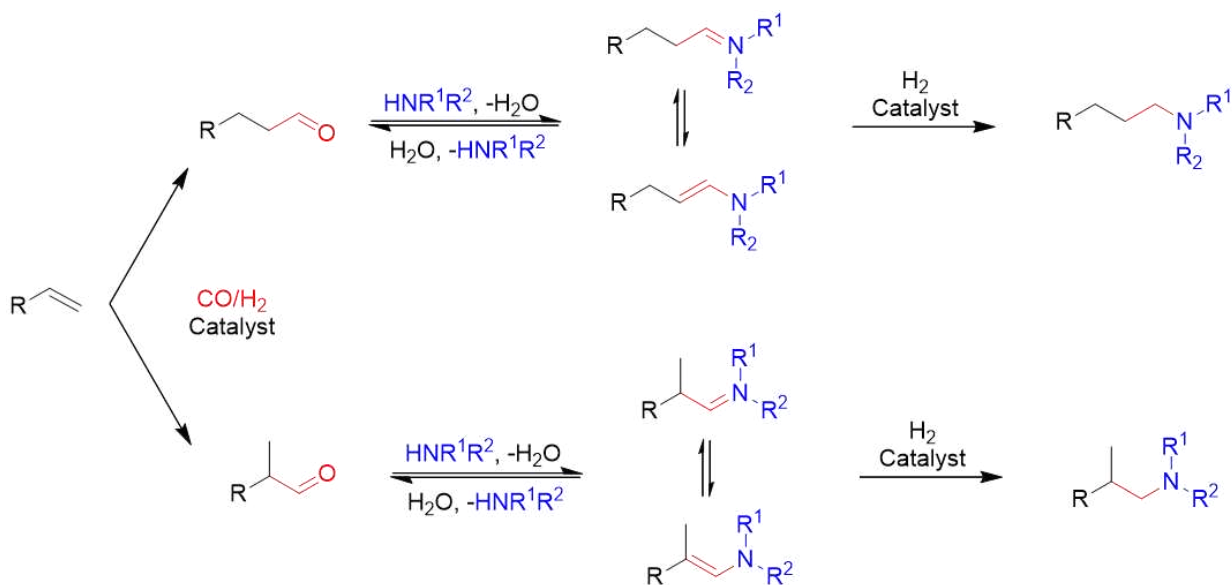
Figure 11. One pot-three steps hydroaminomethylation (HAM) of terminal olefins.

HAM is a one pot-three steps reaction that starts with a first catalysed hydroformylation (HF), the direct functionalization of a double bond by addiction of a mixture of carbon monoxide (CO) and hydrogen (H_2) in presence of a metal (i. e. Rh, Ru, Co, Pt, Fe) catalyst and a ligand, mostly phosphine or phosphite ligands, that leads to the obtainment of linear and branched aldehydes. These compounds then react in situ with a primary or secondary amines already present in the reaction environment to give the correspondent hydroxylamine which provides the corresponding imine or enamine, in equilibrium, by loss of a molecule of water. The last step is the hydrogenation of the imine/enamine, that provides the desired final amine exploiting the H_2 pressure of syngas and, usually, the same catalytic system that also catalyses the first reaction of HF. For this reason, it is important to find a catalytic system adapted for both hydroformylation and hydrogenation steps.

HAM was firstly developed by Reppe and co-workers at BASF.[195] They found that amines could be obtained by reaction of acetylene with carbon monoxide in presence of ammonia and water, a stoichiometric amount of $Fe(CO)_5$ and very hard conditions of temperature (T > 300 °C) and pressure (P > 150 bar). Then, it was demonstrated that HAM reaction could proceed more efficiently with a catalytic amount of Co catalyst and that pressure could be lowered by using $Co_2(CO)_8$ precursor in presence of diphospines.[196]

Rh, Ru and Ir catalysts, in particular their complexes with ligands, resulted to be much better catalysts for the HAM of alkenes. Among them, Rh complexes are the more active and selective catalysts for both hydroformylation and hydrogenation steps.

1.6.1 Rhodium catalysed hydroaminomethylation

Rhodium catalysed HAM was firstly described in 1971, when Iqbal and co-workers used Rh_2O_3 as main catalyst for the HAM of cyclohexene, founding it was a better catalyst compared to $Fe(CO)_5$ previously used by Reppe and co-workers.[197] In fact, the use of Rh catalyst alone afforded amines with higher yields (> 80%) than that obtained with $Fe(CO_5)$ (6%), while the combination of the catalysts provided even an higher yield (>90%), together with a suppression of the formation of by-products. Rh_2O_3 was used as unmodified catalyst, without using any ligand.

Another unmodified catalyst, very used for example by Eilbracht and co-workers, is $[Rh_2(\mu-Cl)_2(COD)_2]$: this is a precursor that under syngas pressure gives raise to the (putative) active specie $[Rh(H)(CO)_3]$ by losing COD (1,5-cycloottadiene) and Cl ligands. This catalyst was used with success in the synthesis of amines in high yields, including biologically active compounds as Difenidol and a Fluspirilene precursors,[197] trimipramine and other analogous compounds,[198] and oxa- and aza-macroeterocycle compounds,[199] valuable intermediates for the synthesis of bioactive compounds.

Use of non-modified Rh catalyst, where CO is the only ligand, is effective, but many efforts have been done to develop more efficient catalysts. Moreover, systems containing only CO ligands determine the formation of both the linear and branched amines.

The introduction of more electron-donating ligands allows the modulation of the coordination sphere of the metal centre and promotes higher rection rates maintaining a high chemoselectivity. Eilbracth and co-workers developed HAM protocols using rhodium salts or combination of a rhodium catalyst and PPh_3 as ligand.[200,201] The major problem with these protocols is the unsatisfactory regioselectivity; the difficulty to separate the regioisomers undermined the possibility to obtain pure products in good yields. Moreover, hydrogenation step resulted very slow.

1.6.2 Diphosphine ligands

Diphosphine ligands are the most used phosphorous based ligands in HF and HAM reactions. They can give better chemo- and regioselectivity due to their steric hindrance and chelating ability. The full Rh catalysed reaction mechanism in presence of diphosphine ligands is represented below (Figure 12).
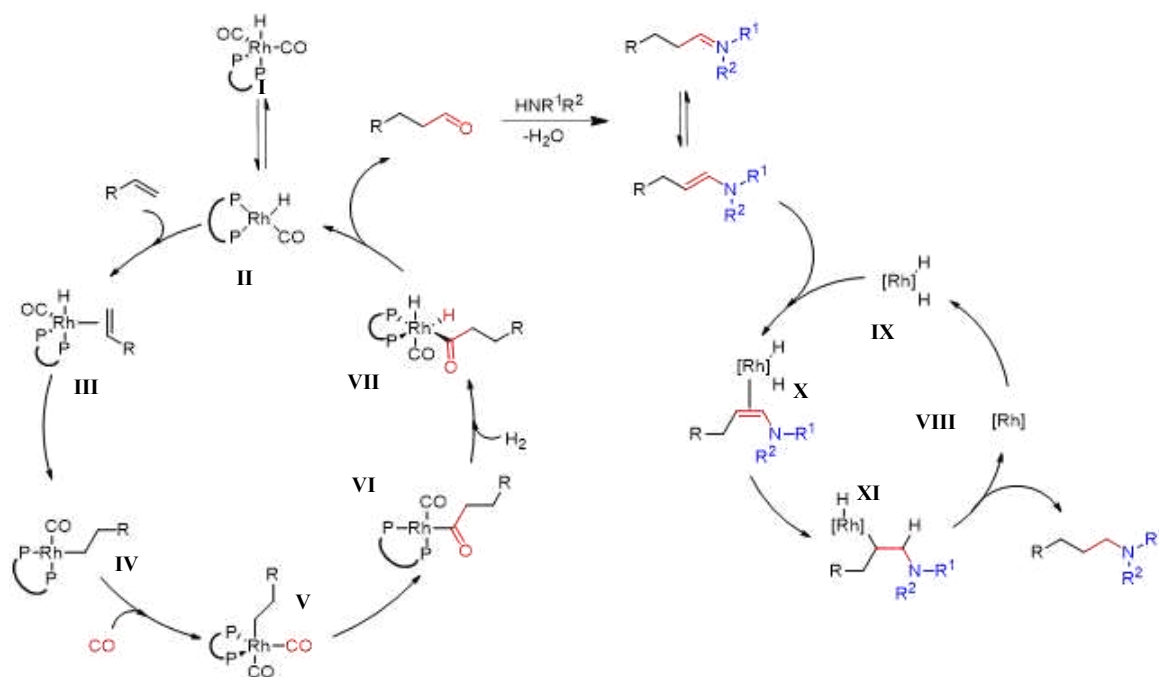
Figure 12. Rhodium catalysed reaction mechanism with diphosphine ligands.

HF step initially involves the formation of a precursor complex of catalyst and ligand, $[Rh(H)(CO)_2L_2]$ (**I**) in equilibrium with a square-planar $[Rh(H)(CO)L_2]$ specie (**II**), which is the active specie able to coordinate the double bond. After the coordination (**III**), the transfer of the hydride ligand on the double bond provides a linear or branched alkyl specie (**IV**). After coordination of these species with one CO (**V**), its migratory insertion leads to the formation of a square-planar acyl specie (**VI**) and the oxidative addition of dihydrogen provides the last specie of the catalytic cycle (**VII**), from which aldehyde is released by reductive elimination of one hydride, with contemporary regeneration of acyl active specie (**II**). To avoid side reactions, principally the hydrogenation or the isomerization of the double bond,[202] insertion of CO and aldehyde formation must be fast. HF step is also determinant for the regioselectivity of the reaction since it is determined by the initial formation of the linear or branched aldehydes: it does not depend on the isomerization of the double bond, but from the rearrangement of complex (**III**), influenced by the nature of the ligand. The introduction of diphosphine ligands based on xantene structure in rhodium catalysed hydroformylation was crucial for this purpose. These ligands have enough large *bite angles* (111-123 °) fundamental to obtain the linear aldehyde, together with a big steric hindrance (Figure 13).

34
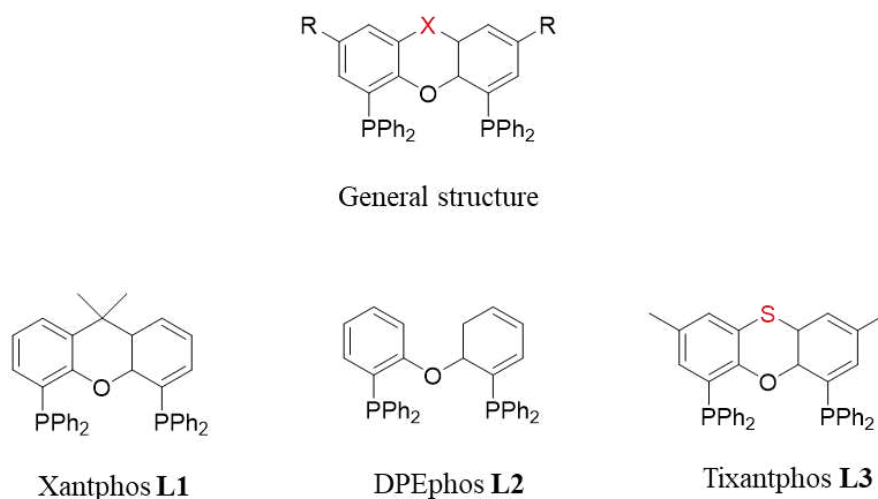
Figure 13. Structure of xantene and its diphosphine ligand derivative Xantphos (**L₁**), DPEphos (**L₂**) and Tixantphos (**L₃**)

These ligands stabilize the catalyst thanks to the different electronic interaction on the metal centre: in particular, they stabilize complex (**III**) by electronic characteristics of electron donation and retro-donation. Basicity of these ligands compensates the partial positive charge localized on the metal centre, most of all in presence of electron-withdrawing substituents on the starting olefin. In case of electron-donating groups on the starting alkene, negative charge on the metal centre is compensated by the retro-donation on the conjugate aromatic system. Moreover, ligands contribute to make a more geometrically rigid system, so the intermediates remain more stable.[203]

Reaction of the aldehydes with amines occurs immediately in the reaction environment, with the linear aldehyde that usually reacts faster than the branched one giving the resultant enamine or imine. Hydrogenation is the rate determining step. After an oxidative addiction of dihydrogen to [Rh] neutral specie (**VIII**), the formed [Rh(H)₂] dihydride (**IX**) coordinates the double bond giving the [Rh(H)₂(enamine)] (**X**). Hydride transfer generates an alkyl specie (**XI**), starting from which a reductive elimination leads to the formation of the desired amine together with the restoration of the original [Rh] active specie (**VIII**). Nature of the ligand involved in the reaction and the coordination sphere that is formed influence this step: a better hydrogenation activity was demonstrated using phosphines endowed with electron withdrawing groups (EWG).[204]

Beller and co-workers demonstrated that steric hindrance and bite angle of the ligands affect the HAM regioselectivity:[205] unlike HF, the presence and influence of amines, that can compete with diphosphines acting as ligands on Rh metal centre, could not be ignored. Chelating ligands, as Xantphos (**L₁**), Iphos (**L₅**) or derivatives, are less favourable to exchange

compared to PPh₃, so the effect of the amines in chelating the catalyst is not significant. These chelating agents also determine a faster hydrogenation rate. According to the studies performed for HF reaction, the bigger is the bite angle of the diphosphine, the higher is the regioselectivity in favour of the formation of the linear amine. Among all the ligands Xantphos demonstrated to have the best qualities balancing quantitative conversion, high chemoselectivity (amine >97%) and regioselectivity (l/b 98:2) and fast hydrogenation rates. Thanks to their bite angle, Xantphos (**L₁**), Naphos (**L₄**) and Iphos (**L₅**) (Figure 14) were also successfully exploited for the one-pot isomerization-hydroaminomethylation of internal alkenes, affording a regioselectivity similar to that of HF and HAM of terminal alkenes.[206]
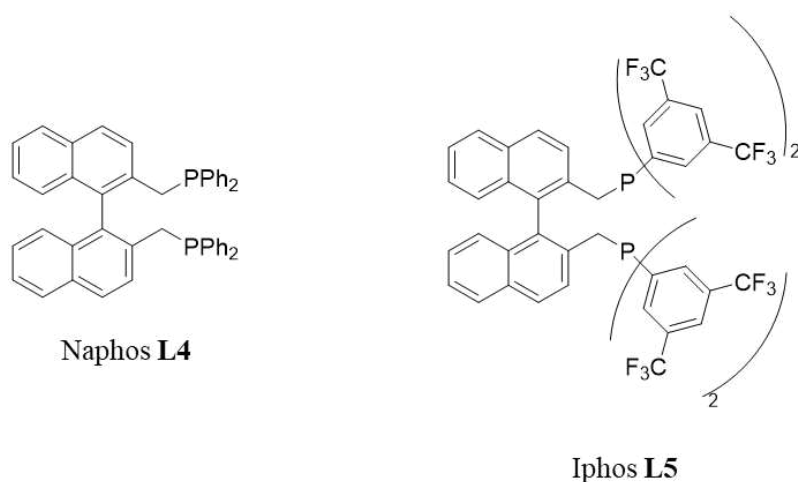
Figure 14. Structures of Naphos and Iphos.

Bis-[(dipyrrolyl)phosphino]xantene ligands (Figure 15), derived from Xantene's core by modification of the backbone with dipirrolylphosphine groups (**L₆**),[207] possess π-acceptor character that enhances the reaction rate due to a facilitated dissociation of CO ligand. The steric hindrance also determines very high selectivity and regioselectivity (l/b 200:1). The limit of these ligands is that their activity is strictly dependent on the acidity of the medium: pKₐ values between 16-17 (EtOH, BuOH) guarantee the best performances, especially in terms of regioselectivity. Less acidic media determine a maintenance of regioselectivity, but chemoselectivity is lower due to the decreased hydrogenation activity and an increase of the double bond isomerization, while in more acidic media high activity is accompanied by side reactions as aldol condensation.
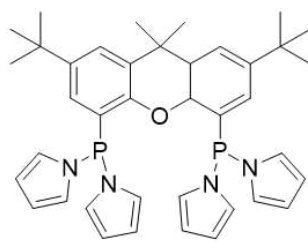
L6

Figure 15. Structure of dipirrolylphosphines.

Very recently, Xantphos derivative N-Xantphos (**L7**) was used with [Rh(acac)(CO)$_2$] and a co-catalyst for the HAM of alkyl and aryl hindered amines in continuous segmented flow reactor with a robust catalyst recover. This protocol also enables a switch from amine to enamine without necessity to change the ligand (Figure 16, left).[208]

Sulfoxatphos (**L8**), a Xantphos analogue endowed with two sulfonic groups, that also guarantee its solubility in water, results very attractive. As example, it was exploited for the HAM of terminal alkenes in ionic liquid/biphasic system with Rh catalysts as [Rh(COD)$_2$BF$_4$] (alone or in combination with [Rh(acac)(CO)$_2$]) or [Rh(COD)Cl$_2$] (Figure 16, right).[209]
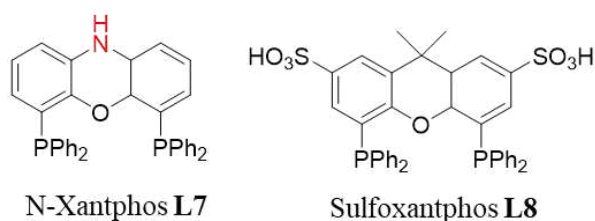
Figure 16. Structures of N-Xantphos and Sulfoxantphos.

1.6.3 Other phosphorus ligands

1.6.3.1 Monophosphurus ligands

Monophosphorus ligands (Figure 17) are less used. Triphenilphosphine sulfide (TPPS) (**L9**) and TBBP (**L10**) guarantee high or excellent selectivity for amine formation, but regioselectivity is obviously low or moderate. Phospholes demonstrated to be promising as ancillary in HAM since its better promotion of reductive amination compared to PPh$_3$. Phospholes were used for the first time for the HAM of estragole with *N*-dibutylamine. The protocol provided the product in high yields and these ligand demonstrated to be very promising demonstrating to promote a faster hydrogenation step than PPh$_3$.[210]

Tuning of electronic and steric properties of monophosphorus ligands is necessary to combine higher activity and selectivity.
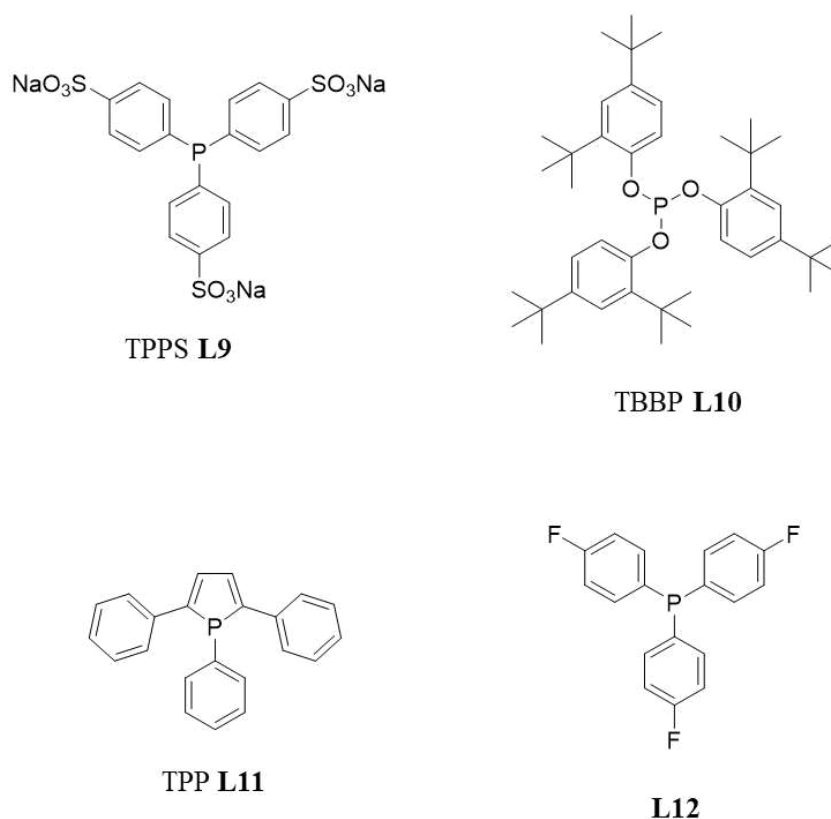

Figure 17. Structures of monophosphurus ligands.

1.6.3.2 Bisphosphite ligands

For a long time, phosphite ligands were not used in HAM protocols because of their sensitivity to hydrolysis. Low yields and hydrogenation of the starting alkenes can represent important problems, even if their good π-acidic character is a very attractive characteristic. Introducing bisphosphite ligand Biphephos (Figure 18), endowed with very crowded bulky aryl substituents, in the rhodium coordination sphere, HAM provides amines in very high regioselectivity for the linear product. Biologically active compounds as the antiarrhythmic ibutilide, the antidepressant aripiprazole and antihistaminic terfenadine and fexofenadine were all synthesized by HAM protocols in very high linear-regioselectivity (from l/b 37:1 to 48:1) using biphephos as ligand.[211]
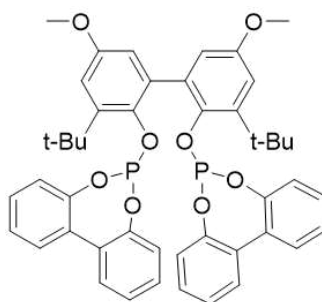
Biphephos **L13**

Figure 18. Structure of Biphephos (**L₁₃**).

1.6.3.3 Tetraphosphorus ligands

Biphenyl backbone based tetraphosphorus ligands (Figure 19) provide highly excellent regioselectivity in the HAM of both terminal and internal alkenes: the higher concentration of phosphines around the metal centre ensures a bigger chelating ability, with a consequent better regioselectivity. Rhodium catalysed HAM with Tetrabi as ligand provides amines in excellent chemoselectivity (> 99% amines) and regioselectivity (97% linear amine, l/b 168:1) both in the HAM of terminal alkenes[212] and in the isomerization-hydroaminomethylation of internal alkenes with piperidine.[213] The high sterically hindrance of tetraphosphoramide (**L₁₅**), together with the electron-withdrawing properties of pyrrole moiety, allows to obtain a linear selective rhodium-catalysed HAM of styrene derivatives with a regioselectivity linear/branched > 99:1, very challenging since styrene naturally provides the branched product in HF and HAM reaction conditions.[214]
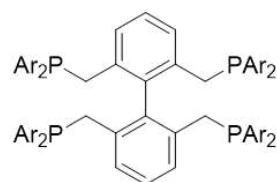
Tetrabi **L14**
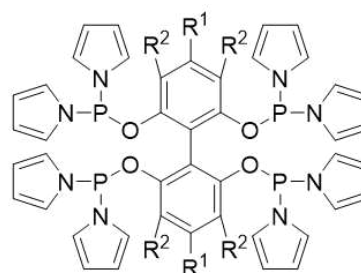
L15

Figure 19. Tetraphosphorus ligands.

1.6.3.4 Non-phosphine-based ligands

Carbene ligands

Carbene ligands were introduced for the HAM by Beller.[215] Rhodium monocarbene complex could solve the problem of the low-hydrogenation activity of rhodium-phosphine catalytic complexes, due to the strong coordination of phosphines.

Moreover, the strong electron-donating properties of carbene ligands have a positive effect on the chemoselectivity of the reaction,[17] avoiding the side reaction of isomerization of the double bond; a simultaneous coordination together with phosphorous containing ligands also provides a higher regioselectivity for linear products. Carbene ligands were exploited for the synthesis of 3,3-diarylpropylamines, which structure can be found in antiallergic, choleretic, antipyretic, coronarodilator, and antispasmodic compounds.[216] Rhodium-carbene mediated HAM showed a better activity and selectivity compared with the previous HAM rhodium-catalysed protocols.

Nitrogen-containing ligands

Hybrid amino-phosphine ligands have a dual coordination mode, with phosphorus ligand always coordinated, while nitrogen nucleus can be both coordinated or not, leaving a vacant position that has a beneficial role in coordination of the alkene and its activation. Dinitrogen ligand N,N,N,N-tetramethylendiamine (TMEDA) was used in Rh-ligand complex used for the synthesis of biological active 2-benzazepines exploiting two different pathways, by intramolecular HAM starting from isoprenyl- or allylamines or starting from 2-isopropenylbenzaldehyde and different anilines.[217]

1.6.4 Rh catalysed HAM in green solvents

Water alone is hardly considered a suitable solvent for HAM protocols, since it is the by-product in the equilibrium reaction of imine/enamine synthesis. Anyway, different alternatives were explored to perform Rh-catalysed HAM avoiding the use of organic solvents.

Vohrolt and co-workers explored the HAM of 1-dodecene using dimethylammonium dimethyl carbamate (dimcarb) as a reactive ionic liquid as amine counterpart, obtaining final amines with an yield of 42%.[209] No extraction is needed and the catalytic complex [Rh(cod)Cl$_2$]/Sulfoxantphos is recycled five times with loss of 10% in yield in the last run.

Vohrolt and co-workers also explored the HAM of water-soluble aliphatic amines and 1-octene in water exploiting the use of alcohols as 1-BuOH, 2-BuOH, tert-BuOH, iso-BuOH and EtOH as cosolvents.[218] The reaction did not occur without co-solvent, but in H_2O/ROH [Rh(cod)Cl$_2$]/Sulfoxantphos system provides final amines in good yields in 6 h under 50 bar of syngas at 100 °C. The protocol was applied to amino-acids and amino polyols and an evaluation of catalyst recycle was made. Unfortunately, chromatographic purification was necessary to obtain final products.

Beller and co-workers reported the first protocol for the synthesis of primary anilines from medium chain alkenes and NH$_3$ in a water/MTBE system:[219] the protocol exploits a Ru/Ir catalyst and affords primary amines in good yields and low formation of secondary amines by-products under 78 bar of syngas and high temperature (130 °C), in relatively short time (10 h).

Cationic surfactant CTAB found different applications in aqueous biphasic systems for HAM protocols. Wang and co-workers showed that the presence of the surfactant accelerates the HAM performed with a water soluble Rh complex in biphasic system, since micelles expand the interfacial area between the phases, enriching the concentration of Rh catalyst at the interface by means of electrostatic interactions between micelles and anionic catalyst.[220] The same principle was exploited for the HAM of limonene with ammonia to obtain a value-added compound with a different water-soluble catalytic complex, where good phase interaction and easier phases separation were obtained.[221] In presence of [Rh(cod)Cl$_2$]/triphenylphosphine trisulfonate and CTAB primary amines were obtained in 25% yield, with a reduction of the isomerization side reaction by optimization of reaction conditions. HAM of limonene,[222] as well as other monoterpenes[223] or eugenol[224] and estragole,[210] is a protocol of great potential for the production of value added amines from biomass derived compounds and is quite explored. Recently an interesting protocol for Rh-catalysed HAM of natural alkenes estragole, limonene, camphene and β-pinene with different amines in green solvents was reported:[225] *p*-cymene and anisole were used as solvents giving similar results compared to toluene, while EtOH also provided better yields for the most "hard" substrates.

Cyclodextrins can be exploited in a similar way of surfactants. Natural cyclodextrins α-cyclodextrin (α-CD), β-cyclodextrin (β-CD), 2-hydroxy-propyl β-cyclodextrin (hp-β-CD), γ-cyclodextrin (γ-CD) and Randomly Methylated β-cyclodextrin (RAME-β-CD) have been used as "surfactants" to perform the Rh catalysed-HAM of bio-renewable eugenol and of its derivatives estragole and anethol in biphasic aqueous medium.[226] The best results were

obtained with RAME-β-CD: benzene ring can be accommodated in the hydrophobic cavity, while the double bond remains outside and is converted in the correspondent amine in excellent yields and acceptable but limited regioselectivity. The system still requires hard reaction conditions (40 bar of syngas, 125 °C), but cyclodextrins can be recycled five times without loss in activity.

RAME-β-CD were successfully used as green mass transfer in water for the scale-up of HAM of 1-decene and diethylamine using a Rh/sulfoxantphos catalytic system.[227] Higher cyclodextrin concentrations support higher mass transfer rates between phases and the stability of the catalytic system. Moreover, they remarkably increase reaction rates and regioselectivity in favour of the formation of linear amine: amines are finally obtained with a chemoselectivity of 80%, and regioselectivity of 35%, with the possibility to recycle the biphasic aqueous system, performing the reaction under 30 bar of syngas and 125 °C in 30 h.

Micellar catalysis is very less exploited for HAM processes. Gall and co-workers used Rh(I) catalyst and amphiphilic triphenylphosphane functionalized poly(2-oxazolines) as macro ligand for the HAM of 1-octene, obtaining modest amines yields and regioselectivity.[228]

For the best of our knowledge, non-ionic surfactants as TPGS-750-M, that demonstrated to bring many advantages in different kind of metal catalysed reactions, has never been exploited for HAM of alkenes.

1.6.5 Microwave-assisted Rh catalysed HAM

HAM usually requires very hard conditions of pressure (>50 bar) and temperature (>100 °C) and very long reaction times (24 h) to be efficient.[17] Microwave heating is scarcely explored for HAM, even if it is clear that this technology enables to perform this kind of reactions in milder conditions. Exploiting the modified microwave apparatus described in paragraph 1.4.2, Petricci, Taddei and co-workers proposed a protocol using Rh(CO)H(PPh$_3$)$_3$/Xantphos complex to perform a regioselective HAM of terminal alkenes in green EtOH, using very mild pressure conditions of 4 bar of syngas in 10 minutes.[155] This protocol allowed to obtain a small library of linear amines in good yields and it was also applied to the HAM of different basic α-amino acids, efficiently prepared both in the Boc-protected form and in the zwitterionic one.

Very recently, the same group published a protocol that exploits microwaves dielectric heating for the obtainment of pyrrolizidine by intramolecular hydroaminomethylation.[229] Hyacintacine A2 (natural alkaloid) benzyl ether and a lentiginouse analogue were obtained in

good yields from 3,4-bis(benzyloxy)-2-[(benzyloxy)methyl]-5-vinylpyrrolidine and *N*-hydroxypyrrolidine in mild conditions in green EtOH. Pirrolyzidine can be purified by separating the product in Strong Cation EXchange (SCX) columns and the recovered ethanolic phase can be recycled for three times without significant impact on yield.

1.6.6 Hydroaminomethylation of anilines

Secondary anilines represent very important products and intermediates for the synthesis of heterocyclic compounds and APIs.[230]

In most cases, anilines production starts from the synthesis of an aliphatic amine (Figure 20), obtained by direct HAM, or passing through an aldehyde intermediate obtained by HF. Aldehydes can be directly transformed in the amines by reductive amination or can be converted in other functional groups as alcohols, halide compounds or nitriles, that provide amines respectively by reactions of hydrogen borrowing, nucleophilic substitutions and reduction. From these aliphatic amines, aniline derivatives are usually obtained with different strategies, as Pd catalysed Buchwald-Hartwig amination,[231,232] Cu catalysed Ullman amination,[233,234] photoredox Ullman amination.[235,236] Even if these reactions provide anilines in a very effective way, most of them suffer from low atom economy and from the necessity to use toxic solvents (i.e. toluene) and high temperature or use of non-suitable catalyst for API production,[237] as Pd, which use is avoided in the last three steps of the synthesis of pharmaceutical compounds.

Many efforts have been done to enhance the sustainability of this transformation, for example applying micellar catalysis in Ullman type reactions,[115,238–240] Buchwald-Hartwig amination,[113,114,241,242] and alkylation of anilines with alcohols through hydrogen borrowing[173] or using water as solvent for Fe-catalysed reductive amination,[243] or performing Ullman C-N coupling in DESs.[244]
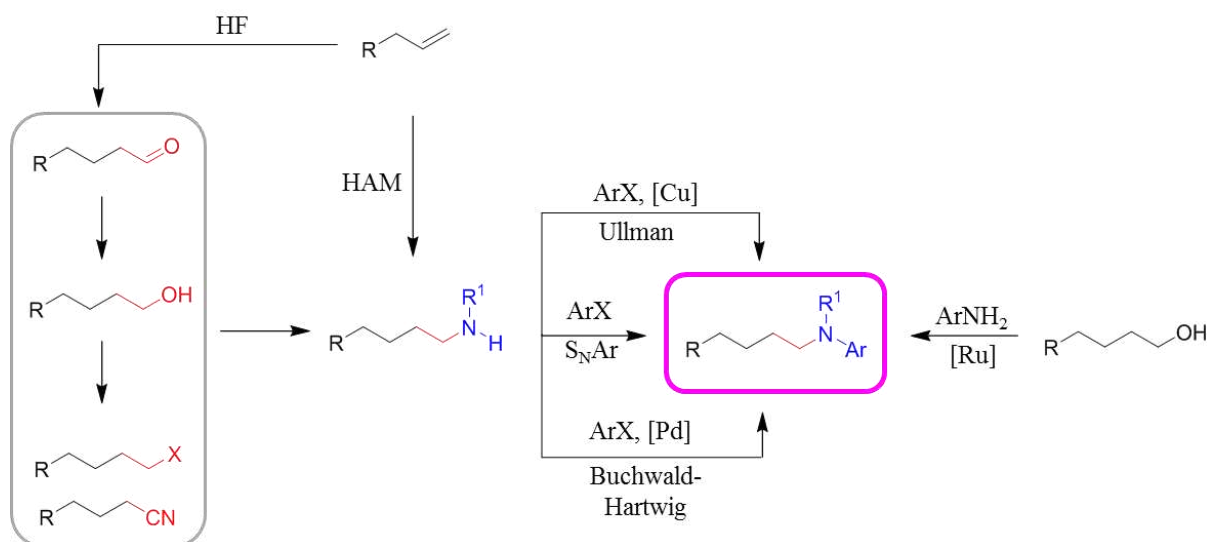
Figure 20. Classical syntheses of anilines.

Very few protocols of HAM for the synthesis of anilines are reported.

Beller and co-workers developed a first protocol for the HAM of arylaretenes to selectively obtain branched amphetamines with a Rh-diphosphine catalyst in relatively mild conditions.[245] The complex [Rh(cod)₂BF₄]/dppf, with addition of little amount of HBF₄ allowed them to obtain the branched product in high yield (>90%) and good regioselectivities in THF under 30 bar of pressure of syngas at 60 °C.

Villa Marco and Xiao proposed a protocol for the HAM of styrene derivative that provides β-chiral amines with high enantioselectivity (88-96%) combining metal and organocatalysis and exploiting the use of a chiral ligand and Hantzsch ester as additional hydrogen source, that inherently impacts the atom economy of the process.[246]

Very recently, Zhang and co-workers developed a very interesting protocol using water as the unique solvent and a water-soluble tailor-made ligand for the branched-selective HAM of styrenes.[247] Catalyst can be recycled two times without effect on the yield and regioselectivity. The use of a tailor-made ligand, as the scarce substrate scope can unfortunately undermine the exploitation of this method at industrial level. Furthermore, in the case of poorly water-soluble substrates the addition of the surfactant sodium dodecylbenzenesufonate (SDBS) is required, thus moving to a more classical micellar catalyzed process.

Chen and co-workers recently published a protocol involving the use of a P, O-ligand able to give a six membered ring chelating [Rh(acac)(CO)₂] centre, providing a complex that

accelerates both the HAM steps giving final anilines in good yields in 4 h, but with very modest regioselectivity.[248]

The most recent work is represented by Qian and co-workers, that developed a Rh(I) polymeric catalyst very effective in the regioselective HAM of olefins with secondary anilines with the possibility of recycling the catalyst almost 20 times. The reaction is performed in THF, at 150 °C and in 18 h provides linear secondary anilines (*l:b* 99:1) in a 98% yield.[249]

1.7 Aim of the work

HAM represents a valid process for the synthesis of amines, potential important intermediates in APIs synthesis. This very important transformation is still very poorly explored on aromatic substrates such as anilines. Moreover, reported processes still present different problematics as the necessity of hard reaction conditions of pressure or temperature and long times of reaction, scarce substrate scopes, limited to only styrene derivatives or only to aniline or methyl aniline, or the necessity to synthesize tailor-made ligands soluble in water to use it as the only solvent. (Paragraph 1.6.6).

Following the interesting results of the research group on HF protocols,[154] including micellar catalyzed green version,[175] and on microwave-assisted HAM,[155,229] the aim of this work is the development of a fully environmentally benign protocol for the regioselective micellar catalyzed HAM of different terminal olefins with different anilines in water,[250] entirely avoiding organic solvents and implementing a full recovery of the water micellar phase retaining both the catalyst and the commercially available ligand that can be reused at least 5 times. The coordination complex formation between the ligand and the utilized Rh metal precursor under isolated and actual reaction conditions with implications for the active catalytic species has been deeply studied.[250] A Life Cycle Assessment (LCA) analysis of this and other protocols applied to the synthesis of substituted anilines is also reported confirming the greenness of this HAM procedure.

2. RESULTS AND DISCUSSION

2.1 Reaction optimization

Table 3. Reaction optimization: catalyst and ligand.
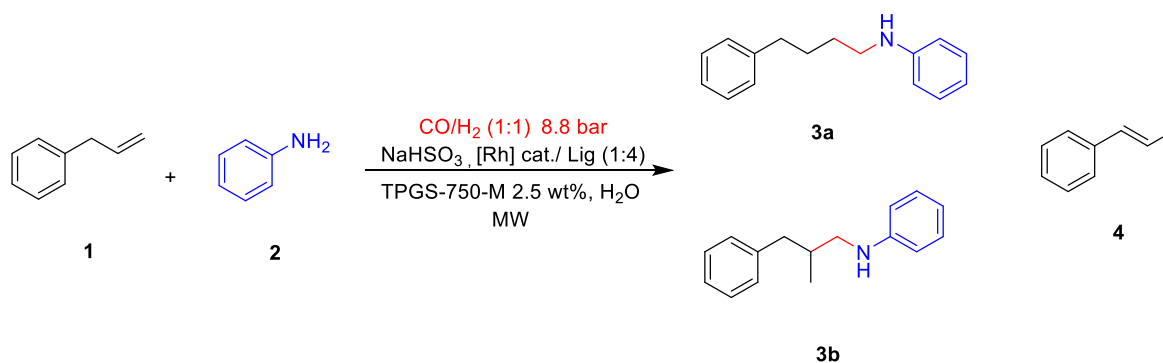
Entry	Cat., Lig., T, time	Conv. [%][a]	3 [%][a] (3a/3b)	4 [%][a]
1[b]	[Rh(CO)H(PPh$_3$)$_3$] 1 mol%, Xantphos (L$_1$), 70 °C, 40 min	43	37 (4:1)	6
2[b]	[Rh(CO)H(PPh$_3$)$_3$] 1 mol%, Xantphos (L$_1$), 70 °C, 60 min	67	52 (6:1)	15
3[b]	[Rh(CO)H(PPh$_3$)$_3$] 1 mol%, Biphephos, 70 °C, 60 min	70	-	70
4[b]	[Rh(CO)H(PPh$_3$)$_3$] 1 mol%, 6-DPPon, 70 °C, 60 min	41	41 (3:1)	-
5[c]	[Rh(CO)H(PPh$_3$)$_3$] 2 mol%, Xantphos (L$_1$), 70 °C, 60 min	50	47 (19:1)	3
6[b]	[Rh(CO)H(PPh$_3$)$_3$] 1 mol%, Xantphos (L$_1$), 70 °C, 2 x 30 min	64	47 (30:1)	17
7[b]	[Rh(acac)(CO)$_2$] 1 mol%, Xantphos (L$_1$), 70 °C, 60 min	60	57 (18:1)	3
8[b]	[Rh(acac)(CO)$_2$] 1 mol%, Biphephos, 70 °C, 60 min	72	-	72
9[b]	[Rh(acac)(CO)$_2$] 1 mol%, 6-DPPon, 70 °C, 60 min	-	-	-
10[b]	[Rh(acac)(CO)$_2$] 1 mol%, Xantphos (L$_1$), 70 °C, 2 x 30 min	63	60 (19:1)	3
11[d]	[Rh(acac)(CO)$_2$] 1 mol%, Xantphos (L$_1$), 70 °C, 2 x 30 min	53	35 (12:1)	18
12[e]	[Rh(acac)(CO)$_2$] 1 mol%, Xantphos (L$_1$), 70 °C, 2 x 30 min	69	65 (20:1)	4

[a] Conversion of **1** into **3** and **4** determined by GC/MS as reported experimental section. [b] **1** (0.75 mmol), **2** (0.9 mmol), Rh catalyst (0.0075 mmol), ligand (0.03 mmol), NaHSO$_3$ (1.12 mmol), CO/H$_2$ (8.8 bar), TPGS-750-M 2.5wt% in H$_2$O (3 mL), MW. [c] **1** (0.75 mmol), **2** (0.9 mmol), Rh cat (0.015 mmol), ligand (0.06 mmol), NaHSO$_3$ (1.12 mmol), CO/H$_2$ (8.8 bar), TPGS-750-M 2.5wt% in H$_2$O (3 mL), MW. [d] **1** (0.75 mmol), **2** (0.9 mmol), Rh cat (0.0075 mmol), ligand (0.03 mmol), NaHSO$_3$ (1.12 mmol), CO/H$_2$ (8.8 bar), TPGS-750-M 5wt% in H$_2$O (3 mL), MW. [e] **1** (0.75 mmol), **2** (0.9 mmol), Rh cat (0.0075 mmol), ligand (0.03 mmol), CO/H$_2$ (8.8 bar), TPGS-750-M 2.5wt% in H$_2$O (3 mL), MW.

In our previous work on the micellar catalysed HF, we found that the addition of $NaHSO_3$ into the reaction mixture plays a key role in obtaining very good reaction yields and in preventing aldol condensation, typically occurring in HFs in aqueous media, due to the formation of aldehyde's Bertagnini's salt.[175]

Bertagnini's salt is also known to be a very good substrate for reductive amination as well:[251] HAM was firstly performed by irradiating with MWs allyl benzene **1** and aniline **2** at 70 °C for 40 minutes with [Rh(CO)H(PPh$_3$)$_3$] and Xantphos, at 8.8 bar of syngas in the presence of $NaHSO_3$, and using a 2.5 wt% suspension of the surfactant TPGS-750M in H_2O as the reaction medium. A 43% of conversion with respect to **1** was observed with a quite good regioselectivity towards the linear amine (*linear/branched*: 4/1). However, β-methylstyrene **4** was obtained (6%) via allylbenzene isomerization (Table 3, entry 1).

Irradiating with MWs in the same conditions but for longer reaction time gave rise to 67% conversion of **1** under formation of amine **3** in 52% yield with a better regioselectivity, together with a 15% of the isomerization side product **4** (Table 3, entry 2).

The use of different ligands did not improve the conversion. Using Biphephos, supposed to increase the regioselectivity due to the higher value of its bite angle, a 70% of conversion in **4** was obtained (Table 3 entry 3), while using 6-DPPon isomerization was not observed, but only 41% of conversion was obtained, with a negative impact on regioselectivity (l/b 3:1) (Table 3, entry 4).

Increasing the amount of catalyst to 2 mol% a better regioselectivity as well as a lower isomerization of allyl benzene (3%) were obtained, but conversion respected to **1** decreased to 50% (Table 3, entry 5). Irradiation of the mixture for two intervals of 30 minutes provided a 47% of conversion in anilines with an excellent regioselectivity (Table 3, entry 6).

However, the use of [Rh(acac)(CO)$_2$] in combination with Xantphos has positive impact on both the selective conversion towards the amines (57%) and the regioselectivity (l/b 18:1) (Table 3, entry 7), especially when the reaction is irradiated at 70 °C for 30 min two times both in presence (60%, l/b 19:1; Table 3, entry 10) and in absence of $NaHCO_3$ (69%, l/b 20:1; Table 3, entry 12), that is not crucial to obtain satisfactory results. A higher concentration of the surfactant (5%) inflicts a negative impact on both conversion, chemo- and regioselectivity (Table 3, entry 11). Irradiating the mixture at 70 °C for 60 min (still in presence of $NaHCO_3$) using of [Rh(acac)(CO)$_2$] and Biphephos, results were superimposable to that obtained with Rh(CO)H(PPh$_3$)$_3$, with a 72% of conversion in **4** (Table 3, entry 8), while in presence of 6-DDPon only the starting material was recovered (table 3 entry 9).

Based on our previous experience on micellar catalysed hydrogen borrowing protocols,[15] we decide to explore the use of aniline hydrochloride instead of the free aniline.

Table 4. Reaction optimization, aniline salts.
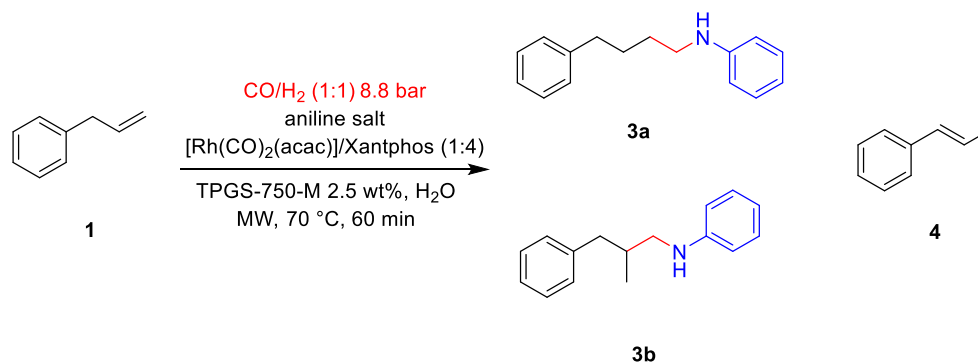
Entry	Aniline salt	Conv. (%)[a]	3 (%)[a] (3a/3b)	4 (%)[a]
1[b]	PhNH$_3$Cl (1 eq)	84	84 (24:1)	-
2[b]	PhNH$_3$Cl (1.2 eq)	98	96 (24:1)	2
3[b]	PhNH$_3$Cl (1.5 eq)	94	91 (19:1)	3
4[b]	PhNH$_3$OAc (1.2 eq)	7	6 (18:1)	1
5[b]	PhNH$_3$OCH=O (1.2 eq)	10	5 (9:1)	1
6[b]	PhNH$_2$ (1.2 eq), CH$_3$COOH/CH$_3$COONa	55	36 (19:1)	19
7[b]	PhNH$_2$ (1.2 eq), HCl (2.4 eq)	70	68 (24:1)	2
8[b]	PhNH$_2$ (1.2 eq), HCl (1.2 eq)	73	70 (24:1)	3
9[b]	PhNH$_2$ (1.2 eq), pTSA (1.2 eq)	71	66 (15:1)	5

[a]Conversion determined by GC/MS as reported experimental section. [b]**1** (0.75 mmol), aniline or aniline salt, [Rh(acac)(CO)$_2$] (0.0075 mmol), Xantphos (0.03 mmol), CO/H$_2$ (8.8 bar), TPGS-750M 2.5wt% in H$_2$O (3 mL), MW.

Surprisingly, we observed an 84% conversion of **1** into **3** as the sole reaction product with good regioselectivity towards the linear isomer **3a** (l/b 24:1) (Table 4, entry 1). Better conversions (96%) were observed by using a slight excess of aniline hydrochloride (1.2 eq), together with a minor formation of **4** (Table 4, entry 2). A further increase of the amount of aniline hydrochloride (1.5 eq) inverted the tendence, providing worse chemo- and regioselectivity (l/b 19:1) (Table 4, entry 3). Both using acetate and formate salts (Table 4, entries 4 and 5), conversion was drastically reduced under 10%. Measuring the pH of the solution before and after the irradiation using aniline hydrochloride, it was observed that the

best results were obtained starting from a pH of 4-5, while finding a pH value of 4 at the end of the reaction. Performing the reaction with aniline in acetate buffer, with a nominal pH of 4-5, a modest conversion in anilines was obtained, together with a higher isomerization of allylbenzene (19% of 4) (Table 4, entry 6). Directly introducing stoichiometric HCl or an excess or stoichiometric pTSA (Table 4, entries 7, 8, 9) an improvement was observed compared to the reaction in acetate buffer, but performances were not acceptable compared with the results obtained with aniline hydrochloride.

These results suggested that hydrochloride not only has a role related to avoiding the possible catalyst poisoning or in a pH function.

As the impact of different salts on the micelles' dimensions and properties is well documented in literature, especially for ionic surfactants,[252,253] the addition of different salts (NaCl, MgBr$_2$, CsF) in catalytic amounts was also investigated, however, without noticing an increased performance with respect to the use of sole aniline hydrochloride. This observation is consistent with our previous findings on HF under micellar catalysis conditions.[175]

Further investigations were performed in presence of aniline hydrochloride.

Table 5. Reaction optimization.
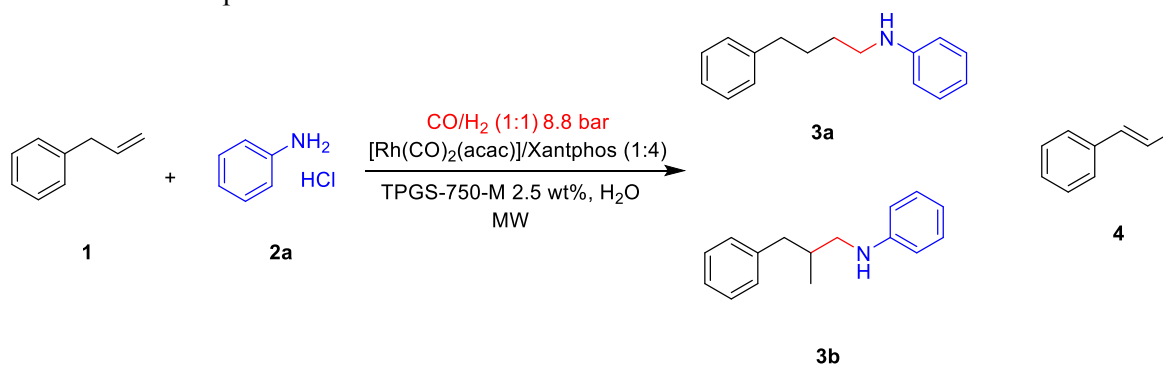
Entry	T (°C), time	Conv. (%)[a]	3 (%)[a] (3a/3b)	4 [a]
1[b]	50 °C, 60 min	49	43 (24:1)	6
2 [b]	60 °C, 60 min	98	98 (32:1)	0
3 [b]	70 °C, 60 min	98	96 (24:1)	1
4 [b]	80 °C, 60 min	86	81 (22:1)	5
5 [b]	90 °C, 60 min	77	70 (22:1)	7
6[c]	60 °C, 40 min	77	73 (23:1)	4
7 [c]	60 °C, 50 min	83	80 (24:1)	3
8 [c]	60° C, 70 min	96	96 (1:0)	0
9[d]	60 °C, 12 h	87	85 (4:1)	2

[a]Conversion determined by GC/MS as reported experimental section. [b]**1** (0.75 mmol), PhNH$_3$Cl (0.9 mmol), CO/H$_2$ (8.8 bar), [Rh(acac)(CO)$_2$] (0.0075 mmol), Xantphos (0.03 mmol), TPGS-750-M 2.5wt%, H$_2$O (3 mL), MW. [c]**1** (1 mmol), PhNH$_3$Cl (0.75 mmol), CO/H$_2$ (8.8 bar), [Rh(acac)(CO)$_2$] (0.0075 mmol), Xantphos (0.03 mmol), TPGS-750-M 2.5wt%, H$_2$O (3 mL), MW. [d]**1** (1 mmol), PhNH$_3$Cl (0.75 mmol), CO/H$_2$ (8.8 bar), [Rh(acac)(CO)$_2$] (0.0075 mmol), Xantphos (0.03 mmol), TPGS-750M 2.5wt%, H$_2$O (3 mL), autoclave.

The reaction was firstly performed at different temperatures. Starting from the result obtained with an irradiation of 70 °C for 60 minutes (Table 5, entry 3), we investigated the reaction behavior at both higher and lower temperature. Increasing the temperature to 80 °C and 90 °C chemo-and regioselectivity were both negatively affected, with a lower conversion in anilines especially at higher temperatures. However, dropping the temperature at 60 °C, an almost quantitative conversion of **1** in **3** was reached, with the highest regioselectivity observed (32:1) (Table 5, entry 2). Further decreasing the temperature to 50 °C conversion of starting material dramatically decreased under 50% (Table 5, entry 1).

Irradiating the reaction mixture at 60 °C for shorter times of 40 and 50 min, lower conversions in anilines, around 70%, were obtained, with a bad impact also on

regioselectivity (Table 5, entries 6 and 7). On the other hand, a longer time of irradiation of 70 min gave almost comparable results, with a 96% of conversion in anilines and an excellent regioselectivity (Table 5, entry 8).

The reaction was also performed heating the mixture with classic heating source in autoclave to have a direct comparison: after 12 h at 60 °C conversion was surprisingly still high, seen the mild conditions of temperature and pressure, while regioselectivity was dramatically worsened with a linear/branched ratio of only 4:1 (Table 5, entry 9).

HAM reaction was performed in different micellar mediums, using both ionic surfactants, as cationic CTAB or anionic SDS, and non-ionic Marlipal.

Table 6. Reaction optimization: surfactants.
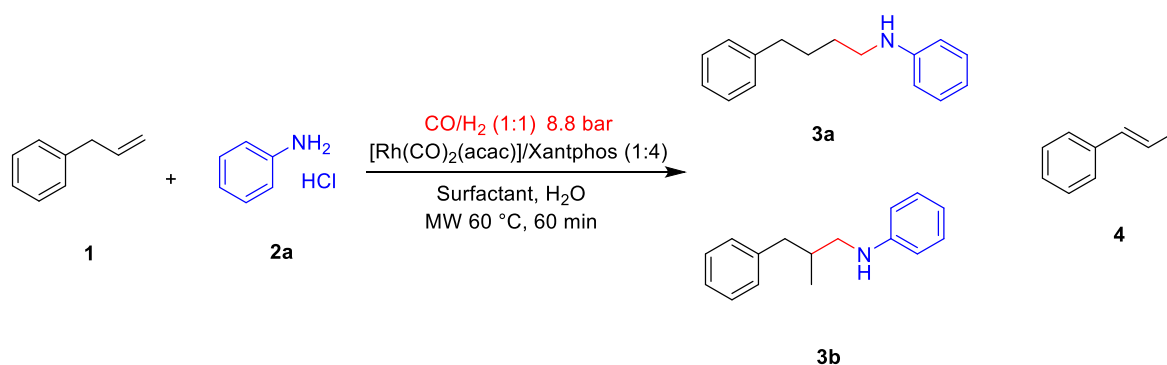
Entry	Surfactant (conc.)	Conv(%)[a]	3 (%)[a] (3a/3b)	4[a]
1[b]	TPGS-750M (2.5 wt%)	98	98 (32:1)	0
2[b]	SDS (2.5 wt%)	46	42 (13:1)	4
3[b]	CTAB (2.5 wt%)	19	18 (17:1)	1
4[b]	Marlipal 24 (2.5 wt%)	51	45 (13:1)	6
5[c]	TPGS-750M (1 wt%)	83	78 (19:1)	5
6[c]	TPGS-750M (1.5 wt%)	82	80 (25:1)	2
7[c]	TPGS-750M (2 wt%)	83	78 (19:1)	3
8[c]	TPGS-750M (5 wt%)	96	96 (18:1)	0

[a]Conversion determined by GC/MS as reported experimental section. [b]**1** (0.75 mmol), PhNH$_3$Cl (0.9 mmol), CO/H$_2$ (8.8 bar), [Rh(acac)(CO)$_2$] (0.0075 mmol), Xantphos (0.03 mmol), H$_2$O (3 mL), MW, 60 °C with different surfactants. [c]**1** (1 mmol), PhNH$_3$Cl (0.75 mmol), CO/H$_2$ (8.8 bar), [Rh(acac)(CO)$_2$] (0.0075 mmol), Xantphos (0.03 mmol), H$_2$O (3 mL), MW, 60 °C with different concentrations of TPGS-750M.

Irradiating the mixture at 60 °C for 60 min, all the surfactants in a concentration of 2.5 wt% provided worst performances compared to TPGS-750-M with a drastic impact on the conversion (Table 6, entries 2-4), with worst results observed with the cationic surfactant (Table 8, entry 3). Results are in line with that obtained for HF, confirming the important role of surfactant's active influence on yield and regioselectivity.

Surprisingly, in the reaction conditions of 60 °C for 60 minutes of irradiation, a higher concentration of TPGS-750-M (5%) did not determine a worst outcome: instead, conversion and chemo-selectivity were almost comparable to values observed with 2.5 wt% of TPGS-750-M in water, while only regioselectivity resulted negatively impacted (*l/b* 18:1) (Table 6, entry 8). However, lower concentrations of surfactant determined both lower conversions and regioselectivity (Table 6, entries 5-7).

Once found that the best conditions for the HAM protocol were MWs irradiation at 60° C, for 60 min at a pressure of 8.8 bar of syngas (CO/H$_2$ 1:1) in a concentration of 2.5 wt% of TPGS-750-M in water, blank reactions were performed without, respectively, syngas, catalyst, ligand, catalyst and ligand. In any case, only allyl benzene was recovered, without conversion in any product. The reaction was then performed in water without presence of surfactant: a very low conversion of 37% was obtained and regioselectivity decreased (l/b 12:2), once again confirming the important role of micelles as nanoreactors in the good outcome of the reaction.

2.2 Purification, scale up and catalyst recycle

Chromatographic purifications always undermine the sustainability of processes since they usually need the major quantity of organic solvents. In our case, the complexity of the reaction mixture required a very slow gradient to obtain satisfactory results and, consequently, a larger quantity of solvents. For this reason, a selective purification of the anilines was necessary to not compromise the sustainability of the process.

The finding that the reaction can provide excellent results using an excess of allylbenzene (**1**, 1 eq) on aniline hydrochloride (**2a**, 0.75 eq), verified by performing the reaction in these conditions, is fundamental to develop a selective recover of the product.

Since anilines are the only basic compounds in the reaction mixture, a selective acidic work up could represent a valid alternative. After the reaction, measured pH solution is slight acidic, nonetheless after extraction with DCM or EtOAc aniline derivatives are not selectively retained in the water phase but pass in the organic phase with the rest of the mixture.

Decreasing pH value could maybe solve this problem, but, in this case after the first extraction in organic solvent to remove the unreacted allyl benzene, catalyst and ligand, aqueous phase should be basified or reported to the original pH and a further extraction with organic solvents to recover anilines should be performed. This would compromise both the possibility to scale-up the reaction, seen the large amount of organic solvent needed for the double extraction, and would risk undermining the possibility of reuse the micellar phase for a possible recycle of catalyst.

The use of Strong Cation EXchange (SCX) columns seemed a valid alternative. These columns are charged with sulfonic -SO_3H groups able to protonate amines or anilines that are retained to the support as salts, while the rest of compounds can be eluted using a polar solvent. Then, basic compounds can be recovered by displacement with an alcoholic solution of NH_3.

After irradiation at 60 °C for 60 minutes, using 1 mmol of allyl benzene and 0.75 mmol of aniline hydrochloride, water micellar phase was extracted with DCM (5 mL) and solvent was evaporated. The crude was solubilized in MeOH and charged on SCX column; it was firstly eluted with MeOH and then with a solution of NH_3 4% in EtOH. Water phase, MeOH and EtOH were checked both by TLC and GC analysis finding an effective separation of anilines, obtained without any impact in yield and regioselectivity and all present only in ethanolic phase, from the rest of the mixture.

To improve the sustainability of the process, DCM was substituted with the more recommended EtOAc. Using the same quantity of solvent, EtOAc revealed to be less effective than DCM in the extraction of anilines. The use of a higher amount of solvent was not considered an improvement, especially looking for the future scale up of the reaction. The idea of flushing the mixture in EtOAc was finally discarded, since it is not perfectly suitable for the selected SCX columns.

The reaction mixture was finally directly filtered over the SCX column after the irradiation, and firstly flushed with EtOH to recover the aqueous phase with catalyst and ligand, and then with ethanolic NH_3 to displace anilines that were recovered with retention of regioselectivity and yield, separated from unreacted allylbenzene, catalyst and ligand eluted in EtOH with aqueous phase.
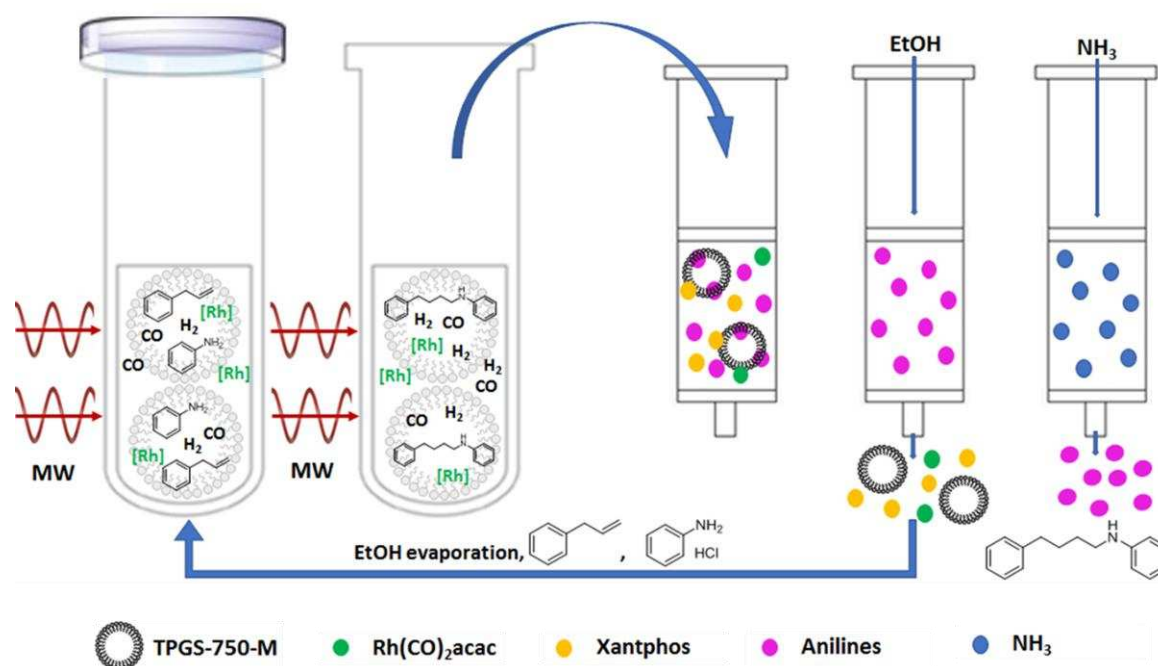
Figure 21. Purification of anilines, catalyst an micelles recycle.

This purification method revealed to be excellent and the possibility to separate only anilines, while the catalyst could be recovered with micellar phase, was very attractive to exploit this procedure to evaluate the possibility of catalyst recycle. The aqueous phase with catalyst and ligand collected after the elution was evaporated to remove EtOH: then, 0.75 mmol of allylbenzene and 0.75 mmol of aniline hydrochloride were added to restore the initial conditions and the reaction mixture was directly subjected to microwave irradiation for 60 min at 60 °C under 8.8 bar of syngas pressure. Anilines were surprisingly obtained without impact on both yield and regioselectivity, demonstrating that this process had the potential for an effective recycle of micellar phase and catalyst.

A pilot reaction with 10 mmol of allylbenzene was performed, maintaining the ratio of 1 equivalent of allylbenzene and 0.75 equivalents of aniline hydrochloride, irradiating the mixture for 60 min at 60 °C under 8.8 bar of syngas pressure. Once ascertained that the results were comparable with the results obtained in smaller scale, reaction was performed again and, after irradiation, the mixture was filtered in SCX columns as explained above. The second cycle was successfully performed without any impact on both regioselectivity and yield. The procedure was repeated for further three times without dramatic impact on both reaction yield and regioselectivity (Figure 22).
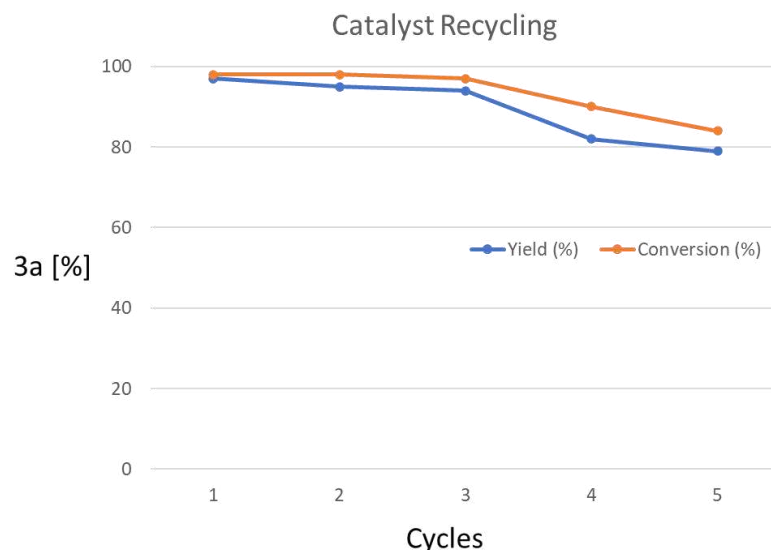
Figure 22. Catalyst recycle cycles. Conversion was determined by GC.

2.3 Substrate scope

No results have ever been obtained using aliphatic amines as the substrates.

Using different primary and secondary amines, both hydrochloride salts and not, high conversions were obtained but only in a large amount of the isomerization product and in aldehyde, while product was never formed (Table 7, entry 1-6), sign that probably bot hydroformylation and hydrogenation steps are slow. Reaction with phenylethylamine gave the best results, with a conversion of 17% in final amines and an excellent regioselectivity (Table 7, entry 7). The reaction was performed using different salts, hydrochloride, formic, and acetate buffer, to investigate a similar effect seen with aniline. Worst results were observed, with a maximum conversion of 7% in the desired product (Table 7, entries 8-11). Since the only promising results were obtain with phenylethyl amine, we supposed that the aromatic ring could play a role in the good outcome of the reaction. The reaction was performed with both benzylamine and its hydrochloride salt, to see if aromatic ring closer to amine moiety could have a different behaviour. Even in this case, a high rate of isomerization was detected, with a very little conversion in imine and final amines (Table 7, entries 12 and 13).

Table 7. Aliphatic amines
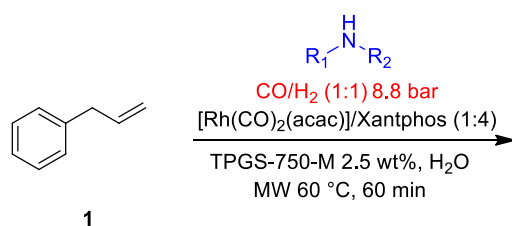
Entry	Amine	Conv. (%)	Product (l/b)	By-products (%)
1	Morpholine	100	0	Enamine (17) Aldehyde (31) Isomer (41)
2	Morpholine HCl	90	0	Aldehyde (40) Isomer (50)
3	Piperidine HCl	80	0	Aldehyde (20) Isomer (60)
4	Dodecyl amine	50	0	Aldehyde (50)
5	Dodecyl amine HCl	70	0	Isomer (70)
6	Cyclohexylamine HCl	90	0	Aldehyde (30) Isomer (90)
7	Phenylethylamine	93	17 (1:0)	Imine (13) Isomer (63)
8	Phenylethylamine HCl	73	4 (1:0)	Imine (1) Isomer (67)
9[a]	Phenylethylamine HCl	66	2 (1:0)	Imine (2) Isomer (62)
10	Phenylethylamine HCOOH	-	-	Aldehyde (60) Isomer (20)
11	Phenylethylamine CH$_3$COOH/CH$_3$COONa		7 (1:0)	Aldehyde (51) Isomer (23)
12	Benzylamine	85	7 (1:0)	Imine (14) Isomer (65)
13	Benzylamine HCl	75	3 (1:0)	Imine (5) Isomer (67)

[a] Catalyst 2 mol%, ligand 8 mol%

To evaluate the applicability of the process, the optimized reaction conditions were exploited to perform the reaction using different starting materials, both alkenes and anilines hydrochloride. The protocol demonstrated versatility and high tolerance for many different functional groups.
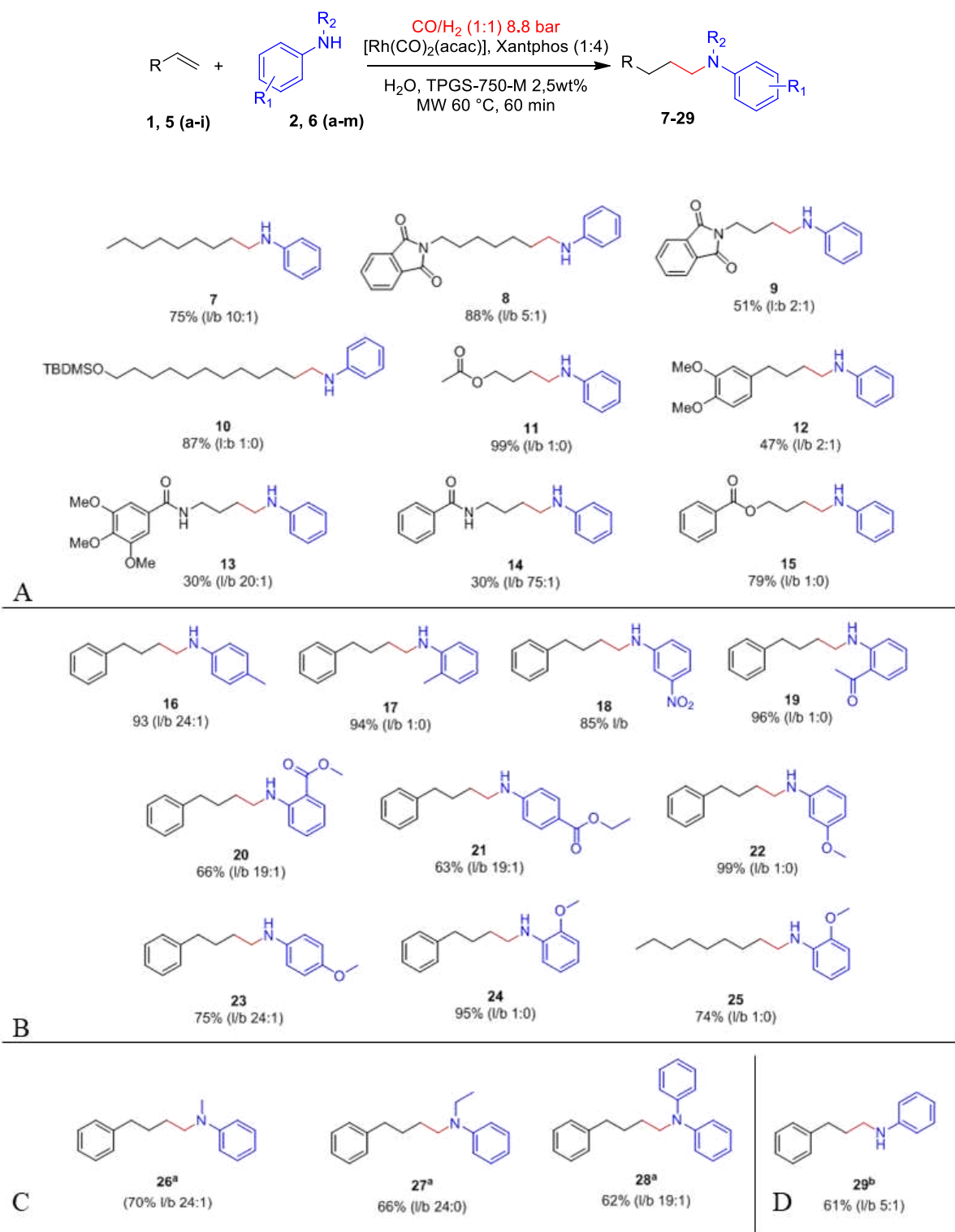
Scheme 1. Substrate scope: different alkenes (A), different anilines hydrochloride (B), secondary anilines (C), styrene (D). [a] CO/H$_2$ 1:5, 8.8 bar. [b] CO/H$_2$ 1:1, 10 bar, BIPHEPHOS.

Alkenes with long alkyl chains or decorated with different functional groups were reacted with aniline hydrochloride. In all the cases, the nature of the alkene does not impact on the regioselectivity (Scheme 1, A). Different functional groups, i. e. esters, amides or

phthalimides are stable in the optimized reaction conditions. Anilines with both electron-donating and electron-withdrawing functional groups in different positions of the ring were used (Scheme 1, B). In this case, regioselectivity was more affected, while isolated yield suffered a very small impact. Once again, different functional groups, even susceptible to hydrogenation as nitro (**18**) demonstrated tolerance to the reaction conditions.

The possibility to perform the reaction even with secondary anilines was evaluated (Scheme 1, C; Table 8).

Table 8. Reaction condition optimization: secondary anilines.
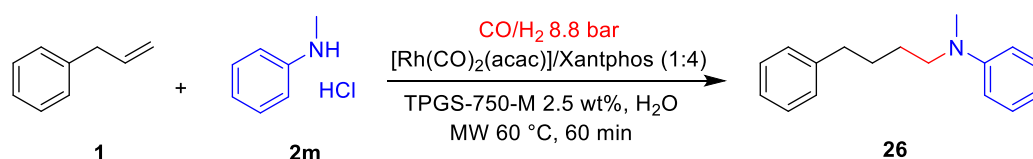
Entry	CO/H$_2$	Conv. (%)	SM (%) isomer	SM (%) reduced	Aldehyde (%)	26 (%) (26a/26b)
1	1:1	25	8	-	16	42 (24:1)
2	1:5	8	-	18	4	70 (24:1)

[a]Conversion is determined by GC/MS as reported experimental section. [b]**1** (1 mmol), PhMeNH$_2$Cl (0.75 mmol), CO/H$_2$ (8.8 bar), [Rh(acac)(CO)$_2$] (0.0075 mmol), Xantphos (0.03 mmol), TPGS-750M 2.5wt% H$_2$O (3 mL), MW, 60 °C

Performing the reaction using *N*-methyl aniline hydrochloride, we initially obtained a lower conversion in the product, while 16% of conversion in aldehyde was detected together with an substantial amount of unreacted allylbenzene. (Table 8, entry 1). We hypothesized that hydrogenation of the enamine was slower in this condition and for this reason the equilibrium was moved toward its hydrolysis. Performing the reaction with a 1:5 CO/H$_2$ ratio conversion in anilines was increased to 70% with very high regioselectivity (Table 8, entry 2). The reaction was then successfully performed with ethyl-aniline and diphenyl aniline hydrochloride.

Using styrene and derivatives, an inverted regioselectivity is usually detected in HF and HAM reactions, with the formation of branched product as major regioisomer. We wanted to see if our protocol was in line with this kind of result: the process can be efficiently applied on styrene, surprisingly obtaining the linear amine **29** in good yield as the major regioisomer (Scheme 1, D) and it is reversed with respect to the data reported in the literature on the same substrate (l/b 1:13).[247] The regioselectivity towards the linear isomer can be increased by

using Biphephos as ligand and 10 bar of syngas, while in this case the conversion is a bit lower.

2.4 Mechanistic investigation

With the aim to elucidate the catalytic process, micellar phase was analysed by Transmission Electron Microscopy (TEM) before and after MW irradiation confirming that after irradiation a more homogenous multi-micelle structure is obtained without Rh nanoparticles formation (Figure 23).
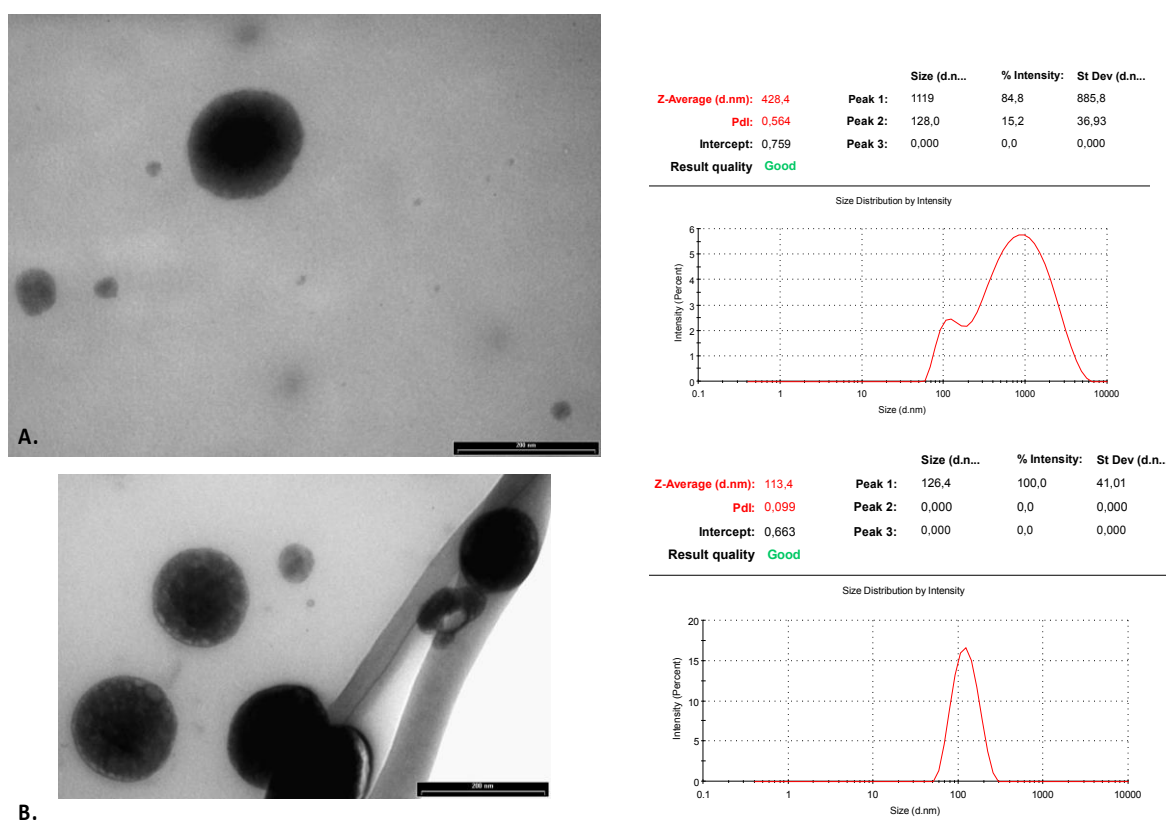

Figure 23. TEM (left) and Zeta-Potential (right) of analysis of: **A)** reaction mixture before irradiation: **1** (0.75 mmol), PhNH$_2$ HCl (0.9 mmol), [Rh(acac)(CO)$_2$] (0.0075 mmol), Xantphos (0.03 mmol), H$_2$O (3 mL), TPGS-750M 2.5wt%; **B)** reaction mixture after irradiation: **1** (0.75 mmol), PhNH$_2$ HCl (0.9 mmol), [Rh(acac)(CO)$_2$] (0.0075 mmol), Xantphos (0.03 mmol), CO/H$_2$ (9 bar) H$_2$O (3 mL), TPGS-750M 2.5wt%, MW, 60 °C, 60 min

Then role of hydrochloride cannot be limited to avoidance of catalyst poisoning or to the necessity to have an acidic pH for the good outcome of the reaction. In fact, similar conditions can be obtained even using other salts that provided inferior results. For this reason, in collaboration with Prof. Robert Langer and Dr. Matthias Vogt, we investigated the role of

aniline hydrochloride by evaluating its possible direct involvement in the formation of the HAM active catalytic species. Therefore, Xantphos and [Rh(acac)(CO)$_2$] were reacted in the presence of aniline hydrochloride (Scheme 2).
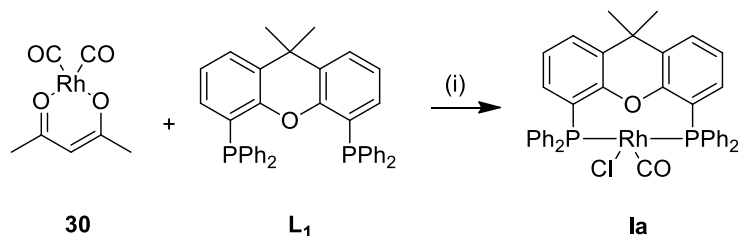
Scheme 2. Synthesis of complex Ia. PhNH$_3$Cl (1.2 eq), PhNH$_2$ (4.7 eq), THF, rt, 2h, Glovebox. Recrystallised from DCM.
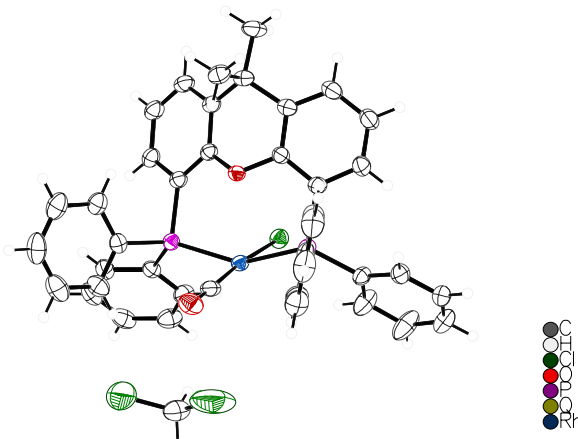
Figure 24. Mercury plot of the molecular structure of [Rh(κ^2-(P,P')xantphos)(CO)Cl] (**Ia**), derived from single crystal X-ray diffraction analysis. Hydrogen atoms and residual solvent molecule (CH$_2$Cl$_2$) omitted for clarity. Thermal ellipsoids at 30% probability. The structure has been previously reported by Haynes and co-workers (CSD deposition # CCDC 864318 with the Cambridge Crystallographic Data Center).

The reaction gave rise to the clean formation of [Rh(κ^2-(P,P')xantphos)(CO)Cl] (Ia).

The bidentate κ^2-P,P' coordination mode of the utilized xantphos ligand (L$_1$) proceeds via formal displacement of a carbonyl ligand in the rhodium precursor and concomitant loss of the protonated acetylacetonate (acacH). Aniline hydrochloride provides a chlorido ligand and furnishes the protonation of the *acac* ligand prior to its displacement. However, coordination of aniline was not observed under these conditions. Rhodium xantphos species related to complex Ia were previously detected in the carbonylation of methanol as well,[254,255] but its possible role as (pre)catalyst in the HAM reaction has never been investigated.

We utilized isolated [Rh(κ^2-(P,P')xantphos)(CO)Cl] (Ia) as (pre)catalyst both [Rh(acac)(CO)$_2$] and xantphos (L$_1$) irradiating the mixture at 70 °C for 2x30 minutes: **3a** was obtained with the same regioselectivity observed in our optimal conditions but with a lower conversion of **1** (68%). In addition, 10% of aldehyde together with propyl benzene (12%) and 9% of **4** were observed by using this catalyst, thus demonstrating that is not optimal for the hydroformylation step. It can be hypothesized that Ia may suffer from significant decomposition under the applied reaction condition and excess of xantphos that can reconstitute the complex, is beneficial with respect to the application of the isolated complex Ia. On the contrary, directly irradiating the imine (obtained from aniline and 4-phenylbutylaldehyde) at 60 °C for 20 minutes in the presence of complex Ia, with 8.8 bar of syngas in a H$_2$O/TPGS-750-M mixture, **3a** was obtained in almost quantitative yields (98%). This finding may corroborate the hypothesis that [Rh(k^2-(P,P')xantphos)(CO)Cl] (Ia) is involved as pre-catalyst or active species in the imine hydrogenation step. The complex [(xantphos)Rh(CO)]$^+$ (Ib), which is possibly obtained after dissociation of the chlorido ligand, is known to be an active hydrogenation catalyst for carbonyl compounds.[256]

As further studies, we premixed free of aniline with HCl until pH 4.5 (2 equiv.) or with a stoichiometric amount of ZnCl$_2$ before the irradiation: both these reactions furnished very good results in the optimized HAM conditions. However, the use of aniline hydrobromide produced the expected product in only 47% isolated yields with lower regioselectivity (l/b 17:1). The excess of chloride ions does not seem to be crucial for the imine hydrogenation step of the HAM sequence and the decisive role of the chloride ion in anilinium salts (Table 4) likely originates from a reaction step involved in the aldehyde formation.

In course of these studies, the compositions of the reaction mixtures at different stages of the reaction (before addition of syngas, after addition of syngas and after the catalytic reaction) was investigated by extraction of the three aqueous reaction mixtures with CD$_2$Cl$_2$, respectively. The ^{31}P{^{1}H} NMR spectrum of the reaction mixture before application of syngas pressure displays four pronounced doublet resonances (indicated by &,§,#, and * in Figure 25) at 20.0 ppm (&, $^1J_{RhP}$ = 110.6 Hz), 20.3 ppm (§, $^1J_{RhP}$ = 107.9 Hz), 24.7 ppm (#, $^1J_{RhP}$ = 98.8 Hz), 25.2 ppm (*, $^1J_{RhP}$ = 98.8 Hz), with the $^1J_{RhP}$ coupling constant being in a typical range for rhodium(III) complexes.[257] The intensity of the latter two resonances decreases upon addition of syngas and the complexes cannot be detected after the catalytic reaction. In addition to the resonance corresponding to the excess xantphos ligand, a very broad resonance at approx. 39 ppm was detected, for which a $^1J_{RhP}$ coupling constant was not resolved.

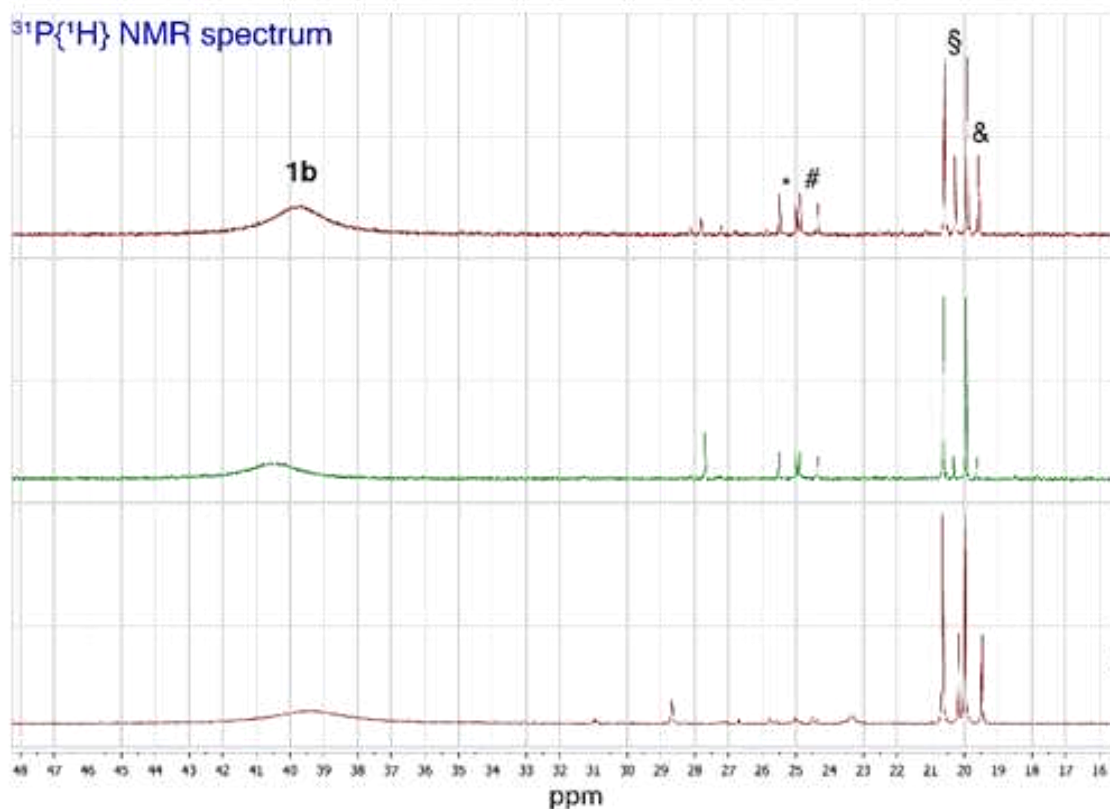**Figure 25.** Stacked ^{31}P {^{1}H} NMR spectra of CD_2Cl_2 extracts of the catalytic reaction mixture before syngas addition (top), after addition of syngas (middle) and after the catalytic reaction (bottom).
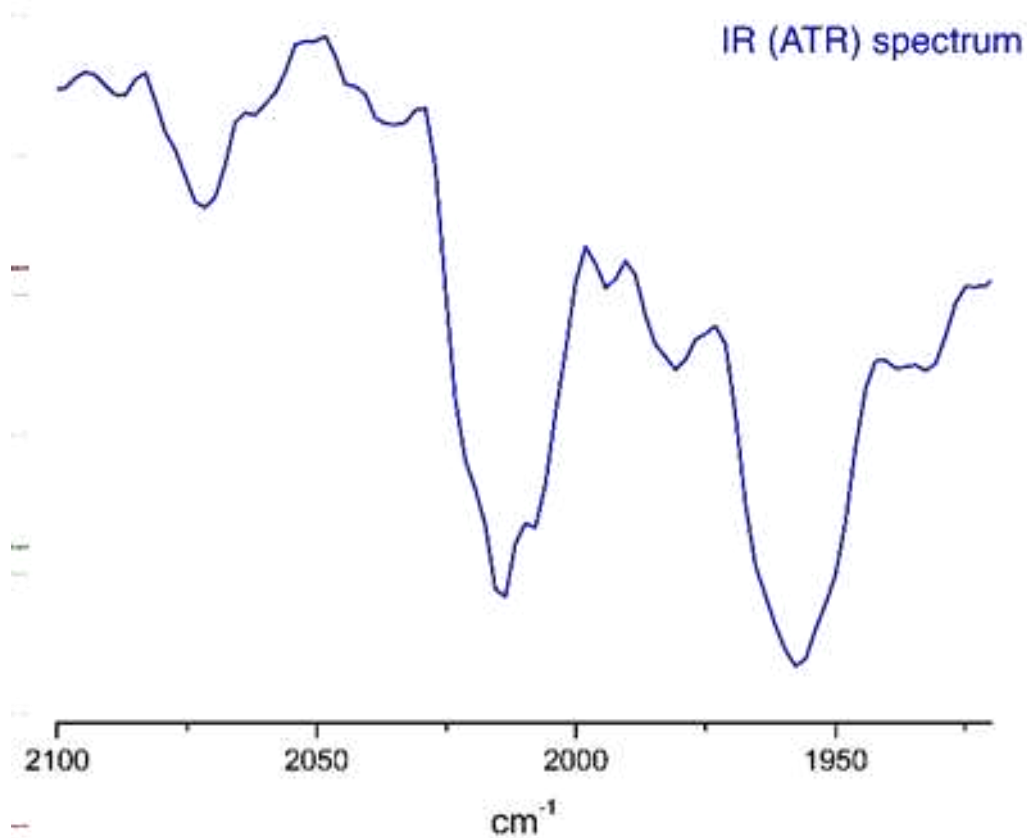

Figure 26. Section of the IR spectrum of the residue after evaporation of the reaction mixture, showing bands associated with the C–O-stretching vibration in Ia.

The chemical shift of 39 ppm is similar to the resonance previously reported for [(xantphos)Rh(CO)]$^+$ (Ib).[255] Interestingly, neither in the ^{31}P{^{1}H}NMR spectrum of the aqueous mixture nor in the CD$_2$Cl$_2$ extracts [(xantphos)Rh(H)(CO)$_2$] (A) could be detected, which was found in previous reports as the only detectable resting state in hydroformylation reactions with rhodium/xantphos system.[258–260] These findings are in line with previous reports, where under slightly acidic conditions [(xantphos)Rh(CO)]$^+$ (Ib) was formed and the partial suppression of the hydroformylation in favour of a catalytic hydrogenation was observed.[208,256] The absence of the typical hydroformylation resting state [(xantphos)Rh(H)(CO)$_2$] (A) was further supported by ^{1}H NMR spectroscopy at different stages, where no resonances corresponding to hydrido ligands were observed. The formation of rhodium (III) species without the involvement of dihydrogen and hydrido ligands suggest that an oxidative addition of the other reactants might be involved in the present example.

The IR spectrum of the evaporated methylene chloride extract of the catalytic reaction mixtures (measured by attenuated total reflection, ATR) showed two bands of low intensity at 1957 cm^{-1} and 2012 cm^{-1}, which are in line with the formation of [Rh(κ^2-(P,P')xantphos)(CO)Cl] (Ia) and/or a cationic rhodium(I) or a rhodium(III) complex (Figure 26). Additional evidence for the rhodium species present in the reported micellar catalysis system was gained by high resolution mass spectrometry (HR-MS) utilizing heated electrospray ionization (HESI) and liquid injection field desorption ionization (LIFDI) techniques. The HESI HR-MS spectra displayed several pronounced ion peaks next to the pattern observed for the surfactant TPGS-750M (Figure 27 top), whose identity was in part confirmed by MS-MS experiments in addition to the exact isotopic pattern.
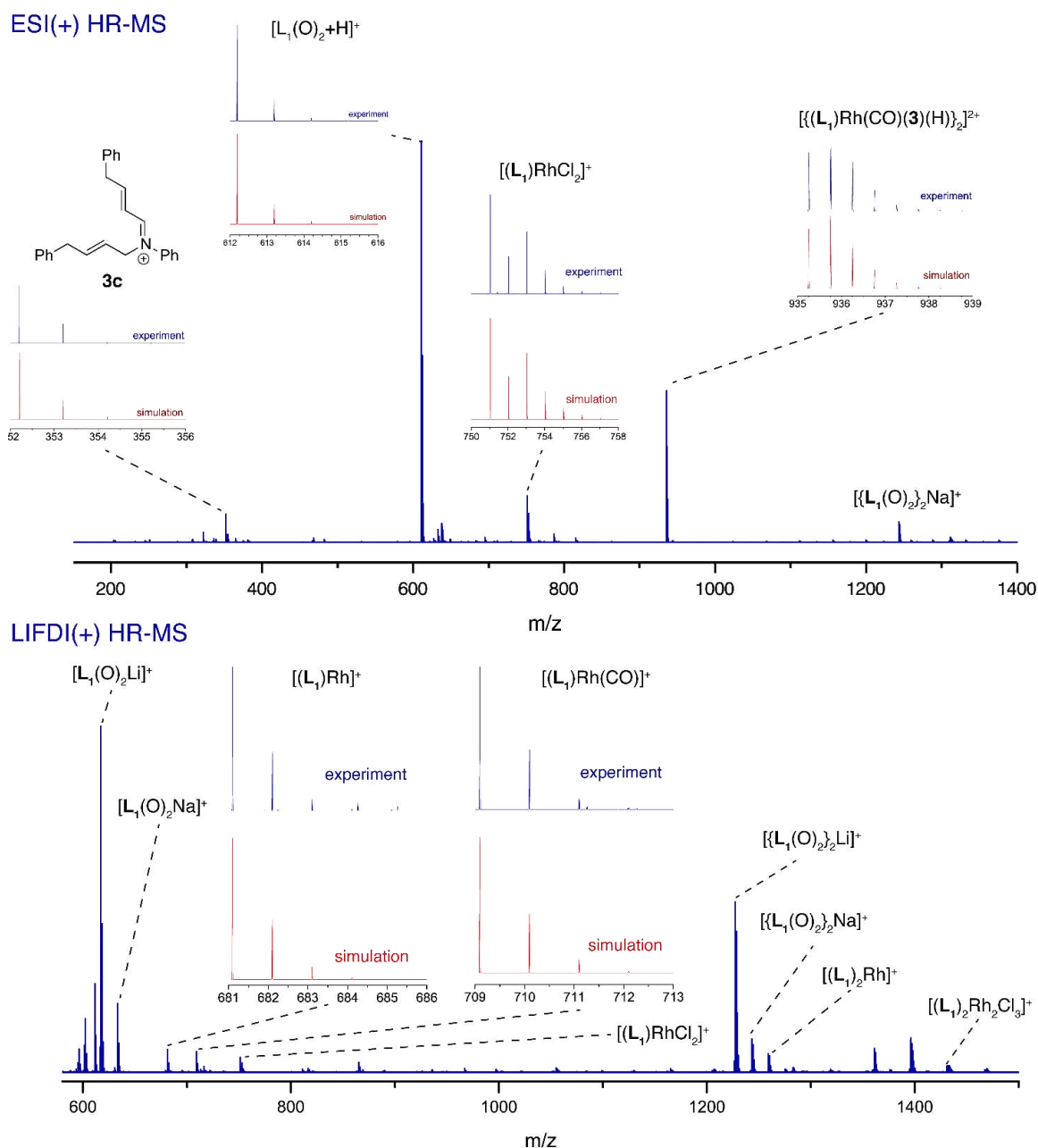
Figure 27. Positive mode HESI (top) and LIFDI (bottom) high resolution mass spectra with insets for selected ions, showing the agreement of measured and simulated isotopic patterns (L 1 = xantphos).

At approx. 226 m/z the protonated product amine (3a/3b) was identified, whereas the composition of the ion with 352 m/z agrees with an iminium salt (3c) formed by an unsaturated secondary amine Ph-CH$_2$-CH=CH-CH$_2$-NH-Ph (formed by the HAM reaction) and an α,β-unsaturated aldehyde Ph-CH$_2$-CH=CH-C(O)H. However, the formation of such a species is not in agreement with the commonly assumed reaction mechanism, which would involve a catalytic hydroformylation followed by imine formation and its subsequent catalytic hydrogenation.

Different ions with the general composition $[\{L_1(O)_2\}M]^+$ (M = H, Li, Na) and $[\{L_1(O)_2\}_2M]^+$ (M = Rh, Li, Na), containing the oxidized xantphos ligand with phosphine oxide groups instead of the terminal phosphines and a metal ion or a proton were detected with both ionization methods in the mass spectra. In addition, the HESI(+) mass spectrum shows a peak of approx. 20% intensity, whose isotopic pattern is in agreement with the rhodium(III) complex $[(L_1)RhCl_2]^+$ (L_1 = xantphos). A second diagnostic peak for a dicationic species is observed a approx. 935 m/z, which is in line with a product-bound (3 = 3a/3b) rhodium(I) dimer of the general composition $[\{(L_1)Rh(3)\}_2(H_2)]^{2+}$ (L_1 = xantphos). The LIFDI(+) mass spectrum (Figure 27 bottom) displays additional rhodium species associated with the catalytic HAM reaction: (i) a series of ions with the general composition $[(L_1)_2Rh_2Cl_n]^+$ (n = 3 – 5) suggest that potential hydrido and carbonyl ligands are replaced by ligands such as chlorido ligands and that oxidation to rhodium(III) species can easily occur; (ii) in addition to $[(L_1)RhCl_2]^+$ m/z $\approx$ 751), $[(L_1)Rh]^+$ m/z $\approx$ 681) and $[(L_1)Rh(CO)]^+$ (Ib, m/z $\approx$ 709) are observed in the LIFDI(+) high-resolution mass spectrum, which is in accordance with the observations made by NMR- and IR spectroscopy.

In previous investigations with rhodium/xantphos-based catalysts for hydroformylation reactions, it has been demonstrated that under slightly acidic conditions (e.g. caused by a silica support) protonation of the hydrido ligand in $[(L_1)Rh(CO)(H)]$ (Ic) and subsequent dihydrogen elimination is observed. In result, the active species for the hydroformylation reaction, $[(L_1)Rh(CO)(H)]$ (Ic), is deactivated by protonation and $[(L_1)Rh(CO)]^+$ (Ib) is formed instead, which is an active hydrogenation catalyst but remains inactive for hydroformylation.[256]

Remarkably, the reaction mixture utilizing the $[Rh(acac)(CO)_2]$/xantphos(L_1) catalytic system in the presence of allyl benzene (**1**) and aniline hydrochloride (**2a**) under 8.8 bar syngas (30 min, no microwave radiation applied) gave rise to the isolation of a few air-stable single crystals from DCM extracts of different batches, which were subjected to XRD analysis. The obtained crystal structure reveals a complex with the general composition $[(L_1)RhCl_2(CH=CH-CH_2Ph)]$ (B) entailing a rhodium centre in a distorted octahedral coordination sphere, where the xantphos ligand (L_1) binds in a tridentate fashion (κ^3-P,O,P') in a meridional mode (Figure 28).

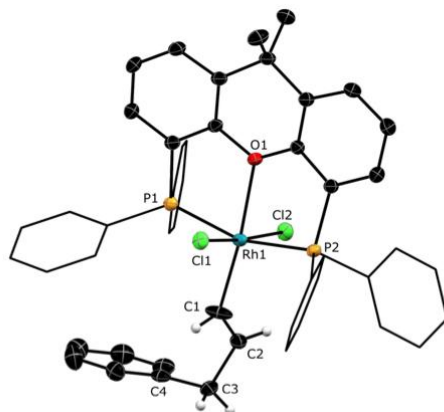**Figure 28.** Mercury plot of the molecular structure of [(L 1)RhCl 2 (CH=CH-CH 2 Ph)]complex (CB) derived from single crystal X-ray diffraction analysis. Hydrogen atoms omitted for clarity, except for vinyl ligand. PPh 2 phenyl rings drawn as wireframe. Thermal ellipsoids at 30% probability (structure deposited at CCDC #2176611).

Two chlorido ligands are located in apical positions (mutual *trans*) to the Rh center. The structure allows for the localization of a further Rh–C bond suggesting the formation of an organometallic Rh(III) complex decorated with a vinyl moiety, as a result of formal C–H-activation of allyl benzene.

A related resting state or termination product, $[(L_1)RhI_2(OAc)]$ (L_1 = xantphos), with an acyl instead of a vinyl ligand has been observed in the carbonylation of methanol with the rhodium-xantphos catalyst system. Moreover, the formation of the vinyl-complex $[(L_1)RhCl_2(CH=CH-CH_2Ph)]$ (B) instead of an η^1-coordinated ally complex appears somewhat surprising.[255]

To gain further insights for these findings, we performed quantum chemical investigations using density functional theory (DFT) on B97D3/def2-TZVP level of theory.
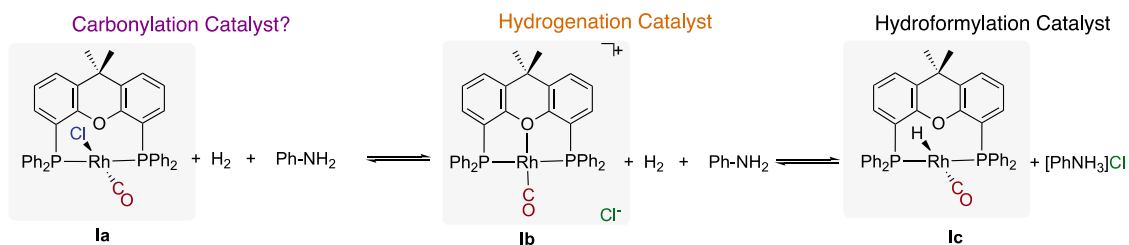
ΔH_{rel} / ΔG_{rel} in kcal/mol			
gas phase	-151.3 / -67.0	-46.8 / -57.9	0 / 0
H_2O (SMD)	-24.1 / 60.2	-13.9 / -25.0	0 / 0
toluene (SMD)	-74.9 / 9.4	-28.6 / -39.6	0 / 0

Scheme 3. Relative stability of possibly species in the presence of anilinium salts, obtained by density functional theory calculations (B97D3/def2-TZVP) for different models of solvation.

As starting point we considered the commonly assumed active species for hydroformylation reaction with rhodium/xantphos(L_1)-based catalysts (Scheme 3), [(L_1)Rh(CO)(H)] (Ic), and its conversion in the presence of anilinium salts to [(L_1)Rh(CO)]$^+$ (Ib) as well as the coordination of chloride counterions to Ib, yielding complex [(L_1)Rh(CO)Cl] (Ia). To estimate the influence of the micellar system on the relative stability of different species, an implicit solvation model based on density (SMD) for water as well as for toluene was used to account for highly polar and non-polar environments and the results were compared with those obtained for the gas phase, which might be taken as a rough approximation for a non-solvated state in a micelle. It turns out that the formation of [(L_1)Rh(CO)]$^+$ (Ib) is exergonic in all cases with respect to [(L_1)Rh(CO)(H)] (Ic). In the gas phase the formation of complex Ia is thermodynamically even more favourable. Moreover, the formation of [(L_1)Rh(CO)Cl] (Ia) is exothermic with respect to Ib and Ic, indicating that the chloride ion coordination to Ib is entropically disfavoured in common solvated systems under standard conditions. However, within a micelle this entropic contribution is likely to be compensated. In view of the possible entropy effects within a micelle and the high chloride ion concentration due to the utilization of [PhNH$_3$]Cl as well as the fact that complex Ia can be even isolated from the reaction with [PhNH$_3$]Cl, the formation of Ia from Ib seems facile, despite the large difference in Gibbs energy in water and toluene. We therefore considered complex Ia and Ib as potential active species for the catalytic reaction reported herein.

As several findings of this investigation contradict a viable hydroformylation mechanism for the reported micellar system (absence of a detectable resting state [(xantphos)Rh(H)(CO)$_2$] (A), detection of unsaturated products and the single crystal XRD structure of the vinyl complex B), we started to investigate alternative pathways of aldehyde formation. As the vinyl ligand in [(L_1)RhCl$_2$(CH=CH-CH$_2$Ph)] (B) is most likely formed by C–H-activation of allyl benzene (**1**), we investigated the C–H-activation of allyl benzene by Ia and Ib as well as the subsequent carbonylation leading to an α,β-unsaturated aldehyde (32) (Eq. 1 and Figure 28).

Eq. 1   **1**   +   CO $\xrightarrow{\text{Ia or Ib}}$ **31**
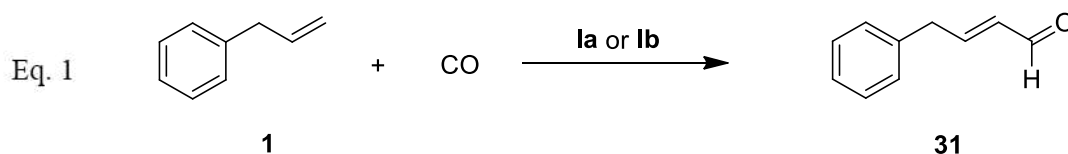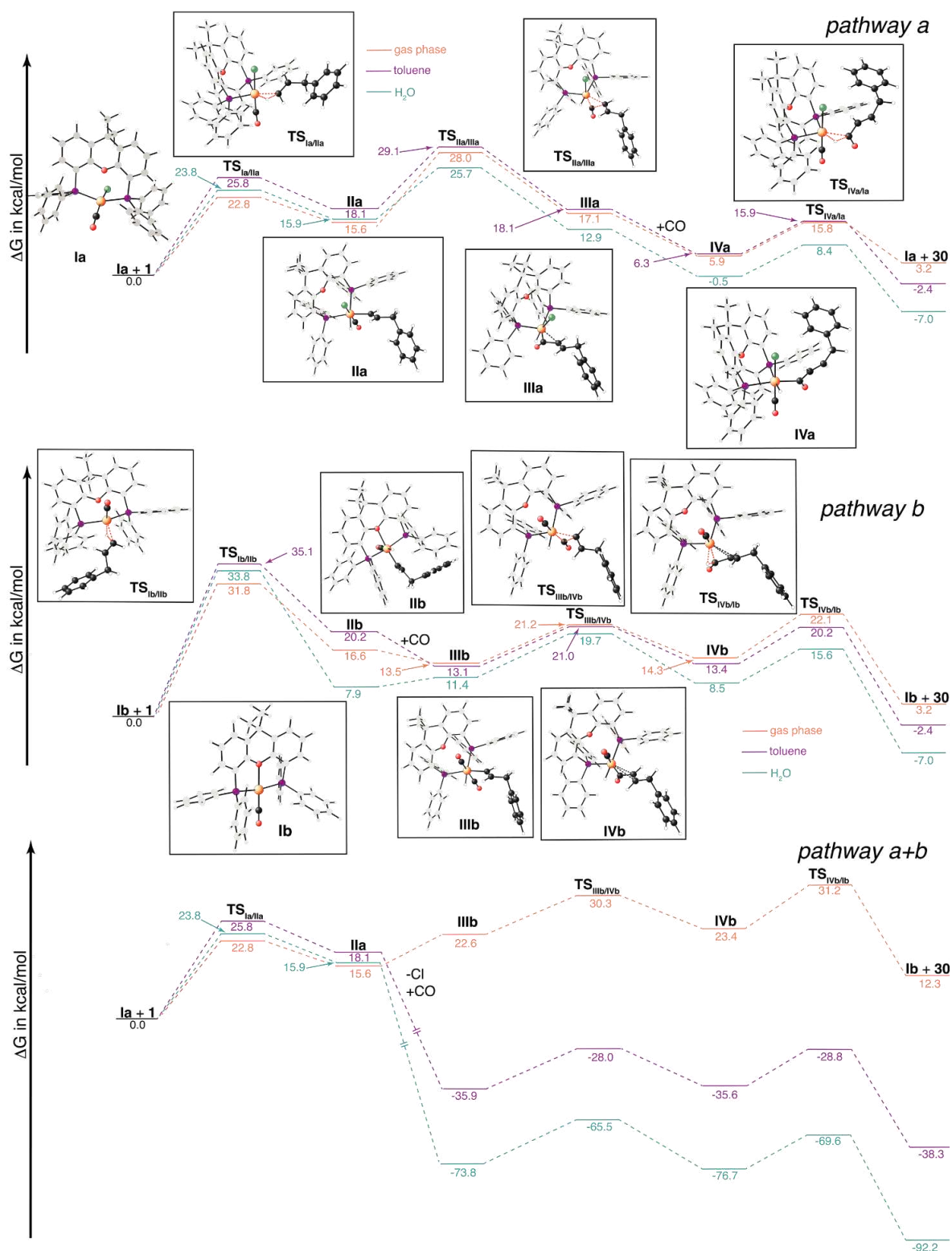
Figure 29. Mechanistic pathways based on density functional theory (DFT) calculations (G16, B97D3/def2-TZVP) with different approximations for the solvation in the present micellar system. For each reaction step different isomers were considered, but only the pathway with the most favourable isomers is drawn.

Previous quantum chemical investigations with the rhodium/xantphos(L_1) system revealed that different isomers of similar stability can be involved in the catalytic mechanism.[258,261] In

the current case we considered for each intermediate different isomers and searched independently for connecting transition states for the different isomers.

The species depicted in Figure 29 represent the isomers of the most favorable pathway among this series. Starting from $[(L_1)Rh(CO)Cl]$ (Ia, pathway a) the actual C–H-activation leading to the hydrido vinyl complex $[(L_1)Rh(CO)(Cl)(H)(CH=CH-CH_2Ph)]$ (IIa) was found to be uphill in Gibbs energy by 15.6…18.1 kcal/mol (depending on the model of solvation) with a barrier ($TS_{Ia/IIa}$) of 22.8…25.8 kcal/mol. Interestingly, the lowest value for the Gibbs energy of IIa and $TS_{Ia/IIa}$ is obtained in the gas phase. Complex IIa was subjected to a migratory insertion step of a carbonyl ligand into the Rh–C bond of the generated vinyl ligand, which is most favorable for the aqueous solvation model with a barrier of 25.7 kcal/mol ($TS_{IIa/IIIa}$) for the formation of the resulting acyl complex $[(L_1)Rh(Cl)(H)(C(O)-CH=CH-CH_2Ph)]$ (IIIa, $\Delta G_{SMD=H2O}$ = 12.9 kcal/mol). In case of IIIa the generated vacant coordination site is not occupied by the central oxygen atom of the xantphos ligand (L_1), which remained κ^2-coordinated. Instead, this intermediate is rather stabilized by an additional interaction of the C=C double bond in acyl ligand with the central rhodium atom.

The coordination of a carbonyl ligand provides further stabilization for the resulting complex $[(L_1)Rh(CO)(Cl)(H)(C\{O\}-CH=CH-CH_2Ph)]$ (IVa, $\Delta G_{SMD=H2O}$ = -0.5 kcal/mol), which is most significant with an aqueous solvation. The α,β-unsaturated aldehyde **31** is finally formed by C–H reductive elimination from IVa with a barrier ($TS_{IVa/Ia}$) of ΔG = 8.9…9.9 kcal/mol with respect to IVa. The formation of the aldehyde 30 from allyl benzene and CO is thermodynamically favourable in an aqueous ($\Delta G_{SMD=H2O}$ = -7.0 kcal/mol) and toluene environment ($\Delta G_{SMD=toluene}$ = -2.4 kcal/mol) as solvation model. With complex Ia as active species the migratory insertion step exhibits the highest barrier within this carbonylation pathway. Notably, the initial C–H activation is expected to be faster in the gas phase (or a non-solvated state within the micelle), while the following steps are more favorable in an aqueous or very polar environment.

An alternative pathway b involves the C–H bond activation of allyl benzene by complex $[(L_1)Rh(CO)]^+$ (Ib), which proceeds via a similar transition state ($TS_{Ib/IIb}$) with respect to Ia ($TS_{Ia/IIa}$), involving a concerted C–H oxidative addition that leads to $[(L_1)Rh(CO)(H)(CH=CH-CH_2Ph)]^+$ (IIb). Again, the relative stability of this intermediate with respect to Ib and allyl benzene strongly depends on the environment, ranging from ΔG = 7.9 kcal/mol for water to ΔG = 20.2 kcal/mol for toluene. Notably, the Gibbs energy of the

connecting transition state $TS_{Ib/IIb}$ was found to be between 31.8 and 35.1 kcal/mol, representing the highest barrier along *pathway b* (Figure 29).

It was found that the migratory insertion of a carbonyl ligand into the Rh–C bond is only facile after coordination of a second carbonyl ligand in *trans*-position to the first one, leading to $[(L_1)Rh(CO)_2(H)(CH=CH-CH_2Ph)]^+$ (IIIb, ΔG = 11.4…13.5 kcal/mol). The following migratory insertion proceeds via $TS_{IIIb/IVb}$ (ΔG = 19.7…21.2 kcal/mol) to the intermediate $[(L_1)Rh(CO)(H)(C\{O\}-CH=CH-CH_2Ph)]^+$ (IVb, ΔG = 8.5…14.3 kcal/mol), which contains the resulting acyl ligand that is additionally coordinated by the C=C double bond. The final C–H reductive elimination via $TS_{IVb/Ib}$ leads to the formation of the product aldehyde **31** and regeneration of Ib. Like in pathway a, all reaction steps apart from the initial C–H activation are expected to be faster in a very polar or aqueous environment. Against this background, the isolated complex $[(L_1)RhCl_2(CH=CH-CH_2Ph)]$ (B) may be formed from the intermediate $[(L_1)Rh(CO)(Cl)(H)(CH=CH-CH_2Ph)]$ (IIa) by protonation of the hydrido ligand, subsequent dihydrogen release after depressurisation and coordination of a second chloride ligand (Scheme 4). As the migratory insertion gives rise to the highest barrier in *pathway a* and as this reaction step can be hampered in cationic vinyl species as well,[81] dissociation of the carbonyl ligand seems likely in the absence of CO pressure, yielding complex B after a change of the xantphos (L_1) coordination mode from κ^2 to κ^3. This finding is supported by a Gibbs energy of -46.2 kcal/mol for the formation of B from IIa according to Scheme 4.
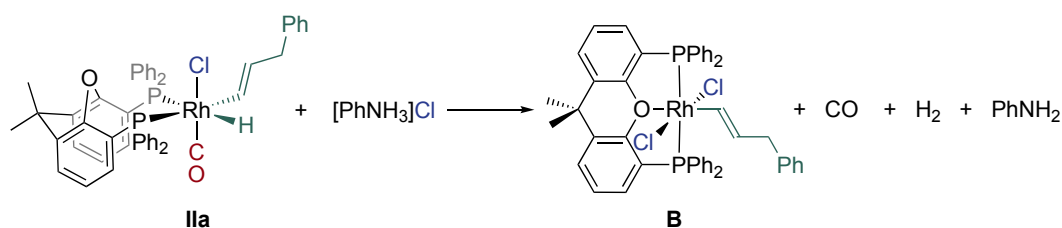
Scheme 4. Possible formation of the isolated complex B from the catalytic intermediate IIa.

The comparison of *pathway a* and *b*, and in particular the comparison of the transition states associated with C–H bond activation ($TS_{Ia/IIa}$ and $TS_{Ib/IIb}$). The proposed reaction mechanism for the carbonylation reaction involving neutral and cationic species is summarized in Scheme 5.
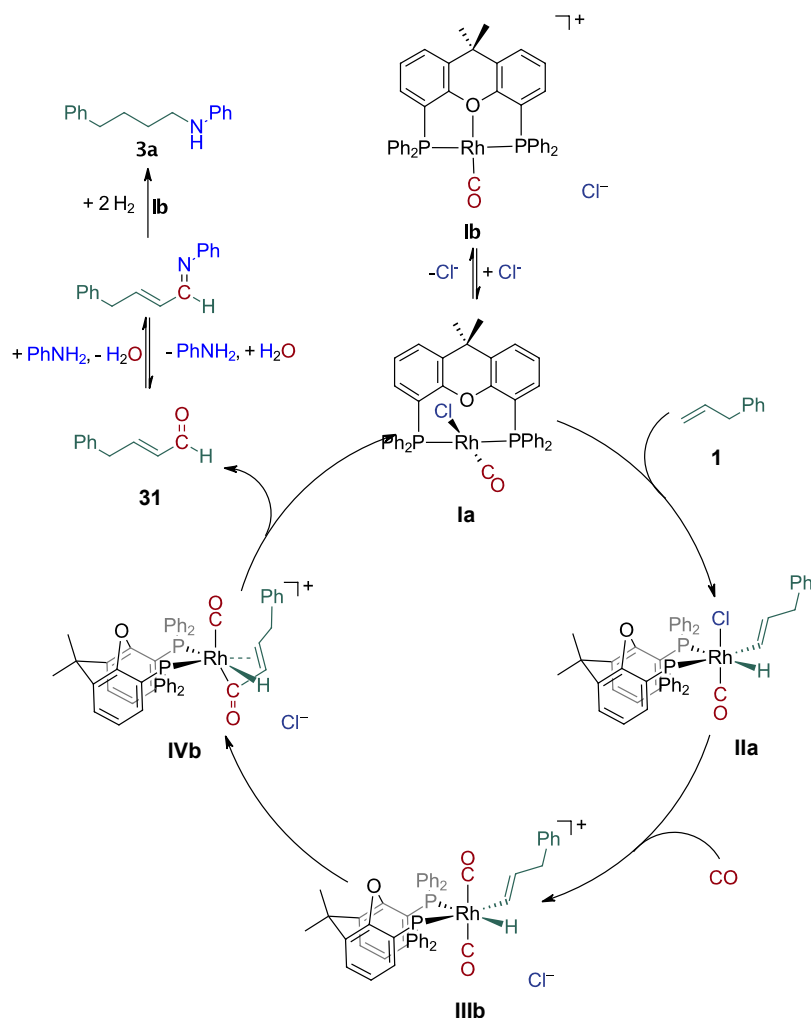
Scheme 5. Proposed carbonylation mechanism with a subsequent imine formation and hydrogenation.

The coordination of a chloride ion to $[(L_1)Rh(CO)]^+$ (Ib→Ia) reduces the barrier for this reaction step. In consequence, the chloride ions in the herein described micellar catalyst system can act as promoters, that accelerate the initial C–H bond activation step. Assuming that chloride ion coordination to Ib is fast and reversible in the described micellar system, the initial C–H bond activation by $[(L_1)Rh(CO)Cl]$ (Ia→IIa) may be followed by substitution of the chlorido- by a carbonyl ligand in $[(L_1)Rh(CO)(Cl)(H)(CH=CH-CH_2Ph)]$ (IIa→IIIb), making the following migratory insertion in $[(L_1)Rh(CO)_2(H)(CH=CH-CH_2Ph)]^+$ (IIIb→IVb) step more favorable by proceeding via *pathway b* (Figure 29 bottom).

A significant drop in Gibbs energy is calculated under standard conditions for the substitution step IIa→IIIb with the implicit solvation model for H_2O and toluene. However, this difference in Gibbs energy may be compensated by the comparably high chloride ion concentration in combination with concentration as well as entropy effects within the micelles.

Overall aqueous micellar systems are expected to provide milieus of different polarity for transition metal complexes and these findings suggest that availability and combination of different milieus along a mechanistic pathway can reduce reaction barriers and facilitate certain reaction sequences. These findings together with potentially high salt concentrations create unique conditions, which in turn, can favor alternative reaction pathways that do not suffer from low (regio)selectivity such as hydroformylation sequences that are commonly assumed to be viable for HAM reactions. Further support for the proposed reaction mechanism is provided by the results observed for the HAM of styrene. With our conditions, the reaction proceeds with a good regioselectivity for the linear product **29** (Scheme 1), confirming the formation of a linear aldehyde as the main product in the first reaction step. As HF of styrene under different conditions usually produces the branched aldehyde as the main reaction product with a low regioselctivity,[154,156,259] and the corresponding HAM process generates branched amines,[155] the reverse regioselectivity observed in the micellar catalytic conditions indicates an alternative mechanistic scenario, such as reported in Scheme 5.

To further investigate the reaction mechanism and the role of chloride ions, the reaction was also performed in NaCl or Bu_4NCl (tert-Butyl acetate, TBAC) solutions at different concentrations (3 M and 4 M). It is interesting to note that NaCl has a detrimental effect in the reaction outcome with an almost full recovery of the starting styrene, while Bu_4NCl furnishes the expected linear product **29** in similar yields (55%) with a slight better selectivity (l/b 6:1). Taking into account that Bu_4NCl probably increases the chloride ion concentration in the micelle, these findings support the hypothesis that (i) C−H activation occurs in the nonpolar/nonsolvated inner part of the micelle, while (ii) the following chlorido ligand dissociation rather takes place in the aqueous part or polar part of the system as the increased NaCl concentration hampers chloride ligand dissociation in the polar/aqueous part after C−H activation. By using free aniline and TBAC, no conversion was observed, and a poor 20% of **29** as a 1:1 mixture of linear/branched product was formed by adding TBAC into the reaction mixture with $Rh(acac)(CO)_2$ without xantphos. Further investigations on the reaction mechanism are actually ongoing with the aim to fully establish the compartments in which this novel type of reaction takes place.

2.5 Life cycle assessment

LCA is usually performed for industrial processes, but we decided, in collaboration with Prof. Maria Laura Parisi, to do the analysis to evaluate the overall impact of our process on the

environment. To do this, we implemented an attributional cradle-to-gate approach according to the ISO14040 family standards and Guidelines,[180,181] and the more completely elaborated ILCD Handbook Guidelines.[262] The unit chosen for the study is 1g of the target product **3a**, to which all the environmental burdens were attributed. We also decided to compare our results with other state-of-the-art procedures reported to obtain the same product (1g) (Scheme 6): an HAM protocol (Process B),[155] a hydrogen borrowing (HB) procedure (Alternative 1),[263] and two cross-coupling procedures (Alternatives 2[264] and 3[265]).
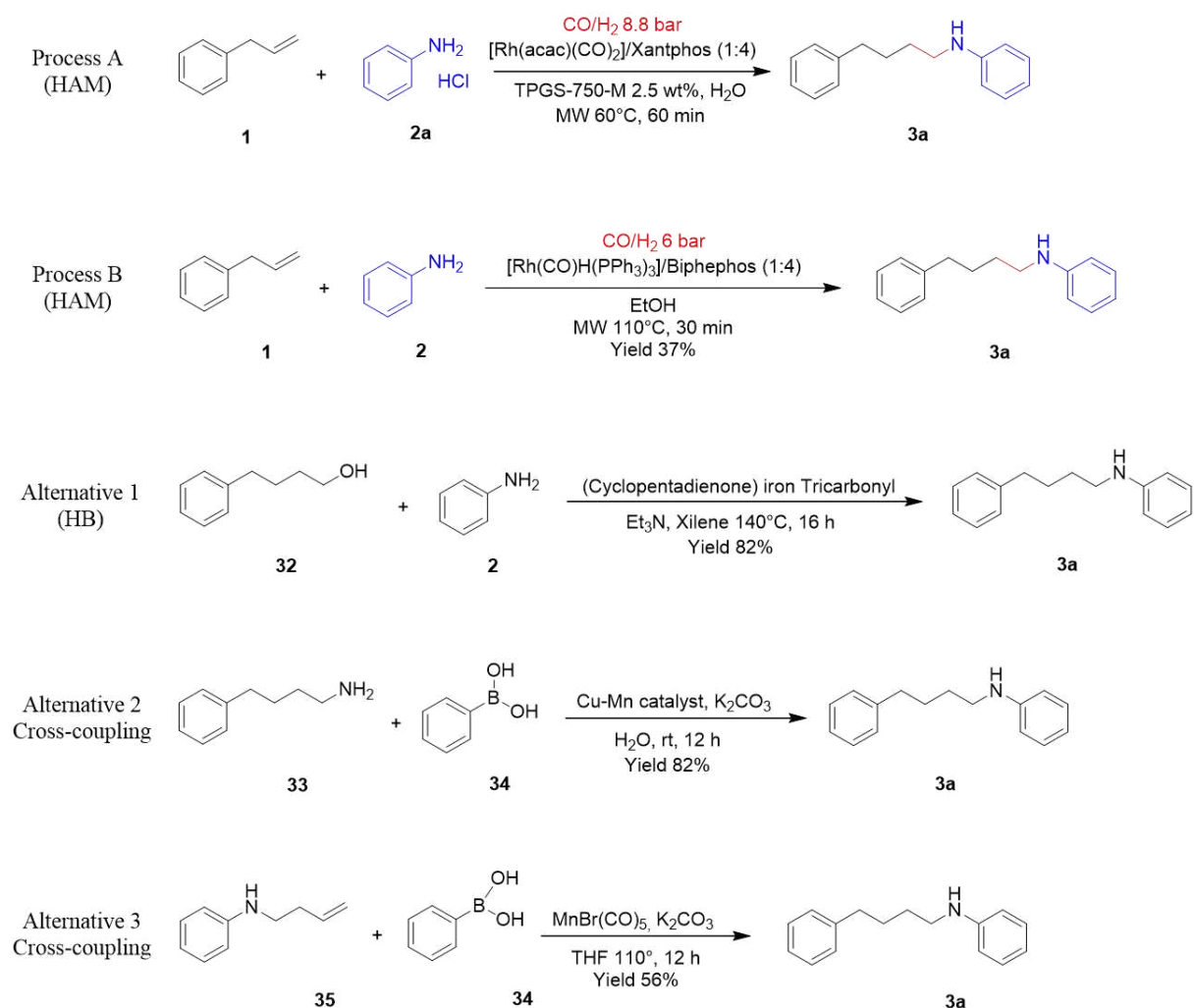
Scheme 6. Selected process for the synthesis of **3a** for th comparison in terms of environmental impact.

The LCI of the process was built based on primary laboratory data and system boundaries were defined to focus the foreground system on the synthetic procedure (Figure 30).

73
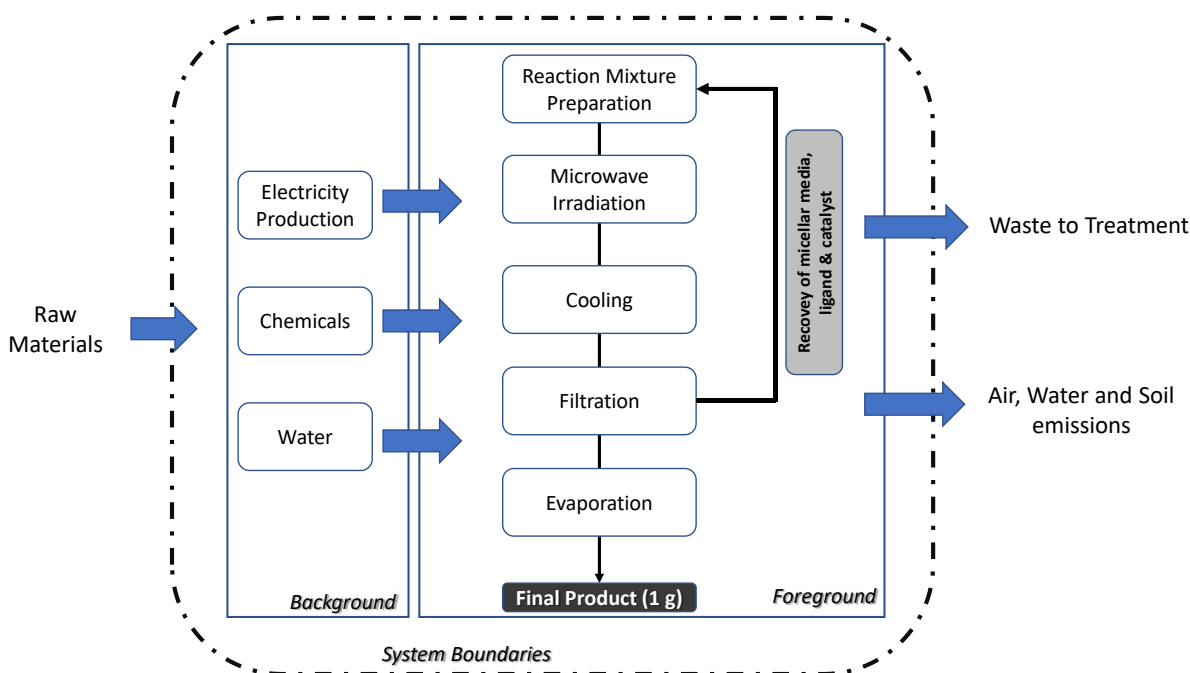
Figure 30. System boundaries of micellar catalysed HAM.

Meta-data, customized to generate data-sets for reactants, catalyst, ligand and reaction micellar media, and secondary data were taken from the Eco-invent database v. 3.6,[266] and equipment and instruments were accounted in terms of energy requirements for their functioning.

For the LCIA, ILCD 2011 Midpoint+ method (version 1.09), developed by the Joint Research Centre - European Commission was chosen. This method allows to obtain single scores, expressed in Eco-Points (Pt), on sixteen impact categories: i) climate change, ii) ozone depletion, iii) human toxicity: cancer effects and iv) non-cancer effects, v) particulate matter, vi) ionizing radiation HH, vii) ionizing radiation E, viii) photochemical ozone formation, ix) acidification, x) terrestrial eutrophication, xi) freshwater eutrophication, xii) marine eutrophication, xiii) freshwater ecotoxicity, xiv) land use, xv) water source depletion and xvi) mineral, fossil and ren resource depletion. LCA calculations are performed with software Simapro v.9. The characterization of the environmental impacts determined by our process is expressed in Figure 31.
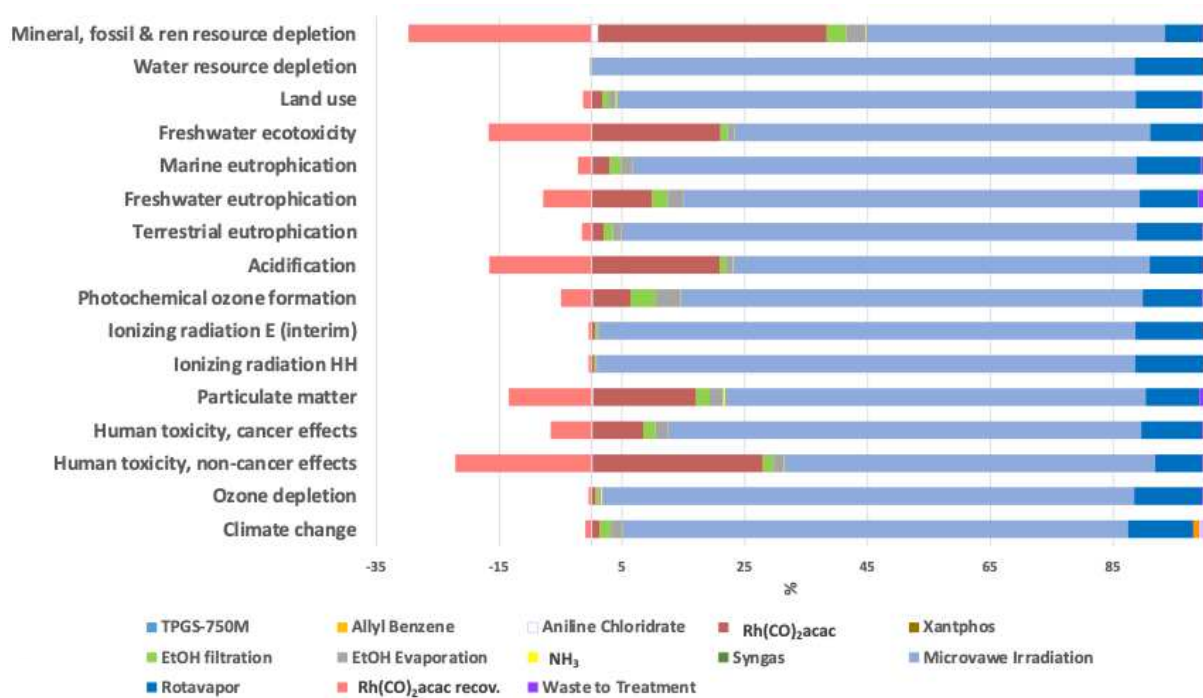
Figure 31. Characterization of the environmental impacts of the HAM process investigated in this work. Method: ILCD 2011 Midpoint+ V1.10 / EC-JRC Global, equal weighting / Characterization..
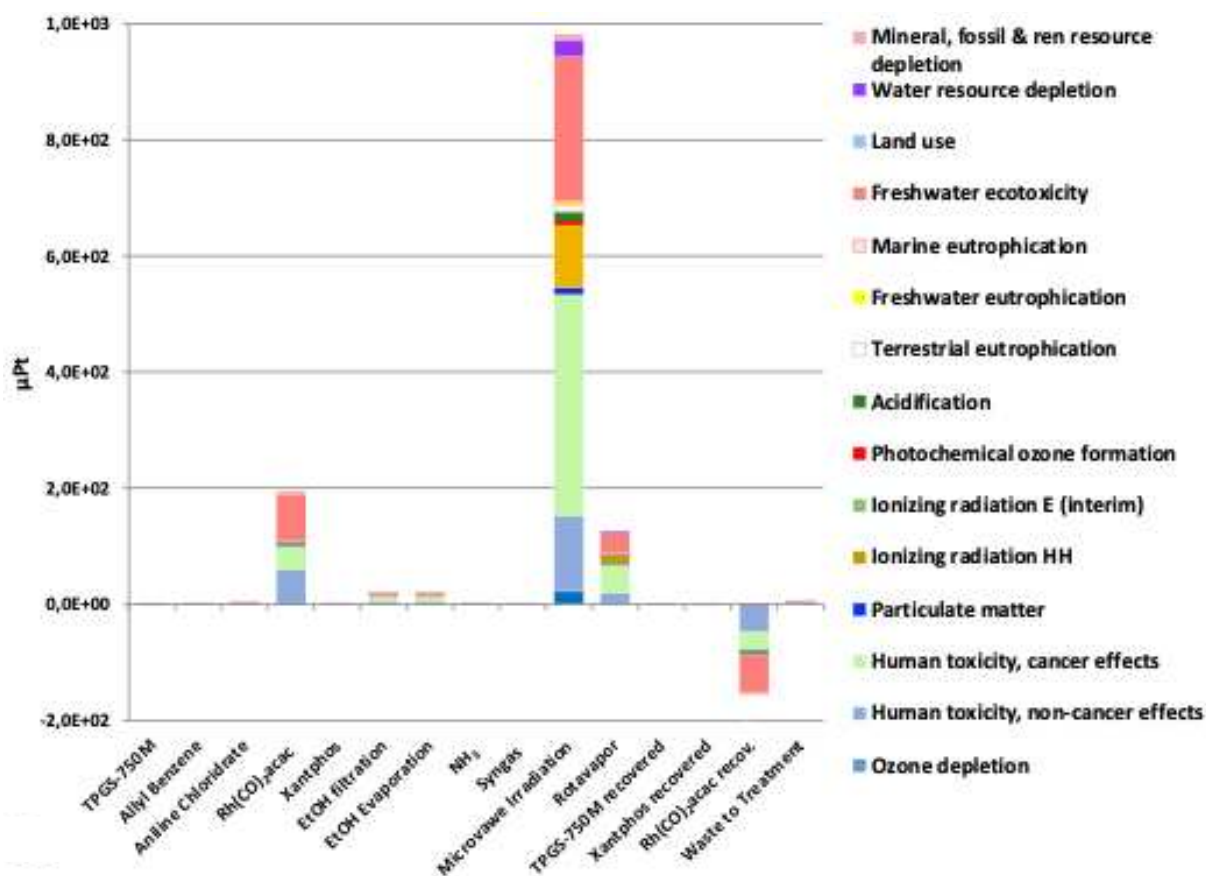
Figure 32. Single score calculation of the HAM process investigated in this work. Method: ILCD 2011 Midpoint+ V1.10 / EC-JRC Global, equal weighting / Single score.

75

The analysis of the single contribution of every component of the process shows that the bigger environmental burden is caused by electricity consumption, due to the use of microwave and rotavapor, the use of the catalyst and the EtOH filtration (Figure 32). The use of rotavapor is already reduced to minimum, since no extraction or chromatographic purification, that requires a big amount of organic solvent to remove under vacuum, are necessary, due to the exploitation of filtration of EtOH on the SCX columns.

The impact of catalyst is completely counterbalanced since it is possible to fully recycle it for several consequent processes. Ligand and micellar water phase do not bring the same contribution since these compounds have a low environmental footprint.

In terms of Eco-Points, the global single score of the process has a value of 1.20 mPt, the better profile between all the procedures compared (Table 9). The calculation of the score of any single component of the reaction confirmed that electricity consumption and the use of catalyst (completely counterbalanced) are the cause of the major impact on environment (Figure 32).

In any case, the micellar HAM protocol showed the better profile between all the procedures compared.

The global Impact of MW irradiation remains high both in relation with the other parameters and in absolute terms. Nonetheless, very good results are obtained in only 60 minutes, impossible in conventional heating condition.

To really evaluate the impact of the energy consumption due to the microwave heating, we decided to calculate the direct and indirect energy consumption of our protocol using CED indicator expressed in MJ and, once again, to compare it with the other procedures considered before (Figure 33).
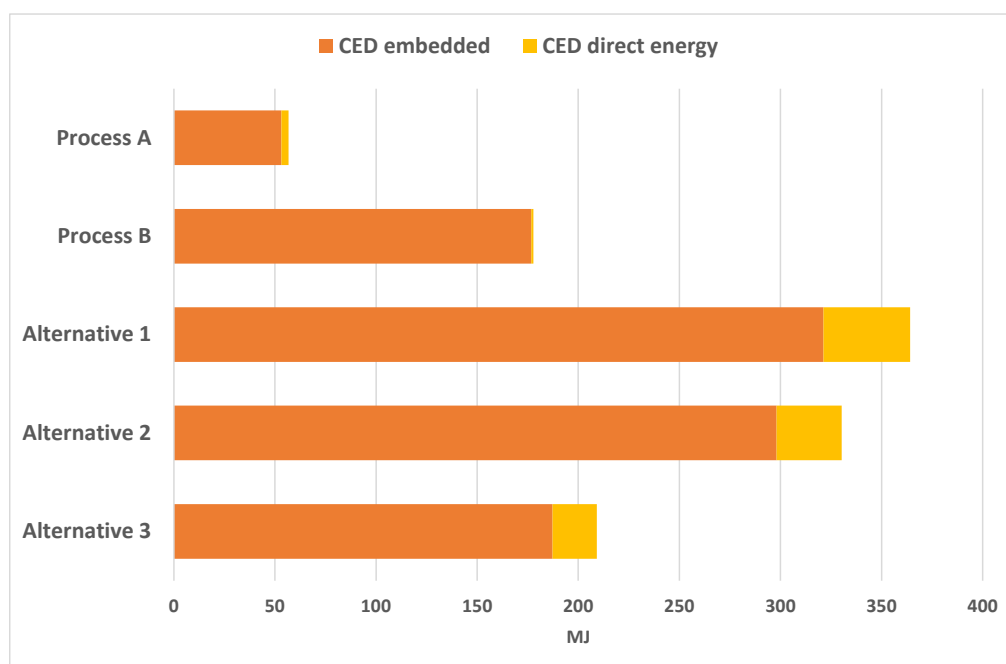
Figure 33. CED indicator results.

The obtained results confirm that our protocol performs better than the other evaluated procedures even in terms of energy demand, with a total consumption of 3.5 MJ of electricity required per gram of final compound and of 53.2 MJ of energy embedded in all the raw material used. Owing to the use of MW irradiation, the resulting high yields, the shorter reaction times, and the milder reaction conditions (in terms of syngas pressure and temperature) lower the overall environmental impact and energy consumption, giving rise to a superior sustainable reaction profile.

The scores of all the procedures, both in terms of global single scores and of energy consumption are reported in Table 9.

Table 9. Comparison of the scores in Eco-Points and MJ of the five processes.

Procedure	Eco-Point (mPt)	CED Embedded (MJ)	CED direct energy (MJ)
HAM (this work)	1.2	53.2	3.5
HAM (Process b)	3.7	176.7	1.1
Hydrogen borrowing (Alt 1)	12.6	321.3	42.8
Cross coupling (Alt 2)	10.3	298.1	32.2
Cross coupling (Alt 3)	8.1	187.3	21.9

3. CONCLUSIONS

In conclusion, the first protocol for the HAM of terminal alkenes with anilines exploiting micellar catalysis in water, without any impact of organic solvents, was developed. This protocol provides linear anilines as major isomers in mild reaction conditions heating with MW at 60 °C for 60 minutes with a low syngas pressure (H_2/CO 1:1 8.8 bar), using commercially available surfactant (TPGS-750-M), Rh catalyst and cheap ligand. The protocol is versatile and ensures high group tolerance as demonstrated by the large substrate scope. Anilines can be purified by filtration on SCX columns and the water-micellar phase with catalyst and ligand can be recycled several times without a dramatic impact on both regioselectivity and yields. A gram scale application was also successfully investigated.

Detailed mechanistic investigations were performed and suggest a different pathway from the expected hydroformylation/condensation/reduction sequence: an initial carbonylation step is viable, in which chlorine plays a decisive role.

LCA analysis demonstrates that the process has a lower environmental impact is in line with both principles of Green and, in some way, of Circular Chemistry.

4. EXPERIMENTAL SECTION

4.1 Material and methods

General informations: all reagents were used as purchased from commercial suppliers (i.e. Merck/Aldrich for surfactant except for Maripal 24/930 that was purchased on knodge.com, fluorochem for ligand, AlfaAesar for Rh catalysts) without further purification. Strata® SCX columns for solid phase extractions were purchased from Phenomenex®: surface area (m^2/g): 440-550; Average Pore size (Å): 58-78; Average Particle size (μm): 40-75. Flash column chromatography was performed in glass columns using Merk silica gel 60 Å, 230-400 mesh particle size Merck aluminium backed plates pre-coated with silica gel 60 (UV254) were used for analytical thin-layer chromatography and were visualized by staining with a solution ninhydrin in EtOH or a $KMnO_4$ solution. ^{1}H-, ^{13}C NMR spectra were recorded on 600 MHz MHz Brücker Advance NMR spectrometers. Deuterated chloroform and methanol were used as the solvents and chemical shift values (δ) are reported in parts per million (ppm) referring to the residual signals of the deuterated solvent (δ 7.26 for ^{1}H and δ 77.6 for ^{13}C in $CDCl_3$, δ 3.34 for ^{1}H and δ 49.00 for ^{13}C in CD_3OD). Data are represented as follows: chemical shift,

multiplicity (s = singlet, d = doublet, dd = doublet of doublets, dt = doublet of triplets, t = triplet, q = quartet, m = multiplet or multiple resonances, bs = broad singlet), coupling constant (J) in Hertz and the integration (δ) in ppm. Mass spectrometry data were collected on Varian Saturn 2000 GC/MS spectrometer with ion trap detector and equipped with 30 m OV-101 capillary column, splitting injector at 240 °C.

Methods for GC analysis: A) 40 °C - 3 min, 40-200 °C 10 °C/min – 17 min, 200-240 °C 20 °C/min – 5 min; B) 40 °C - 3 min, 40-200 °C 10 °C/min-1 min, 200-240 °C 20 °C/min – 8 min, 240-280 °C 20 °C/min, 8 min. Reactions carried out under MW dielectric heating were performed with a modified Discover microwave oven equipped with the 80 mL vial for reaction under pressure.

Scanning transmission electron microscopy (STEM) and Energy-dispersive X-ray spectroscopy (EDS) analysis was done using a FIB/SEM TESCAN GAIA 3 installed at the Microscopy Center (Ce.me.) at ICCOM-CNR (Firenze). DLS, Z-potential measurements were done using a Zetasizer NanoZS90 instrument (Malvern, Worcestershire, UK).

Computational methods: all reported structures were optimized by the density functional theory (DFT)[86] with Grimme's B97D3 functional[87] and the def2svp basis set[88,89] in the gas phase using Gaussian16.[90] Frequency analysis calculations of optimized structures were performed at the same level of theory (B97D3/def2svp) to characterize the structures to be minima (no imaginary frequency). Based on the B97D3/def2svp optimized geometries, the energy results were further refined by calculating the single point energy at the B97D3/def2tzvp level of theory.

4.2 Experimental procedures

4.2.1. Preparation of not commercially available starting alkenes

2-(Dec-9-en-1-yl)-1,3-dioxolane (1b)
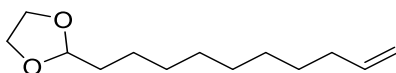
10-undecenal (2.38 mL, 12.0 mmol) was dissolved in anhydrous ethylene glycol (136 mL, 2436.0 mmol) and a catalytic amount of pTSA (193 mg, 1.02 mmol) in 40 mL of anhydrous toluene was added. The resulting mixture was heated at reflux for 1 h. The mixture was extracted with CH_2Cl_2 (3x50 mL), and the organic layer was evaporated after drying with anhydrous Na_2SO_4 furnishing the protected aldehyde. **YIELD**: 81%. **GC-MS** (*m/z*): 212; R_t = 16.563 (Method A). **^{1}H NMR** (600 MHz, CDCl$_3$) δ 5.83 – 5.68 (m, 1H), 4.95 (d, *J* = 17.1 Hz, 1H), 4.89 (d, *J* = 10.0 Hz, 1H), 4.80 (t, *J* = 4.5 Hz, 1H), 3.98 – 3.87 (m, 2H), 3.85 – 3.77 (m, 2H), 2.00 (q, *J* = 6.5 Hz, 2H), 1.66 – 1.59 (m, 2H), 1.41 – 1.22 (m, 12H). **^{13}C NMR** (151 MHz, CDCl$_3$) δ 139.1, 114.1, 104.7, 64.8, 33.9, 33.7, 29.5, 29.5, 29.3, 29.1, 28.9, 24.0.

2-(7-(phenylamino)heptyl)isoindolin-1,3-dione (1c).
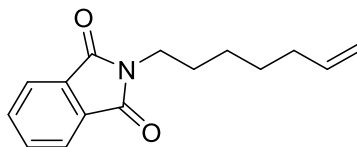
To a solution of phthalimide (0.400 g, 2.72 mmol) in dry CH_3CN (10 mL) were added K_2CO_3 (1.50 g, 10.88 mmol) and 1-bromoheptene (792 μL, 5.44 mmol). After the solution was refluxed for 15 h, CH_2Cl_2 (30 mL) was added to the reaction mixture, and this latter was then washed with H_2O (3x15 mL). The organic layer was evaporated under reduced pressure after drying with dry Na_2SO_4 The mixture was filtered, concentrated *in vacuo*, and the crude was purified by flash chromatography on silica gel (20% EtOAc in petroleum ether) to afford a clear product as a colorless oil. **^{1}H NMR** (600 MHz, $CDCl_3$) δ 7.83 (m, 2H), 7.70 (m, 2H), 5.78 (ddt, 1H), 5.00 (m, J = 17.1, 1.7 Hz,1H), 4.93 (ddt, J = 10.2, 2.3, 1.2 Hz, 2H), 3.68 (t, J = 7.3 Hz, 2H), 2.08 (q, J = 7.02 Hz, 2H), 1.69 (m, 2H), 1.44 (m, 2H) **^{13}C NMR** (151 MHz, $CDCl_3$) δ 168.46, 138.29, 133.88, 132.17, 123.18, 114.89, 99.99, 37.87, 33.26, 28.05, 26.10.

2-Allylisoindolin-1,3-dione (1d)
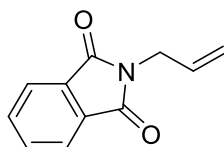
To a solution of phthalimide (1.5 g, 10.2 mmol) in DMF (10 mL) were added K_2CO_3 (1.41 g, 10.2 mmol) and allyl bromide (882 μL, 10.2 mmol). After the solution was stirred for 16 h at room temperature, EtO_2 (30 mL) was added to the reaction mixture, and this latter was then washed with $NaCl_{ss}$ (3x15 mL). The organic layer was evaporated under reduced pressure after drying with anhydrous Na_2SO_4 to afford the desired compound. **YIELD**: 87%. **GC-MS** (*m/z*): 187; R_t = 16.7 (Method A). **^{1}H NMR** (600 MHz, $CDCl_3$) δ 7.86 (dd, J = 5.3, 3.1 Hz, 2H), 7.72 (dd, J = 5.3, 3.1 Hz, 2H), 5.95 – 5.81 (m, 1H), 5.25 (dd, J = 17.0, 0.9 Hz, 1H), 5.20 (d, J = 10.2 Hz, 1H), 4.30 (d, J = 5.7 Hz, 2H). **^{13}C NMR** (151 MHz, $CDCl_3$) δ 167.9, 134.0, 132.1, 131.5, 123.3, 117.8, 40.1.

tert-Butyldimethyl(undec-10-en-1-yloxy)silane (1e)

TBDMSO ~~~~~⟨~~~⟩~7~=
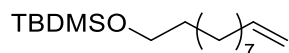
$NaBH_4$ (900 mg, 23.8 mmol) was added to a solution of 10-undecenal (2.38 mL, 11.9 mmol) in dry MeOH (50 mL) at 0 °C. After stirring for 1 h at 0 °C, NH_4Cl_{ss} (25 mL) was added. The organic phase was separated and evaporated after drying with anhydrous Na_2SO_4. Imidazole (1.16 g, 16.97 mmol) and TBDMSCl (2.56 g, 16.97 mmol) were added to a solution of the alcohol (11.31 mmol) in dry CH_2Cl_2 (35 mL) at 0 °C. Stirring was continued at room temperature for 4 h. H_2O (20 mL) was added and the organic layer was washed with $NaCl_{ss}$ (20 mL) and concentrated after drying with dry Na_2SO_4. The crude was purified by column chromatography on silica gel (20% EtOAc in petroleum ether) to afford the title compound as a colorless liquid. **YIELD**: 65%. **GC-MS** (*m/z*): 284; R_t = 17.9 min (Method A). **^{1}H NMR** (600 MHz, $CDCl_3$) δ 5.81 (ddt, *J* = 17.1, 10.2, 6.8 Hz, 1H), 5.03-4.98 (m, 1H), 4.95-4.91 (m, 1H), 3.59 (t, *J* = 6.7 Hz, 2H), 2.10-2.02 (m, 2H), 1.57-1.48 (m, 2H), 1.41-1.36 (m, 2H), 1.33-1.23 (m, 10H), 0. 09 (s, 9H), 0.05 (s, 6H). **^{13}C NMR** (151 MHz, $CDCl_3$) δ 139.2, 114.2, 63.3, 33.8, 32.8, 29.5, 29.4, 29.2, 28.9, 26.

Allyl benzoate (1f)
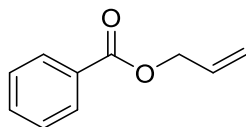
In a dry round bottom flask charged with benzoic acid (1.5 g, 12.30 mmol) and dry CH_2Cl_2 (40 mL) allyl alcohol (557 μL, 8.2 mmol) and DMAP (100 mg, 0.82 mmol) were added. The solution was cooled to 0 °C and stirred for 15 minutes before the addition of DCC (3.4 g, 16.4 mmol). The reaction was stirred at room temperature for 16 h under N_2. The mixture was filtered, concentrated *in vacuo*, and the crude was purified by flash chromatography on silica gel (20% EtOAc in petroleum ether) to afford a clear product as a colourless oil. **YIELD**: 53 %. **GC-MS** (*m/z*) 163; R_t= 12.670 min (Method A). **^{1}H NMR** (600 MHz, CDCl$_3$) δ 8.04 (d, *J* = 8.0 Hz, 2H), 7.52 (t, *J* = 7.3 Hz, 1H), 7.41 (t, *J* = 7.2 Hz, 2H), 6.02 (ddt, *J* = 16.3, 10.7, 5.4 Hz, 1H), 5.32 (dd, *J* = 50.5, 14.1 Hz, 2H), 4.80 (d, *J* = 5.4 Hz, 2H). **^{13}C NMR** (151 MHz, CDCl$_3$) δ 166.3, 133.1, 132.2, 130.1, 129.7, 128.5, 118.3, 65.6

4.2.2 General methods for the synthesis of benzoyl allyl amides

A mixture the appropriate carboxylic acid (16 mmol) in freshly distilled $SOCl_2$ (12 mL) was heated to reflux for 2 h, then cooled to room temperature and evaporated under vacuum to dryness to afford quantitatively corresponding acid chlorides. In a dried flask under N_2 atmosphere, a solution of allylamine (1.8 mL, 24 mmol) and Et$_3$N (3.3 mL, 24 mmol) in dry CH_2Cl_2 (25 mL) was cooled in an ice bath to 0 °C. Then, the appropriate benzoyl chloride (16 mmol) was added dropwise. The solution was allowed to warm to room temperature and then stirred for 16 h. H_2O (15 mL) was added and the organic layer was separated. The aqueous layer was extracted with CH_2Cl_2 (2 x 30 mL). The combined organic phases were washed with NaCl$_{ss}$ (15 mL), dried over dry Na_2SO_4 and the solvent removed. The crude product was purified by precipitation or column chromatography on silica gel.

N-Allyl-3,4,5-trimethoxybenzamide (1g)
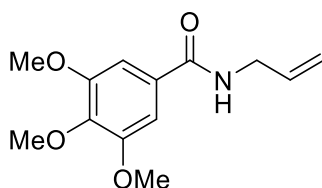
The crude was solubilized in the minimum amount of CH_2Cl_2 (10 mL) and petroleum ether (50 mL) was added slowly in order to obtain a white precipitate that was filtered on Büchner washing with cold petroleum ether. **YIELD**: 70%. **^{1}H NMR** (600 MHz, CDCl$_3$) δ 7.02 (s, 2H), 6.42 (bs, 1H), 5.96 – 5.55 (m, 1H), 5.20 (dd, J = 45.4, 13.7 Hz, 2H), 4.04 (d, J = 5.7 Hz, 2H), 3.87 (s, 9H). **^{13}C NMR** (151 MHz, CDCl$_3$) δ 167.1, 153.2, 140.9, 134.2, 129.9, 116.7, 104.4, 60.9, 56.4, 42.7.

N-Allyl-benzamide (1h)
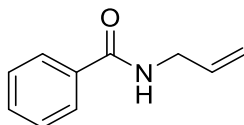
The product was purified by means of flash chromatography using EtOAc in petroleum ether. Yield: 78%. **^{1}H NMR** (600 MHz, CDCl$_3$) δ 8.28 (d, J = 8.4 Hz, 2H), 7.96 (d, J = 8.4 Hz, 2H), 6.45 (s, 1H), 6.01 – 5.88 (m, 1H), 5.28 (d, J = 17.1 Hz, 1H), 5.22 (d, J = 10.2 Hz, 1H), 4.11 (t, J = 5.3 Hz, 2H). **^{13}C NMR** (151 MHz, CDCl$_3$) δ 165.4, 149.6, 140.0, 133.4, 128.2, 123.9, 117.4, 42.8.

### 4.2.3 General methods for the hydroaminomethylation reaction

Method A (primary anilines): A 80 mL MW tube was charged with a solution of TPGS-750 M (2.5 wt% in H$_2$O, 3 mL), alkene (1 mmol) and aniline hydrochloride (0.75 mmol) were added and the mixture was stirred for 3- 5 minutes. Then, Xantphos (17 mg, 0.03 mmol) and [Rh(acac)(CO)$_2$] (2 mg, 0.0075 mmol) were added. The mixture was subjected to 3 cycles of vacuum/syngas inside the microwave cavity. Syngas was added since 130 psi (8.8 bar, syngas ratio H$_2$/CO 1:1) are detected and irradiated at 60 °C for 60 minutes cooling while heating

with a fixed power of 300 Watt. After irradiation, the mixture was cooled down to room temperature and the internal gas released by opening the external pressure valve.

The mixture was filtrated on SCX columns with EtOH (9 mL) to recover micellar phase with catalyst and ligand and NH_3 4% in EtOH (9 mL) to recover the final amine after evaporation. When necessary, the crude was purified by chromatography on silica gel (see single methods for ratios). The yields are referred to the isolated linear products. If not described, the branched products were not isolated from the crude materials.

Method B (secondary anilines): A 80 mL MW tube was charged with a solution of TPGS-750 M (2.5 wt% in H_2O, 3 mL), alkene (0.75 mmol) and aniline hydrochloride (0.90 mmol) were added and the mixture was stirred for 3- 5 minutes. Then, Xantphos (17 mg, 0.03 mmol) and [Rh(CO)$_2$acac] (2 mg, 0.0075 mmol) were added. The mixture was subjected to 3 cycles of vacuum/syngas inside the microwave cavity. Syngas was added since 130 psi (8.8 bar, syngas ratio H_2/CO 5:1) are detected and irradiated at 60 °C for 60 minutes cooling while heating with a fixed power of 300 Watt. After irradiation, the mixture was cooled down to room temperature and the internal gas released by opening the external pressure valve.

The mixture was filtrated on SCX columns with EtOH (9 mL) to recover micellar phase with catalyst and ligand and NH_3 4% in EtOH (9 mL) to recover the final amine after evaporation. When necessary, the crude was purified by chromatography on silica gel (see single methods for ratios). The yields are referred to the isolated linear products. If not described, the branched products were not isolated from the crude materials.

Method C (crystallized Rh-complex): A 80 mL MW tube was charged with a solution of TPGS-750 M (2.5 wt% in H_2O, 3 mL), alkene benzene (0.75 mmol) and aniline hydrochloride (0.90 mmol) were added and the mixture was stirred for 3 - 5 minutes. Then, [Rh(xant)(CO)Cl] (5.6 mg, 0.0075 mmol) were added. The mixture was subjected to 3 cycles of vacuum/syngas inside the microwave cavity. Syngas was added since 130 psi (8.8 bar) are detected and irradiated at 60 °C for 60 minutes cooling while heating with a fixed power of 300 Watt. After irradiation, the mixture was cooled down to room temperature and the internal gas released by opening the external pressure valve.

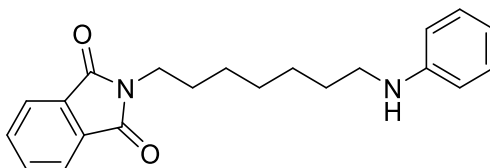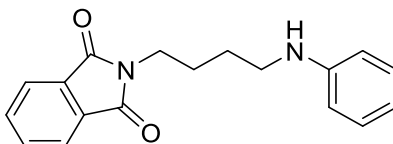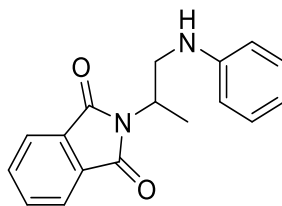## *N*-(4-phenylbutyl)aniline (3a)
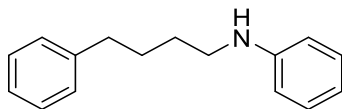
The titled compound was obtained following the general method A. Purification: 2% EtOAc in petroleum ether. **YIELD**: 92%. **GC/MS** (*m/z*): 225.0, R_t = 21.9 min (Method A). **¹H NMR** (600 MHz, CDCl₃) δ 7.31 (t, *J* = 7.5 Hz, 2H), 7.21 (m, 5H), 6.73 (t, *J* = 7.3 Hz, 1H), 6.64 (d, *J* = 7.8 Hz, 2H), 3.16 (t, *J* = 6.7 Hz, 2H), 2.69 (t, *J* = 7.7 Hz, 2H), 1,77 (m, 2H), 1.72-1.68 (m, 2H). **¹³C NMR** (151 MHz, CDCl₃) δ 148.21, 142.22, 129.28, 128.44, 128.38, 125.85, 117.44, 112.95, 44.05, 35.68, 29.11, 28.95.
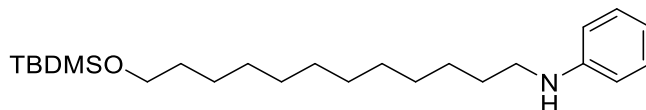
N-nonylaniline (7)
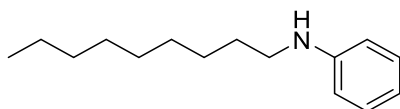
The titled compound was obtained following the general method A. Purification: 1% EtOAc in petroleum ether. **YIELD**: 69%. GC/MS (*m/z*): 220.7, R_t = 19.9 min (Method A). **¹H NMR** (600 MHz, CDCl₃) δ 7.19 (t, *J* = 7.5 Hz, 2H), 6.72 (t, *J* = 7.3 Hz, 1H), 6.66 (d, *J* = 7.74, 2H), 3.11 (t, *J* = 7.3 Hz, 2H), 1.63 (m, 2H), 1.41-1.37 (m, 2H), 1.29 (m, 12H), 0.89 (t, *J* = 7.1 Hz, 3H). **¹³C NMR** (151 MHz, CDCl₃) δ 148.02, 129.26, 117.57, 113.13, 44.38, 31.90, 29.58, 29.47, 29.43, 29.30, 27.18, 22.69, 14.14.

2-(7-(phenylamino)heptyl)isoindoline-1,3-dione (8)

The titled compound was obtained following the general method A. Purification: 1.5% EtOAc in petroleum ether. **YIELD**: 72%. **GC/MS** (*m/z*): 269.0 R_t = 35.7 min (Method B). **^{1}H NMR** (600 MHz, CDCl$_3$) δ 7.84 (m, 2H), 7.72 (m, 2H), 7.17 (t, 2H, *J* = 8.0 Hz), 6.70 (t, 1H, *J* = 7.4 Hz), 6.62 (d, *J* = 8.0 Hz, 2H), 3.69 (t, *J* = 7.4 Hz, 2H), 3.10 (t, *J* = 7.1 Hz, 2H), 1.69 (t, *J* = 6.7 Hz, 2H), 1.62 (t, *J* = 6.7 Hz, 2H), 1.39 (m, 6H). **^{13}C NMR** (151 MHz, CDCl$_3$) δ 168.51, 148.51, 133.90, 132.17, 129.24, 123.20, 117.0, 112.95, 112.69, 50.20, , 44.11, 37.97, , 34.09, 32.84, 28.82, 28.65, 28.52, 27.00, 26.77.

2-(4-(phenylamino)butyl)isoindoline-1,3-dione (9)

The titled compound was obtained following the general method A. Purification: 10% EtOAc in petroleum ether. **YIELD**: 34%. **GC/MS** (*m/z*): 294.0, R_t = 31.4 min (Method B). **^{1}H NMR** (600 MHz, CDCl$_3$) δ 7.83 (m, 2H), 7.71 (m, 2H), 7.15 (t, *J* = 7.6 Hz, 2H), 6.70 (t, *J* = 7.2 Hz, 1H), 6.64 (d, *J* = 7.7 Hz, 2H), 3.72 (t, *J* = 7.1 Hz, 2H), 3.15 (t, *J* = 6.6 Hz, 2H), 1.80-1.76 (m 2H), 1.69-1.64 (m, 2H). **^{13}C NMR** (151 MHz, CDCl$_3$) δ 168.60, 147.44, 134.23, 134.05, 132.00, 129.28, 123.49, 123.28, 117.99, 113.39, 43.89, 37.65, 26.44.
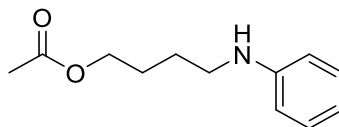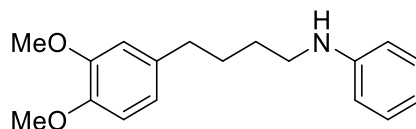
2-(1-(phenylamino)propan-2-yl)isoindoline-1,3-dione (9b)

The titled compound was obtained following the general method A. Purification: 9% EtOAc in petroleum ether. YIELD: 17%. **GC/MS** (*m/z*): 294, R_t = 28.7 min (Method B). **^{1}H NMR** (600 MHz, CDCl$_3$) δ 7.85 (m, 2H), 7.73 (m, 2H), 7.17 (t, *J* = 7.4 Hz, 2H), 6.72 (t, *J* = 7.3 Hz, 1H), 6.64 (d, *J* = 7.1 Hz, 2H), 3.78-3.74 (m, 1H), 3.72-3.68 (m, 1H), 3.07, (m, 1H), 1.04 (d, *J* = 6.9 Hz, 3H). **^{13}C NMR** (151 MHz, CDCl$_3$) δ 168.97, 134.11, 131,95, 129.32, 123.37, 113.40, 47.99, 41.40, 32.89, 16.24.

N-(12-(((tert-butyldimethylsilyl)oxy)dodecyl)aniline (10)

The titled compound was obtained following the general method A. Purification: 2% EtOAc in petroleum ether. **YIELD**: 87%. **^{1}H NMR** (600 MHz, CDCl$_3$) δ 7.18 (t, *J* = 7.6 Hz, 2H), 6.70 (t, *J* = 7.3 Hz, 1H), 6.62 (d, *J* = 7.8 Hz, 2H), 3.61 (t, *J* = 6.5 Hz, 2H), 3.11 (t, *J* = 7.1 Hz, 2H), 1.61 (m, 4H), 1.51 (m, 4H), 1,29 (m, 12H), 0.9 (s, 9H), 0.07 (s, 6H). **^{13}C NMR** (151 MHz, CDCl$_3$) δ 129.25, 117.44, 113.01, 63.37, 44.28, 32.91, 29.65, 29.61, 29.47, 27.19, 32.63, 29.65, 29.61, 29.47, 27.19, 26.02, 25.83, -5.23.

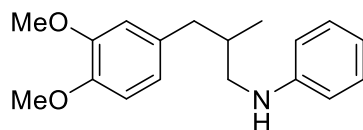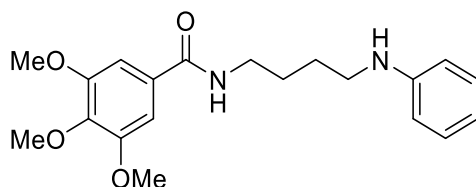## 4-(phenylamino)butyl acetate (11)

The titled compound was obtained following the general method A. Purification: 5% EtOAc in petroleum ether. **YIELD**: 99%. **GC/MS** (*m/z*): 207.2, R_t = 18.9 min (Method A). **^{1}H NMR** (600 MHz, CDCl$_3$) δ 7.18 (t, *J* = 7.5 Hz, 2H), 6.71 (t, *J* = 7.32 Hz, 1H), 6.62 (d, *J* = 7.7 Hz, 2H), 4.12 (t, *J* = 6.5 Hz, 2H), 3.17 (t, *J* = 6.7 Hz, 2H), 2.06 (s, 3H), 1.77 (m, 2H), 1.70 (m, 2H). **^{13}C NMR** (151 MHz, CDCl$_3$) δ 171.17, 147.94, 129.63,117.74, 112.99, 64.14, 43.74, 26.28, 25.99, 20.98.

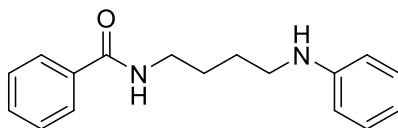## *N*-(4-(3,4-dimethoxyphenyl)butyl)aniline (12)

The titled compound was obtained following the general method A. Purification: 8% EtOAc in petroleum ether. **YIELD**: 31% **GC/MS** (*m/z*): 285.3, R_t = 27.0 min. (Method A). **^{1}H NMR** (600 MHz, CDCl$_3$) δ 7.60 (t, *J* = 8.0 Hz, 2H), 6.80-6.79 (d, *J* = 7.9 Hz, 1H), 6.76 (t, *J* = 6.8, 1H), 6.73-6.69 (m, 4H), 3.89 (s, 3H), 3.87 (s, 3H), 3.16 (t, 2H), 2.60 (t, *J* = 7.4 Hz, 2H), 1.72-1.69 (m, 4H). **^{13}C NMR** (151 MHz, CDCl$_3$) δ 148.81, 147.16, 134.80, 129.33,), 120.16, (113.81), 111.65, 111.16, (), 55.94, 44.65, 35.24, 29.11, 28.79.

N-(3-(3,4-dimethoxyphenyl)-2-methylpropyl)aniline (12b)

The titled compound was obtained following the general method A. Purification: 15% EtOAc in petroleum ether. **YIELD:** 11% **GC/MS** (*m/z*): 285.1, R_t = 25.1 min. (Method A). **¹H NMR** (600 MHz, CDCl₃) δ 7.16 (t, *J* = 8.0 Hz, 2H), 6.84 (d, J = 8.1, 2H), 6.79 (d, *J* = 8.0 Hz, 2H), 6.62 (d, *J* = 7.7 Hz, 2H), 3.88 (s, 3H), 3.86 (s, 3H), 3.09 (m, 1H), 2.97 (m, 1H), 2.70 (m, 1H), 2.49 (m, 1H), 1.78 (m, 1H), 0,99 (d, 3H). **¹³C NMR** (151 MHz, CDCl₃) δ 129.57, 129.36, 129.17, 121.06, 119.84, 112.14, 111.31, 111.02, 110.89, 55.89, 40.63, 29.72, 27.22, 18.16, 11.93.

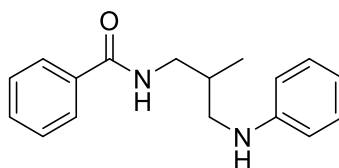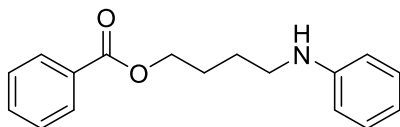### 3,4,5-trimethoxy-*N*-(4-(phenylamino)butyl)benzamide (13)

The titled compound was obtained following the general method A. Purification: 40% EtOAc in petroleum ether. **YIELD**: 29%. **¹H NMR** (600 MHz, CDCl₃) δ 7.15 (t, 2H, *J* = 7.56 Hz), 6.99 (s, 2H), 6.69 (t, *J* = 7.3 Hz, 1H), 6.61-6.60 (d, *J* = 7.7 Hz, 2H), 3.86 (s, 3H), 3.84 (s, 6H), 3.48-3.45 (m, 2H), 3.15 (t, *J* = 6.18 Hz, 2H), 1.75-1.68 (m, 4H). **¹³C NMR** (151 MHz, CDCl₃) δ 167.38, 153.16, 148.10, 140.82, 130.10, 129.26, 117.58, 112.97, 104.36, 60.88, 56.27, 56.22, 43.75, 39.93, 26.88, 23.87.

N-(4-(phenylamino)butyl)benzamide (14)

The titled compound was obtained following the general method A. Purification: 40% EtOAc in petroleum ether. **YIELD**: 30%. **¹H NMR** (600 MHz, CDCl₃) δ 7.75-7.74 (d, *J* = 7.3 Hz, 2H), 7.48 (t, *J* = 7.4, 1H), 7.40 (t, *J* = 7.6, 2H), 7.18 (t, *J* = 8.2 Hz, 2H), 6.72 (t, *J* = 7.3, 1H), 6.64-6.62 (d, *J* = 7.7 Hz, 2H), 6.44 (s, 1H), 3.50 (q, *J* = 6 Hz, 2H), 3.17 (t, *J* = 6.42, 2H), 1.77-1.70 (m, 4H). **¹³C NMR** (151 MHz, CDCl₃) δ 167.67, 148.07, 134.60, 131.42, 129.32, 128.57, 126.88, 117.59, 113.0, 43.69, 39.80, 27.34, 26.84.

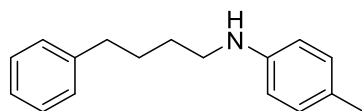## *N*-(2-methyl-3-(phenylamino)propyl)benzamide (14b)

The titled compound was obtained following the general method A. Purification: 40% EtOAc in petroleum ether. **YIELD**: 1%. **¹H NMR** (600 MHz, CDCl₃) δ 7.73 (d, *J* = 8.3 Hz, 2H), 7.49 (t, *J* = 7.4 Hz, 1H), 7.41 (t, *J* = 7.4 Hz, 2H), 7.19 (t, *J* = 8.4, 2H), 6.72 (t, *J* = 7.26 Hz, 1H), 6.67- (d, *J* = 7.7 Hz, 2H), 6.60 (s, 1H), 3.67-3.63 (m, 1H), 3.39-3.34 (m, 1H), 3.16 (m, 1H), 3.08 (m, 1H), 2.15 (m, 1H), 1.07 (d, *J* = 6.84 Hz, 3H). **¹³C NMR** (151 MHz, CDCl₃) δ 167.83, 148.13, 134.54, 131.47, 129.36, 117.63, 113.15, 48.29, 44.10, 33.31, 16.39.
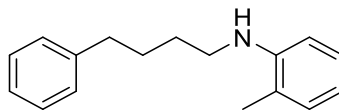
4-(phenylamino)butyl benzoate (15)

The titled compound was obtained following the general method A. Purification: 1.5% EtOAc in petroleum ether. **YIELD**: 79%. **GC/MS** (*m/z*): 269 R_t = 25.3 min (Method B). **¹H NMR** (600 MHz, CDCl₃) δ 8.04 (d, *J* = 7.3 Hz, 2H), 7.57 (t, *J* = 7.4 Hz, 1H), 7.44 (t, *J* = 7.5 Hz, 2H), 7.20 (t, *J* = 7.8 Hz, 2H), 6.76 (t, *J* = 7.0 Hz, 1H), 6.70 (d, *J* = 7.6 Hz, 2H), 4.38 (t, *J* = 6.4 Hz, 2H), 3.24 (t, *J* = 7.0 Hz, 2H), 1.91 (m, 2H), 1.82 (m, 2H). **¹³C NMR** (151 MHz, CDCl₃) δ 172.05, 133.81, 130.24, 129.58, 129.42, 128.51, 128.40, 119.26, 114.48, 64.54, 44.94, 26.36, 25.62.
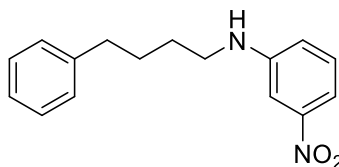
4-methyl-*N*-(4-phenylbutyl)aniline (16)

The titled compound was obtained following the general method A. **Purification**: 2% EtOAc in petroleum ether. **YIELD**: 89%. **GC/MS** (*m/z*): 239.8, R_t = 22.7 min (Method A). **¹H NMR** (600 MHz, CDCl₃) δ 7.31 (t, *J* = 7.4 Hz, 2H), 7.22 (m, 3H), 7.02 (d, *J* = 8.1 Hz, 2H), 6.57 (d, *J* = 8.3, 2H), 3.14 (t, *J* = 7.0 Hz, 2H), 2.68 (t, *J* = 7,6 Hz, 2H), 2.27 (s, 3H), 1-78-1.74 (m, 2H), 1.70-1.67 (m, 2H). **¹³C NMR** (151 MHz, CDCl₃) δ 145.96, 142.26, 129.76, 128.44, 128.36, 126.67, 125.82, 113.16, 44.43, 35.69, 29.75, 28.97, 20.41.
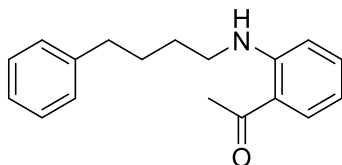
2-methyl-*N*-(4-phenylbutyl)aniline (17)

The titled compound was obtained following the general method A. Purification: 1% EtOAc in petroleum ether. **YIELD**: 94%. **GC/MS** (*m/z*): 239.8, R_t = 22.5 min min. (Method A). **¹H NMR** (600 MHz, CDCl₃) δ 7.33 (t, *J* = 7.4 Hz, 2H), 7.32 (d, *J* = 6.4 Hz, 2H), 7.16 (t, *J* = 6.8 Hz, 2H), 7.08 (d, *J* = 7.1 Hz, 1H), 6.69 (t, *J* = 7.4 Hz, 1H), 6.64 (d, *J* = 7.9 Hz, 1H), 3.21 (t, *J* = 6.9 Hz, 2H), 2.72 (t, *J* = 7.6 Hz, 2H), 2.15 (s, 3H), 1.81 (m, 2H), 1.75 (q, *J* = 6.8 Hz, 2H). **¹³C NMR** (151 MHz, CDCl₃) δ 128.88, 128.37, 127.23, 125.86, 60.40, 35.55, 29.72, 28.87, 21.05.

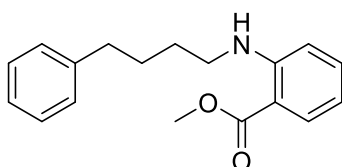## 3-nitro-N-(4-phenylbutyl)aniline (18)

The titled compound was obtained following the general method A. Purification: 4% EtOAc in petroleum ether. **YIELD**: 83%. **GC/MS** (*m/z*): 270.5, R_t = 28.8 min (Method B). **¹H NMR** (600 MHz, CDCl₃) δ 7.56 (d, *J* = 7.8 Hz, 1H), 7.44 (s, 1H), 7.31-7.27 (m, 3H), 7.20 (m, 3H), 6.91 (d, *J* = 7.2 Hz, 1H), 3.20 (t, *J* = 6.9 Hz, 2H), 2.69 (t, *J* = 7.5 Hz, 2H), 1.78-1.75 (m, 2H), 1.73-1.68 (m, 2H). **¹³C NMR** (151 MHz, CDCl₃) δ 144.44, 141.91, 129.71, 129.06, 128.43, 128.42, 125.96, 118.95, 112.04, 106.42, 43.89, 35.55, 29.74, 28.77, 28.64.

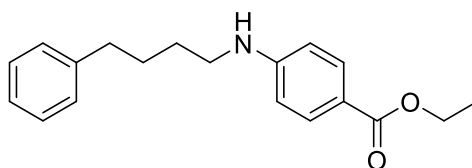## 1-(2-((4-phenylbutyl)amino)phenyl)ethan-1-one (19)

The titled compound was obtained following the general method A. Purification: 8% EtOAc in petroleum ether. **YIELD**: 96% **GC/MS** (*m/z*): 267.6, R_t = 24.9 min. (Method B) **¹H NMR** (600 MHz, CDCl₃) δ 7.81 (d, *J* = 7.9 Hz, 1H), 7.44 (t, *J* = 7.9 Hz, 1H), 7.27 (m, 2H), 7.16 (m, 3H), 6.99 (d, *J* = 8.2 Hz, 1H), 6.79 (t, 7.4 Hz, 1H), 3.24 (t, *J* = 6.2 Hz, 2H), 2.68 (t, *J* = 5.7 Hz, 2H), 2.62 (s, 3H), 1.81-1.77 (m, 4H). **¹³C NMR** (151 MHz, CDCl₃) δ 142.09, 135.06, 132.75, 131.75, 128.43, 128.34, 125.81, 112.32, 43.00, 35.59, 28.88, 28.54, 27.92.

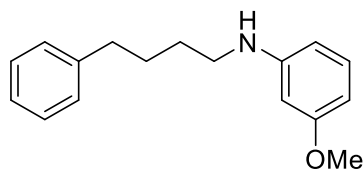## Methyl 2-((4-phenylbutyl)amino)benzoate (20)

The titled compound was obtained following the general method A. Purification: 2.5% EtOAc in petroleum ether. **YIELD**: 63% **GC/MS** (*m/z*): 283.0, R_t = 25.2 min (Method B). **¹H NMR** (600 MHz, CDCl₃) δ 7.94 (d, *J* = 9.4 Hz, 2H), 7.44 (t, *J* = 7.0 Hz, 1H), 7.27 (m, 2H), 7.20 (m, 3H), 6.97 (d, *J* = 7.9 Hz, 1H), 6.79 (t, *J* = 7.1 Hz, 1H), 3.89 (s, 3H), 3.25 (t, *J* = 6.8 Hz, 2H), 2.68 (t, *J* = 6.7 Hz, 2H), 1.81-1.78 (m, 4H). **¹³C NMR** (151 MHz, CDCl₃) δ 141.95, 134.88, 131.67, 128.43, 128.38, 125.87, 51.94, 35.52, 28.76, 28.14.

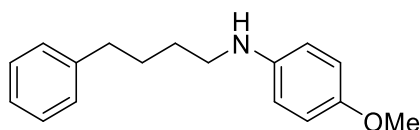## Ethyl 4-((4-phenylbutyl)amino)benzoate (21)

The titled compound was obtained following the general method A. Purification: 8% EtOAc in petroleum ether. **YIELD**: 60 % **GC/MS** (*m/z*): 294.0. R_t = 31.2 min (Method B). **¹H NMR** (600 MHz, CDCl₃) δ 7.87 (d, *J* = 8.64 Hz, 2H), 7.28 (t, *J* = 7.5 Hz, 2H), 7.19 (m, 3H), 6.55 (d, *J* = 8.5 Hz, 2H), 4.31 (q, *J* = 7.0 Hz, 2H), 3.18 (t, *J* = 6.4 Hz, 2H), 2.66 (t, *J* = 7.5 Hz, 2H), 1,76-1.73 (m, 2H), 1.68-1.66 (m, 2H), 1.36 (t, *J* = 7.1, 3H). **¹³C NMR** (151 MHz, CDCl₃) δ 171.19, 166.85, 141.96, 131.50, 129.09, 128.39, (126.14), 125.91, 111.67, 60.21, 43.53, 41.33, 28.75, 14.47.

3-methoxy-*N*-(4-phenylbutyl)aniline (22)

The titled compound was obtained following the general method A. Purification: 5% EtOAc in petroleum ether. **YIELD**: 99%. **GC/MS** (*m/z*): 256.0, R_t = 24.4 min (Method B). **¹H NMR** (600 MHz, CDCl₃): δ 7.30 (t, *J* = 7.4 Hz, 2H), 7.20 (m, 3H), 7.09 (t, *J* = 8.1 Hz, 1H), 6.29 (d, *J* = 8.0 Hz, 1H), 6.25 (d, *J* = 8.0 Hz, 1H), 6.19 (m, 1H), 3.78 (s, 3H), 3.14 (t, *J* = 6.9 Hz, 2H), 2.67 (t, *J* = 7.7 Hz, 2H), 1.78-1.73 (m, 2H), 1.70-1.66 (m, 2H). **¹³C NMR** (151 MHz, CDCl₃) 160.88, 149.50, 142.19, 129.98, 128.42, 128.36, 125.83, 106.20, 102.60, 98.93, 55.11, 44.07, 35.65, 29.04, 28.92.
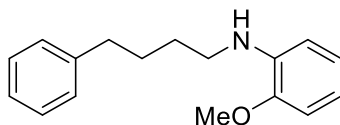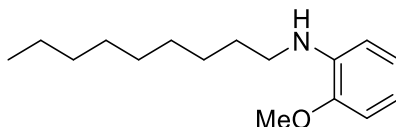
4-methoxy-*N*-(4-phenylbutyl)aniline (23)

The titled compound was obtained following the general method A. Purification: 2.5% EtOAc in petroleum ether. **YIELD**: 72%. **GC/MS** (*m/z*): 256.0, R_t = 24.2 min (Method B). **^{1}H NMR** (600 MHz, CDCl$_3$): δ 7.28 (m, 2H), 7.19 (m, 3H), 6.79 (d, *J* = 8.7 Hz, 2H), 8.28 (d, *J* = 8.3 Hz, 2H), 3.76 (s, 3H), 3.11 (t, *J* = 6.6 Hz, 2H), 2.65 (t, *J* = 7.6 Hz, 2H), 1.76 (m, 4H). **^{13}C NMR** (151 MHz, CDCl$_3$) δ 151.76, 141.72, 127.90, 127.83, 125.29, 114.40, 113.90, 55.32, 44.62, 35.16, 28.63, 28.44.

2-methoxy-*N*-(4-phenylbutyl)anilin (24)

The titled compound was obtained following the general method A. Purification: 2% EtOAc in petroleum ether. **YIELD**: 95% **GC/MS** (*m/z*): 254.8, R_t = 23.3 min (Method B). **^{1}H NMR** (600 MHz, CDCl$_3$) δ 7.30 (t, *J* = 7.2 Hz, 2H), 7.22 (d, *J* = 7.26 Hz, 3H), 6.89 (t, *J* = 7.5 Hz, 1H), 6.79 (d, *J* = 7.8 Hz, 1H), 6.69 (t, *J* = 7.6 Hz, 1H), 6.64 (d, *J* = 7.6 Hz, 1H), 3.86 (s, 3H), 3.17 (t, *J* = 6.6 Hz, 2H), 2.69 (t, *J* = 7.5 Hz, 2H), 1.79-1.71 (m, 4H). **^{13}C NMR** (151 MHz, CDCl$_3$) δ 146.31, 141.77, 137.66, 127.91, 125.26, 120.79, 115.88, 109.47, 108.88, 54.88, 43.18, 35.17, 29.21, 28.56, 28.48.

2-methoxy-*N*-nonylaniline (25)

The titled compound was obtained following the general method A. **Purification**: 5% EtOAc in petroleum ether. **YIELD**: 74% **GC/MS** (*m/z*): 249.2, R_t = 21.0 min (Method A). **^{1}H NMR** (600 MHz, CDCl$_3$) δ 6.89 (m, 1H), 6.80 (m, 3H), 3.87 (s, 3H), 3.14 (t, *J* = 6.8 Hz, 2H), 1.69 (m, 2H), 1.39 (m, 2H), 1.26 (m, 10H), 0.89 (t, *J* = 6.6 Hz, 3H). **^{13}C NMR** (151 MHz, CDCl$_3$) δ 155.50, 121.31, 55.50, 31.89, 29.72, 29.56, 29.45, 29.29, 28.97, 27.19, 22.69, 14.13.

N-methyl-*N*-(4-phenylbutyl)aniline (26)
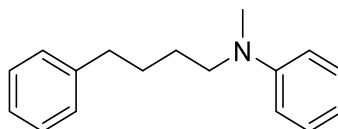
The titled compound was obtained following the general method B. Purification: 3% EtOAc in Hexane. YIELD: 67% **GC/MS** (*m/z*): 239.1, R_t = 21.9 min. (Method B). **^{1}H NMR** (600 MHz, CDCl$_3$) δ 7.29-7.19 (m, 7H), 6.70 (m, 3H), 3.33 (t, *J* = 8.1, 2H), 2.92 (s, 3H), 2.65 (t, *J* = 7.1, 2H), 1.65-1.62 (m, 4H). **^{13}C NMR** (151 MHz, CDCl$_3$) δ 129.17, 128.39, 125.78, 115.91, 112.14, 52.41, 35.81, 29.72, 29.02.

_N_-ethyl-_N_-(4-phenylbutyl)aniline (27)

The titled compound was obtained following the general method B. Purification: 3% EtOAc in Hexane. **YIELD**: 66% **GC/MS** (_m/z_): 253.0, R_t = 22.2 min (Method B). **^{1}H NMR** (600 MHz, CDCl₃) δ 7.32 (t, _J_ = 7.3 Hz, 2H), 7.24 (m, 5H), 6. 68 (m, 3H), 3.38 (q, _J_ = 6.7 Hz, 2H), 3.31 (t, _J_ = 6.5 Hz, 2H), 2.70 (t, _J_ = 7.1 Hz, 2H), 1.73-1.69 (m, 4H), 1.17 (t, _J_ = 6.84 Hz, 3H). **^{13}C NMR** (151 MHz, CDCl₃) δ 148.01, 142.38, 129.29, 128.43, 128.37, 125.82, 115.38, 111.88, 50.29, 44.97, 35.87, 29.08, 27.28, 12.30.
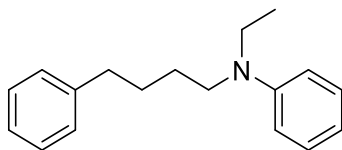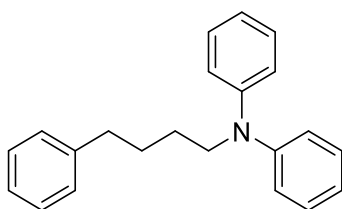
_N_-phenyl-_N_-(4-phenylbutyl)aniline (28)

The titled compound was obtained following the general method B. Purification: 3% Et₂O in petroleum ether. **YIELD**: 59% **GC/MS** (_m/z_): 301.0, R_t = 25.4 min (Method B). **^{1}H NMR** (600 MHz, CDCl₃): δ 7.29 (m, 6H), 7.19 (m, 6H), 6.63 (m, 3H), 3.26 (t, _J_ = 6.2 Hz, 2H), 2.64 (t, _J_ = 7.3 Hz, 2H), 1.68-1.63 (m, 4H). **^{13}C NMR** (151 MHz, CDCl₃) δ 129.21, 128.38, 125.78, 115.32, 111.83, 50.88, 35.81, 30.17, 27.10.

N-(3-phenylpropyl)aniline (29)

The titled compound was obtained following the general method A. Purification: 2% EtOAc in petroleum ether. Yield: 50%. **GC/MS** (*m/z*): 212.0, R_t = 20.964 min (Method A). **^{1}H NMR** (600 MHz, CDCl$_3$) δ 7.29 (t, *J* = 7.3 Hz, 2H), 7.21 (t, 5H), 6.80 (t, *J* = 7.3 Hz, 3H), 6.74 (d, *J* = 7.8 Hz, 1H), 3.18 (t, 7.2 Hz, 2H), 2.24 (t, *J* = 7.7 Hz, 2H), 2.03-1.98 (m, 2H). **^{13}C NMR** (151 MHz, CDCl$_3$) δ 141.39, 129.5, 129.36, 126.02, 119.00, 114.30, 44.71, 30.46, 29.71.

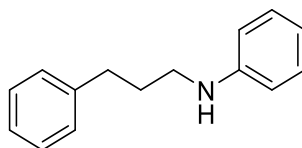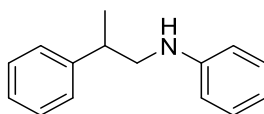## N-(2-methyl-3-phenylpropyl)aniline (29b)

the titled compound was obtained following the general method A. Purification: 2% EtOAc in petroleum ether. Yield: 10%. **GC/MS** (*m/z*): 212.0, R_t = 19.8 min. **^{1}H NMR** (600 MHz, CDCl$_3$): δ 7.34 (t, *J* = 7.1 Hz, 2H), 7.24 (m, 3H), 7.17 (t, *J* = 7.6 Hz, 2H), 6.71 (t, *J* = 7.2 Hz, 1H), 6.61-6.60 (d, *J* = 7.9 Hz, 2H), 3.35 (m, 1H), 3.08 (m, 1H), 1.52 (d, 3H). **^{13}C NMR** (151 MHz, CDCl$_3$) δ 133.86, 129.25, 128.69, 127.26, 127.65, 123.18, 113.18, 51.08, 39.18, 19.75.

4.2.4 Investigation of the pre-catalyst via stoichiometric reaction of ligand and metal precursor and isolation of [rh(κ^2-(p,p')xantphos)(CO)cl] (complex i)

Synthesis: [Rh(κ^2-(P,P')xantphos)(CO)Cl] (Complex I) can be prepared in a straightforward reaction starting from [Rh(acac)(CO)$_2$] precursor and xantphos. Bidentate coordination via the phosphine moieties is observed via the formal displacement of a carbonyl ligand and concomitant loss of the *acetylacetone*. The aniline hydrochlorid likely servs as the acid providing a chloro ligand and furnishing protonation of *acac*.

All manipulations were performed in a Glovebox under inert argon atmosphere.

A 25 mL vial equipped with a magnetic stir bar was charged with 58 mg (0.1 mmol, 1 eq) of xantphos and [Rh(acac)(CO)$_2$] was added (26 mg, 0.1 mmol, 1 eq). Subsequently, the mixture was dissolved in 3 mL dry THF. Upon vigorous gas formation, a clear red solution was formed and 15 mg (12 eq) aniline hydrochloride was added. The hydrochloride was only sparsely soluble in the mixture. Addition of 44 mg of aniline (4.7 eq.) and 2 mL of THF gave rise to a slow formation of a clear orange solution. However, an orange microcrystalline product started slowly to precipitate. The mixture was allowed to stir for 2 h at rt before the mother liquor was decanted.

The obtained orange solid was subsequently dissolved in 0.8 mL CH$_2$Cl$_2$ and layered with *n*-hexane to give single crystals of [Rh(κ^2-(P,P')xantphos)(CO)Cl] x CH$_2$Cl$_2$ (**complex I**) also suitable for XRD analysis. The compound has been previously reported and fully characterized by Deb et al. (see J. Mol. Catal. A: Chem. 2020, 326, 21) via the reaction of [Rh(CO)$_2$Cl]$_2$ and xantphos (1:1 in CH$_2$Cl$_2$). The crystal structure has been previously reported by Haynes and co-workers. The compound has been synthesized in a similar way as reported by Deb et al. but using EtOH as solvent instead of CH$_2$Cl$_2$ (Organometallics 2011, 30, 6166-6179). The mother liquor (THF) can be layered with Et$_2$O and *n*-hexane (2:1:2) to give a second fraction of compound **I**. After 24 h at r.t. red crystals formed, which were subjected to another X-ray diffraction study. The structure confirms the structure obtained from the crystallization in CH$_2$Cl$_2$. However, THF was found co-crystallized instead of CH$_2$Cl$_2$.

4.2.5 Investigation of the catalytic mixture

A 80 mL MW tube was charged with a solution of TPGS-750-M (2.5 % in H$_2$O, 3 mL), allyl benzene (11.25 mmol) aniline hydrochloride (13.50 mmol), xantphos (255 mg, 0.45 mmol) and [Rh(acac)(CO)$_2$] (30 mg, 0.11 mmol) were added and the mixture was stirred at room temperature for 5-10 min. The mixture was subsequently subjected to three cycles of vacuum/syngas. The mixture was finally pressurized with syngas until a pressure of 130 psi (8.8 bar) was detected. The mixture was allowed to react for 30 min at r.t. before the pressure was released. A few single crystals formed slowly from the reaction mixture, which were subjected to scXRD analysis.

4.3 LCA calculations

Impact Category	Unit	TPGS-750M	Allyl Benzene	Aniline Chloridrate	Rh(CO)acac	Xantphos	EtOH filtration	EtOH Evaporation	NH3	Syngas	MW Irradiation	Rotavapor	TPGS-750M recovered	Xantphos recovered	Rh(CO)acac recovered	Waste to Treatment
CC	kg CO2 eq	7,43E-06	1,04E-03	3,61E-03	3,32E-02	7,74E-05	5,02E-02	5,02E-02	3,20E-03	6,08E-05	2,30E+00	2,96E-01	-5,94E-06	-6,19E-05	-2,66E-02	5,48E-02
OD	kg CFC-11 eq	7,85E-13	3,90E-11	1,90E-10	1,62E-09	8,15E-11	1,39E-09	1,39E-09	4,97E-10	2,06E-11	2,55E-07	3,28E-08	-6,28E-13	-6,52E-11	-1,30E-09	1,18E-09
HT-nce	CTUh	1,23E-11	9,83E-11	1,10E-09	1,38E-07	2,31E-11	8,72E-09	8,72E-09	4,35E-10	1,96E-11	3,01E-07	3,87E-08	-9,83E-12	-1,85E-11	-1,10E-07	1,80E-09
HT-ce	CTUh	1,17E-12	4,55E-11	1,61E-10	7,61E-09	3,98E-12	1,84E-09	1,84E-09	6,01E-11	4,18E-12	7,10E-08	9,15E-09	-9,37E-13	-3,18E-12	-6,09E-09	4,60E-10
PM	kg PM2.5 eq	1,41E-08	1,08E-06	2,66E-06	1,95E-04	6,58E-08	2,59E-05	2,59E-05	3,06E-06	3,10E-08	7,99E-04	1,03E-04	-1,13E-08	-5,27E-08	-1,56E-04	1,00E-05
IR-HH	kBq U235 eq	1,04E-06	5,62E-06	1,31E-04	2,29E-03	2,22E-05	8,77E-04	8,77E-04	1,41E-04	2,39E-05	3,94E-01	5,08E-02	-8,33E-07	-1,78E-05	-1,83E-03	4,05E-04
IR-E	CTUe	3,75E-12	2,11E-11	4,91E-10	6,45E-09	1,43E-10	3,15E-09	3,15E-09	8,63E-10	7,91E-11	9,97E-07	1,28E-07	-3,00E-12	-1,15E-10	-5,16E-09	1,54E-09
POF	kg NMVOC eq	5,56E-08	5,36E-06	1,30E-05	3,81E-04	6,07E-07	2,47E-04	2,47E-04	5,92E-06	1,77E-07	4,63E-03	5,97E-04	-4,45E-08	-4,86E-07	-3,05E-04	2,83E-05
Ac	molc H+ eq	1,33E-07	5,23E-06	2,43E-05	4,05E-03	7,20E-07	2,17E-04	2,17E-04	1,32E-05	3,87E-07	1,32E-02	1,71E-03	-1,07E-07	-5,76E-07	-3,24E-03	5,31E-05
TE	molc N eq	4,14E-07	7,90E-06	4,88E-05	5,55E-04	9,33E-07	4,11E-04	4,11E-04	1,66E-05	5,52E-07	2,44E-02	3,14E-03	-3,31E-07	-7,46E-07	-4,44E-04	1,11E-04
FE	kg P eq	5,95E-09	3,06E-07	1,02E-06	8,22E-05	2,00E-08	2,12E-05	2,12E-05	2,82E-07	3,95E-08	6,25E-04	8,05E-05	-4,76E-09	-1,60E-08	-6,57E-05	9,14E-06
ME	kg N eq	9,07E-08	7,68E-07	3,76E-06	5,56E-05	8,69E-08	3,82E-05	3,82E-05	1,55E-06	5,47E-08	1,67E-03	2,15E-04	-7,26E-08	-6,95E-08	-4,45E-05	1,29E-05
Fecotox	CTUe	3,47E-04	3,62E-03	2,50E-02	4,31E+00	5,46E-04	2,32E-01	2,32E-01	1,16E-02	5,62E-04	1,40E+01	1,80E+00	-2,77E-04	-4,37E-04	-3,45E+00	5,04E-02
LU	kg C deficit	8,79E-05	4,47E-04	2,75E-03	4,21E-02	8,01E-04	2,69E-02	2,69E-02	5,93E-03	2,25E-04	2,09E+00	2,70E-01	-7,03E-05	-6,41E-04	-3,37E-02	1,13E-02
WRD	m3 water eq	4,45E-07	1,87E-06	4,11E-06	-4,21E-05	9,84E-08	1,01E-06	-1,01E-06	1,29E-05	3,23E-07	2,81E-02	3,62E-03	-3,56E-07	-7,87E-08	3,37E-05	1,08E-07
MF&RD	kg Sb eq	1,29E-09	1,86E-09	6,91E-07	2,28E-05	4,54E-09	1,94E-06	1,94E-06	7,64E-08	2,15E-09	2,98E-05	3,84E-06	-1,03E-09	-3,63E-09	-1,82E-05	1,79E-07

Characterization results for HAM process investigated in this work (Process A). Method: ILCD 2011 Midpoint+ V1.10 / EC-JRC Global, equal weighting / Characterization. Impact categories acronyms: climate change – CC; ozone depletion – OD; Human toxicity, non-cancer effects – HT-nce; Human toxicity, cancer effects – HT-ce; Particulate matter – PM; Ionizing radiation HH – IR-HH; Ionizing radiation E (interim) – IR-E; Photochemical ozone formation – POF; Acidification -Ac; Terrestrial eutrophication – TE; Freshwater eutrophication – FE; Marine eutrophication – ME; Freshwater ecotoxicity – Fecotox; Land use – LU; Water resource depletion – WRD; Mineral, fossil & ren resource depletion – MF&RD

Label	Climate change	Ozone depletion	Human toxicity, non-cancer effects	Human toxicity, cancer effects	Particulate matter	Ionizing radiation HH	Ionizing radiation E (interim)	Photochemical ozone formation	Acidification	Terrestrial eutrophication	Freshwater eutrophication	Marine eutrophication	Freshwater ecotoxicity	Land use	Water resource depletion	Mineral, fossil & ren resource depletion
TPGS-750M	7,01E-05	4,29E-06	0,0053	0,0063	0,0002	0,0003	0	8,19E-05	0,0002	0,0002	6,06E-05	0,0002	0,0062	1,13E-06	0,0004	0,0004
Allyl Benzene	0,0098	0,0002	0,0423	0,2446	0,0142	0,0016	0	0,0079	0,0062	0,0032	0,0031	0,0017	0,0646	5,73E-06	0,0018	0,0006
Aniline Chloridrate	0,034	0,001	0,4722	0,864	0,035	0,0362	0	0,0191	0,0289	0,0198	0,0104	0,0083	0,4454	3,53E-05	0,004	0,2388
Rh(CO)acac	0,3134	0,0089	59,3024	40,9056	2,5698	0,6334	0	0,5606	4,8108	0,2257	0,8375	0,122	76,9115	0,0005		7,8696
Xantphos	0,0007	0,0004	0,0099	0,0214	0,0009	0,0061	0	0,0009	0,0009	0,0004	0,0002	0,0002	0,0097	1,03E-05	9,52E-05	0,0016
EtOH filtration	0,4732	0,0076	3,7505	9,8725	0,3406	0,2425	0	0,3642	0,258	0,167	0,216	0,0837	4,1346	0,0003		0,6716
EtOH Evaporation	0,4732	0,0076	3,7505	9,8725	0,3406	0,2425	0	0,3642	0,258	0,167	0,216	0,0837	4,1346	0,0003		0,6716
NH3	0,0302	0,0027	0,1872	0,3232	0,0402	0,039	0	0,0087	0,0157	0,0068	0,0029	0,0034	0,2064	7,61E-05	0,0125	0,0264
Syngas (H:CO)	0,0006	0,0001	0,0084	0,0225	0,0004	0,0066	0	0,0003	0,0005	0,0002	0,0004	0,0001	0,01	2,88E-06	0,0003	0,0007
Microwave Irradiation	21,6722	1,391	129,3037	381,7929	10,5092	108,9932	0	6,8183	15,7329	9,908	6,3689	3,6562	248,7716	0,0269	27,1612	10,2817
Rotavapor	2,7933	0,1793	16,6658	49,2087	1,3545	14,048	0	0,8788	2,0278	1,277	0,8209	0,4712	32,0638	0,0035	3,5008	1,3252
TPGS-750M recovered	-5,61E-05	-3,43E-06					0	-6,55E-05			-4,85E-05			-9,02E-07		
Xantphos recovered							0							-8,22E-06	-7,62E-05	
Rh(CO)acac recovered			-47	-33	-2	-1	0		-4		-1		-62		0,0326	-6
Waste to Treatment	0,5164	0,0065	0,7727	2,4713	0,1316	0,112	0	0,0417	0,063	0,045	0,0932	0,0282	0,8985	0,0001	0,0001	0,0619

Single score calculation of the HAM process investigated in this work (Process A). Method: ILCD 2011 Midpoint+ V1.10 / EC-JRC Global, equal weighting / Single score

Label	HAM process	TPGS-750M	Allyl Benzene	Aniline Chloridrate	Rh(CO)2acac	Xantphos	EtOH filtration	EtOH Evaporation	NH3	Syngas (H2:CO)	Microwave Irradiation	Rotavapor	Rh(CO)2acac recovered	Waste to Treatment
Climate change	0	0,0003	0,0372	0,1294	1,1907	0,0028	1,798	1,798	0,1147	0,0022	82,3506	10,614	-1	1,9622
Ozone depletion	0	0,0003	0,0133	0,0648	0,5522	0,0277	0,4718	0,4718	0,169	0,007	86,6508	11,1683		0,4029
Human toxicity, non-cancer effects	0	0,0025	0,0197	0,2204	27,6763	0,0046	1,7504	1,7504	0,0874	0,0039	60,3459	7,7779	-22	0,3606
Human toxicity, cancer effects	0	0,0013	0,0493	0,1743	8,2537	0,0043	1,992	1,992	0,0652	0,0045	77,0356	9,929	-7	0,4987
Particulate matter	0	0,0012	0,0924	0,2285	16,7553	0,0056	2,2205	2,2205	0,262	0,0027	68,5217	8,8316	-13	0,8579
Ionizing radiation HH	0	0,0002	0,0012	0,0291	0,5093	0,0049	0,195	0,195	0,0314	0,0053	87,6422	11,2961		0,09
Ionizing radiation E (interim)	0	0,0003	0,0019	0,043	0,5653	0,0126	0,276	0,276	0,0756	0,0069	87,3489	11,2583		0,135
Photochemical ozone formation	0	0,0009	0,087	0,2107	6,1848	0,0099	4,018	4,018	0,0961	0,0029	75,2169	9,6946	-5	0,4601
Acidification	0	0,0007	0,0268	0,1245	20,7336	0,0037	1,1117	1,1117	0,0679	0,002	67,8061	8,7394	-17	0,2719
Terrestrial eutrophication	0	0,0014	0,0272	0,1677	1,9094	0,0032	1,4127	1,4127	0,0572	0,0019	83,822	10,8037	-2	0,3808
Freshwater eutrophication	0	0,0007	0,0365	0,1214	9,7735	0,0024	2,5204	2,5204	0,0336	0,0047	74,32	9,579	-8	1,0875
Marine eutrophication	0	0,0045	0,0378	0,185	2,7369	0,0043	1,8769	1,8769	0,0762	0,0027	81,998	10,5686	-2	0,6322
Freshwater ecotoxicity	0	0,0017	0,0176	0,1211	20,9194	0,0026	1,1246	1,1246	0,0561	0,0027	67,664	8,7211	-17	0,2444
Land use	0	0,0035	0,018	0,1108	1,6981	0,0323	1,0826	1,0826	0,239	0,009	84,3926	10,8772	-1	0,4542
Water resource depletion	0	0,0014	0,0059	0,0129		0,0003			0,0407	0,001	88,4332	11,398	0,1062	0,0003
Mineral, fossil & ren resource depletion	0	0,0021	0,003	1,129	37,2084	0,0074	3,1754	3,1754	0,1247	0,0035	48,6129	6,2656	-30	0,2926

Characterization of the environmental impacts of the HAM process investigated in this work (Process A). Method: ILCD 2011 Midpoint+ V1.10 / EC-JRC Global, equal weighting / Characterization

II – Synthesis of SIRT1 potential inhibitors

1. INTRODUCTION

1.1 Sirtuins (SIRTs) family

Silent Information Regulator 2 (SIR2) is the funding member of a large family of proteins named sirtuins, involved in the regulation of important biological pathways in *Archea*, bacteria and eukaryotes.[267] It was identified by screening of genes that regulate transcriptional silence[268] and, in fact, it regulates transcriptional silencing by deacetylation of histone H4 in a reaction that consume adenine dinucleotide (NAD$^+$).[269]

Sirtuins are NAD$^+$ dependent substrate specific deacetylases and ADP-ribosyl transferases, that perform deacetylation at modified lysins with a unique, elegant mechanism (Figure 34): NAD$^+$ cleaves amides providing the formation of nicotinamide (NAM) and an ADP-ribose (ADPR) peptide-imidate intermediate forms *O*-acyl-ADP-ribose (ADPPR) while the deacetylated substrate is released.
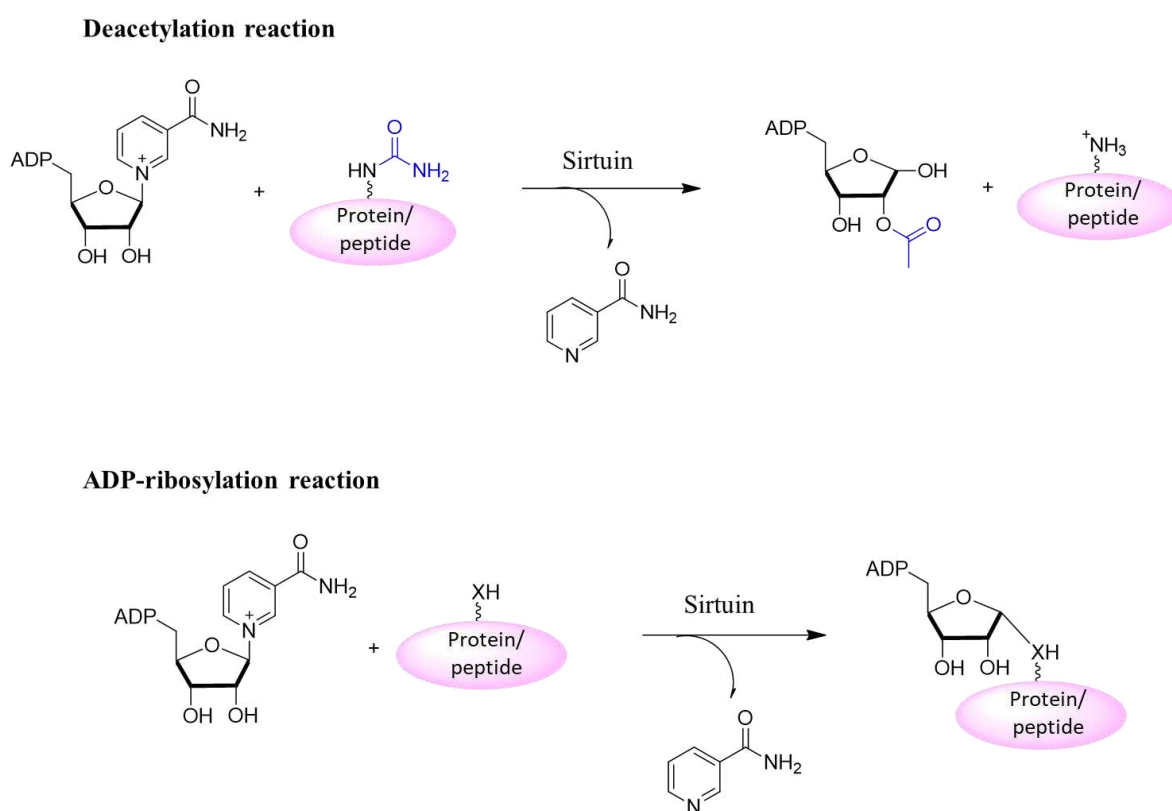

Figure 34. Sirtuins are NAD+ dependent substrate specific deacetylases and ADP-ribosyl transferases mechanisms.

More in detail, an ADP-ribosyl transferase catalyses the nucleophilic attack of the amide bond of an acyl-lysine to the anomeric position of the NAD$^+$ ribose, that provides the formation of an ADP-ribosylated alkylamidate intermediate together with the release of NAM (Figure 35).[270] A conserved histidine residue in the active site, fundamental for the activity, acts as base deprotonating 2'-OH: deprotonated oxygen attacks the alkylamidate forming a cyclic intermediate that decomposes to form 2'-O-acyl-ADP-ribose, which non-enzymatically isomerizes to 3'-O-acyl-ADP-ribose.
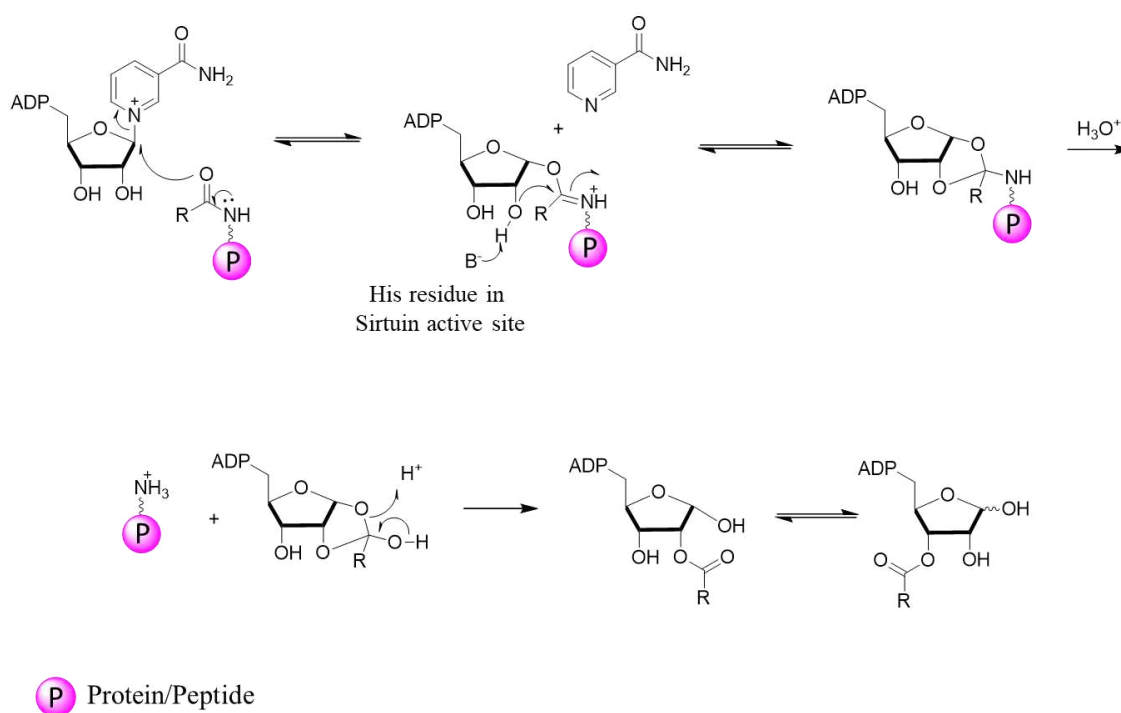
Figure 35. Mechanism of deacetylation of SIRTs.

The catalytic core of 250 amino acidic residues shared by Sirtuins is divided in two domains: a larger one, that adopts a Rossman fold, a mononucleotide binding motif that binds to NAD$^+$, and a smaller globular domain with a structural role, composed by two insertions in the Rossman fold, one of them binding Zinc with four conserved cysteine residues. Acylated peptide and NAD$^+$ bind between these two domains.[271]

Mammalians possess seven Sirtuins, SIRT1-7, with a highly conserved central NAD$^+$-binding and catalytic domain,[272] named sirtuin core domain, and different -N and -C terminal regions;[273] for this reason, they possess divergent biological functions due to i) different enzymatic activities, ii) unique binding partners and substrates and distinct subcellular localization and regulation (Table 10).

Table 10. Summary of the mammalian sirtuins[273]

Sirtuins	Location	Interactions	Biological activity
SIRT1	Nucleus, (cytosol)	FOXO, PCG1α, NF-kB, p300, p53	Metabolism, stress
SIRT2	Cytosol	Tubulin, H4, FOXO	Cell Cycle
SIRT3	Mitochondria	AceCS2, GDH, complex I	Thermogenesis, ATP production
SIRT4	Mitochondria	GDH, IDE, ANT	Insulin secretion
SIRT5	Mitochondria	CPS1	Urea cycle
SIRT6	Nucleus	Histone H3, NF-kB	Base excision repair, metabolism
SIRT7	Nucleolus	Pol I	rDNA transcription

Abbreviations: AceCS2, acetyl-CoA-synthetase 2; ANT, adenine nucleotide translocator; CPS1, carbamoyl phosphate synthetase 1; FOXO, forehead box, subgroup O; GDH, glutamate dehydrogenase; IDE, insulin degrading enzyme; NF-κB, nuclear factor kappa B; PGC-1α, peroxisome proliferator activated receptor gamma coactivator 1 alpha; Pol I, DNA polymerase I; rDNA, recombinant DNA.

SIRT1, SIRT2 and SIRT3 present a NAD^+ deacetylases activity. SIRT6 perform both auto-ADP-ribosyl transferase and deacetylase and substrate-specific deacetylase activity but not all sirtuins carry out deacetylation as primary activity. SIRT4, SIRT5 and SIRT7 have very weak or no detectable deacetylase activity,[274] and, in particular, SIRT5 shows a more active demalonylase and desuccynilase activities.[275]

1.1.1 SIRT1

SIRT1 is a post-translational modified protein of 120 kDa:[276] it is encoded by a gene located at 10q21.3, with a length of 33.715 bp, with nine exons that encode for 747 amino acids[277] and presents a highly structured deacetylase domain, NAD^+ binding domains and long and very flexible *N*- and *C*-terminal regions; *C*-terminal region controls the activity of SIRT1 by stabilization of the catalytic domain performed by a short segment named ESA.[278]

SIRT1 can both deacetylate histones and non-histones targets, as transcription factors and other enzymes.[279,280] SIRT1 is predominantly found in the nucleus of the cell,[280] where it mainly deacetylases the transcriptional coactivators peroxisome proliferator-activated receptor gamma coactivator-1α (PGC-1α) and p300[281] and can directly increase the transcriptional activities of other important nuclear regulators.[282] By the deacetylation and stimulation of

PGC-1α, SIRT1 also promotes transcriptional activities of Forehead box protein O1 (FOXO1), proliferator-activated receptor α (PPARα), and proliferator-activated receptor γ (PPARγ), while through the deacetylation and inhibition of p300, SIRT1 reduces transcriptional activities of tumour protein 53 (p53) and nuclear factor κ-light-chain-enhancer of activated B cells (NF-κB).[283] SIRT1 possesses not only two nuclear localization signals, but also two nuclear export signals that may dictate a cytosolic localization, where it has important effects on regulation of cytoplasmic proteins.

SIRT1 is known to have a role in a large number of physiological processes[284] as apoptosis, cell differentiation, development and autophagy.[285] It also has a role in brain disfunctions, as synaptic plasticity, endocrine regulation,[286] neurodegenerative diseases,[287] and drug addiction.[288] Moreover, SIRT1 has a role in metabolism, health span[289] and in pathologies as cardiovascular diseases[290–292] and cancer.[293–295]

1.1.2 SIRT1 roles in anxiety and depression

SIRT1 was recognized as one of two genes linked to major depression, revealed in both genders and in different populations.[296] However, animal studies sometimes produced conflicting results regarding the role of SIRT1 in depression and anxiety. SIRT-mediated control of these disorders seems to depend on several factors, as cell type, genetic background of studied animals or brain region analysed.[297]

Higuchi and co-workers reported that the pharmacological inhibition of hippocampal SIRT1/2 in depressed model mice leaded to a depression-like behaviour, while their activation led to stress resilience. On the other hand, other studies on rats revealed contradictory results.[298,299]

SIRT1 activity in medial prefrontal cortex (mPFC) neurons is a key regulator of sex-specific depression-related behaviours:[300] its knock-down in mPFC of male mice induces depressive-like behaviours, while reducing mitochondrial density and the expression levels of genes involved in mitochondrial biogenesis. As aforementioned, SIRT1 affects the transcriptional activity of PGC-1α, master regulator of mitochondrial biogenesis and function:[301] the ablation of SIRT1 gene decreases mitochondrial density in mPFC neurons and reduces PGC-1α gene expression in the prelimbic mPFC, evidence that mitochondrial dysfunction in this area contributes to the development of depression symptomatology. The injection of a SIRT1 activator of wild-type mice produces an anti-depressant like effect.

In Nucleus Accumbens (NAc) SIRT1 also mediates anxiety and depression-like behaviour in susceptible mice with a cell- and circuit-specific manner:[302] an overexpression of SIRT1 level

in Dopamine D1 subpopulation of medium spiny neurons (MSNs) of NAc provides an increase in anxiety- and depression-like behaviours, while the ablation of the protein was associated to their decrease. Nonetheless, the injection of resveratrol, a Sirtuins activator,[303] provokes an increase of anxiety- and depression-like behaviours, decreased by the injection of a SIRT1 inhibitor.

Emotional disorders are known comorbid conditions that exacerbate chronic pain.[304] Zhou and co-workers also demonstrated a role of SIRT1 in decreasing emotional pain vulnerability by its deacetylation action of CaMKIIα in central amygdala: a reduced SIRT1 protein level, associated with a downregulation of CaMKIIα, was found in mice vulnerable to develop anxiety and depression associated with chronic pain.

Depression is related with the alteration and insufficiency of neurotransmitter as serotonin (5-HT), norepinephrine and dopamine.[305] In amygdala, SIRT1 activates monoamine oxidase A (MAO-A) promoter by deacetylation of transcription factor nescient helix-loop-helix 2 (NHLH2) on lysine 49,[306] determining a decrease of serotonin and dopamine, associated with humoral disorders. Other studies also suggest that SIRT1 could have a role even the expression of receptor of acetylcholine, that can regulate mood and anxiety in the brain[307] and that also can contribute to the regulation of GABA expression,[308] demonstrating the high involvement of SIRT1 in the level of neurotransmitters in the brain.

SIRT1 may also control the inflammatory response in depression: in fact, it is involved in inflammatory mechanisms through antiapoptotic pathways as i) modulation of the nuclear translocation of Forehead box-containing protein O (FOXO), associated with the anti-apoptotic factor Bcl-2; ii) inhibition of p53 and NF-kB signals, and iii) inhibition of the release of pro-inflammatory cytokines in microglia.

1.2 Aim of the work

Prof Federica Pellati's group recently found an interesting inhibitory activity on SIRT-1 in vivo models of neuropathies as anxiety and depression of an extract of *Helicrisum Stoaches*. The main component of this extract is represented by compound **36** (Figure 36).

The docking of **36** with SIRT1 let Prof. Manetti's group develop a pharmacophoric model. For the validation of this model the synthesis of the analogues **36-40** was necessary.
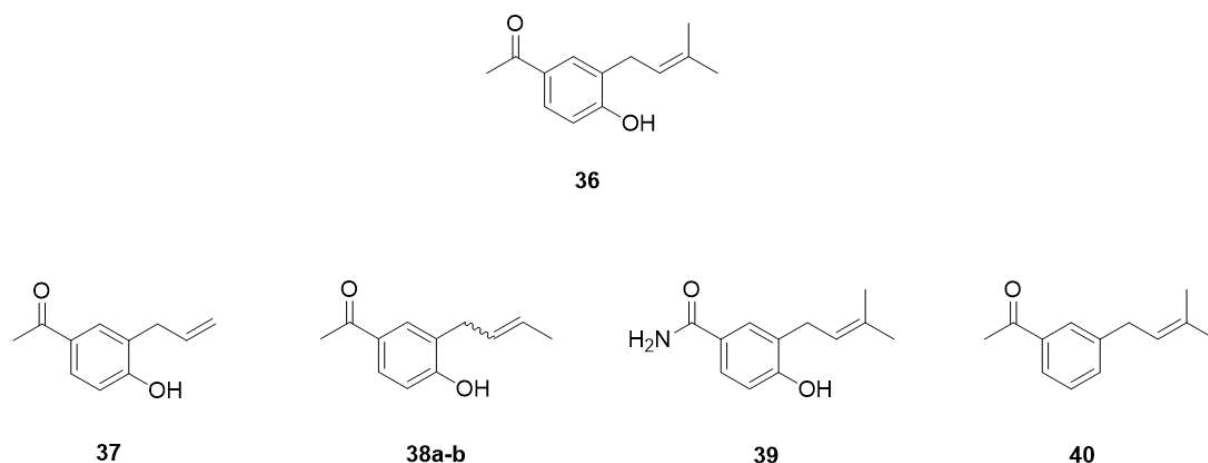
Figure 36. Structure of compound **36** extracted from *Helicrisum Stoaches*, and compounds **37-40**.

The aim of this work was the synthesis compounds **36-40** to test them and confirm the preliminary data obtained from computational studies.

2. RESULTS AND DISCUSSION

Phenolic compounds **a** can generally be obtained by Claisen rearrangement from compounds **b**, that can be provided by alkylation by compounds with general structure **c** (Scheme 7).
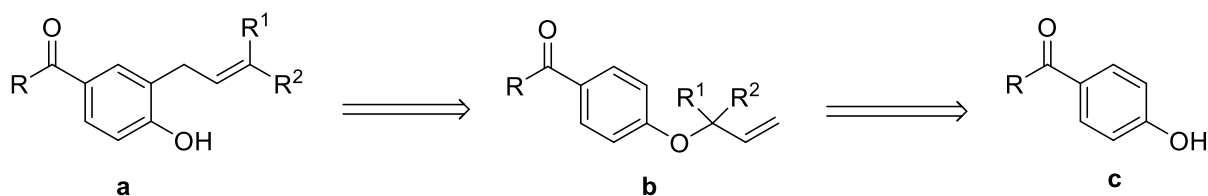
Scheme 7. Retrosynthetic strategy for the obtainment of phenolic compounds. R = -CH$_3$, -NH$_2$, R$_1$ = -H, -CH$_3$, R$_2$ = -H, -CH$_3$.

Starting from the preparation of **37**, 4-hydroxyacetophenone (**41**) was used as the starting material and treated with allyl bromide thus obtaining after 5 h of reflux in acetone compound **42** in 91% yield (Scheme 8). After Claisen rearrangement under microwave irradiation, **37** was obtained in 60% yield.
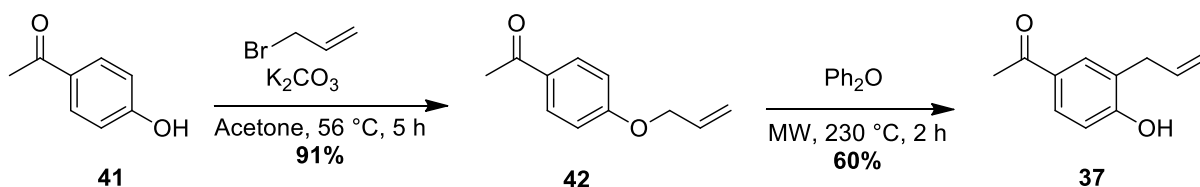
Scheme 8. Synthesis of compound **37**.

The same synthetic approach has been applied to the synthesis of **38**. In this case, both Mitsunobu's conditions and nucleophilic substitution were investigated for the alkylation step (Table 11).

**Table 11.** Reaction conditions for the synthesis of compound **43**.
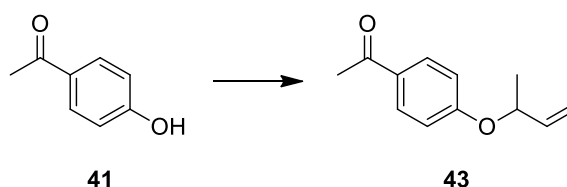
Entry	Conditions	Yield
1	3-buten-2-ol (1.3 eq), PPh₃ (1.3 eq), DIAD (1.3 eq) dry THF, 0 °C to 66 °C, 48 h	-
2	3-buten-2-ol (1.2 eq), PPh₃ (2 eq), DIAD (2 eq) dry THF, 0 °C to r.t., sonication, 48 h	50%
3	3-chloro-1-butene (1.2 eq), K₂CO₃ (2 eq) Acetone, reflux, 16 h	15%
4	3-chloro-1-butene (1.2 eq), K₂CO₃ (2 eq), KI (0.5 eq) dry DMF, 50 °C, 16 h	60%

The alkylation of 4-hydroxyacetophenone was initially performed refluxing 3-buten-2-ol in THF for 16 h in the presence of an excess of Ph₃P and DIAD: only starting materials were recovered (Table 11, entry 1). Sonication can sometimes have a good impact on Mitsunobu's reaction of phenols with hindered alcohols.[309] After stirred for 12 h, the solution of 4-hydroxyacetophenone and 3-buten-2-ol, in presence of a higher amount of both PPh₃ and DIAD was sonicated for 40 minutes. After further 24 h of regular stirring, **43** was obtained in 50% yield (Table 11, entry 2).

The use of a nucleophilic substitution with 3-chloro-1-butene was also explored. Using a similar procedure applied for the synthesis of **42**, refluxing **41** and 3-chloro-1-butene in

presence of K$_2$CO$_3$ in acetone for 12 h, **43** was obtained in a very low yield of 10% (Table 11, entry 3). The low yield observed is probably mostly related to the use of a secondary chloride, less reactive than allyl bromide. Therefore, performing the reaction in DMF adding KI to the reaction mixture, to perform an exchange of the chlorine atom with the better leaving group iodine in the Filkenstein's conditions, at 50 °C let the isolation of **43** possible in 60% yield (Table 11, entry 4).
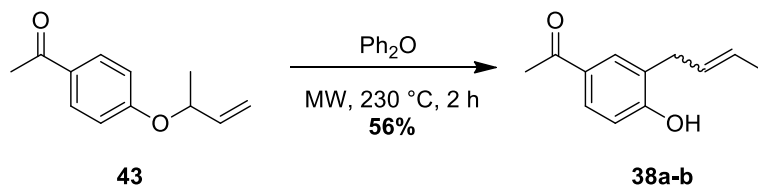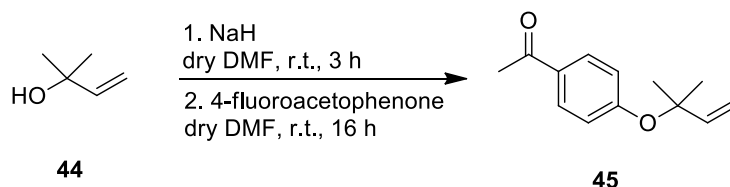

Scheme 9. Synthesis of compounds *(E, Z)* **38a-b**.

Then, **43** was subjected to Claisen rearrangement in the previously developed conditions, affording **38a-b** as a mixture of isomers, not separable by chromatography, in 56% yield (Scheme 9).

Synthesis of **36** was more challenging. Alkylation by nucleophilic substitution with 3-chloro-3-methyl-butene, that proceed via SN$_1$ mechanism, would afford two isomers due to the isomerization of double bond in a more stable conformation. Moreover, 3-chloro-3-methyl-1-butene can easily go towards elimination in alkaline conditions, side-reaction favoured by the formation of a stable conjugated diene.

These problems could be theoretically overcome trying to provide **36** though a nucleophilic aromatic substitution on 4-fluoroacetophenone using 2-methylbut-3-en-2-ol. The reaction was firstly performed following the first step of a S$_N$Ar/Claisen rearrangement successful procedure with fluoro-benzophenone derivatives.[310]
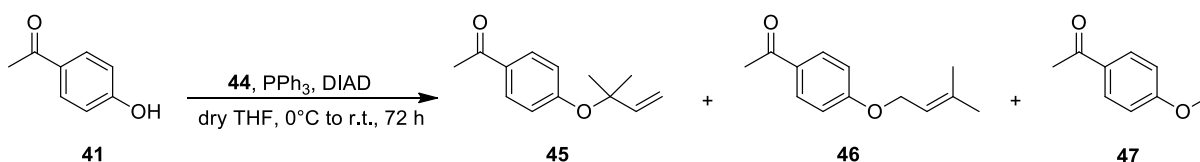

Scheme 10. Synthesis of compound **45** via S$_N$Ar.

Deprotonation of 2-methylbut-3-en-2-ol was accomplished stirring the alcohol in dry DMF in presence of NaH as strong base. After 1 h, the solution was added to a solution of 4-

fluorobenzophenone in anhydrous DMF and the mixture was stirred rt for 16 h. Unfortunately, only starting material was collected (Scheme 10). Assuming that the amount of NaH (0.67 eq) was not enough to afford the deprotonation of the alcohol (1 eq), the reaction was performed using a slight excess of base (1.2 eq) and the solution was stirred for 3 h before the addition to the solution of 4-fluorobenzophenone. After 16 h, once again the desired product was not achieved.

Alongside, the possibility to exploit 2-methylbut-3-en-2-ol to obtain **45** by Mitsunobu reaction was investigated, while knowing that it would be very challenging. Mitsunobu reaction for tertiary alcohols is only occasionally reported[311] and the problem of double bond isomerization still remained, since after the formation of the P-O intermediate a carbocation would be formed.

Scheme 11. Synthesis of compound **45** and by-products.

Firstly, the alkylation to obtain **45** from **41** was performed with 2-methylbut-3-en-2-ol (**44**) in the same reaction conditions seen for the alkylation with secondary alcohol. Starting phenol was totally consumed and, as expected, a mixture of isomers **45** and **46** in 1:1 ratio was collected, but they were isolated only in traces (Scheme 11). Interestingly, methylated phenol **47** was obtained as the major product of the reaction, as confirmed by mass spectrum and ^{1}H NMR (Scheme 11).

Since no explanation was found assuming a ionic mechanism, the intercourse of a radical mechanism was hypothesized. To verify this theory, the reaction was performed in the same conditions in presence of 2,2,6,6-tetramethyl-1-piperidinyloxy (TEMPO) as radical scavenger. Surprisingly, the amount of by-product **47** was significantly reduced, confirming the theory of radical mechanism.
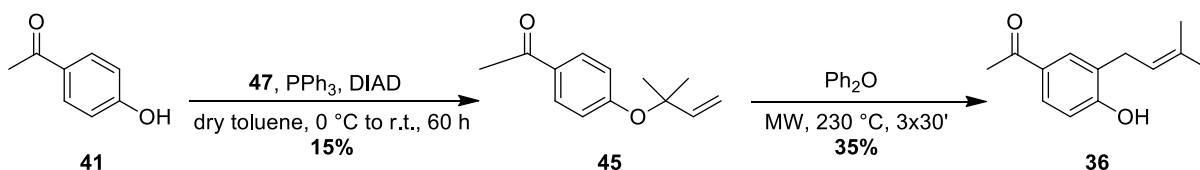

Scheme 12. Synthesis of compound **36**.

By substitution of THF with toluene, the reaction was naturally slower, with a lower conversion of the starting phenol, but the formation of the methylated by-product was extremely reduced (Scheme 12). **45** and **46** ratio was unfortunately confirmed to be 1:1 both adding DIAD as last reactive in the reaction mixture and adding phenol to the "complex" alcohol/PPh$_3$/DIAD (Scheme 12). Purification of the mixture by chromatography was very challenging, since the isomers have very similar structure and close Rf. **45** was finally isolated in very poor yield (15%). **36** was obtained by Claisen rearrangement from **45** in 35% yield, heating the mixture with microwaves at 230 °C for three intervals of 40 min in presence of Ph$_2$O.

Wang et. al reported the synthesis and use of a tailor-made iridium catalyst for the obtainment of aromatic amides from aromatic aldehydes in water.[312] Among them, 2-hydroxybenzamide was obtained from 4-hydroxybenzaldehyde, starting material for the synthesis of **39.**

The half sandwich iridium catalyst was synthesized as reported in literature (Scheme 13).
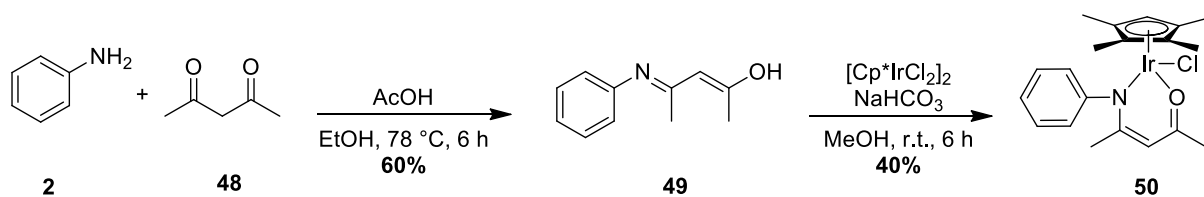
**Scheme 13.** Synthesis of half iridium sandwich **50.**

Aniline (**2**) and 2,4-pentanedione (**48**) were solubilized in anhydrous EtOH, in presence of a catalytic amount of AcOH, and the mixture was refluxed for 6 h purging the reaction in N$_2$ atmosphere (Schlenk technique) (Scheme 13): **49** was obtained in a 60% yield. Then, it was mixed with [Cp*IrCl$_2$]$_2$ and NaHCO$_3$ in anhydrous MeOH and the mixture was stirred at room temperature for 6 h under N$_2$ purged atmosphere (Schlenk technique), and **50** was obtained in moderate yield (40%).
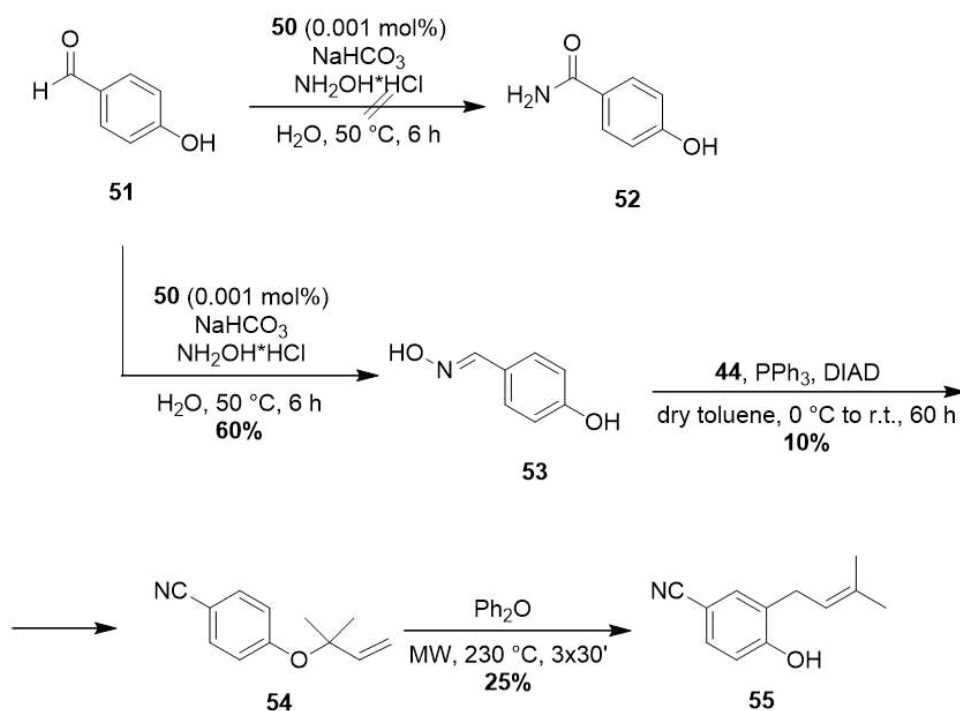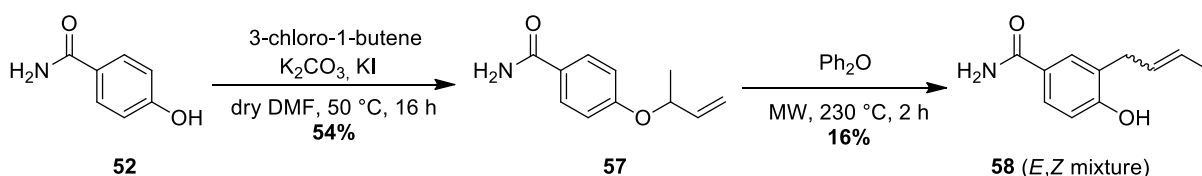
Scheme 14. Synthesis of compound **55.**

4-hydroxybenzaldehyde (**51**) was then reacted with NH_2OH hydrochloride, in presence of $NaHCO_3$ and **50** in water, heating the mixture at 50 °C for 6 h. At the end of this time, only the aldoxime intermediate **53** was recovered instead of 4-hydroxybenzamide **52**, according with the NMR spectra of the isolated compound (Scheme 14). Anytime reaction was repeated the same result was obtained, probably for reasons arising from a wrong manipulation of the catalyst.

53 was reacted with 2-methylpent-4-en-2-ol (**44**) in anhydrous toluene, in the same conditions seen for the synthesis of compound **45,** and **54** was obtained in 10% yield together with its isomer (Scheme 14). Aldoximes give the correspondent nitrile compounds by hydration on heating[313] or MWs conditions. In this case, Mitsunobu conditions[314] together with sonication probably determined the dehydration of the oxime to nitrile: ^{1}H NMR and ^{13}C NMR of isomers obtained did not show anymore the peak of oxime group hydrogen and carbon, while mass and both NMR spectra were attributable to the products of dehydration **54. 54** was then diluted in Ph_2O and submitted to 3 cycles of 40 minutes of MW irradiation providing **55** in a 25% yield.
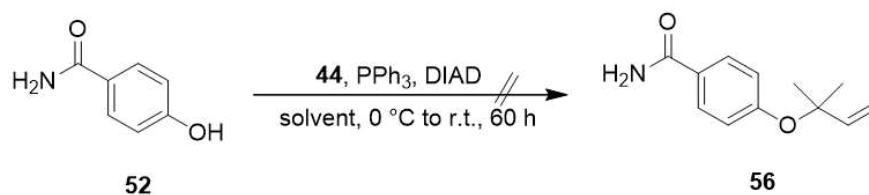
**Scheme 15.** Synthesis of compound **56.** Solvents: toluene, THF, DMF.

4-hydroxybenzamide (**52**) was directly used in the Mitsunobu reaction with 2-methylpent-4-en-2-ol to obtain the intermediate **56** (Scheme 15). Performing the reaction in anhydrous toluene in the optimized conditions only starting material was recovered. The reaction was then performed even in THF and after 48 hours only starting material was recovered and not even the methylated by-product was formed. A last attempt was made performing the reaction in DMF, with the same result. Mitsunobu conditions with a tertiary alcohol together with the scarce solubility of **52** in all these solvents are probably the reasons of the unsuccess of the procedure.

Scheme 16. Synthesis of compound **58** (*E,Z* mixture)**.**

However, **52** was successfully alkylated with 3-chloro-1-butene following the procedure used for the synthesis of the analogue ketone **43**. **57** was obtained in 54% yield and subjected to Claisen rearrangement. After 2 h of MW irradiation in presence of Ph$_2$O, **60** was isolated in 16% yield (Scheme 16).

Since the lack of phenolic moiety, a different strategy was designed for the synthesis of compound **42.**

Table 12. Conditions for the synthesis of compound **60.**
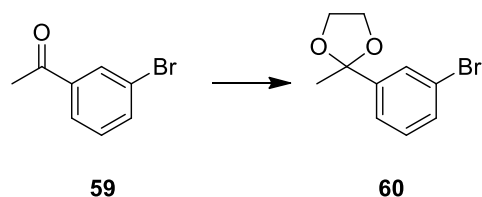
| Entry	Conditions	Yield
1	Ethylene glycol (1.5 eq), *p*TSA (0.085 eq) dry toluene, reflux, 16 h	16%
2	Ethylene glycol (203 eq), *p*TSA (0.085 eq) dry toluene, reflux, 5 h	15%
3	Ethylene glycol (1.5 eq), I_2 (cat.) dry toluene, reflux, 16 h	20%
4	Ethylene glycol (10 eq) I_2 (cat.) MW, 50 °C, 1 h	26%
5	Ethylene glycol (10 eq), I_2 (cat.) MW, 80 °C, 1 h	40%

Since the procedures described in literature provided **60** in a quantitative yield,[315] 3-bromoacetophenone (**59**) was refluxed in toluene with ethylene glycol and catalytic *p*-toluensulfonic acid (*p*TSA). Unexpectedly and curiously, only part of **59** was converted. Chromatographic separation was very challenging, since the difficulty to separate the product from the starting material (SM), and **60** was obtained only in 16% yield (Table 12, entry 1). Performing the reaction with a very large amount of ethylene glycol (200 eq), following a different procedure used in the laboratory for the synthesis of other acetals, result did not change and **60** was isolated in 15% yield (Table 12, entry 2). Another attempt was made using a catalytic amount of I_2 instead of *p*TSA. A slight improvement was obtained in terms of isolated yield (20%) (Table 12, entry 3).

With a tan δ of 1.375 ethylene glycol is very active towards microwaves. Irradiating **59** in a large excess of 10 equivalents of ethylene glycol with a catalytic amount of I_2 at 50 °C and 80 °C for 1 h, **60** was obtained in 26% and 40% yield respectively (Table 12, entries 4, 5).

The low reactivity of the ketone, due to a stability given by its conjugation with the aromatic ring, seem to be refute by literature, as well as the instability of the formed acetal.

Nonetheless, after few times, spontaneous hydrolysis of the acetal was noticed, confirming a poor stability of the final product.

To avoid this problem, **60** was synthesized and immediately used to form a Grignard reagent (Scheme 17).
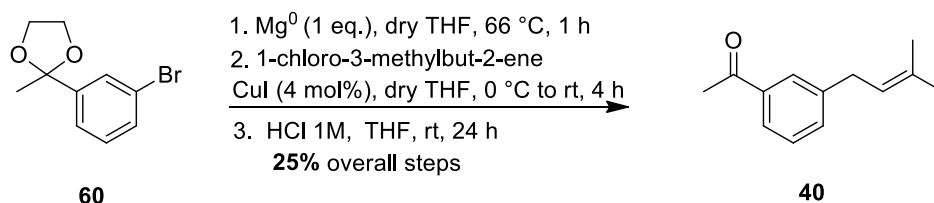
Scheme 17. Synthesis of compound **40**.

Attempts were made both adding a solution of **60** in carefully dried THF and Et$_2$O to Mg: at room temperature no reaction occurred, not even when Mg was previously activated with iodine. After refluxing the mixture in dry THF for 1 h, Mg was completely consumed: a solution of 1-chloro-3-methylbut-2-ene and 4 mol% of CuI were added at 0 °C to the solution of Grignard reagent and the mixture was stirred at room temperature for 4 h. After purification a mixture of ketone **40** and its acetal was obtained, as confirmed by ^{1}H NMR spectrum. The mixture was stirred with HCl 1 M in THF for 48 hour and pure **40** was obtained in 25% yield overall two steps (Scheme 17).

Preliminary tests on SIRT1 show a lower activity of the synthesized compounds with respect to the nicotinamide used as the gold standard (Figure 37).
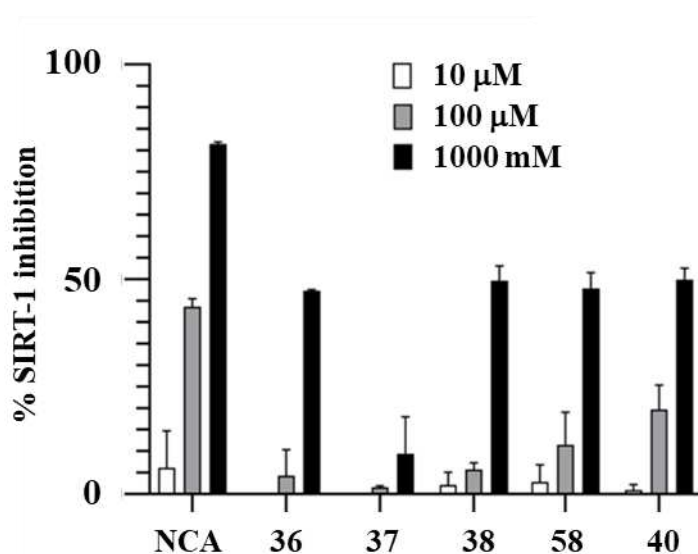

Figure 37. Inhibitory activity of compound **36-38**, **40**, **58**, also compared with nicotinamide (NCA).

Since none of the compounds shows an improvement in activity compared to Nicotinamide, for the moment, it was decided to not proceed with the determination of their IC_{50} or other tests.

3. CONCLUSIONS

In conclusion, five compounds (**36**, **37**, **38, 40**, **58**) were synthesized and tested to evaluate their inhibitory activity on SIRT1. The inhibitor activity of all the compounds resulted inferior compared to that of Nicotinamide. Compounds **38**, **40** and **58** only determined a little improvement of activity at 100 µM compared to **36**, but not enough to continue with assays as the determination of the IC_{50}. Ketone or amide moiety seem not determine a substantial difference in the inhibition profile.

As future perspectives, from a chemical point of view a deeper investigation of the radical mechanism that intercourse in the Mitsunobu reaction with phenols and tertiary alcohols would be such interesting. Moreover, nucleophilic aromatic substitution for the obtainment of the intermediates could be taken into consideration, for example, by exploitation of micellar catalysis. In fact, the chemistry exploited for the first development of potential SIRT1 inhibitors synthesis is in contrast with all of the Green Chemistry principles described in the introduction of Section I; as future perspective, the possible optimization of the synthetic route should be carried out taking the sustainability of the process into great consideration as well.

# 4. EXPERIMENTAL SECTION

4.1 Materials and methods

All reagents were used as purchased from commercial suppliers without further purification. The reactions were carried out in oven dried vessels. Solvents were dried and purified by conventional methods prior use or, if available, purchased in anhydrous form. Flash column chromatography was performed with Merck silica gel Å 60, 0.040-0.063 mm (230-400 mesh). MPLC Syncore Büchi on highly resistant PP cartridges Normal Phase silica gel NP 40 – 63 μm particle size and 60 Å pore size (Si60) withstand a maximum pressure of 10 bar (145 psi) column with PE (Eluent A) and EtOAc (Eluent B) as mobile phase.

Merck aluminium backed plates pre-coated with silica gel 60 (UV254) were used for analytical thin layer chromatography and were visualized by staining with a KMnO4 or Ninidrine solution. NMR spectra were recorded at 25 °C or at 37 °C with 400 or 600 MHz for 1H and 101 or 151 MHz for 13C Brücker Advance NMR spectrometers. The solvent is specified for each spectrum. Splitting patterns are designated as s, singlet; d, doublet; t, triplet; q, quartet; m, multiplet; bs, broad singlet. Chemical shifts (δ) are given in ppm relative to the resonance of their respective residual solvent peaks.

Mass spectra (LC-MS) were acquired using an Agilent 1100 LC-MSD VL system (G1946C) with an electrospray ionization source (ESI). Data were obtained by a direct injection with a 0.4 mL/min flow rate using a binary solvent system of 95/5 MeOH/H_2O. UV detection was monitored at 254 nm. Mass spectra were acquired in positive and negative mode scanning over the mass range 105-1500 (m/z), using a variable fragmentor voltage of 10–70 mV (0-70).

4.2 Synthetic procedures

1-(4-(allyloxy)phenyl)ethan-1-one (42)
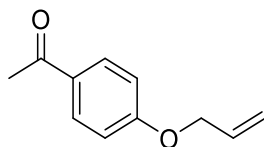
To a solution of 4-hydroxyacetophenone **41** (953.1 mg, 7 mmol) in acetone (15 mL) allyl bromide (0,667 mL, 7.7 mmol) and K_2CO_3 (1451 mg, 10.5 mmol) were added and the mixture was refluxed for 5 h. After cooling, the mixture was filtered and concentrated in vacuo. The residue was dissolved in EtOAc and washed with H_2O and Brine. The organic layer was dried over Na_2SO_4 and filtrated. The solvent was evaporated under vacuum and the product was obtained as a yellow oil. **YIELD:** 91%. **^{1}H NMR** (400 MHz, CDCl$_3$) δ 7.88 (d, J = 9.0 Hz, 2H), 6.90 (d, J = 8.9 Hz, 2H), 6.00 (m, 1 H), 5.30 (dd, 2H), 4.56 (d, 2H), 2.51 (s, 3H). **^{13}C NMR** (101 MHz, CDCl$_3$) δ 196.7, 162.4, 132.5, 130.4, 118.1, 114.4, 68.8, 26.3. **LC-MS** (*m/z*) (ES+): 199.1 [M+Na]$^+$

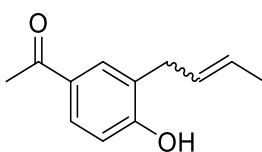### 1-(3-allyl-4-hydroxyphenyl)ethan-1-one (37)
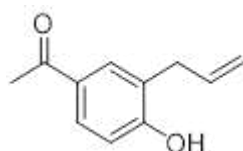
42 (100 mg, 0.5681 mmol) was charged in a MW vessel under inert atmosphere. Ph_2O was added and the reaction was heated MW 230 °C, 3x40 min, at a fixed power of 300 Watt. After cooling, the mixture was purified with by chromatography (2% EtOAc in petroleum ether) and obtained as a yellowish solid. **YIELD**: 60%. **^{1}H NMR** (600 MHz, CDCl$_3$) δ 7.81 (m, 2h), 6.94 (d, J = 8.3 Hz, 1H), 6.05 (ddt, 1H), 5.18 (dd, 2H), 3.48 (d, J = 6.4 Hz), 2.60 (s, 3H) **^{13}C NMR** (151 MHz, CDCl$_3$) δ 198.28, 159.36, 135.78, 131.42, 129.96, 129.27, 126.10, 116.80, 115.53, 34.65, 26.32 **LC-MS** (*m/z*) (ES-); 175.1 [M-H]$^-$

1-(4-(but-3-en-2-yloxy)phenyl)ethan-1-one (43)
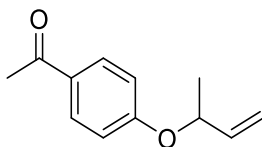
To a solution of 4-hydroxyacetophenone **41** (204 mg, 1.5 mmol) in dry DMF (5mL) under N_2 flux, K_2CO_3 (414 mg, 3 mmol) and KI (124.5 mg, 0.75 mmol) were added Then a solution of 3-chloro-1-butene (0.182 mL, 1.8 mmol) in dry DMF was slowly added dropwise at room temperature and the mixture was then stirred at 50 °C for 16 h. After cooling, the mixture was diluted with EtOAc and the organic phase was washed with H_2O and Brine, dried over Na_2SO_4, filtrated, and evaporated under vacuum. The mixture was purified by flash chromatography (20% EtOAc in petroleum ether) and obtained as a yellow oil. **YIELD: 60%.**
¹H NMR (400 MHz, CDCl₃) δ 7.88 (d, *J* = 8.9 Hz, 2H), 6.91 (d, *J* = 8.9 Hz, 2H), 5.90 (m, 1 H), 5.25 (dd, 2H), 4.87 (q, *J* = 7.8 Hz, 2H), 2.53 (s, 3H), 1.44 (d, *J* = 9.7 Hz, 3H). **¹³C NMR** (101 MHz, CDCl₃) δ 196.8, 161.9, 138.3, 125.3, 116.1, 115.3, 114.3, 74.7, 68.8, 29.7, 26.3, 21.2, 17.8. **LC-MS** (*m/z*) (ES+): 213.0 [M+Na]⁺

(*E, Z*) 1-(3-(but-2-en-1-yl)-4-hydroxyphenyl)ethan-1-one (38a-b)
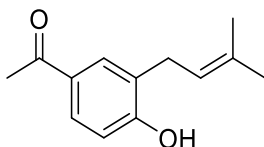

43 (150 mg, 0.7895 mmol) was charged in a MW vessel under inert atmosphere. Ph_2O was added and the reaction was heated MW 230 °C, 3x40 min, at a fixed power of 300 Watt. After cooling, the mixture was purified by flash chromatography (2% EtOAc in petroleum ether) and obtained as a white solid. **YIELD**: 57%. **¹H NMR** (600 MHz, CDCl₃) δ 7.77 (m, 2H), 6.86 (m, 1H), 5.65 (m, 2H), 3.40 (d, *J* = 4.4 Hz, 2H), 2.55 (s, 3H), 1.73 (d, *J* = 4.7, 3H). **¹³C NMR** (151 MHz, CDCl₃) δ 197.3, 159.4, 141.7, 131.2, 129.2, 128.2, 127.9, 126.5, 115.6, 33.8, 26.3, 17.9. **LC-MS** (*m/z*) (ES-): [M-H]⁻, 189.0 [M-H]

**1-(4-((2-methylbut-3-en-2-yl)oxy)phenyl)ethan-1-one (45)**
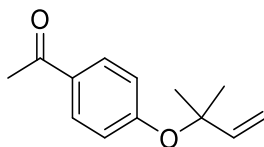
To a solution of 2-methyl-3-buten-2-ol (**44**) (0.513 mL, 4.9 mmol) and PPh₃ (1611 mg, 6.15 mmol) in dry toluene (8mL) under N₂ atmosphere, cooled at 0° C, DIAD (1.210 mL, 6.15 mmol) was slowly added dropwise. After 30 min, the mixture was allowed to reach room temperature and 4-hydroxyacetophenone (**41**) was added. The mixture was stirred at room temperature for 12 h, then sonicated for 40 min, and stirred at room temperature for further 48 h. Toluene was evaporated under vacuum and the mixture was diluted in EtOAc. H₂O was added and the mixture was extracted with EtOAc. The combined organic layers were dried over Na₂SO₄, filtrated and the solvent was evaporated in vacuum. The mixture was purified by automatic chromatography (?) and obtained as yellow oil. **YIELD**: 15%. **¹H NMR** (400 MHz, CDCl₃) δ 7.82 (d, J = 13.6 Hz, 2H), 6.98 (d, J = 13.5 Hz, 2H), 6.61 (dd, 1H), 5.20 (dd, 2H), 2.52 (s, 3H), 1.50 (s, 6H) **¹³C NMR** (101 MHz, CDCl₃) δ 196.2, 160.8, 143.7, 130.6, 129.8, 119.4, 113.9, 80.3, 27.2, 26.3. **LC-MS** (*m/z*) (ES-): 227.0 [M+Na]⁻

## 1-(4-hydroxy-3-(3-methylbut-2-en-1-yl)phenyl)ethan-1-one (36)

45 (150 mg, 0.7895 mmol) was charged in a MW vessel under inert atmosphere. Ph_2O was added and the reaction was heated MW 230 °C, 3x40 min, at a fixed power of 300 Watt. After cooling, the mixture was purified by flash chromatography (2% EtOAc in petroleum ether) and obtained as a yellowish solid. **YIELD**: 35%. **^{1}H NMR** (600 MHz, CDCl$_3$) δ 7.78 (m, 2H), 6.88 (d, J = 8.2 Hz), 5.32 (t, J = 6 Hz, 1H), 3.40 (d, J = 7.1 Hz, 2H), 2.56 s, 3H), 1,78 (s, 6H). **^{13}C NMR** (151 MHz, CDCl$_3$) δ 197.9, 159.3, 135.2, 130.9, 130.1, 128.9, 127.3, 121.2, 115.5, 29.4, 26.3, 25.8, 17,9. **LC-MS** (*m/z*) (ES-): 203.0 [M-H]$^-$. Melting point 95-100 °C.

## (2E,4E)-4-(phenylimino)pent-2-en-2-ol (49)
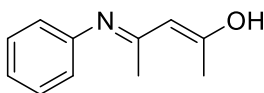
Acetylacetone (**48**) (0.099 mL, 1.1 mmol), aniline (0.103 mL, 1 mmol) and AcOH (drops) were mixed in EtOH under N_2 atmosphere (Schlenk technique) and the mixture was refluxed for 6 h. After cooling, EtOH was evaporated under vacuum and the mixture was purified by flash chromatography (5% EtOAc in petroleum ether). **YIELD:** 60%. **^{1}H NMR** (400 MHz, CDCl$_3$) δ 12.43 (s, 1H), 7.29 (t, J = 8.1 Hz, 2H), 7.14 (t, J = 7.5 Hz, 1H), 7.06 (d, J = 7.5 Hz, 2H), 5.15 (s, 1H), 2.05 (s, 3H), 1.95 (s, 3H). **^{13}C NMR** (101 MHz, CDCl$_3$) δ 196.1, 160.3, 138.7, 129.1, 125.6, 124.7, 97.6, 29.1, 19.8. **LC-MS** (*m/z*) (ES+): 176.3 [M+H]$^+$, 198.2 [M+Na]$^+$

Half sandwich Iridium Complex (50)
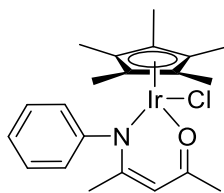
A mixture of [Cp*IrCl$_2$]$_2$, (40 mg, 0,050 mmol), NaHCO$_3$ (16.8 mg, 0.2 mmol), and **49** (17.5 mg, 0.1 mmol) were dissolved in dry purged methanol under N$_2$ atmosphere (standard Schlenk technique) and the mixture was stirred at room temperature for 7 hours. The solvent was evaporated under vacuum and the crude was purified by flash chromatography (EtOAc 30% in petroleum ether) and the product was obtained as red/orange solid. **YIELD:** 40%. **^{1}H NMR** (600 MHz, CDCl$_3$) δ 7.32 (m, 4H), 7.08 (m, 1H), 4.83 (s, 1H), 1.97 (s, 3H), 1.56 (s, 1H), 1.23 (s, 15H). **LC-MS** (*m/z*) (ES+): 502.2 [M-Cl]$^+$

4-hydroxybenzaldehyde oxime (53)
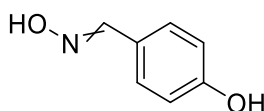
4-hydroxybenzaldehyde (**51**) (366 mg, 3mmol), NH$_2$OH*HCl (210 mg, 3 mmol), NaHCO$_3$ (302.4 mg, 3.6 mmol) and **50** (1.6 mg, 0.003 mmol) were added to H$_2$O (6 mL) in a round bottom flask and the mixture was stirred at 50 °C for 6 h. After cooling, the reaction was extracted with EtOAc and the combined organic layers were dried over Na$_2$SO$_4$, filtrated and evaporated under vacuum. The crude was purified by flash chromatography (10% EtOAc) to obtain a white solid. **YIELD:** 60%. **^{1}H NMR** (400 MHz, MeOD) δ 7.95 (s, 1H), 7.40 (d, *J* = 8.5 Hz, 2H), 6.75 (d, *J* = 8.7 Hz, 2H). **^{13}C NMR** (101 MHz, MeOD) δ 158.7, 149.0, 128.0, 124.2, 115.1. **LC-MS** (*m/z*) (ES-): 136.0 [M-H]$^-$

4-((2-methylbut-3-en-2-yl)oxy)benzonitrile (54)
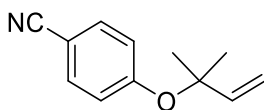
To a solution of **53** in dry toluene under N_2 atmosphere, 2-methyl-3-buten-2-ol (**44**), PPh$_3$ were added. The solution was cooled to 0 °C and DIAD was slowly added dropwise. After 30 min, the reaction was allowed to reach room temperature and stirred at room temperature for 12 h. Then, it was sonicated for 40 min and stirred at room temperature for 48 h. Toluene was removed under vacuum and the crude was diluted with EtOAc. H_2O was added and the crude was extracted with EtOAc. The combined organic layers were dried over Na_2SO_4, filtrated, and evaporated under vacuum. The crude was purified by flash chromatography (2% EtOAc in petroleum ether) and the product was obtained as intense yellow oil. **YIELD**: 15%. **^{1}H NMR** (400 MHz, CDCl$_3$) δ 7.48 (d, J =8.9 Hz, 2H), 6.99 (d, J = 8.9, 2H), 6.07 (m, 1H), 5.20 (dd, 2H), 1.49 (s, 6H). **^{13}C NMR** (101 MHz, CDCl$_3$) δ 160.2, 143.4, 120.1, 114.6, 27.1, 21.6. **LC-MS** (m/z) (ES+): 225.0 [M+Na]$^+$

4-hydroxy-3-(3-methylbut-2-en-1-yl)benzonitrile (55)
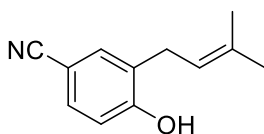
54 (150 mg, 0.7895 mmol) was charged in a MW vessel under inert atmosphere. Ph$_2$O (0.470 mL) was added and the reaction was heated MW 230 °C, 3x40 min, at a fixed power of 300 Watt. After cooling, the mixture was purified by flash chromatography (2% EtOAc in petroleum ether) and obtained as a brown solid. **YIELD**: 35%. **^{1}H NMR** (600 MHz, CDCl$_3$) δ 7.41 (m, 2H), 6.85 (d, J = 8 Hz, 1H), 5.29 (m, 1H), 3.36 (d, J = 7.0 Hz, 2H), 1,81 (s, 3H), 1.77 (s, 3H). **^{13}C NMR** (151 MHz, CDCl$_3$) δ 158.28, 137.4, 133.9, 132.0, 128.4, 120.1, 119.4, 116.4, 110.8, 103.8, 29.8, 29.0, 25.8. **LC-MS** (*m/z*) (ES-): 186.0 [M-H]$^-$

4-(but-3-en-2xyloxy)benzamide (57)
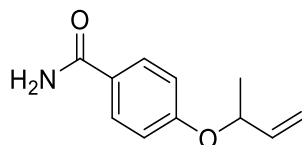
To a solution of 4-hydroxybenzamide **52** (205 mg, 1.5 mmol) in dry DMF (5mL) under N_2 flux, K_2CO_3 (414 mg, 3 mmol) and KI (124.5 mg, 0.75 mmol) were added Then a solution of 3-chloro-1-butene (0.182 mL, 1.8 mmol) in dry DMF was slowly added dropwise at room temperature and the mixture was then stirred at 50 °C for 16 h. After cooling, the mixture was diluted with EtOAc and the organic phase was washed with H_2O and Brine, dried over Na_2SO_4, filtered, and evaporated under vacuum. The mixture was purified by flash chromatography (20% EtOAc in petroleum ether) and obtained as a yellow oil. **YIELD:** 54%. **¹H NMR** (400 MHz, MeOD) δ 7.78 (d, J = 8.8 Hz, 2H), 6.94 (d, J = 8.8 Hz, 2H), 5.89 (m, 1H), 5.26 (m, 1H), 5.15 (m, 1H), 4.93 (m, 1H), 1.40 (d, J = 6.4 Hz, 3H) **¹³C NMR** (101 MHz, MeOD) δ 170.62, 161.07, 138.66, 129.15, 129.04, 115.04, 114.79, 74.36, 20.15 **LC-MS** (*m/z*) (ES-): 214.0 [M+Na]⁺

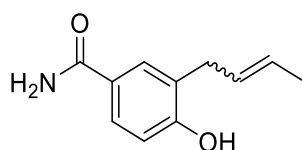## (*E, Z*) 4-hydroxy-3-(methylbut-2-en-1-yl)benzamide (58)

57 (80 mg, 0.41 mmol) was charged in a MW vessel under inert atmosphere. Ph_2O (0.240 mL) was added and the reaction was heated MW 230 °C, 3x40 min, at a fixed power of 300 Watt. After cooling, the mixture was purified by flash chromatography (2% EtOAc in petroleum ether) and obtained as a brown solid. **YIELD**: 35%. **¹H NMR** (400 MHz, MeOD) δ 8.48 (s, 1H), 7.92 (s, 1H), 7.60 (m, 2H), 5.60 (m, 2H), 3.36 (d, 2H), 1.65 (d, 2H) **¹³C NMR** (101 MHz, MeOD) δ 171.57, 158.20, 129.46, 128.82, 127.29, 126.75, 125.47, 124.20, 113,96, 32.04, 18.72 **LC-MS** (*m/z*) (ES-): 186.0 [M-H]⁻

2-(3-bromophenyl)-2-methyl-1,3-dioxolane (60)
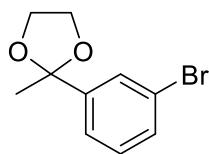
To a solution of 3-bromo-acetophenone (**59**) (0.354 mL, 2.5 mmol) in ethylene glycole (1.5 mL, 25 mmol), a catalytic amount of I_2 was added and the mixture was stirred MW, 3x20 min at 80 °C (power fixed at 150 W). The reaction was quenched with a saturated solution of $Na_2S_2O_3$ and the aqueous phase was extracted with EtOAc. The combined organic layers were dried over Na_2SO_4, filtrated and evaporated under vacuum. The crude was purified by chromatography (Hexane) and product was obtained as yellowish oil. **YIELD**: 40%. [1]**H NMR** (600 MHz, CDCl$_3$) δ 7.62 (m, 1H), 7.38 (m, 2H), 7.19 (m, 1H), 4.02 (m, 2H), 3.75 (m, 2H), 1.61 (s, 3H). **LC-MS** (*m/z*) (ES+): 267.1 [M+Na]$^+$

1-(3-(3-methylbut-2-en-1-yl)phenyl)ethan-1-one (40)
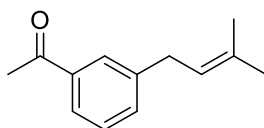
Mg turning (25 mg, 1 mmol) was charged in a two necks flask under N_2 atmosphere. Then a solution of **61** (240 mg, 1 mmol) in dry THF (1 mL) was added and the mixture was refluxed for 1h. Then it was allowed to reach room temperature and CuI (7.6 mg, 0.04 mmol) and 1-chloro-3-methyl-2-butene (0.075 mL, 0.67 mmol) were slowly added at 0 °C and then the mixture was stirred rt for 4 h. The mixture was quenched with NH_4Cl ss, and the aqueous phase was extracted with EtOAc. The combined organic layers were dried over Na_2SO_4, filtrated, and the solvent was evaporated under vacuum. After purification, a mixture of ME **42** and its derivative acetals derivative acetal was obtained and it was used for the next step without further purification.

To a solution of a mixture of **42** and its acetal derivative (80 mg), in THF (2.5 mL), HCl 1N was slowly added dropwise and the mixture was stirred rt for 48 h. NaOH 2N was added, and the aqueous phase was extracted with EtOAc. The combined organic layers were dried over Na_2SO_4, filtrated and evaporated under vacuum. The crude was purified by flash chromatography (1% EtOAc in petroleum ether) and obtained as a white solid. **YIELD:** 25% (overall two steps). **^{1}H NMR** (600 MHz, CDCl$_3$) δ 7.77 (m, 2H), 7.38 (m, 2H), 5.32 (t, J = 7.1 Hz, 1H), 3.50 (d, J = 7,1 Hz, 2H), 2.59 (s, 3H), 1.76 (s, 3H), 1.74 (s, 3H). **^{13}C NMR** (151 MHz, CDCl$_3$) δ 198.4, 142.4, 137.3, 133.4, 133.2, 128.6, 128.1, 125.9 122.5, 34.2, 26.7, 25.7, 17.9. **LC-MS** (*m/z*) (ES-): 211 [M+Na]$^+$

III – Design of a 2-alkyl-4-hydroxyquinoline derivative photoaffinity labelling probe

1. INTRODUCTION

1.1 Photoaffinity labelling

Photoaffinity labelling (PAL) is a technique originally developed by Singh and Westheimer in 1962[316] that represents a very effective method of investigation of small molecules-protein interaction with atomic level precision; for this reason, it represents a very important tool for drug discovery, that can be exploited for i) binding sites identification of known targets, ii) the identification of unknown novel or alternative binding sites or targets or even for iii) the elucidation of protein structures. In this context, small molecules target identification is one of the most common fields of application of PALs, but they are largely used also for ligandability profiling, to survey for ligand binding sites or to screen possible competing molecules in the site of action.[317]

In small molecules target identification, an active small molecule is generally derivatized in a photoaffinity probe (PAP) that preserves parent's molecule phenotypic characteristics.[318] A PAP is generally constituted by an affinity (or specificity) unit (blue), a photoreactive moiety or photoactivable group (PAG) (red), a linker and an identification (or reporting) tag (green) (Figure 38).

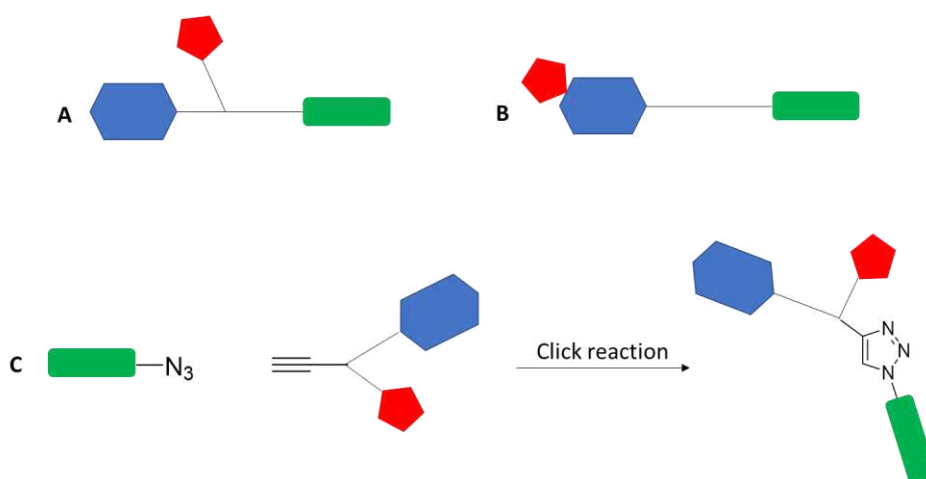**Figure 38.** (A) PAL probe with photo group, pharmacophore and reporter tag remote from one another and connected by linkers. (B) PAL probe with photo group directly incorporated within the pharmacophore. (C) Two-component PAL probe with pharmacophore and protogroup in a separate molecule to the reporter tag, then connected by a conjugation step through 1,3-cycloaddition reaction (click chemistry) between alkyne and azide.[318]

The affinity (or specificity) unit is a small molecule that shares a high structural similarity with the active parent compound and ensures the formation of an initial reversible bond with the protein of interest. The identification (or reporting) tag, instead, is necessary for the detection and isolation of the ligand-protein adduct, i. e. biotin, a radioisotope or a fluorescent dye.
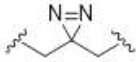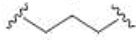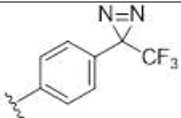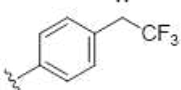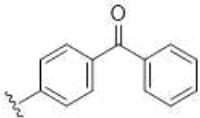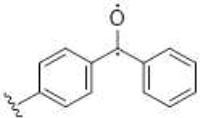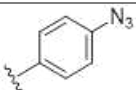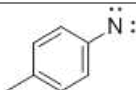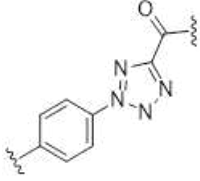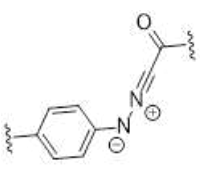
PAGs are usually placed on the linker or, sometimes, on the affinity unit. When irradiated with a light of a specific wavelength, the photoreactive group generates a reactive intermediate that reacts very fast with a molecule in the proximity, ideally the target-protein, creating a permanent bond with it.

Originally, Singh and Westheimer used a α-keto diazo functional group,[316] in particular a diazoacetate, to map the architecture of chemotripsin, but in the years several functional groups with different sizes and able to generate different reactive species were developed:[319] among that alkyl diazirines,[320] trifluoromethyl diazirines,[321] benzophenones,[322] aryl azides,[323] and, most recently, 2-aryl-5-carboxytetrazoles[324] are the most employed (Table 13).

Labelling is most influenced by two factors: i) the amino acidic composition of the binding interface, since some probes present a specificity for some amino acids, and ii) the lifetime of the reactive intermediate, that is related to the labelling radius.[325] Generally, short half-lives increase the labelling specificity by limiting the diffusion of the probe to nearby proteins after the formation of the reactive specie.

Once synthesized, PAP is incubated in cells or lysates and, once the affinity group binds the target, it is activated with light to trigger crosslinking.[318] After the click reaction, if it is necessary, labelled and tagged proteins are separated by affinity purification using the reporter tag and an SDS-PAGE allows to visualise labelled proteins using specific reagents. Proteins are excised from the gel and undergo multiple protein digests to produce peptide fragments analysed by LC-MS/MS.

Table 13. Principal PAGs.[319]

PAG	Main reactive specie	Wavelength	Half-life	Amino acids
Diazirine	Carbene	350-380 nm	2 ns	none
Diazirine	Carbene	350-380 nm	2 ns	none
Benzophenone	Diradical	350-365 nm	30-40 µs	Met
Aril azide	Nitrene	300 nm	0.1-1 ns	nucleophiles
Tetrazole	Nitril imine	300 nm	7.5 s	Glu, Asp

Secondary reactive products are not reported.[319]

1.1.1 Alkyl-diazirines

Diazirines are three-membered ring systems that contain two nitrogen atoms, in a N=N double bond, and a carbon atom:[319,326,327] their high reactivity, small size and rapid solvent quenching make them very attractive PAGs. Diazirines are stable at room temperature, to acids and bases and in oxidative and mild reaction conditions and they are unreactive towards nucleophiles and electrophiles.

Irradiation of a diazirine with UV-light at a λ of 350 nm triggers the formation of a reactive carbene (Scheme 18), together with the isomerization to a diazo compound that undergoes protonation and recombination of ion pair and can react selectively with acidic amino acids in a pH-dependent manner.[328] Carbene singlet can undergo concerted XH reactions, with a rapid insertion into nearby O-H, N-H or C-H bonds of the target or interconvert in a triplet carbene

specie that undergoes to a stepwise XH abstraction/recombination (Scheme 18). Carbenes have an estimated half-life of 1-2 ns which limits their distance of diffusion to 2-4 nm before it is quenched by the solvent[328] and can theoretically label all the amino acids, with a slight preference for the nucleophilic ones.[329]
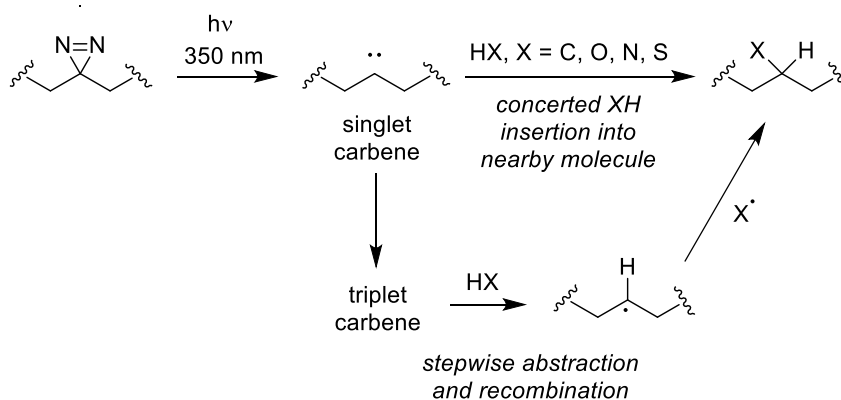
Scheme 18. Photolysis of alkyl diazirines to carbene. The carbene is generated as a singlet in equilibrium with a triplet carbene which can label nearby amino acids.

Alkyl diazirine are usually obtained from ketones present in the parent molecule in three steps:[327] i) addition of liquid ammonia to obtain the correspondent N-H imine, followed by ii) the addition of hydroxylamine-*O*-sulfonic (HOSA) acid to form the diaziridine moiety and iii) the final oxidation of the diaziridine in diazirine by use of oxidating agents as I_2 and Et_3N (most common) or Hunig's base, AgO_2 or Jones reagent (Scheme 19). Moreover, slightly different strategies were developed.
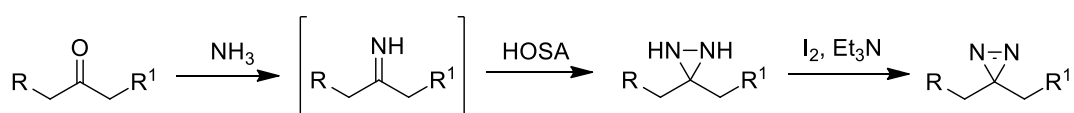
Scheme 19. Classical synthesis of diazirines.

In alternative, a molecule can be functionalized by trifunctional tags endowed with the diazirine, a triple bond for biorthogonal click chemistry and an alcohol for the attachment to the parent molecule.[319]

1.2 2-alkyl-4-hydroxyquinolines

2-alkyl-4-hydroxyquinolines (AQs) compounds are a group of natural microbial metabolites that are usually substituted with different alkyl chains and different degrees of unsaturation in

position 2, the most known produced by *Pseudomonas Aeruginosa*.[330,331] Pseudomonas Quinolone Signal (PQS), that is also an auto-inducer, and its biosynthetic precursor hydroxy-2-heptilquinoline (HHQ), play an important role in Quorum Sensing (QS), intraspecies signals involved in the formation of biofilm and motility,[332] in the production of virulence factors[333] and in the modulation of the immune response (Figure 39).[334]
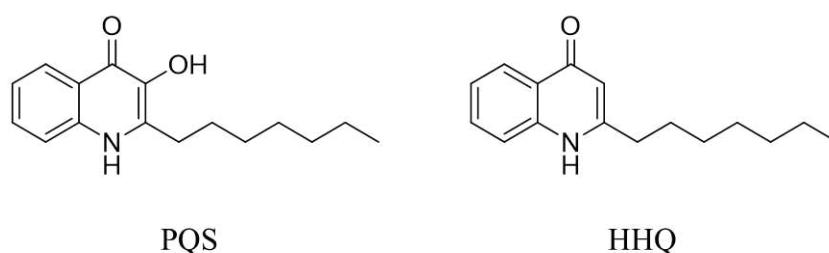
Figure 39. Structures of PQS and HHQ.

2-alkyl-4-quinolone *N*-oxides (AQNOs) produced by bacteria also have antibacterial effects attributed to the inhibition of cytochromes in the respiratory chains of bacteria, but they are not involved in QS.[335]

Similar molecules are also produced by other bacteria as *Pseudonocardia*[336] *Burkolderia*[337] and *Streptomyces*,[338] and other alkyl-quinolones responsible for QS were individuated.[332]

1.2.1 2-alkyl-4-hydroxyquinolines: antibacterial activity

Pseudomonas Aeruginosa and *Staphylococcus Aureus* (together with species of genus *Burkholderia*) are the leading cause of comorbidity and mortality in polymicrobial chronic pulmonary infections that affect patients with cystic fibrosis.[339] Their cooperative or competitive interactions influence their survival and persistence, as well as the antibiotic susceptibility or resistance and, consequently, the progression of the disease.[340] While *Pseudomonas Aeruginosa* produces and expels respiratory inhibitors, like pyocyanin and quinoline *N*-oxides, that block the electron transport pathway and suppress the growth of *Staphylococcus Aureus*, on the other hand it survives by adapting to a respiration-defective small colony variant (SCV), antibiotic resistant phenotype that causes persistent and recurrent infections.

As aforementioned, PQS is an auto-inductor. When a threshold extracellular concentration is reached, PQS actives the transcriptional regulator PqsR. The complex PQS-PqsR binds the promoter of *pqsA,* ligase responsible of the first step of the synthesis of PQS and HHQ.

Antagonists of PqsR, potentially including 2-alkyl-4-hydroxyquinolines can represent an attractive alternative to conventional antibacterial therapies.[341] Lu and co-workers identified three antagonists of PqsR with a IC$_{50}$ in nanomolar range.[342] These compounds, analogues of HHQ and endowed with a strong electron-withdrawing group in position 6 of the ring, are not only efficient competitors for PqsR, but they are also able to reduce the production of the factor of virulence pyocyanin.

Saturated and unsaturated 2-alkyl-4(1H)-quinolone N-oxides of *Pseudomonas* (AQNOs) and *Burkholderia* (MAQNOs) possess antibiotic activity against *Staphilococcus aureus* with antagonist action on cytochromes:[335,343] AQNO can inhibit the respiratory chain blocking the menaquinone binding-site by miming the function of menaquinone (MH)/menaquinol (MKH$_2$), that shuttles electrons in the respiratory chain.[344,345] AQNO would directly inhibit the cytochrome in aerobic conditions, while in anaerobic ones the inhibition activity would be performed on nitro-reductase. Unsaturation of the alkyl chain or methylation of the quinoline improves the activity of these compounds.[343] 3-methylation of MAQNOs contributes in a significant way to the long-lasting inhibition growth and metabolic activity, increasing the structural resemblance of quinolone-N-oxide to menaquinone. On the other hand, unsaturation of AQNOs and MAQNOs in Δ^1-position increases antibiotic activity compared to Δ^2-position, the position of unsaturation in menaquinones, probably because it reduces structural flexibility of the inhibitors in the binding site of the target proteins improving the activity (Figure 40).
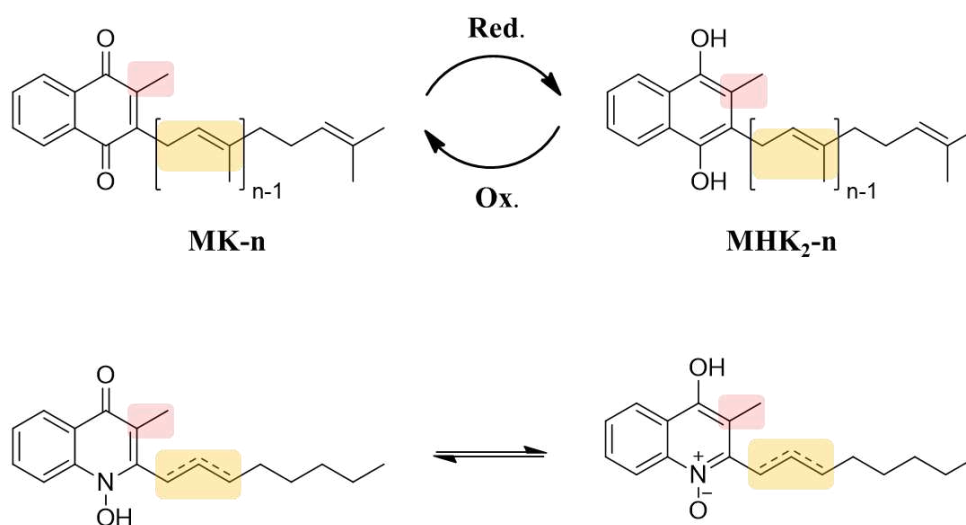
Figure 40. Structural analogy of the menaquinone (MK)/menaquinol (MKH2) redox couple and the tautomers of quinolone N-oxides.[343]

Non oxidized 2-alkyl-4-hydroxyquinolines also showed activity on *Staphylococcus Aureus*. Thierbach and co-workers synthesized selectively methylated derivatives of AQs, HHQ, PQS and HQNO and some of them, as HQNO methylated derivatives and *N*-Me-PQS showed an interesting activity on *Staphylococcus aureus*, superior to natural compounds.[346]

1.2.2 2-alkyl-4-hydroxyquinolines and photolabelling

Two interesting examples of 2-alkyl-4-hydroxyquinolines modified for the synthesis of PAPs used to highlights the role of PQS and HHQ in QS are reported in literature.

In 2017, Baker and co-workers developed two probes mimics of PQS and HHQ choosing aryl azides as photoreactive groups:[347] in their studies on *Escherichia Coli* and *Pseudomonas Aeruginosa* they found that PQS probably binds a protein involved in phenazine biosynthesis and the regulatory protein Rhlh, that would possibly be a high attractive target for anti-virulence strategy.

In 2018, Meijler group developed two different probes endowed with a diazirine photoreactive group still based on the structure of PQS and HHQ to identify their unknown protein targets in living cells miming the activity of the parent compounds.[348] In this case, one of the most interesting finding was that PQS and HHQ show a remarkable promiscuity in different pathways, some of that with key roles in pathogenicity of *Pseudomonas Aeruginosa*. They also identified all the proteins of the previous work, except for Rhlh and Pfpl, with the difference that 182 proteins were found, compared to the 11 found by Baker and co-workers. This suggests a significant overlap between the two kinds of probes, with a difference probably due to the alternative photoreactive groups, which difference in photo crosslinker had been already reported for carbohydrates.

1.3 Aim of the work

In the past few years, Dr. Luc Rocheblave and co-workers synthesized a library of 4-hydroxyquinoline compounds with a good antibacterial activity on *Staphylococcus Aureus*.[349] These compounds act as antagonists, some of them with a Minimal Inhibitory Concentration (MIC) of 4 or 8 mg/mL. The most active compounds of the series present a monounsaturated aliphatic chain length of 10-13 carbons with a non-conjugate double bond in position 3 (Figure 41 left).

The aim of this work was the evaluation of efficient synthetic routes for the synthesis of a derivative molecule decorated with a ketone, in replacement of the double bond, precursor of a reactive moiety as diazirine, as starting point for the synthesis of a photolabeling probe useful to better elucidate the interaction between these compounds and bacteria (Figure 41, right).
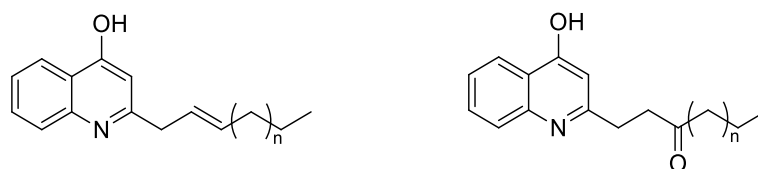
Figure 41. General structure of 4-hydroxyquinoline compounds and of probe precursor.

2. RESULTS AND DISCUSSION

Original synthesis of 4-hydroxyquinolines easily provided a chlorinated intermediate (**62**) in three steps starting from kynurenic acid, interesting as starting material for the synthesis of desired ketone compound (Scheme 20).[349]
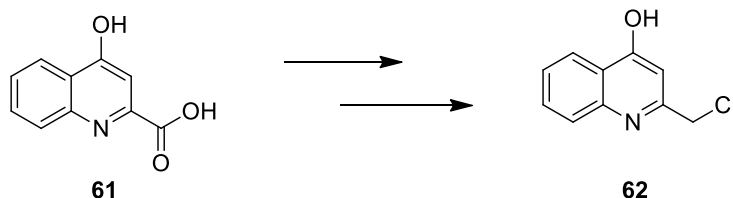
Scheme 20. Synthesis of intermediate **62**.

Benzylic chloride moiety can represent an interesting leaving group, exploitable for alkylation or Grignard reaction; on the other hand, mobile proton of free phenol could represent an obstacle to the good outcome of the reaction. Moreover, benzyl chloride moiety can compete with a lot of reagents useful to put a protecting group.

A different synthetic route was delighted to obtain a protected compound with a similar reactive moiety (Scheme 21).
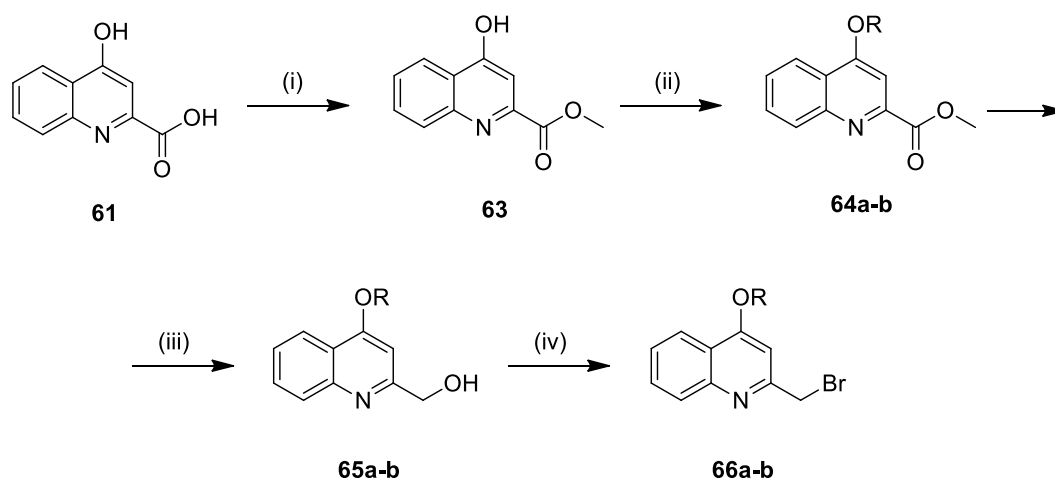
a: R = PMB
b: R =CH$_2$-CH$_2$=CH$_2$

Scheme 21. Synthesis of compounds **66a-b**. i) H$_2$SO$_4$, MeOH, 66 °C, 16 h, 90%; ii) a) 4-methoxybenzyl chloride, K$_2$CO$_3$, KI, DMF, 60 °C, 5 h, 78%; b) allyl bromide K$_2$CO$_3$, KI, DMF, 60 °C, 5 h, 70%; iii) NaBH$_4$, THF/MeOH 1:1, 66 °C, 3 h a) 90%, b) 34%; iv) NaBH$_4$, THF/MeOH 1:1, 66 °C, 3 h, a) 90%; b) 20%.

Kynurenic acid was firstly converted into methyl ester heating a solution in MeOH and H$_2$SO$_4$: stirring the reaction mixture at reflux for 16 h, ester derivative **63** was obtained in 90% yield. 4-methoxybenzyl (PMB) and allyl groups were firstly used to protect the phenolic moiety. **63** was reacted with both 4-methoxybenzil chloride and allyl bromide in DMF in presence of K$_2$CO$_3$ and KI: the reactions were stirred at 60 °C for 5 h and compounds **64a-b** were obtained in yields over 70% by precipitation in EtOAc, in which they are scarcely soluble, without chromatographic purification. Both esters were easily converted in alcohols by reduction with NaBH$_4$ in THF/MeOH, stirring the mixture at reflux for 3 h. The reaction was quenched, the solvent was evaporated and **65a** was easily obtained by precipitation of the product in H$_2$O. The white solid obtained was filtrated and washed with H$_2$O, in which boric salts are soluble, and the product was obtained in 90% yield. The same procedure could not be exploited for **65b**, that had to be recovered by chromatographic purification. The affinity of the product for silica made the purification very challenging and the product was finally recovered in 34% yield.

Table 14. Synthesis of **66a**.

65a → 66a
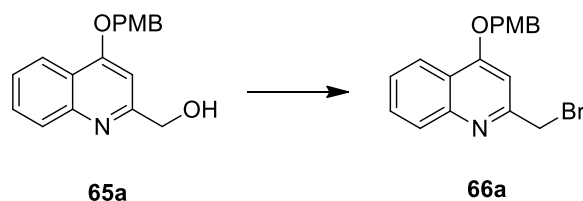
Entry	Conditions	Yield
1	PPh$_3$ (x eq), NBS (1.2 eq) dry DCM, 0 °C to r.t., 16 h	54%
2	PPh$_3$ (1.4 eq), CBr$_4$ (1.4 eq) dry DCM, 0 °C to r.t., 16 h	55%
3	PPh$_3$ (1.2 eq), CBr$_4$ (1.2 eq) dry DCM, 0 °C to r.t., 4 h	80%
4	PPh$_3$ (1.2 eq), CBr$_4$ (1.2 eq) dry Et$_2$O/ACN 3:1, 0 °C to r.t., 3 h	70%

At this point, it was decided to substitute the chloride with a better leaving group. Attempts to obtain an iodine derivative were failures, probably because of the great reactivity of this leaving group in this position; for this reason, bromine was selected. Different conditions were evaluated to obtain the bromination of the alcohol (Table 14).

Alcohol **65a** was reacted with different brominating agents in presence of PPh$_3$, using dry DCM as solvent (Table 14, entries 1-3) under inert atmosphere. Firstly, *N*-bromosuccinimide (NBS) was used as brominating agent: after the addition of PPh$_3$ and NBS at 0 °C, the reaction mixture was stirred at room temperature: after16 h, alcohol was still present and **66a** was obtained in a 54% yield (Table 14, entry 1). Using CBr$_4$ (1.4 eq) as brominating agent and PPh$_3$ (1.4 eq) SM was completely converted, but yield did not improve. According to the LC-MS spectrum, it was hypothesized the formation of a double brominated compound both in the desired position and in an activated position on the aromatic ring. Unfortunately, the by-product was not isolated, so its structure was not confirmed. To avoid a possible double bromination, a lower amount of CBr$_4$ (1.2 eq) and PPh$_3$ (1.2 eq) (Table 14, entry 3) were used in the same conditions and the reaction provided **66a** in 80% yield, with a complete consumption of SM and avoiding the formation of by-products. Unexpectedly, the same

reaction conditions in presence of **65b** as starting alcohol, provided **66b** in very poor yields (20%).

The reaction was also performed replacing dry DCM with in anhydrous ACN/Et$_2$O mixture as solvent (Table 14, entry 4), with the purpose of precipitate phosphinoxide in the reaction environment and obtain **66a** by filtration in DCM, to separate it from the excess of PPh$_3$ not reacted. Phosphinoxide was precipitated with petroleum ether and filtrated but, unfortunately, precipitation resulted incomplete. Moreover, the low solubility of compound **66a** in petroleum ether determined a bad separation and chromatography was necessary: even in this case, the reaction provided **66a** in good yield (70%).

All the synthetic route was also scaled up to gram scale without any impact in yields, with an exception for bromuration step. In fact, increasing the amount of starting alcohol only SM was recovered. Since the presence of phosphinoxide was detected in LC-MS, the first idea was that, even trying to work in dry conditions, water was still present in the reaction mixture and produced back the starting reactant due to a further substitution. To avoid it, the reaction was performed in anhydrous conditions in presence of activated molecular sieves, but the same result was obtained. For this reason, it was preferable to divide a larger amount of SM in parallel reactions to afford an effective "scale-up".

Once obtained **66a** in large amounts, different strategies for the obtainment of the ketone were evaluated. The faster way to obtain the ketone was find the direct alkylation of **66a** with ketones of different alkyl chains (Scheme 22).
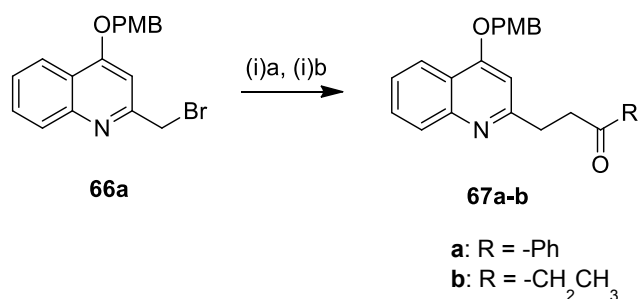
Scheme 22. i) a: acetophenone, NaH, dry THF, -10 °C to rt, 16 h, 25%; b: 2-butanone, LDA, dry THF, -78 °C to r.t., 16 h, 20% (mix).

To evaluate the possibility to successfully perform the reaction, a first attempt was made using acetophenone as ketone, since the formation of only one enolate is possible in presence of strong bases. Reacting acetophenone and **66a** with NaH at -10 °C in anhydrous THF, **67a** was obtained in a promising 25% yield (Scheme 22, a).

The reaction was then performed in small scale (50 mg) using 2-butanone as starting ketone. In this case, LDA was prepared in situ and used as base to guarantee the formation of the kinetic enolate, which was reacted with **66a** at -78° C in anhydrous THF for 3 h purging the solution with Ar (Scheme 22, b). The formation of the product was detected in LC-MS, but the isolated compound was recovered in too small amount for an exhaustive characterization with NMR, necessary to confirm the formation of the right isomer. For this reason, the same reaction was performed in a bigger scale (250 mg) in the same reaction conditions. Since after 3 h reaction seemed to not occur, it was stirred at room temperature for 16 h. Then, TLC showed a completely consumption of the SM, and the formation of different compounds. Every spot was isolated and check in the LC-MS and NMR. The spot responding to the mass of **67b** resulted to be a mixture of both the isomers derived from the formation of both the kinetic and thermodynamic enolates. From these results it was understood that reaction was possible, but reactivity of **66a** at -78°C needed to be improved to totally avoid the formation of the thermodynamic enolate, seen the difficulty to separate the isomers by flash chromatography.

The following optimization was directly performed using a ketone with a long alkyl chain.

Table 15. Synthesis of compound **69**.
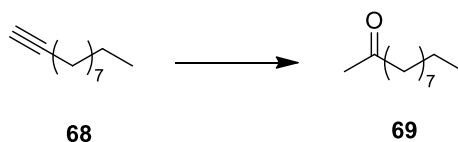
Entry	Conditions	Yield
1	H$_2$O, PdCl$_2$ 1,4-dioxane, 80 °C, 20 h	-
2	H$_2$O, pTSA, Hg (II) acetate Acetone, r.t., 16 h	85%

1-undecyn (**68**) was firstly stirred in presence of H$_2$O and catalytic PdCl$_2$ in 1,4-dioxane at 80 °C for 20 h, but only starting material was recovered (Table 15, entry 1). According to literature, mercuric salts guarantee very good results in this kind of transformation. In fact, performing the reaction in presence of Hg (II) acetate and pTSA in acetone at room temperature, after 16 h a full conversion was obtained and compound **69** was isolated with an 85% yield (Table 15, entry 2).

Once obtained the ketone, it was used for the alkylation of **66a** (Table 16).

Table 16. Synthesis of compounds **70** and **71**.
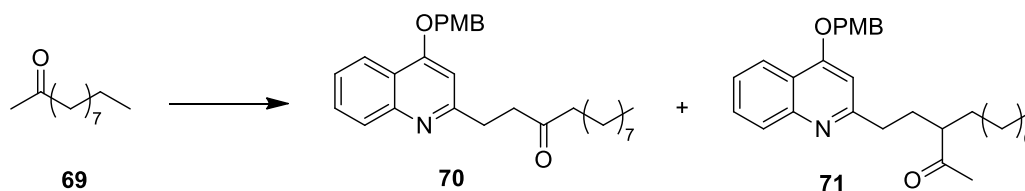
Entry	Conditions	Yield
1	LDA (1.2 eq), **66a** (1.2 eq) dry THF, -78 °C to r.t., 3 h	**70**, 10%
2	LDA (3 eq), **66a** (1.2 eq), TBAI (0.12 eq) dry THF, -78 °C, 2 h	-
3	LDA (1.5 eq), **66a** (1.2 eq), TBAI (0.12 eq) dry THF, -78 °C, 2 h	**71**
4	LiHDMS (1.5 eq), **66a** (1.2 eq), TBAI (0.12 eq) dry THF, -78 °C, 2 h	-

LDA was again synthesized in situ with redistilled diisopropylamine and titrated *n*-BuLi. The reaction was stirred at -78 °C in dry THF for 2 h, but only SM was detected in TLC an LC-MS. To push the reaction, the temperature was led to -10 °C and stirred for 1 h at this temperature, then the reaction was stirred for a further hour at room temperature. After purification, compound **70** was isolated in the right isomer in very poor yield (10%) (Table 16, entry 1).

To push the reaction, LDA was added by cannulation in high excess (3 eq; Table 16, entry 2). Tetrabutylammonium iodide (TBAI) was also added to the reaction mixture in catalytic amount, to obtain a better leaving group by exploitation of Finkelstein like conditions. According to both TLC and LC-MS, after stirring the reaction for 2 h at -78 °C in dry THF, SM was completely consumed. The temperature was slowly lead at room temperature during 12 h before the work up was performed, then different products were isolated by flash chromatography, all of them by-products of degradation (Table 16, entry 2).

Thinking that the problem was represented by the excess of base, the reaction was performed using 1.5 equivalents of LDA, maintaining all the other reaction conditions. Once again, the

reaction provided different products, among them, unexpectedly, **71**, as confirmed by NMR spectrum, while **70** was not isolated (Table 16, entry 3).

The more hindered non nucleophile base LiHMDS was used instead of LDA in the same conditions, to favour the formation of the kinetic enolate, but the reaction did not provide nor **70** or **71** (Table 16, entry 4).

Seen the great difficulty to obtain **70** by alkylation in an efficient and reproducible way, an alternative synthetic route was evaluated. In particular, the possibility to synthesize the ketone on the quinoline and make it react with a long chain bromine was attractive: it was then evaluated the possibility to put a triple bond at two carbons of distance from the quinoline ring to obtain a methyl ketone in the desired position by hydration, exploiting the procedure successfully used for the obtainment of **69**.

The possibility to react vinyl bromide and **66a** with a Grignard reaction was explored.

Table 17. Synthesis of compound **74**.
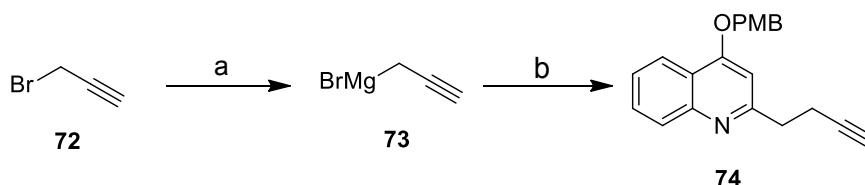
Entry	a	b	Yield
1	Mg^0 (1 eq) dry THF, r.t. to reflux, 1 h	**66a** (0.67 eq), CuI (4 mol%) dry THF, 0 °C to r.t., 4 h	-
2	Mg^0 (1 eq), Hg_2Cl_2 cat. dry THF, r.t. to reflux, 1 h	**66a** (0.67 eq) dry THF, 0 °C to r.t., 4 h	-
3	Mg^0 (1 eq), Hg_2Cl_2 (10 mol%) dry Et_2O, r.t., 1 h	**66a** (0.3 eq) dry THF, 0 °C to r.t., 16 h	20%
4	Mg^0 (1eq), $ZnBr_2$ dry THF, reflux, 3 h	-	-

Firstly, propargyl bromide was reacted with Mg turnings in anhydrous THF, purging the reaction with Argon and, after the mixture was refluxed for 1 h purging the reaction with Argon, Mg seemed to be completely consumed (Table 17, entry 1). A solution of **66a** and CuI in anhydrous THF were added, but after stirring for 16 h **74** was not provided. The same reaction was performed adding a catalytic amount of Hg_2Cl_2, as auxiliary in the formation of

the Grignard reagent, but, even in this case, product **74** was not obtained, while only **66a** was recovered (Table 17, entry 2). At least, THF was substituted with anhydrous Et₂O and 10 mol% of Hg₂Cl₂ were added to Mg turning: after 1 h Mg was consumed and a solution of **66a** in anhydrous THF was added (Table 17, entry 3). The reaction was stirred for 16 h and **74** was obtained in low yield (20%).

One attempt was performed using ZnBr₂, instead of HgCl₂, to perform the Grignard formation in a safer way, that also should selectively guarantee the maintenance of triple bond without the formation of the allene.[350] **66a** was reacted with Mg⁰ in presence of ZnCl₂ in dry THF and the mixture was refluxed for 3 h. Unfortunately, reaction didn't occur, since all Mg⁰ was still present unreacted (Table 17, entry 4).

For the best of our knowledge, the attempt to synthesize Grignard reagent on the quinoline decorated with a benzylic bromide was never described in literature. Stirring **66a** and Mg in anhydrous THF purging the mixture with Argon did not afford the desired Grignard, not even under refluxing the solution for few hours.

Seen the different problematics found, as the drastic conditions needed to obtain the product in low yields and the possibility to finally obtain the allene instead of the triple bond after the reaction, it was decided to replace the alkyne with a double bond.
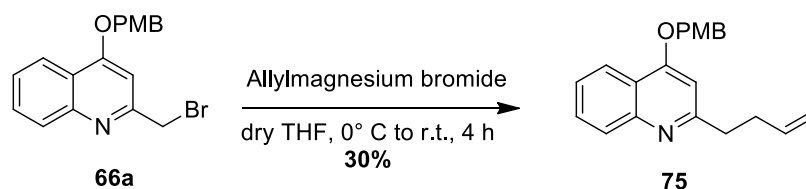
Scheme 23. Synthesis of **75.**

75 was easily obtained in moderate yield (30%) by stirring **66a** in presence of allyl magnesium bromide for 4 h in dry THF under anhydrous atmosphere (Scheme 23). The double bond could represent an interesting versatile moiety, potential precursor not only of a methyl ketone, by hydration and oxidation of the alcohol obtained under Markovnikov conditions, but also of different interesting functional groups, like aldehydes, alcohols or epoxides.
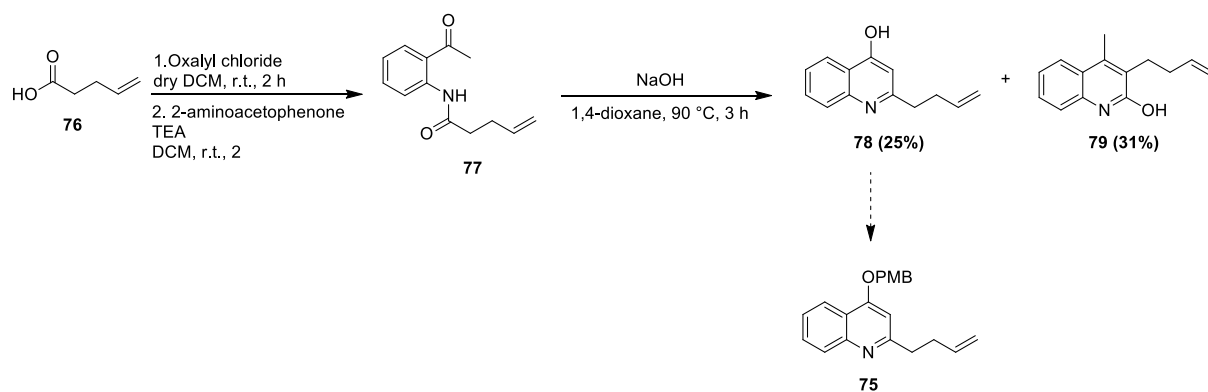
Scheme 24. Synthesis by Conrad-Limpach cyclization.

A more rapid way for the obtainment of **75** was considered, following Conrad-Limpach cyclization reaction conditions (Scheme 24).

Pentenoic acid (**76**) was activated as acyl chloride by stirring it with oxalyl chloride in dry DCM at room temperature for 2 h. Then, after the evaporation of volatiles, the acyl chloride was reacted with 2-aminoacetophenone in dry DCM for 16 h to afford **77**. Product was not purified. After the evaporation of the solvent, the crude was stirred in 1,4-dioxane for 3 hours at 80 °C in presence of NaOH. Purification by crystallization of the product was tried exploiting several solvents without success, and only after a very challenging chromatographic purification to separate them, both isomers **78** and **79** were recovered in moderate yield, respectively 27% and 31%. Since cyclization provided **78** as minor isomer the previous synthetic way that, instead, directly provides **75** in acceptable to excellent yields, in gram scale and without necessity of chromatographic purification for most of the steps, was preferred.

Starting from **75**, the first attempt was the transformation of the double bond in an epoxide, to subsequently open it by reaction with a long chain alkyl magnesium bromide to obtain a secondary alcohol which could finally be oxidized providing the desired ketone. Two side reactions were predicted for this kind of transformation: i) the formation of the *N*-oxide, taken as granted as side reaction and ii) the cleavage of the -PMB, usually cleaved in mild oxidative conditions. The simultaneous formation of the *N*-oxide and the epoxide was considered less problematic: in fact, *N*-oxide could be further reduced with an additional step, or optionally maintained, seen the interesting activity of these compounds. For these reasons, attention was firstly focused in finding a procedure that would guarantee the maintenance of the PMB protecting group, to avoid at least the necessity of a further step to reintroduce it in the molecule.

143
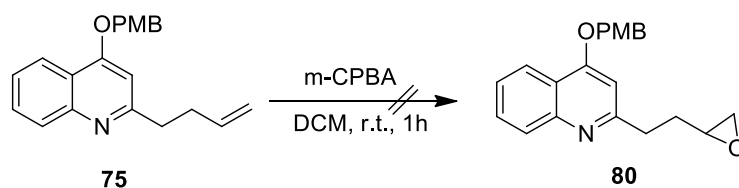
Scheme 25. Synthesis of compound **80**.

75 was reacted with a little excess of m-CPBA in DCM (Scheme 25). After 3 h at room temperature, starting material seemed mostly consumed, and the formation of a compound with mass attributable to epoxide or *N*-oxide products was confirmed by LC-MS. Interestingly, after chromatographic purification, a large amount of SM was recovered. To be sure of a real complete conversion of the starting material, the same reaction was performed stirring the mixture at room temperature for 16 h. Even in this case, SM seemed to be completely absent according to TLC, but, after purification, it resulted to be the only recovered product. Since both epoxide and *N*-oxide are usually stable in the purification conditions used, it was difficult to hypothesize what kind of labile product was formed in these conditions. For this reason, NMR spectrum of the crude mixture was performed. Unfortunately, NMR was also unhelpful to understand what effectively happens in the reaction.

3. CONCLUSIONS

In conclusion the first attempts to obtain a versatile synthesis for the obtainment of a precursor of a future photolabeling probe, starting from antibacterial 4-hydroxyquinoline compounds were performed. The main goal to obtain compound decorate with a ketone in replacement of the original double bond, as precursor for a future reactive moiety in a photolabeling probe, was not achieve. Nonetheless, different interesting synthetic routes were deeply studied and promising intermediates for the successful continuation of this project.

3.1 Future perspectives

As future perspective for this work, a further investigation of the epoxide formation reaction should be performed and different work-up or chromatographic conditions should be evaluated. The reaction could maybe be performed in larger amounts, to see if it's possible to isolate and characterize even a small amount of the formed product.

As alternative, the Markovnicov hydration of the double bond to obtain a secondary alcohol or a ketone must be evaluated.

Grignard reaction with bromo-derivative quinoline compounds is unexpectedly very promising and, for the best of our acknowledgement, never described in literature. An investigation of the reaction, its optimization and its possible application with different quinolines or Grignard reagents would be particularly interesting.

75 is an interesting versatile product and its use as intermediate even for different purposes should be considered.

4. EXPERIMENTAL SECTION

4.1 Materials and methods

All reagents were used as purchased from commercial suppliers without further purification. The reactions were carried out in oven dried vessels. Solvents were purchased in anhydrous form.

Flash column chromatography was performed with Merck silica gel Å 60, 0.040-0.063 mm (230-400 mesh). MPLC Syncore Büchi on highly resistant PP cartridges Normal Phase silica gel NP 40 – 63 μm particle size and 60 Å pore size (Si60) withstand a maximum pressure of 10 bar (145 psi) column with PE (Eluent A) and EtOAc (Eluent B) as mobile phase.

Merck aluminium backed plates pre-coated with silica gel 60 (UV254) were used for analytical thin layer chromatography and were visualized by staining with a KMnO4 or Ninidrine solution.

NMR spectra were recorded at 25 °C With 400 MHz for ^{1}H and 101 MHz for ^{13}C Brücker Advance NMR spectrometers. The solvent is specified for each spectrum. Splitting patterns are designated as s, singlet; d, doublet; t, triplet; q, quartet; m, multiplet; bs, broad singlet. Chemical shifts (d) are given in ppm relative to the resonance of their respective residual solvent peaks. Mass spctra (LC-MS) were acquired using Agilent uHPLC/MS 1290 Infinity system with a binary pump, degasser, autosampler, thermostated column compartment, 1260 Diode Array Detector and 6120 single quadrupole mass spectrometer. The entire system was controlled by Chemstation software (Agilent technologies). The column was an Agilent Poroshell 120 SB-C18, 2.7 mm, 2.1 x 50 mm. The samples were analyzed in the positive ion mode of the Electro Spray Ionization (ESI) source, whose conditions were as follow: gas

temperature, 350 °C, drying gas at 12.0 L/min, nebulizer gas at 35 psig, Vcap. at 3000 V, fragmentor at 60 V.

4.2 Synthetic procedures

methyl 4-hydroxy-2-naphthoate (63)
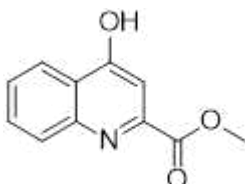
H_2SO_4 (90 m) was added to MeOH (10 mL) at 0 °C, then the solution was added to hydrated kynurenic acid (2g, 9.66 mmol) at 0 °C and the mixture was refluxed for 24 h. After cooling, the reaction mixture was cooled to 0 °C and $NaHCO_3$ (80g) was added portion wise under stirring. The solvent was evaporated under vacuum, 500 mL of H_2O was added and the aqueous phase was extracted with EtOAc. The combined organic layers were dried over Na_2SO_4, filtrated and the solvent was evaporated under vacuum. **63** was obtained without any further purification as a yellow solid **YIELD** 75% **¹H NMR** δ 8.22 (m, 1H), 7.62 (m, 2H), 7.33 (ddd, J = 8.1 Hz, 6.0 Hz, 2.0 Hz, 1H), 6.94 (s, 1H), 3.95 (s, 3H) **¹³C NMR** 180.86, 150.75, 141.78, 133.98, 126.00, 125.67, 125.48, 119.40, 109.63, 42.79

methyl 4-hydroxyquinoline-2-carboxylate (64a)
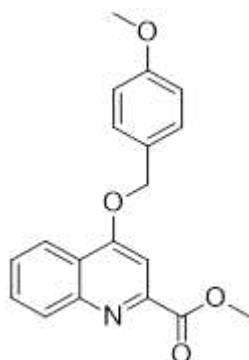
To a solution of **63** (2g, 10 mmol) in DMF (50 mL) K_2CO_3 (2.760g, 20 mmol) and KI (830 mg, 5 mmol) were added. Then, 4-methoxybenzylchloride (1.628 mL, 6 mmol) was added dropwise at room temperature and the mixture was then stirred at 60 °C for 16 h. After cooling, the mixture was diluted with EtOAc and the organic phase was washed with H_2O and Brine, dried over Na_2SO_4, filtrated and evaporated under vacuum. Collected solid was carefully washed with EtOAc and **64a** was obtained as a white/yellowish solid. **YIELD** 78%.
^{1}H NMR (400 MHz, CDCl₃) δ 8.17 (m, 2H), 7.68 (m, 1H), 7.61 (s, 1H), 7.50 (m, 1H), 7.37 (d, J = 8.8 Hz, 2H), 6.89 (d, J = 8.8 Hz, 2H), 5.21 (s, 2H), 4.00 (s, 3H), 3.76 (s, 3H) **^{13}C NMR** (100 MHz, CDCl₃) δ166.31, 162.45, 159.88, 149.02, 148.52, 130.54, 130.19, 129.58, 127.62, 127.37, 122.37, 122.01, 114.19, 101.15, 70.62, 55.35, 53.34 **LC-MS** (ES+) *(m/z)*: 324.2 [M+H]$^+$

methyl 4-(allyloxy)quinoline-2-carboxylate (64b)
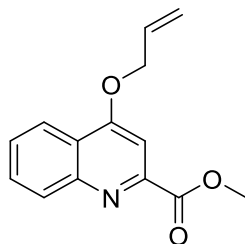
To a solution of **3** (1g, 5 mmol) in DMF (25 mL) K$_2$CO$_3$ (1.380g, 10 mmol) and KI (415 mg, 2.5 mmol) were added. Then, allyl bromide (0.519 mL, 6 mmol) was added dropwise at room temperature and the mixture was then stirred at 60 °C for 16 h. After cooling, the mixture was diluted with EtOAc and the organic phase was washed with H$_2$O and Brine, dried over Na$_2$SO$_4$, filtrated and evaporated under vacuum. Collected solid was carefully washed with EtOAc and **64b** was obtained as a white/yellowish solid. **YIELD** 70%. **^{1}H NMR** (400 MHz, CDCl$_3$) δ 8.20 (dd, J = 8.3 Hz, 0.9 Hz, 1H), 8.15 (m, 1H), 7.69 (m/ddd, 1H), 7.58 (m/ddd, 1H), 7.51 (s, 1H), 6.09 (ddt, 1H), 5.48 (dq, J = 17.2 Hz, 1.4 Hz, 1H), 5.36 (dq, J = 10.5 Hz, 1.4 Hz, 1.4Hz, 1H), 4.78 (dt, J = 5.3 Hz, 1.4 Hz. 1.4 Hz), 4.00 (s, 3H) **^{13}C NMR** (101 MHz, CDCl$_3$) δ 166.27, 162.19, 148.98, 148.53, 130.63,130.53, 130.22, 127.63, 122.30, 121.87, 118.81, 101.05, 69.43, 53.32 **LC-MS** (ES+) *(m/z)*: 244.2 [M+H]$^+$

(4-((4-methoxybenzyl)oxy)quinolin-2-yl)methanol (65a)
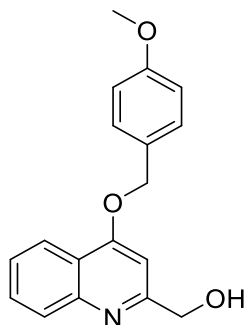
To a suspension of **64a** (1 g, 3.09 mmol) in dry THF (10 mL), stirred at room temperature under inert atmosphere, NaBH$_4$ (703.6, 18.54 mmol) was added and the mixture was heated at 65 °C and refluxed for 15 min. MeOH (10 mL) was added dropwise and the mixture was refluxed for 3h. After cooling, reaction was carefully quenched with water and solvents were evaporated. The white solid was precipitated in water, filtrated on Buchner and washed with water, and **65a** was collected as white solid **YIELD** 63% **^{1}H NMR** (400 MHz, CDCl$_3$) δ 8.13 (dd, J = 8.3 Hz, 1.7 Hz, 1H), 7.92 (d, J = 9.2 Hz, 1H), 7.62 (m, 1H), 7.38 (m, 1H), 7.35 (d, J = 8.7 Hz, 2H), 6.89 (d, J =8.8 Hz, 2H), 6.63 (s, 1H), 5.13 (s, 2H), 4.78 (s, 2H), 3.77 (s, 3H) **^{13}C NMR** (101 MHz, CDCl$_3$) δ 161.89, 160.26, 159.81, 147.68, 130.11, 129.36, 128.10, 127.58, 125.44, 122.15, 121.06, 114.18, 97.79, 70.26, 64.39, 55.36 **LC-MS** (ES+) *(m/z)*: 296.2 [M+H]$^+$

(4-(allyloxy)quinolin-2-yl)methanol (65b)
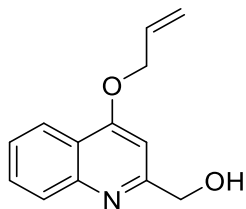
To a suspension of **64a** (400 mg, 1.65 mmol) in dry THF (5.3 mL), stirred at room temperature under inert atmosphere, NaBH$_4$ (378 mg, 10 mmol) was added and the mixture was heated at 65 °C and refluxed for 15 min. MeOH (5.3 mL) was added dropwise and the mixture was refluxed for 3h. After cooling, reaction was carefully quenched with water and solvents were evaporated. The mixture was purified by flash chromatography (10% MeOH in DCM) and **65b** was obtained as white solid **YIELD** 34% **^{1}H NMR** (400 MHz, CDCl$_3$) δ 8.13 (dd, J = 8.4 Hz, 1.7, 1H), 7.91 (d, J = 8.3 Hz, 1H) 7.61 (m, 1H), 7.41 (m, 1H), 6.54 (s, 2H), 6.06 (ddt, 1H), 5.44 (dq, J = 17.4 Hz, 1.5 Hz, 1H), 5.31 (dq, J = 10.7 Hz, 1.3 Hz, 1H), 4.77 (s, 2H), 4.67 (d, 5.1 Hz, 2H) **^{13}C NMR** (101 MHz, CDCl$_3$) δ 161.71, 160.41, 147.63, 131.82, 130.14, 128.01, 125.46, 122.01, 120.96, 118.53, 97.75, 69.11, 64.42 **LC-MS** (ES+) *(m/z)*: 216.1[M+H]$^+$

2-(bromomethyl)-4-((4-methoxybenzyl)oxy)quinoline (66a)
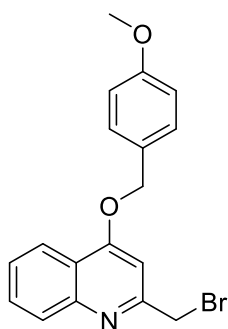
To a solution of **65a** (295 mg, 1 mmol) in dry CH_2Cl_2 (6.6 mL) PPh$_3$ (314,4 mg, 1.2 mmol) was added. Then, CBr$_4$ (398 mg, 1.2 mmol) was added at 0°C and the mixture was stirred rt 16 h. The mixture was filtrated with CH_2Cl_2 and the solvent was evaporated. The crude was purified purified by flash chromatography (15% EtOAc in cyclohexane) to obtain **66a** as white solid **YIELD** 80% **^{1}H NMR** (400 MHz, CDCl$_3$) δ 8.12 (dd, J = 8.32 Hz, 1 Hz, 1H), 7.91 (d, J = 8.4 Hz, 1H), 7.62 (m, 1H), 7.38 (m, 1H), 7.35 (d, J = 8.6 Hz, 2H), 6.90 (d, J = 8.5 Hz, 2H) 6.89 (s, 1H), 5.15 (s, 2H), 4.58 (s, 2H), 3.76 (s, 3H) **^{13}C NMR** (400 MHz, CDCl$_3$) δ 162.20, 159.85, 157.99, 130.29, 148.48, 130.29, 129.50, 128.72, 128.72, 127.53, 120.73, 114.19, 100.87, 70.53, 55.36, 35.14 **LC-MS** (ES+) *(m/z)* 358.6 [M+H]$^+$

4-(allyloxy)-2-(bromomethyl)quinoline (66b)
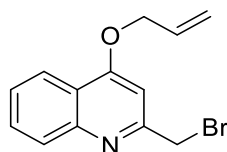
To a solution of **65b** (210 mg, 0.98 mmol) in dry CH_2Cl_2 (6.5 mL) PPh$_3$ (308 mg, 1.17 mmol) was added. Then, CBr$_4$ (389 mg, 1.17 mmol) was added at 0°C and the mixture was stirred rt 16 h. The mixture was filtrated with DCM and the solvent was evaporated. The crude was purified by flash chromatography (15% EtOAc in cyclohexane) to obtain **66b** as white solid **YIELD** 20% **^{1}H NMR** (400 MHz, CDCl$_3$) δ 8.14 (dd, *J* = 11.5 Hz, 1.1 Hz, 1H), 7.91 (d, *J* = 11.4 Hz, 1H), 7.63 (m, 1H), 7.43 (m, 1H), 6.82 (s, 1H), 6.08 (ddt, 1H), 5.46 (m, 1H), 5.32 (dq, *J* = 14.0 MHz, 1.8 Hz, 1H) 4.70 (s, 2H), 4.57 (s, 2H) **^{13}C NMR** (101 MHz, CDCl$_3$) δ 161.93, 157.94, 148.45, 131.78, 130.29, 128.70, 126.14, 121.83, 120.67, 118.66, 100.78, 69.20, 47.81, 35.03 **LC-MS** (ES+) *(m/z)*: 279.2 [M+H]$^+$

undecan-2-one (69)
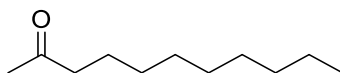
To a solution of 1-undecyn (**68**) (0.197 ml, 1 mmol) in acetone (6.3 mL), H$_2$O (0.090 mL, 5 mmol), p-toluensulfonic acid (190 mg, 1 mmol) and (CH$_3$COO)$_2$Hg were added and the mixture was stirred at room temperature for 16 h. The mixture was filtrated on silica and washed with acetone. The mixture was then purified by flash chromatography an **69** was obtained as colourless oil **YIELD** 85% **^{1}H NMR** (400 MHz, CDCl$_3$) δ 2.35 (t, *J* = 7.6 Hz, 2H), 2.06 (s, 3H), 1.50 (m, 2H), 0.80 (t, *J* = 7.1 Hz, 3H) **^{13}C NMR** (101 MHz, CDCl$_3$) δ 209.48, 43.84, 31.87, 30.95, 29.87, 29.44, 29.41, 29.27, 29.18, 23.87, 22.67, 14.11

1-(4-((4-methoxybenzyl)oxy)quinolin-2-yl)dodecan-3-one (70)
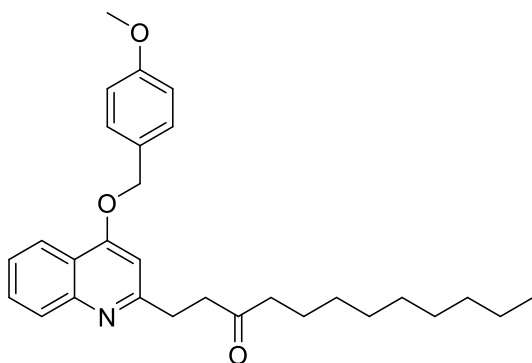
A solution of freshly prepared LDA (0.70 mmol) in THF (1.8 mL) was cannulated in a solution of **69** (110 mg, 0.59 mmol) in dry THF (1.2 mL) stirred at -78 °C under Ar atmosphere. After 15 min, TBAI (33 mg, 0.140 mmol) and a solution of **66a** (250 mg, 0.70 mmol) were added at -78 °C and stirred under Ar atmosphere for 1 h, then it was stirred at 0 °C for 1 h, and rt for 1h. The reaction was quenched with NH₄Cl ss and the aqueous phase was extracted with EtOAc. The combined organic layers were dried over Na₂SO₄, filtrated and the solvent was evaporated under vacuum. The mixture was purified by flash chromatography (20% EtOAc in cyclohexane) to obtain **70** as a yellow oil. **YIELD**: 5% **¹H NMR** (400 MHz, CDCl₃) d 8.09 (dd, J = 8.32 Hz, 1.7 Hz, 1H), 7.85 (d, J = 7.2 Hz, 1H), 7.57 (m, 1H), 7.35 (d, 8.7 Hz, 2H), 7.22 (m, 1H), 6.89 (d, J = 8.8 Hz, 2H), 6.69 (s,1H), 3.87 (s, 3H), 3.12 (t, J = 6.8 Hz, 2H), 2.94 (t, J = 7.4 Hz, 2H), 2.40 (t, 7.7 Hz, 2H), 1.50 (m, 2H), 1.18 (m, 12H), 0.80 (t, J = 6.8 Hz, 3H) **¹³C NMR** (101 MHz, CDCl₃) d 210.77, 162.33, 161.47, 159.73, 148.73, 129.76, 129.43, 128.67, 128.07, 124.92, 121.92, 120.23, 114.12, 113.94, 101.49, 70.05, 55.35, 43.13, 41.43, 33.02, 31.91, 29.45, 29.33, 29.28, 22.93, 22.70, 14.15 **LC-MS** (ES+) *(m/z)* 448.7[M+H]⁺

2-(but-3-en-1-yl)-4-((4-methoxybenzyl)oxy)quinoline (75)
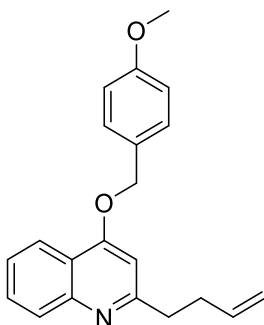
A solution of **66a** (600 mg, 1.68 mmol) in dry THF (3 mL) stirred under Ar atmosphere was cooled at 0 °C and a solution 1M of allyl-magnesium bromide in Et$_2$O (3.36 ml, 3.36 mmol) was slowly added dropwise. The reaction was then stirred rt for 4 h and quenched with NH$_4$Cl ss. The combined organic layers were dried over Na$_2$SO$_4$, filtrated and the solvent was evaporated under vacuum. The mixture was purified by flash chromatography (12% EtOAc in cyclohexane) and **75** was obtained as yellow solid. **YIELD** 35% **^{1}H NMR** (400 MHz, CDCl$_3$) δ 8.11 (dd, *J* = 8.3 Hz, 1Hz, 1H), 7.90 (d, *J* = 8.4 Hz, 1H), 7.59 (m, 1H), 7.36 (d, *J* = 8.8 Hz, 2H), 7.35 (m, 1H), 6.89 (d, *J* = 8.8 Hz, 2H), 6.65 (s, 1H), 5.85 (ddt, 1H), 5.13 (s, 2H), 5.01 (dq, *J* = 17,1 Hz, 1.8 Hz, 1H), 4.92 (m, 1H), 3.77 (s, 3H), 2.94 (t, *J* = 8.1, 2H), 2.50 (m, 2H) **^{13}C NMR** (101 MHz, CDCL$_3$) δ 163.16, 161.49, 165.93, 148.88, 137.80, 129.79, 129.32, 128.23, 127.88, 124.89, 121.87, 120.19, 115.22, 114.13, 101.08, 70.01, 55.36, 39.33, 33.94 **LC-MS** (ES+) *(m/z):* 320.2 [M+H]$^+$

N-(2-acetylphenyl)pent-4-enamide (77)
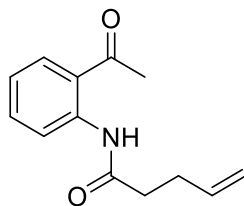
To a solution of 4-pentenoic acid (**76**) (0.153 mL, 1.5 mmol) in dry DCM (5), oxalyl chloride (4.5 mmol) and a drop of DMF were added and the mixture was stirred for 2 h under Argon atmosphere. The mixture was evaporated and resolubilized in dry DCM (14 mL) and TEA (0.332 mL, 4.5 mmol) and 2-aminoacetophenone (0.273 mL, 2.25 mmol) were added at 0 °C and the mixture was stirred rt for 2 h. The mixture was diluted with HCl 0.1 N and the aqueous phase was extracted with DCM. The combined organic layers were dried over Na$_2$SO$_4$, filtrated and the solvent was evaporated under vacuum. The crude was used for the following step without any purification. **LC-MS** (ES+) *(m/z):* 218.2 [M+H]$^+$

2-(but-3-en-1-yl)quinolin-4-ol (78)
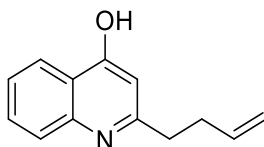
To a solution of **77** (mix) crude in 1,4-dioxane (18 mL), NaOH (92 mg) was added and the mixture was stirred at 110 °C for 3 hours under Ar atmosphere. After cooling, solvent was evaporated and the mixture was purified by flash chromatography (EtOAc 50% in cyclohexane) and compound **78** was obtained as yellowish solid. **YIELD** 27% **^{1}H NMR** (400 MHz, CDCl$_3$) δ 12.69 (s, 1H), 8.28 (dd, *J* = 8.2 Hz, 1.6 Hz,1H), 7.74 (d, *J* = 7.3 Hz, 1H), 7.51 (m, 1H), 7.26 (m, 1H), 6.20 (s, 1H), 5.67 (ddt, 1H), 4.87 (m, 2H), 2.74 (t, *J* = 8.2 Hz, 2H), 2.41 (q, *J* = 7.7 Hz, 2H) **^{13}C NMR** (101 MHz, CDCl$_3$) δ 178.86, 154.70, 140.74, 136.30, 131.91, 125.15, 124.87, 123.76, 118,76, 116.13, 108.18, 108.18, 40.96, 33.57, 32.91 **LC-MS** (ES+) *(m/z):* 200.1 [M+H]$^+$

3-allyl-4-methylquinolin-2-ol (79)
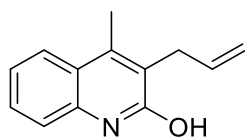
To a solution of **77** (mix) crude in 1,4-dioxane (18 mL), NaOH (92 mg) was added and the mixture was stirred at 110 °C for 3 hours under Ar atmosphere. After cooling, solvent was evaporated and the mixture was purified by flash chromatography (EtOAc 45% in cyclohexane) and compound **78** was obtained as yellow/orange solid. **YIELD** 27% **¹H NMR** (400 MHz, CDCl₃) δ 12.05 (s, 1H), 7.64 (dd, *J* = 8.2 Hz, 1.3 Hz, 1H), 7.39 (m, 1H), 7.32 (dd/m, 1H), 7.14 (m, 1H), 5.94 (ddt, 1H), 4.98 (m, 2H), 3.54 (d, *J* = 6Hz, 2H), 2.41 (s, 3H) **¹³C NMR** (101 MHz, CDCl₃) δ 163.61, 144.67, 137.01, 135.16, 129.50, 128.49, 124.32, 122.28, 120.96, 116.22, 115.12, 30.89, 15.12 **LC-MS** (ES+) *(m/z)*: 200.1 [M+H]⁺

Bibliography

1   J. O. Metzger, *Angewandte Chemie*, 1997, **109**, 812–813.

2   C. W. Anastas, Paul T., Warner, *Green Chemistry: Theory and Practice*, 1998.

3   S. L. Y. Tang, R. L. Smith and M. Poliakoff, *Green Chemistry*, 2005, **7**, 761–762.

4   P. Tundo, *Pure and Applied Chemistry*, 2001, **73**, 1117–1124.

5   H. C. Erythropel, J. B. Zimmerman, T. M. de Winter, L. Petitjean, F. Melnikov, C. H. Lam, A. W. Lounsbury, K. E. Mellor, N. Z. Janković, Q. Tu, L. N. Pincus, M. M. Falinski, W. Shi, P. Coish, D. L. Plata and P. T. Anastas, *Green Chemistry*, 2018, **20**, 1929–1961.

6   T. Keijer, V. Bakker and J. C. Slootweg, *Nature Chemistry*, 2019, **11**, 190–195.

7   E. C. I. Council, 2017.

8   T. E. Graedel, in *Handbook of Green Chemistry and Technology*, Blackwell Science Ltd, Oxford, UK, 2002, pp. 56–61.

9   C. Das Neves Gomes, O. Jacquet, C. Villiers, P. Thuéry, M. Ephritikhine and T. Cantat, *Angewandte Chemie International Edition*, 2012, **51**, 187–190.

10   H. Mutlu and L. Barner, *Macromolecular Chemistry and Physics*, 2022, **223**, 2200111.

11   EPA United States Environmental Protection Agency, 2002.

12   A. Abera Tsedalu, *Journal of Chemistry*, 2021, **2021**, 1–14.

13   T. Dalton, T. Faber and F. Glorius, *ACS Central Science*, 2021, **7**, 245–261.

14   J. Jiang, L. Du and Y. Ding, *Mini-Reviews in Organic Chemistry*, 2020, **17**, 26–46.

15   C. S. G. Seo and R. H. Morris, *Organometallics*, 2019, **38**, 47–65.

16   B. Liu, Y. Wang, N. Huang, X. Lan, Z. Xie, J. G. Chen and T. Wang, *Chem*, 2022, **8**, 2630–2658.

17   P. Kalck and M. Urrutigoïty, *Chemical Reviews*, 2018, **118**, 3833–3861.

18   L. A. Evans, N. S. Hodnett and G. C. Lloyd-Jones, *Angewandte Chemie International Edition*, 2012, **51**, 1526–1533.

19   R. Ye, J. Zhao, B. B. Wickemeyer, F. D. Toste and G. A. Somorjai, *Nature Catalysis*, 2018, **1**, 318–325.

20   D. J. Cole-Hamilton, *Science*, 2003, **299**, 1702–1706.

21   O. Walter, *Angewandte Chemie International Edition*, 2006, **45**, 2005–2005.

22   O. Wachsen, K. Himmler and B. Cornils, *Catalysis Today*, 1998, **42**, 373–379.

23   P. Chirik and R. Morris, *Accounts of Chemical Research*, 2015, **48**, 2495–2495.

24   J. G. Hernández and E. Juaristi, *Chemical Communications*, 2012, **48**, 5396–5409.

25   M. P. van der Helm, B. Klemm and R. Eelkema, *Nature Reviews Chemistry*, 2019, **3**, 491–508.

26   I. R. Shaikh, *Journal of Catalysts*, 2014, **2014**, 1–35.

27   V. Polshettiwar and R. S. Varma, *Green Chemistry*, 2010, **12**, 743–756.

28   A. El Kadib, A. Finiels and D. Brunel, *Chemical Communications*, 2013, **49**, 9073–9076.

29   R. A. Sheldon, *Green Chemistry*, 2016, **18**, 3180–3183.

30   G. W. Huisman and S. J. Collier, *Current Opinion in Chemical Biology*, 2013, **17**, 284–292.

31   J. P. Adams, M. J. B. Brown, A. Diaz-Rodriguez, R. C. Lloyd and G. Roiban, *Advanced Synthesis & Catalysis*, 2019, **361**, 2431–2432.

32   U. T. Bornscheuer, G. W. Huisman, R. J. Kazlauskas, S. Lutz, J. C. Moore and K. Robins, *Nature*, 2012, **485**, 185–194.

33   B. Trost, *Science*, 1991, **254**, 1471–1477.

34   A. M. Martín Castro, *Chemical Reviews*, 2004, **104**, 2939–3002.

35   N. Graulich, *WIREs Computational Molecular Science*, 2011, **1**, 172–190.

36   S. Bräse, C. Gil, K. Knepper and V. Zimmermann, *Angewandte Chemie International Edition*, 2005, **44**, 5188–5240.

37   N. Miyaura, K. Yamada and A. Suzuki, *Tetrahedron Letters*, 1979, **20**, 3437–3440.

38   S. Reisman, R. Nani and S. Levin, *Synlett*, 2011, **2011**, 2437–2442.

39   S. Kotha, A. S. Chavan and D. Goyal, *ACS Combinatorial Science*, 2015, **17**, 253–302.

40   C. M. Marson, *Chemical Society Reviews*, 2012, **41**, 7712–7722.

41   R. A. Sheldon, *Green Chemistry*, 2017, **19**, 18–43.

42   T. V. T. Phan, C. Gallardo and J. Mane, *Green Chemistry*, 2015, **17**, 2846–2852.

43   D. Cespi, E. S. Beach, T. E. Swarr, F. Passarini, I. Vassura, P. J. Dunn and P. T. Anastas, *Green Chemistry*, 2015, **17**, 3390–3400.

44   C. J. Clarke, W.-C. Tu, O. Levers, A. Bröhl and J. P. Hallett, *Chemical Reviews*, 2018, **118**, 747–800.

45   D. J. C. Constable, C. Jimenez-Gonzalez and R. K. Henderson, *Organic Process Research & Development*, 2007, **11**, 133–137.

46   C. Jimenez-Gonzalez, C. S. Ponder, Q. B. Broxterman and J. B. Manley, *Organic Process Research & Development*, 2011, **15**, 912–917.

47   R. A. Sheldon, *Current Opinion in Green and Sustainable Chemistry*, 2019, **18**, 13–19.

48   L. J. Diorazio, D. R. J. Hose and N. K. Adlington, *Organic Process Research & Development*, 2016, **20**, 760–773.

49   C. M. Alder, J. D. Hayler, R. K. Henderson, A. M. Redman, L. Shukla, L. E. Shuster and H. F. Sneddon, *Green Chemistry*, 2016, **18**, 3879–3890.

50   K. Alfonsi, J. Colberg, P. J. Dunn, T. Fevig, S. Jennings, T. A. Johnson, H. P. Kleine, C. Knight, M. A. Nagy, D. A. Perry and M. Stefaniak, *Green Chem.*, 2008, **10**, 31–36.

51   D. Prat, O. Pardigon, H.-W. Flemming, S. Letestu, V. Ducandas, P. Isnard, E. Guntrum, T. Senac, S. Ruisseau, P. Cruciani and P. Hosek, *Organic Process Research & Development*, 2013, **17**, 1517–1525.

52   D. Prat, J. Hayler and A. Wells, *Green Chem.*, 2014, **16**, 4546–4551.

53   D. Prat, A. Wells, J. Hayler, H. Sneddon, C. R. McElroy, S. Abou-Shehada and P. J. Dunn,

Green Chemistry, 2016, **18**, 288–296.

54   Z. Lei, B. Chen, Y.-M. Koo and D. R. MacFarlane, *Chemical Reviews*, 2017, **117**, 6633–6635.

55   C. Dai, J. Zhang, C. Huang and Z. Lei, *Chemical Reviews*, 2017, **117**, 6929–6983.

56   S. N. Pedro, C. S. R. Freire, A. J. D. Silvestre and M. G. Freire, *Encyclopedia*, 2021, **1**, 324–339.

57   R. Ferraz, V. Teixeira, D. Rodrigues, R. Fernandes, C. Prudêncio, J. P. Noronha, Ž. Petrovski and L. C. Branco, *RSC Adv.*, 2014, **4**, 4301–4307.

58   M. M. Santos, C. Alves, J. Silva, C. Florindo, A. Costa, Ž. Petrovski, I. M. Marrucho, R. Pedrosa and L. C. Branco, *Pharmaceutics*, 2020, **12**, 694-.

59   G. K. K. Reddy and Y. V. Nancharaiah, *Frontiers in Microbiology*, 2020, **11**, 730.

60   R. Ferraz, J. Costa-Rodrigues, M. H. Fernandes, M. M. Santos, I. M. Marrucho, L. P. N. Rebelo, C. Prudêncio, J. P. Noronha, Ž. Petrovski and L. C. Branco, *ChemMedChem*, 2015, **10**, 1480–1483.

61   L. Cicco, G. Dilauro, F. M. Perna, P. Vitale and V. Capriati, *Organic & Biomolecular Chemistry*, 2021, **19**, 2558–2577.

62   L. Cicco, S. Sblendorio, R. Mansueto, F. M. Perna, A. Salomone, S. Florio and V. Capriati, *Chemical Science*, 2016, **7**, 1192–1199.

63   X. Marset, A. Khoshnood, L. Sotorríos, E. Gómez-Bengoa, D. A. Alonso and D. J. Ramón, *ChemCatChem*, 2017, **9**, 1269–1275.

64   N. Yasukawa, H. Yokoyama, M. Masuda, Y. Monguchi, H. Sajiki and Y. Sawama, *Green Chemistry*, 2018, **20**, 1213–1217.

65   B. Díaz-Reinoso, A. Moure, H. Domínguez and J. C. Parajó, *Journal of Agricultural and Food Chemistry*, 2006, **54**, 2441–2469.

66   Y. Hu, D. J. Birdsall, A. M. Stuart, E. G. Hope and J. Xiao, *Journal of Molecular Catalysis A: Chemical*, 2004, **219**, 57–60.

67   S. E. Lyubimov, E. A. Rastorguev, P. V. Petrovskii, E. S. Kelbysheva, N. M. Loim and V. A. Davankov, *Tetrahedron Letters*, 2011, **52**, 1395–1397.

68   M. Berthod, G. Mignani and M. Lemaire, *Tetrahedron: Asymmetry*, 2004, **15**, 1121–1126.

69   M. Herrero, J. A. Mendiola and E. Ibáñez, *Current Opinion in Green and Sustainable Chemistry*, 2017, **5**, 24–30.

70   D. Liu, Z. Xie, W. K. Snavely, R. Chaudhari and B. Subramaniam, *Reaction Chemistry & Engineering*, 2018, **3**, 344–352.

71   S. M. Mercer, T. Robert, D. V. Dixon and P. G. Jessop, *Catalysis Science & Technology*, 2012, **2**, 1315–1318.

72   D. Vinci, M. Donaldson, J. P. Hallett, E. A. John, P. Pollet, C. A. Thomas, J. D. Grilly, P. G. Jessop, C. L. Liotta and C. A. Eckert, *Chemical Communications*, 2007, **14**, 1427–1429.

73   V. Pace, P. Hoyos, L. Castoldi, P. Domínguez de María and A. R. Alcántara, *ChemSusChem*,

2012, **5**, 1369–1379.

74   Z. Zhang, *ChemSusChem*, 2016, **9**, 156–171.

75   J. Molleti, M. S. Tiwari and G. D. Yadav, *Chemical Engineering Journal*, 2018, **334**, 2488–2499.

76   P. A. Son, S. Nishimura and K. Ebitani, *RSC Advances*, 2014, **4**, 10525.

77   K.-C. Jiang, L. Wang, Q. Chen, M.-Y. He, M.-G. Shen and Z.-H. Zhang, *Synthetic Communications*, 2021, **51**, 94–102.

78   I. Anastasiou, F. Ferlin, O. Viteritti, S. Santoro and L. Vaccaro, *Molecular Catalysis*, 2021, **513**, 111787.

79   F. Valentini, F. Ferlin, S. Lilli, A. Marrocchi, L. Ping, Y. Gu and L. Vaccaro, *Green Chemistry*, 2021, **23**, 5887–5895.

80   Z. Khorsandi, A. R. Hajipour, M. R. Sarfjoo and R. S. Varma, *Green Chemistry*, 2021, **23**, 5222–5229.

81   R. A. Sheldon, *Green Chemistry*, 2005, **7**, 267–278.

82   D. C. Rideout and R. Breslow, *Journal of the American Chemical Society*, 1980, **102**, 7816–7817.

83   S. Narayan, J. Muldoon, M. G. Finn, V. V. Fokin, H. C. Kolb and K. B. Sharpless, *Angewandte Chemie International Edition*, 2005, **44**, 3275–3279.

84   F. Zhou, Z. Hearne and C.-J. Li, *Current Opinion in Green and Sustainable Chemistry*, 2019, **18**, 118–123.

85   C. W. Kohlpaintner, R. W. Fischer and B. Cornils, *Applied Catalysis A: General*, 2001, **221**, 219–225.

86   G. Galli and D. Pan, *Proceedings of the National Academy of Sciences*, 2013, **110**, 6250–6251.

87   G. La Sorella, G. Strukul and A. Scarso, *Green Chemistry*, 2015, **17**, 644–683.

88   D. Myers, *Surfactant Science and Technology*, John Wiley & Sons, Inc., Hoboken, NJ, USA, 2005.

89   A. Sorrenti, O. Illa and R. M. Ortuño, *Chemical Society Reviews*, 2013, **42**, 8200–8219.

90   M. Cortes-Clerget, J. R. A. Kincaid, N. Akporji and B. H. Lipshutz, in *Supramolecular Catalysis*, Wiley, 2022, pp. 467–487.

91   B. Samiey, C.-H. Cheng and J. Wu, *Journal of Chemistry*, 2014, **2014**, 1–14.

92   J. N. N. Israelachvili, *Intermolecular and Surface Forces*, Elsevier, 2011.

93   B. H. Lipshutz, *Current Opinion in Green and Sustainable Chemistry*, 2018, **11**, 1–8.

94   F. Ballistreri, R. Toscano, M. Amato, A. Pappalardo, C. Gangemi, S. Spidalieri, R. Puglisi and G. Trusso Sfrazzetto, *Catalysts*, 2018, **8**, 129.

95   A. K. Godha, J. Thiruvengadam, V. Abhilash, P. Balgi, A. V. Narayanareddy, K. Vignesh, A. V. Gadakh, A. M. Sathiyanarayanan and S. Ganesh, *New Journal of Chemistry*, 2019, **43**, 16041–16045.

96   E. H. Wanderlind, C. R. Bittencourt, A. M. Manfredi, A. P. Gerola, B. S. Souza, H. D. Fiedler and F. Nome, *Journal of Physical Organic Chemistry*, 2019, **32**, e3837.

97   R. V. Maaskant, E. A. Polanco, R. C. W. van Lier and G. Roelfes, *Organic & Biomolecular Chemistry*, 2020, **18**, 638–641.

98   A. Chandra and M. Singh, *Inorganic Chemistry Frontiers*, 2018, **5**, 233–257.

99   D. Goswami, *Applied Biochemistry and Biotechnology*, 2020, **191**, 744–762.

100   B. H. Lipshutz, S. Ghorai, A. R. Abela, R. Moser, T. Nishikata, C. Duplais, A. Krasovskiy, R. D. Gaston and R. C. Gadwood, *The Journal of Organic Chemistry*, 2011, **76**, 4379–4391.

101   B. H. Lipshutz and S. Ghorai, *Aldrachimica Acta*, 2008, **41**, 59–72.

102   P. Klumphu and B. H. Lipshutz, *The Journal of Organic Chemistry*, 2014, **79**, 888–900.

103   B. H. Lipshutz, *Johnson Matthey Technology Review*, 2017, **61**, 196–202.

104   C. Salomé, P. Wagner, M. Bollenbach, F. Bihel, J.-J. Bourguignon and M. Schmitt, *Tetrahedron*, 2014, **70**, 3413–3421.

105   B. H. Lipshutz, T. B. Petersen and A. R. Abela, *Organic Letters*, 2008, **10**, 1333–1336.

106   B. H. Lipshutz and B. R. Taft, *Organic Letters*, 2008, **10**, 1329–1332.

107   B. H. Lipshutz, G. T. Aguinaldo, S. Ghorai and K. Voigtritter, *Organic Letters*, 2008, **10**, 1325–1328.

108   K. Voigtritter, S. Ghorai and B. H. Lipshutz, *The Journal of Organic Chemistry*, 2011, **76**, 4697–4702.

109   B. H. Lipshutz, Z. Bošković, C. S. Crowe, V. K. Davis, H. C. Whittemore, D. A. Vosburg and A. G. Wenzel, *Journal of Chemical Education*, 2013, **90**, 1514–1517.

110   N. A. Isley, F. Gallou and B. H. Lipshutz, *Journal of the American Chemical Society*, 2013, **135**, 17707–17710.

111   S. Handa, E. D. Slack and B. H. Lipshutz, *Angewandte Chemie*, 2015, **127**, 12162–12166.

112   M. Parmentier, M. Wagner, R. Wickendick, M. Baenziger, A. Langlois and F. Gallou, *Organic Process Research & Development*, 2020, **24**, 1536–1542.

113   R. R. Thakore, K. S. Iyer and B. H. Lipshutz, *Current Opinion in Green and Sustainable Chemistry*, 2021, **31**, 100493.

114   E. B. Landstrom, N. Akporji, N. R. Lee, C. M. Gabriel, F. C. Braga and B. H. Lipshutz, *Organic Letters*, 2020, **22**, 6543–6546.

115   A. Steven, *Synthesis*, 2019, **51**, 2632–2647.

116   C. M. Gabriel, M. Parmentier, C. Riegert, M. Lanz, S. Handa, B. H. Lipshutz and F. Gallou, *Organic Process Research & Development*, 2017, **21**, 247–252.

117   N. R. Lee, F. Gallou and B. H. Lipshutz, *Organic Process Research & Development*, 2017, **21**, 218–221.

118   M. Shi, N. Ye, W. Chen, H. Wang, C. Cheung, M. Parmentier, F. Gallou and B. Wu, *Organic Process Research & Development*, 2020, **24**, 1543–1548.

119   M. Parmentier, C. M. Gabriel, P. Guo, N. A. Isley, J. Zhou and F. Gallou, *Current Opinion in Green and Sustainable Chemistry*, 2017, **7**, 13–17.

120   B. S. Takale, R. R. Thakore, F. Y. Kong and B. H. Lipshutz, *Green Chemistry*, 2019, **21**, 6258–6262.

121   J. Yu, K. S. Iyer and B. H. Lipshutz, *Green Chemistry*, 2022, **24**, 3640–3643.

122   J. R. A. Kincaid, R. D. Kavthe, J. C. Caravez, B. S. Takale, R. R. Thakore and B. H. Lipshutz, *Organic Letters*, 2022, **24**, 3342–3346.

123   N. Fleck, R. M. Thomas, M. Müller, S. Grimme and B. H. Lipshutz, *Green Chemistry*, 2022, **24**, 6517–6523.

124   B. S. Takale, R. R. Thakore, R. Mallarapu, F. Gallou and B. H. Lipshutz, *Organic Process Research & Development*, 2020, **24**, 101–105.

125   M. Cortes-Clerget, N. Akporji, J. Zhou, F. Gao, P. Guo, M. Parmentier, F. Gallou, J.-Y. Berthon and B. H. Lipshutz, *Nature Communications*, 2019, **10**, 2169.

126   R. Adamik, B. Buchholcz, F. Darvas, G. Sipos and Z. Novák, *Chemistry – A European Journal*, 2022, **28**, e202103967.

127   T. Lorenzetto, G. Berton, F. Fabris and A. Scarso, *Catalysis Science & Technology*, 2020, **10**, 4492–4502.

128   R. R. Thakore, B. S. Takale, Y. Hu, S. Ramer, J. Kostal, F. Gallou and B. H. Lipshutz, *Tetrahedron*, 2021, **87**, 132090.

129   N. R. Lee, M. Cortes-Clerget, A. B. Wood, D. J. Lippincott, H. Pang, F. A. Moghadam, F. Gallou and B. H. Lipshutz, *ChemSusChem*, 2019, **12**, 3159–3165.

130   D. Chen, Y. Zhang, X. Pan, F. Wang and S. Huang, *Advanced Synthesis & Catalysis*, 2018, **360**, 3607–3612.

131   Y. Yang, X. Meng, B. Zhu, Y. Jia, X. Cao and S. Huang, *European Journal of Organic Chemistry*, 2019, **2019**, 1166–1169.

132   J. Brals, J. D. Smith, F. Ibrahim, F. Gallou and S. Handa, *ACS Catalysis*, 2017, **7**, 7245–7250.

133   M. Cortes-Clerget, S. E. Spink, G. P. Gallagher, L. Chaisemartin, E. Filaire, J.-Y. Berthon and B. H. Lipshutz, *Green Chemistry*, 2019, **21**, 2610–2614.

134   A. Sanzone, S. Mattiello, G. M. Garavaglia, A. M. Calascibetta, C. Ceriani, M. Sassi and L. Beverina, *Green Chemistry*, 2019, **21**, 4400–4405.

135   A. R. Markande, D. Patel and S. Varjani, *Bioresource Technology*, 2021, **330**, 124963.

136   D. M. P. Mingos and D. R. Baghurst, *Chemical Society Reviews*, 1991, **20**, 1–47.

137   S. Maramai and M. Taddei, in *Sustainable Organic Synthesis*, Royal Society of Chemistry, Cambridge, 2021, pp. 488–521.

138   A. de la Hoz and A. Loupy, Eds., *Microwaves in Organic Synthesis*, Wiley, 2012.

139   C. O. Kappe and A. Stadler, *Microwaves in Organic and Medicinal Chemistry*, Wiley, 2005.

140   E. V. Van der Eycken, *Angewandte Chemie International Edition*, 2009, **48**, 2828–2829.

141   S. G. Aitken and A. D. Abell, *Australian Journal of Chemistry*, 2005, **58**, 3–13.

142   A. de la Hoz, A. Díaz-Ortiz and A. Moreno, *Journal of Microwave Power and Electromagnetic Energy*, 2006, **41**, 45–66.

143   C. O. Kappe, B. Pieber and D. Dallinger, *Angewandte Chemie International Edition*, 2013, **52**, 1088–1094.

144   S. B. Ajmer Singh Grewal, Karunesh Kumar, Sonika Redhu, *International Research Journal of Pharmaceutical and Applied Sciences*, 2013, 278–285.

145   E. Petricci, E. Cini and M. Taddei, *European Journal of Organic Chemistry*, 2020, **2020**, 4435–4446.

146   E. Cini, E. Petricci and M. Taddei, *Catalysts*, 2017, **7**, 89.

147   W. Chen, B. Gutmann and C. O. Kappe, *ChemistryOpen*, 2012, **1**, 39–48.

148   M. Gupta and W. Wai Leong Eugene, *Microwaves and Metals*, John Wiley & Sons (Asia) Pte Ltd, Singapore, 2007.

149   S. Horikoshi, A. Osawa, M. Abe and N. Serpone, *The Journal of Physical Chemistry C*, 2011, **115**, 23030–23035.

150   S. Horikoshi, A. Osawa, S. Sakamoto and N. Serpone, *Applied Catalysis A: General*, 2013, **460–461**, 52–60.

151   E. Petricci, C. Risi, F. Ferlin, D. Lanari and L. Vaccaro, *Scientific Reports*, 2018, **8**, 1–10.

152   B. H. P. van de Kruijs, M. H. C. L. Dressen, J. Meuldijk, J. A. J. M. Vekemans and L. A. Hulshof, *Organic & Biomolecular Chemistry*, 2010, **8**, 1688–1694.

153   B. Gutmann, A. M. Schwan, B. Reichart, C. Gspan, F. Hofer and C. O. Kappe, *Angewandte Chemie*, 2011, **123**, 7778–7782.

154   E. Petricci, A. Mann, A. Schoenfelder, A. Rota and M. Taddei, *Organic Letters*, 2006, **8**, 3725–3727.

155   E. Petricci, A. Mann, J. Salvadori and M. Taddei, *Tetrahedron Letters*, 2007, **48**, 8501–8504.

156   E. Airiau, C. Chemin, N. Girard, G. Lonzi, A. Mann, E. Petricci, J. Salvadori and M. Taddei, *Synthesis*, 2010, **2010**, 2901–2914.

157   M. Pineiro, L. D. Dias, L. Damas, G. L. B. Aquino, M. J. F. Calvete and M. M. Pereira, *Inorganica Chimica Acta*, 2017, **455**, 364–377.

158   G. Vanier, *Synlett*, 2007, **2007**, 0131–0135.

159   A. S. Sharma and H. Kaur, *New Journal of Chemistry*, 2018, **42**, 18935–18941.

160   F. Bucciol, S. Tabasso, G. Grillo, F. Menegazzo, M. Signoretto, M. Manzoli and G. Cravotto, *Journal of Catalysis*, 2019, **380**, 267–277.

161   S. Bouasla, J. Amaro-Gahete, D. Esquivel, M. López, C. Jiménez-Sanchidrián, M. Teguiche and F. Romero-Salguero, *Molecules*, 2017, **22**, 2072.

162   S. J. Song, S. J. Cho, D. K. Park, T. W. Kwon and S. A. Jenekhe, *Tetrahedron Letters*, 2003, **44**, 255–257.

163   D. Dallinger and C. O. Kappe, *Chemical Reviews*, 2007, **107**, 2563–2591.

164   A. K. Rathi, M. B. Gawande, R. Zboril and R. S. Varma, *Coordination Chemistry Reviews*, 2015, **291**, 68–94.

165   Y. Le, Y. Zhang, Q. Wang, N. Rao, D. Li, L. Liu, G. Ouyang and L. Yan, *Tetrahedron Letters*, 2021, **68**, 152903.

166   Y. Tian, J. Wang, X. Cheng, K. Liu, T. Wu, X. Qiu, Z. Kuang, Z. Li and J. Bian, *Green Chemistry*, 2020, **22**, 1338–1344.

167   J. M. Kremsner and C. O. Kappe, *European Journal of Organic Chemistry*, 2005, **2005**, 3672–3679.

168   J. K. Lee, D.-C. Kim, C. Eui Song and S. Lee, *Synthetic Communications*, 2003, **33**, 2301–2307.

169   Y. Peng and G. Song, *Catalysis Communications*, 2007, **8**, 111–114.

170   K. M. Taylor, Z. E. Taylor and S. T. Handy, *Tetrahedron Letters*, 2017, **58**, 240–241.

171   S. Tabasso, E. Calcio Gaudino, E. Acciardo, M. Manzoli, B. Bonelli and G. Cravotto, *Frontiers in Chemistry*, 2020, **8**, 253.

172   A. Kumar, Y. E. Jad, J. M. Collins, F. Albericio and B. G. de la Torre, *ACS Sustainable Chemistry & Engineering*, 2018, **6**, 8034–8039.

173   C. Risi, M. Calamante, E. Cini, V. Faltoni, E. Petricci, F. Rosati and M. Taddei, *Green Chemistry*, 2020, **22**, 327–331.

174   C. Risi, E. Cini, E. Petricci, S. Saponaro and M. Taddei, *European Journal of Inorganic Chemistry*, 2020, **2020**, 1000–1003.

175   F. Migliorini, F. Dei, M. Calamante, S. Maramai and E. Petricci, *ChemCatChem*, 2021, **13**, 2794–2806.

176   A. Mitic and K. V. Gernaey, *Chemical Engineering & Technology*, 2015, **38**, 1699–1712.

177   L. Vaccaro, *Sustainable Flow Chemistry*, Wiley-VCH Verlag GmbH & Co. KGaA, Weinheim, Germany, 2017.

178   D. Kralisch, D. Ott and D. Gericke, *Green Chemistry*, 2015, **17**, 123–145.

179   *Ecoinvent, v3.1, Ecoinvent Centre, Swiss Centre for Life Cycle Inventories, Dübendorf, Switzerland*, 2014.

180   *International Organization for Standardization, ISO 14040:2006 – Environmental Management - Life Cycle Assessment - Principles and Framework*.

181   *International Organization for Standardization, ISO 14044:2006 – Environmental Management – Life Cycle Assessment – Requirements*.

182   M. Z. Hauschild, M. Goedkoop, J. Guinée, R. Heijungs, M. Huijbregts, O. Jolliet, M. Margni, A. De Schryver, S. Humbert, A. Laurent, S. Sala and R. Pant, *The International Journal of Life Cycle Assessment*, 2013, **18**, 683–697.

183   O. Jolliet, M. Margni, R. Charles, S. Humbert, J. Payet, G. Rebitzer and R. Rosenbaum, *The*

International Journal of Life Cycle Assessment, 2003, **8**, 324.

184 M. Goedkoop, *Eco-indicator 99 Manual for Designers, Ministry of Housing, Spatial Planning and the Environment*, 2000.

185 M. Goedkoop, R. Heijungs, M. Huijbregts, A. D. Schryver, R. V. Zelm and J. Struijs, *ReCiPE 2008: A life cycle impact assessment method which comprises harmonised category indicators at the midpoint and the endpoint level. Ministerie van Volkshuisvesting, Ruimtelijke Ordering en Milieubeheer, Den Hague*, 2013.

186 *VDI-Standard: VDI 4600, Cumulative energy demand (KEA) – Terms, definitions, methods of calculation, The Association of German Engineers (VDI), Düsseldorf, Germany*, 2012.

187 R. A. Sheldon, *ACS Sustainable Chemistry & Engineering*, 2018, **6**, 32–48.

188 G. Rebitzer, T. Ekvall, R. Frischknecht, D. Hunkeler, G. Norris, T. Rydberg, W.-P. Schmidt, S. Suh, B. P. Weidema and D. W. Pennington, *Environment International*, 2004, **30**, 701–720.

189 M.-W. Siegert, A. Lehmann, Y. Emara and M. Finkbeiner, *The International Journal of Life Cycle Assessment*, 2020, **25**, 1436–1454.

190 H. B. Rose, B. Kosjek, B. M. Armstrong and S. A. Robaire, *Current Research in Green and Sustainable Chemistry*, 2022, **5**, 100324.

191 A. D. Curzons, C. Jiménez-González, A. L. Duncan, D. J. C. Constable and V. L. Cunningham, *The International Journal of Life Cycle Assessment*, 2007, **12**, 272–280.

192 V. Isoni, L. L. Wong, H. H. Khoo, I. Halim and P. Sharratt, *Green Chemistry*, 2016, **18**, 6564–6572.

193 S. D. Roughley and A. M. Jordan, *Journal of Medicinal Chemistry*, 2011, **54**, 3451–3479.

194 O. I. Afanasyev, E. Kuchuk, D. L. Usanov and D. Chusov, *Chemical Reviews*, 2019, **119**, 11857–11911.

195 W. Reppe and H. Vetter, *Justus Liebigs Annalen der Chemie*, 1953, **528**, 133–161.

196 US2497310A, *US2497310A*, 1946.

197 A. F. M. Iqbal, *Helvetica Chimica Acta*, 1971, **54**, 1440–1445.

198 T. Rische, K.-S. Mu¨ller and P. Eilbracht, *Tetrahedron*, 1999, **55**, 9801–9816.

199 C. L. Kranemann and P. Eilbracht, *European Journal of Organic Chemistry*, 2000, **2000**, 2367–2377.

200 T. Rische, L. Bärfacker and P. Eilbracht, *European Journal of Organic Chemistry*, 1999, **1999**, 653–660.

201 T. Rische, B. Kitsos-Rzychon and P. Eilbracht, *Tetrahedron*, 1998, **54**, 2723–2742.

202 B. Breit and W. Seiche, *Synthesis*, 2001, **2001**, 0001–0036.

203 Y. Jiao, M. S. Torne, J. Gracia, J. W. (Hans) Niemantsverdriet and P. W. N. M. van Leeuwen, *Catalysis Science & Technology*, 2017, **7**, 1404–1414.

204 J. A. Fuentes, P. Wawrzyniak, G. J. Roff, M. Bühl and M. L. Clarke, *Catalysis Science & Technology*, 2011, **1**, 431–436.

205 M. Ahmed, A. M. Seayad, R. Jackstell and M. Beller, *Journal of the American Chemical Society*, 2003, **125**, 10311–10318.

206 A. Seayad, M. Ahmed, H. Klein, R. Jackstell, T. Gross and M. Beller, *Science*, 2002, **297**, 1676–1678.

207 B. Hamers, E. Kosciusko-Morizet, C. Müller and D. Vogt, *ChemCatChem*, 2009, **1**, 103–106.

208 M. Y. S. Ibrahim and M. Abolhasani, *Nature Communications*, 2022, **13**, 2441.

209 T. A. Faßbach, R. Kirchmann, A. Behr and A. J. Vorholt, *Green Chem.*, 2017, **19**, 5243–5249.

210 K. C. B. Oliveira, S. N. Carvalho, M. F. Duarte, E. V. Gusevskaya, E. N. dos Santos, J. El Karroumi, M. Gouygou and M. Urrutigoïty, *Applied Catalysis A: General*, 2015, **497**, 10–16.

211 J. R. Briggs, J. Klosin and G. T. Whiteker, *Organic Letters*, 2005, **7**, 4795–4798.

212 G. Liu, K. Huang, C. Cai, B. Cao, M. Chang, W. Wu and X. Zhang, *Chemistry - A European Journal*, 2011, **17**, 14559–14563.

213 G. Liu, K. Huang, B. Cao, M. Chang, S. Li, S. Yu, L. Zhou, W. Wu and X. Zhang, *Organic Letters*, 2012, **14**, 102–105.

214 S. Li, K. Huang, J. Zhang, W. Wu and X. Zhang, *Organic Letters*, 2013, **15**, 3078–3081.

215 A. M. Seayad, K. Selvakumar, M. Ahmed and M. Beller, *Tetrahedron Letters*, 2003, **44**, 1679–1683.

216 M. Ahmed, C. Buch, L. Routaboul, R. Jackstell, H. Klein, A. Spannenberg and M. Beller, *Chemistry - A European Journal*, 2007, **13**, 1594–1601.

217 T. O. Vieira and H. Alper, *Organic Letters*, 2008, **10**, 485–487.

218 T. A. Faßbach, F. O. Sommer and A. J. Vorholt, *Advanced Synthesis & Catalysis*, 2018, **360**, 1473–1482.

219 B. Zimmermann, J. Herwig and M. Beller, *Angewandte Chemie International Edition*, 1999, **38**, 2372–2375.

220 W. Yingyong, M. Luo, H. Chen and C. Zhang, *Arkivok*, 2008, **11**, 165–174.

221 A. Behr and A. Wintzer, *Chemical Engineering & Technology*, 2015, **38**, 2299–2304.

222 C. S. Graebin, M. de F. Madeira, J. K. U. Yokoyama-Yasunaka, D. C. Miguel, S. R. B. Uliana, D. Benitez, H. Cerecetto, M. González, R. G. da Rosa and V. L. Eifler-Lima, *European Journal of Medicinal Chemistry*, 2010, **45**, 1524–1528.

223 D. S. Melo, S. S. Pereira-Júnior and E. N. dos Santos, *Applied Catalysis A: General*, 2012, **411–412**, 70–76.

224 K. C. B. Oliveira, A. G. Santos and E. N. dos Santos, *Applied Catalysis A: General*, 2012, **445–446**, 204–208.

225 A. de Oliveira Dias, M. G. P. Gutiérrez, J. A. A. Villarreal, R. L. L. Carmo, K. C. B. Oliveira, A. G. Santos, E. N. dos Santos and E. V. Gusevskaya, *Applied Catalysis A: General*, 2019, **574**, 97–104.

226 S. A. Jagtap, S. P. Gowalkar, E. Monflier, A. Ponchel and B. M. Bhanage, *Molecular*

166

Catalysis, 2018, **452**, 108–116.

227   K. U. Künnemann, D. Weber, C. Becquet, S. Tilloy, E. Monflier, T. Seidensticker and D. Vogt, *ACS Sustainable Chemistry & Engineering*, 2021, **9**, 273–283.

228   B. Gall, M. Bortenschlager, O. Nuyken and R. Weberskirch, *Macromolecular Chemistry and Physics*, 2008, **209**, 1152–1159.

229   E. Petricci, S. Zurzolo, C. Matassini, S. Maramai, F. Cardona, A. Goti and M. Taddei, *Molecules*, 2022, **27**, 4762.

230   E. Vitaku, D. T. Smith and J. T. Njardarson, *Journal of Medicinal Chemistry*, 2014, **57**, 10257–10274.

231   P. A. Forero-Cortés and A. M. Haydl, *Organic Process Research & Development*, 2019, **23**, 1478–1483.

232   R. Dorel, C. P. Grugel and A. M. Haydl, *Angewandte Chemie International Edition*, 2019, **58**, 17118–17129.

233   F. Ullmann and J. Bielecki, *Berichte der deutschen chemischen Gesellschaft*, 1901, **34**, 2174–2185.

234   D. Ma, Y. Zhang, J. Yao, S. Wu and F. Tao, *Journal of the American Chemical Society*, 1998, **120**, 12459–12467.

235   A. H. Sandtorv and D. R. Stuart, *Angewandte Chemie International Edition*, 2016, **55**, 15812–15815.

236   X.-D. An and S. Yu, *Tetrahedron Letters*, 2018, **59**, 1605–1613.

237   European Medicines Agency (EMA), 2008.

238   A. Monopoli, P. Cotugno, G. Palazzo, N. Ditaranto, B. Mariano, N. Cioffi, F. Ciminale and A. Nacci, *Advanced Synthesis & Catalysis*, 2012, **354**, 2777–2788.

239   X. Ge, S. Zhang, X. Chen, X. Liu and C. Qian, *Green Chemistry*, 2019, **21**, 2771–2776.

240   M. Bollenbach, P. Wagner, P. G. V. Aquino, J.-J. Bourguignon, F. Bihel, C. Salomé and M. Schmitt, *ChemSusChem*, 2016, **9**, 3244–3249.

241   D. Yousif, M. Monti, A. Papagni and L. Vaghi, *Tetrahedron Letters*, 2020, **61**, 152511.

242   T. N. Ansari, A. Taussat, A. H. Clark, M. Nachtegaal, S. Plummer, F. Gallou and S. Handa, *ACS Catalysis*, 2019, **9**, 10389–10397.

243   E. Petricci, N. Santillo, D. Castagnolo, E. Cini and M. Taddei, *Advanced Synthesis & Catalysis*, 2018, **360**, 2560–2565.

244   A. Shaabani and R. Afshari, *Journal of Colloid and Interface Science*, 2018, **510**, 384–394.

245   L. Routaboul, C. Buch, H. Klein, R. Jackstell and M. Beller, *Tetrahedron Letters*, 2005, **46**, 7401–7405.

246   J. Zhang, C. Liu, X. Wang, J. Chen, Z. Zhang and W. Zhang, *Chemical Communications*, 2018, **54**, 6024–6027.

247   L. Zhang, Y. Ning, B. Ye, T. Ru and F.-E. Chen, *Green Chemistry*, 2022, **24**, 4420–4424.

248   X.-C. Chen, T. Lan, K.-C. Zhao, L. Guo, Y. Lu and Y. Liu, *Journal of Catalysis*, 2022, **411**, 158–166.

249   C. Qian, Q. Zheng, J. Chen, B. Tu and T. Tu, *Green Chemistry*, 2023, **25**, 1368–1379.

250   F. Migliorini, E. Monciatti, G. Romagnoli, M. L. Parisi, J. Taubert, M. Vogt, R. Langer and E. Petricci, *ACS Catalysis*, 2023, **13**, 2702–2714.

251   F. Cardullo, D. Donati, G. Merlo, A. Paio, E. Petricci and M. Taddei, *Synlett*, 2009, **2009**, 47–50.

252   V. K. Aswal and P. S. Goyal, *Chemical Physics Letters*, 2002, **364**, 44–50.

253   B. H. Lipshutz, S. Ghorai, W. W. Y. Leong, B. R. Taft and D. V. Krogstad, *The Journal of Organic Chemistry*, 2011, **76**, 5061–5073.

254   B. Deb and D. K. Dutta, *Journal of Molecular Catalysis A: Chemical*, 2010, **326**, 21–28.

255   G. L. Williams, C. M. Parks, C. R. Smith, H. Adams, A. Haynes, A. J. H. M. Meijer, G. J. Sunley and S. Gaemers, *Organometallics*, 2011, **30**, 6166–6179.

256   A. J. Sandee, J. N. H. Reek, P. C. J. Kamer and P. W. N. M. van Leeuwen, *Journal of the American Chemical Society*, 2001, **123**, 8468–8476.

257   E. . W.-V. W. Wiley-VCH, Ed., *PS Pregosin. NMR in Organometallic Chemistry*, 2012.

258   E. Zuidema, L. Escorihuela, T. Eichelsheim, J. J. Carbó, C. Bo, P. C. J. Kamer and P. W. N. M. van Leeuwen, *Chemistry - A European Journal*, 2008, **14**, 1843–1853.

259   M. Kranenburg, Y. E. M. van der Burgt, P. C. J. Kamer, P. W. N. M. van Leeuwen, K. Goubitz and J. Fraanje, *Organometallics*, 1995, **14**, 3081–3089.

260   G. Makado, T. Morimoto, Y. Sugimoto, K. Tsutsumi, N. Kagawa and K. Kakiuchi, *Advanced Synthesis & Catalysis*, 2010, **352**, 299–304.

261   J. J. Carbó, F. Maseras, C. Bo and P. W. N. M. van Leeuwen, *Journal of the American Chemical Society*, 2001, **123**, 7630–7637.

262   *European Commission, 2010; International Reference Life Cycle Data System (ILCD) Handbook: Framework and Requirements for Life Cycle Impact Assessment Models and Indicators*, .

263   T. J. Brown, M. Cumbes, L. J. Diorazio, G. J. Clarkson and M. Wills, *The Journal of Organic Chemistry*, 2017, **82**, 10489–10503.

264   S. D. Sawant, M. Srinivas, K. A. Aravinda Kumar, G. Lakshma Reddy, P. P. Singh, B. Singh, A. K. Sharma, P. R. Sharma and R. A. Vishwakarma, *Tetrahedron Letters*, 2013, **54**, 5351–5354.

265   T. Liu, Y. Yang and C. Wang, *Angewandte Chemie*, 2020, **132**, 14362–14366.

266   G. Wernet, C. Bauer, B. Steubing, J. Reinhard, E. Moreno-Ruiz and B. Weidema, *The International Journal of Life Cycle Assessment*, 2016, **21**, 1218–1230.

267   A. A. Sauve, C. Wolberger, V. L. Schramm and J. D. Boeke, *Annual Review of Biochemistry*, 2006, **75**, 435–465.

268   D. Shore, M. Squire and K. A. Nasmyth, *The EMBO Journal*, 1984, **3**, 2817–2823.

269   S. Imai, C. M. Armstrong, M. Kaeberlein and L. Guarente, *Nature*, 2000, **403**, 795–800.

270   P. Bheda, H. Jing, C. Wolberger and H. Lin, *Annual Review of Biochemistry*, 2016, **85**, 405–429.

271   J. L. Avalos, I. Celic, S. Muhammad, M. S. Cosgrove, J. D. Boeke and C. Wolberger, *Molecular Cell*, 2002, **10**, 523–535.

272   R. A. Frye, *Biochemical and Biophysical Research Communications*, 2000, **273**, 793–798.

273   M. C. Haigis and D. A. Sinclair, *Annual Review of Pathology: Mechanisms of Disease*, 2010, **5**, 253–295.

274   E. Michishita, J. Y. Park, J. M. Burneskis, J. C. Barrett and I. Horikawa, *Molecular Biology of the Cell*, 2005, **16**, 4623–4635.

275   J. Du, Y. Zhou, X. Su, J. J. Yu, S. Khan, H. Jiang, J. Kim, J. Woo, J. H. Kim, B. H. Choi, B. He, W. Chen, S. Zhang, R. A. Cerione, J. Auwerx, Q. Hao and H. Lin, *Science*, 2011, **334**, 806–809.

276   F. Zhang, S. Wang, L. Gan, P. S. Vosler, Y. Gao, M. J. Zigmond and J. Chen, *Progress in Neurobiology*, 2011, **95**, 373–395.

277   T. Huhtiniemi, C. Wittekindt, T. Laitinen, J. Leppänen, A. Salminen, A. Poso and M. Lahtela-Kakkonen, *Journal of Computer-Aided Molecular Design*, 2006, **20**, 589–599.

278   A. M. Davenport, F. M. Huber and A. Hoelz, *Journal of Molecular Biology*, 2014, **426**, 526–541.

279   Y. Fang, S. Tang and X. Li, *Trends in Endocrinology & Metabolism*, 2019, **30**, 177–188.

280   S. Michan and D. Sinclair, *Biochemical Journal*, 2007, **404**, 1–13.

281   X. Hou, D. Rooklin, H. Fang and Y. Zhang, *Scientific Reports*, 2016, **6**, 38186.

282   S. Zhu, Z. Dong, X. Ke, J. Hou, E. Zhao, K. Zhang, F. Wang, L. Yang, Z. Xiang and H. Cui, *Seminars in Cancer Biology*, 2019, **57**, 59–71.

283   T. Lou, Q. Huang, H. Su, D. Zhao and X. Li, *Journal of Ethnopharmacology*, 2021, **268**, 113657.

284   Y. Yang, W. Fu, J. Chen, N. Olashaw, X. Zhang, S. V. Nicosia, K. Bhalla and W. Bai, *Nature Cell Biology*, 2007, **9**, 1253–1262.

285   C. Xu, L. Wang, P. Fozouni, G. Evjen, V. Chandra, J. Jiang, C. Lu, M. Nicastri, C. Bretz, J. D. Winkler, R. Amaravadi, B. A. Garcia, P. D. Adams, M. Ott, W. Tong, T. Johansen, Z. Dou and S. L. Berger, *Nature Cell Biology*, 2020, **22**, 1170–1179.

286   T. Yang, M. Fu, R. Pestell and A. A. Sauve, *Trends in Endocrinology & Metabolism*, 2006, **17**, 186–191.

287   Y. Fujita and T. Yamashita, *Frontiers in Neuroscience*, 2018, **12**, 778.

288   W. Renthal, A. Kumar, G. Xiao, M. Wilkinson, H. E. Covington, I. Maze, D. Sikder, A. J. Robison, Q. LaPlant, D. M. Dietz, S. J. Russo, V. Vialou, S. Chakravarty, T. J. Kodadek, A.

Stack, M. Kabbaj and E. J. Nestler, *Neuron*, 2009, **62**, 335–348.

289   R. H. Houtkooper, E. Pirinen and J. Auwerx, *Nature Reviews Molecular Cell Biology*, 2012, **13**, 225–238.

290   Y. Lee and E. Im, *Antioxidants*, 2021, **10**, 377.

291   Z. Z. Chong, S. Wang, Y. C. Shang and K. Maiese, *Future Cardiology*, 2012, **8**, 89–100.

292   N. D'Onofrio, L. Servillo and M. L. Balestrieri, *Antioxidants & Redox Signaling*, 2018, **28**, 711–732.

293   Z. Lin and D. Fang, *Genes & Cancer*, 2013, **4**, 97–104.

294   D. K. Alves-Fernandes and M. G. Jasiulionis, *International Journal of Molecular Sciences*, 2019, **20**, 3153.

295   L. M. Garcia-Peterson and X. Li, *Biochimica et Biophysica Acta (BBA) - General Subjects*, 2021, **1865**, 129952.

296   L. Kovanen, K. Donner and T. Partonen, *PLOS ONE*, 2015, **10**, e0141001.

297   N. Abe-Higuchi, S. Uchida, H. Yamagata, F. Higuchi, T. Hobara, K. Hara, A. Kobayashi and Y. Watanabe, *Biological Psychiatry*, 2016, **80**, 815–826.

298   C. L. Ferland, W. R. Hawley, R. E. Puckett, K. Wineberg, F. D. Lubin, G. P. Dohanich and L. A. Schrader, *Biological Psychiatry*, 2013, **74**, 927–935.

299   C. L. Ferland and L. A. Schrader, *Neuroscience*, 2011, **174**, 104–114.

300   Y. Lei, J. Wang, D. Wang, C. Li, B. Liu, X. Fang, J. You, M. Guo and X.-Y. Lu, *Molecular Psychiatry*, 2020, **25**, 1094–1111.

301   B. L. Tang, *Molecules and Cells*, 2016, **39**, 87–95.

302   H.-D. Kim, J. Hesterman, T. Call, S. Magazu, E. Keeley, K. Armenta, H. Kronman, R. L. Neve, E. J. Nestler and D. Ferguson, *Journal of Neuroscience*, 2016, **36**, 8441–8452.

303   M. T. Borra, B. C. Smith and J. M. Denu, *Journal of Biological Chemistry*, 2005, **280**, 17187–17195.

304   C. Zhou, Y. Wu, X. Ding, N. Shi, Y. Cai and Z. Z. Pan, *The Journal of Neuroscience*, 2020, **40**, 2332–2342.

305   T. C. Long, in *The New England journal of medicine*, Springer-Verlag, Berlin/Heidelberg, 2008.

306   S. Libert, K. Pointer, E. L. Bell, A. Das, D. E. Cohen, J. M. Asara, K. Kapur, S. Bergmann, M. Preisig, T. Otowa, K. S. Kendler, X. Chen, J. M. Hettema, E. J. van den Oord, J. P. Rubio and L. Guarente, *Cell*, 2011, **147**, 1459–1472.

307   P.-S. Huang, J.-H. Son, L. C. Abbott and U. H. Winzer-Serhan, *Neuroscience*, 2011, **196**, 189–202.

308   G. J. Prud'homme, Y. Glinka, O. Udovyk, C. Hasilo, S. Paraskevas and Q. Wang, *Biochemical and Biophysical Research Communications*, 2014, **452**, 649–654.

309   S. D. Lepore and Y. He, *The Journal of Organic Chemistry*, 2003, **68**, 8261–8263.

310   M. Mochizuki, Y. Fujimoto, H. Yanai and T. Matsumoto, *Synlett*, 2020, **31**, 1511–1516.

311   J. E. Green, D. M. Bender, S. Jackson, M. J. O'Donnell and J. R. McCarthy, *Organic Letters*, 2009, **11**, 807–810.

312   Y. Wang, W. Guo, A.-L. Guan, S. Liu and Z.-J. Yao, *Inorganic Chemistry*, 2021, **60**, 11514–11520.

313   H. C. Aspinall, O. Beckingham, M. D. Farrar, N. Greeves and C. D. Thomas, *Tetrahedron Letters*, 2011, **52**, 5120–5123.

314   E. Whiting, M. E. Lanning, J. A. Scheenstra and S. Fletcher, *The Journal of Organic Chemistry*, 2015, **80**, 1229–1234.

315   M. Achmatowicz, J. Chan, P. Wheeler, L. Liu and M. M. Faul, *Tetrahedron Letters*, 2007, **48**, 4825–4829.

316   A. Singh, E. R. Thornton and F. H. Westheimer, *Journal of Biological Chemistry*, 1962, **237**, PC3006–PC3008.

317   K. M. Lum, Y. Sato, B. A. Beyer, W. C. Plaisted, J. L. Anglin, L. L. Lairson and B. F. Cravatt, *ACS Chemical Biology*, 2017, **12**, 2671–2681.

318   E. Smith and I. Collins, *Future Medicinal Chemistry*, 2015, **7**, 159–183.

319   A. V. West and C. M. Woo, *Israel Journal of Chemistry*, 2022, **63**, e202200081.

320   D. W. GOLDMAN, J. S. POBER, J. WHITE and H. BAYLEY, *Nature*, 1979, **280**, 841–843.

321   R. A. G. Smith and J. R. Knowles, *Journal of the American Chemical Society*, 1973, **95**, 5072–5073.

322   C. C. Yip, C. W. Yeung and M. L. Moule, *Journal of Biological Chemistry*, 1978, **253**, 1743–1745.

323   P. E. Nielsen and O. Buchardt, *Photochemistry and Photobiology*, 2008, **35**, 317–323.

324   K. Bach, B. L. H. Beerkens, P. R. A. Zanon and S. M. Hacker, *ACS Central Science*, 2020, **6**, 546–554.

325   J. V. Oakley, B. F. Buksh, D. F. Fernández, D. G. Oblinsky, C. P. Seath, J. B. Geri, G. D. Scholes and D. W. C. MacMillan, *Proceedings of the National Academy of Sciences*, 2022, **119**, e2203027119.

326   R. A. Moss, *Accounts of Chemical Research*, 2006, **39**, 267–272.

327   S.-S. Ge, B. Chen, Y.-Y. Wu, Q.-S. Long, Y.-L. Zhao, P.-Y. Wang and S. Yang, *RSC Advances*, 2018, **8**, 29428–29454.

328   D. A. Modarelli, S. Morgan and M. S. Platz, *Journal of the American Chemical Society*, 1992, **114**, 7034–7041.

329   A. V. West, G. Muncipinto, H.-Y. Wu, A. C. Huang, M. T. Labenski, L. H. Jones and C. M. Woo, *Journal of the American Chemical Society*, 2021, **143**, 6691–6700.

330   E. E. Hays, I. C. Wells, P. A. Katzman, C. K. Cain, F. A. Jacobs, S. A. Thayer, E. A. Doisy, W. L. Gaby, E. C. Roberts, R. D. Muir, C. J. Carroll, L. R. Jones and N. J. Wade, *Journal of*

Biological Chemistry, 1945, **159**, 725–750.

331   I. C. Wells, W. H. Elliott, S. A. Thayer and E. A. Doisy, *Journal of Biological Chemistry*, 1952, **196**, 321–330.

332   J.-F. Dubern and S. P. Diggle, *Molecular BioSystems*, 2008, **4**, 882–888.

333   F. Witzgall, T. Depke, M. Hoffmann, M. Empting, M. Brönstrup, R. Müller and W. Blankenfeldt, *ChemBioChem*, 2018, **19**, 1531–1544.

334   M. E. Skindersoe, L. H. Zeuthen, S. Brix, L. N. Fink, J. Lazenby, C. Whittall, P. Williams, S. P. Diggle, H. Froekiaer, M. Cooley and M. Givskov, *FEMS Immunology & Medical Microbiology*, 2009, **55**, 335–345.

335   J. W. Lightbown and F. L. Jackson, *Biochemical Journal*, 1956, **63**, 130–137.

336   S. M. Geddis, T. Coroama, S. Forrest, J. T. Hodgkinson, M. Welch and D. R. Spring, *Beilstein Journal of Organic Chemistry*, 2018, **14**, 2680–2688.

337   D. Li, N. Oku, A. Hasada, M. Shimizu and Y. Igarashi, *Beilstein Journal of Organic Chemistry*, 2018, **14**, 1446–1451.

338   H. Kim, J.-Y. Hwang, B. Chung, E. Cho, S. Bae, J. Shin and K.-B. Oh, *Marine Drugs*, 2019, **17**, 133.

339   A. J. Fischer, S. B. Singh, M. M. LaMarche, L. J. Maakestad, Z. E. Kienenberger, T. A. Peña, D. A. Stoltz and D. H. Limoli, *American Journal of Respiratory and Critical Care Medicine*, 2021, **203**, 328–338.

340   L. Biswas and F. Götz, *Frontiers in Cellular and Infection Microbiology*, 2022, **11**, 1383.

341   V. Soheili, A. S. Tajani, R. Ghodsi and B. S. F. Bazzaz, *European Journal of Medicinal Chemistry*, 2019, **172**, 26–35.

342   C. Lu, B. Kirsch, C. Zimmer, J. C. de Jong, C. Henn, C. K. Maurer, M. Müsken, S. Häussler, A. Steinbach and R. W. Hartmann, *Chemistry & Biology*, 2012, **19**, 381–390.

343   D. Szamosvári, M. Prothiwa, C. L. Dieterich and T. Böttcher, *Chemical Communications*, 2020, **56**, 6328–6331.

344   D. Szamosvári and T. Böttcher, *Synlett*, 2018, **29**, 542–547.

345   D. Szamosvári and T. Böttcher, *Angewandte Chemie International Edition*, 2017, **56**, 7271–7275.

346   S. Thierbach, M. Wienhold, S. Fetzner and U. Hennecke, *Beilstein Journal of Organic Chemistry*, 2019, **15**, 187–193.

347   Y. R. Baker, J. T. Hodgkinson, B. I. Florea, E. Alza, W. R. J. D. Galloway, L. Grimm, S. M. Geddis, H. S. Overkleeft, M. Welch and D. R. Spring, *Chem. Sci.*, 2017, **8**, 7403–7411.

348   R. Dandela, D. Mantin, B. F. Cravatt, J. Rayo and M. M. Meijler, *Chemical Science*, 2018, **9**, 2290–2294.

349   B. Gioia, *Synthèse et évaluation biologique des dérivés de la 4-hydroxyquinoléine, dans l'étude des interactions antagonistes entre Pseudomonas aeruginosa et Staphylococcus aureus, chez*

les patients atteints de mucoviscidose., 2020.

350   H. P. Acharya, K. Miyoshi and Y. Kobayashi, *Organic Letters*, 2007, **9**, 3535–3538.